MARINE MICROBIAL INTACT POLAR DIACYLGLYCEROLIPIDS AND THEIR APPLICATION IN THE STUDY OF NUTRIENT STRESS AND BACTERIAL PRODUCTION

By
Kimberly J. Popendorf
B.S. California Institute of Technology, 2006

Submitted in partial fulfillment of the requirements for the degree of
Doctor of Philosophy

at the
MASSACHUSETTS INSTITUTE OF TECHNOLOGY
and the
WOODS HOLE OCEANOGRAPHIC INSTITUTION

February 2013

Author

_____

Joint Program in Oceanography/Applied Ocean Science and Engineering
Massachusetts Institute of Technology
and Woods Hole Oceanographic Institution
September 21, 2012

Certified by

_____

Dr. Benjamin A.S. Van Mooy
Associate Scientist with Tenure of Marine Chemistry and Geochemistry, WHOI
Thesis Supervisor

Accepted by

_____

Dr. Bernhard Peucker-Ehrenbrink
Senior Scientist of Marine Chemistry and Geochemistry, WHOI
Chair, Joint Committee for Chemical Oceanography
Woods Hole Oceanographic Institution

MARINE MICROBIAL INTACT POLAR DIACYLGLYCEROLIPIDS AND THEIR APPLICATION IN THE STUDY OF NUTRIENT STRESS AND BACTERIAL PRODUCTION

By

Kimberly J. Popendorf

Submitted to the MIT/WHOI Joint Program in Oceanography in partial fulfillment of the requirements for the degree of Doctor of Philosophy in the field of Chemical Oceanography

THESIS ABSTRACT

Intact polar diacylglycerolipids (IP-DAGs) were used to study microbial dynamics in the surface ocean. IP-DAGs from surface ocean seawater were quantified using high performance liquid chromatography-mass spectrometry (HPLC-MS), after first developing a sensitive, high throughput molecular ion independent triple quadrupole MS method for quantification. Using this analytical technique I examined the distribution of the nine most abundant classes of IP-DAGs across the Mediterranean, and found that phospholipids as a percent of total IP-DAGs correlated with phosphate concentration. Furthermore, phospholipids were a higher percent of total particulate phosphorus where phosphate was higher, ranging from 1-14%. Thus IP-DAGs can play not only a significant but also a dynamic role in defining planktonic nutrient needs and cellular C:N:P ratios in the environment. Additionally, microcosm incubations were amended with phosphate and ammonium, and in the course of several days this elicited a shift in the ratios of IP-DAGs. This study was the first to demonstrate the dynamic response of membrane lipid composition to changes in nutrients in a natural, mixed planktonic community, and indicated that the change in IP-DAG ratios in response to changing nutrients may be a useful indicator of microbial nutrient stress.

In the surface waters of the western North Atlantic I used three experimental approaches to identify the microbial sources of the nine most abundant classes of IP-DAGs. Phytoplankton are the primary source of one class of sulfolipid, sulfoquinovosyldiacylglycerol, and one class of betaine lipid, diacylglyceryl-trimethyl-homoserine, while heterotrophic bacteria are the dominant source of the phospholipids phosphatidylglycerol and phosphatidylethanolamine. In regrowth experiments in the Sargasso Sea and the North Pacific I demonstrated that phospholipid specific production rate is representative of heterotrophic bacterial cell specific growth rate. I measured phospholipid specific production rate and bacterial production rate using uptake of ^{3}H-leucine (^{3}H-Leu) and ^{3}H-thymidine (^{3}H-TdR) across the North Atlantic, across the Mediterranean, and in the North Pacific subtropical gyre. I found that phospholipid specific production rates estimate heterotrophic bacterial cell specific growth rates that are on the order of 1 per day, an order of magnitude faster than cell specific growth rates suggested by uptake of ^{3}H-Leu and ^{3}H-TdR.

Thesis supervisor: Dr. Benjamin Van Mooy
Title: Associate Scientist with Tenure, Department of Marine Chemistry and Geochemistry, WHOI

Acknowledgements

There are so many people to thank for helping me through this process that is grad school, and making it a wonderful, fun, insightful, exciting, empowering and ultimately rewarding experience along the way.

A huge thank you to my advisor Ben Van Mooy. He has provided endless resources and support, and has always pushed for my best scientific interests. He's a phenomenal scientist to have gotten to work with, and I feel lucky to have joined his lab. I'm grateful for the many, many hours he's spent talking science with me, doing benchwork side by side in rocking rad vans, working things out on the white board, and listening to me babble incoherently with a table full of graphs spread in front of us—he would always draw meaning from my quagmires of data and help direct my research into productive avenues. I have learned so much about how to do science and how to be a scientist from you in my years in the Van Mooy lab, thank you Ben!

Helen Fredricks is responsible for everything I know about liquid chromatography, mass spectrometry, and my ability to identify and quantify lipids—the backbone of my thesis. Her encyclopedic knowledge of lipid ions is unparalleled, and watching her read mass spectra like a book still blows me away. Her graceful fixes for all sorts of lab quandaries are my inspiration, when faced with a puzzling problem on an instrument or flummoxed by a method in lab, my best route to a solution is usually to think "what would Helen do?" She has been my shoulder to lean on since way back when I was a summer student, and her sage advice, motherly encouragement and drawer of chocolate have gotten me through so many trials and tribulations in lab and in my life. Thank you for everything Mama Helen.

To the rest of the amazing Van Mooy lab, a huge debt of thanks and gratitude to everyone who has been a part of this awesome team in the time I've been here. Thanks to Laura Hmelo for being the first, trail-blazing grad student in the lab and a great friend and mentor; to Krista Longnecker for instruction, advice, and insight on so many aspects of my projects, being a statistical analysis guru, helping with matlab, bacterial production, flow cytometry, and rad work on cruises; to Byron Pedler and Tim Shanahan for being there at the start and helping me get going; to Justin Ossolinski for his amazing ability to juggle everyone's needs and equipment on cruises and keep his cool; to the most upbeat and organized lab tech extraordinaire and sock-puppet star, Laura Sofen; to my awesome officemates Jamey Fulton and Patrick Martin for so many helpful conversations and brain-picking sessions over coffee; to Suni Shah for insightful conversations, career advice and encouragement; and to Bethanie Edwards and Jamie Collins, the awesome grad students carrying on the lab traditions.

My defense chair, Phoebe Lam, has been an important mentor throughout my grad school odyssey. I doubt I would have made it this far without your advice, guidance, and support—thank you for opening your office door to me in my first year and leaving it open ever since.

To each member of my committee, Dan Repeta, Sonya Dyhrman, and Janelle Thompson, many thanks for your time and energy helping guide my thesis throughout the process—the following pages owe a lot to your insights and suggestions.

My housemates for the entirety of the time I've been in Woods Hole, Maya Yamato and Ann Allen, have seen me through so much and have been phenomenal friends and supporters. Coming home to good conversations and warm and supportive friends made a world of difference at the end of long days in lab. Thank you for putting up with my crazy hours and commuter weekends, for feeding Finnigan, and for keeping me sane and happy.

Carly Buchwald has been my comrade-in-arms throughout my time in the joint program, from midnight sessions in the MIT student center powering through problem sets, to keeping me

company during late nights in lab, helping me cram last-minute cruise supplies into crazy and inventive containers, all the way through company, encouragement, and a well-caffeinated environment for writing right up to the end. Talking shop with her has helped me think through a lot of science, and I look forward many more fast-paced discussions and good times ahead.

My officemate for three formative years in the Fye Trailer, Karin Lemkau, has been my sounding board at every stage of progress, from surviving generals through the thesis proposal, developing manuscripts, sorting out intercalibration craziness, and putting it all together into a thesis. Thank you for listening to me ad-infinitum and for helping me make sense of myself and my science.

The students of Fye over the years have all provided encouragement, advice, company for pizza dinners in lab, and friendship: my fellow trailermates Dave Griffith and Maya Bhatia, my trailer predecessors James Saenz and Eoghan Reeves, Kristin Pangallo, and the new wave of Fye students Jill McDermott, Britta Voss and Winn Johnson. My JP cohort made the first few years of grad school not only manageable but fun, with special thanks to Erin Bertrand, Stephanie Owens, Jong-Mi Lee, Meredith White, Elizabeth Halliday, Dan Ohnemus, Jeff Kaeli, and Li Ling Hamady.

Thank you to the awesome people of Fye from whom I have borrowed/acquired equipment, time, advice, and science know-how: Liz Kujawinski, Melissa Soule, Carl Johnson, Chris Reddy, Sean Sylva, Bob Nelson, Catherine Carmichael, Tim Eglinton, Daniel Montlucon, Valier Galy, Jeff Seewald, and Amanda Spivak.

Many thanks to the people who have made it possible for me to go on cruises and provided invaluable help at sea: at BIOS, Mike Lomas, John Casey and Amanda Burke; in the Mediterranean, France Van Wambeke, Thierry Moutin, my rad van comrades Agathe Talarmin and Romain Mauriac, Dominique Lamy, Karin Nordkvist; on Pacific and Atlantic cruises, Isabel Ferrera, Mikhail Koblizek, Rick Keil and his team.

The administrative support at WHOI is unparalleled and has made all the difference throughout my time here: in APO Julia Westwater, always an open door and a willing ear, Marsha (Gomes) Armando, Tricia Gebbie, Jim Yoder, Meg Tivey; chemistry education coordinator Mark Kurz; in MC&G Sheila Clifford and Donna Mortimer. Thanks to the JP's tireless champion at MIT, Ed Boyle, for continuing to look out for our welfare at MIT, and to Ronni Schwartz for helping us navigate the northern campus.

I wouldn't be here without the endless support of my incredible family. Thank you to my dad for teaching me to ask the right questions, and my brother for always being a science inspiration, and to my mom for teaching me to approach every problem with creativity, energy, and passion, and to make time to enjoy the good things. Thank you to my grandparents for your unfailing love and support. Thank you to my family of friends for everything over the years, Jenny Fisher, Linda Strubbe, Julia Ma, Jon Simon, Eva Balog, and Jenna Forsyth.

To John, your support and encouragement have meant everything to me. I cannot express how lucky I am to have you in my life. Thank you for putting up with, and helping with, everything this thesis has entailed.

This research was supported by a National Science Foundation Graduate Research Fellowship, a National Defense Science and Engineering Graduate Fellowship, and grants from the U.S. Office of Naval Research (N00014-09-1-0091 and N00014-06-1-0134) and the U.S. National Science Foundation (OCE-1031143, OCE-1029687, and OCE-0646944).

TABLE OF CONTENTS

Chapter 1

An introduction to intact polar membrane lipids as molecular tools to study marine microbes in the surface ocean

Introduction to intact polar membrane lipids as molecular tools to study marine microbes in the surface ocean

Marine microbes play a critical role in global biogeochemical cycles through the myriad chemical transformations that they mediate (Azam et al., 1983; Karl, 2002). In the quest to understand biogeochemial cycles, a great deal of effort is invested in accurately measuring the abundance of microbes, and the magnitude and rate of the chemical reactions they are performing. Given the diversity of microbes in the ocean, and the complex environment in which they live, these parameters are not easily measured. Direct assessment of many key processes, including primary production and bacterial production, is difficult if not impossible (Gasol et al., 2008). Therefore estimates of the magnitude and rate of many processes rely on measurement of representative biochemicals. To measure the abundance of microbes and their rate of cellular production, many molecular tools look to the three major classes of cellular compounds for a suitable biochemical tracer: proteins, nucleic acids (DNA and RNA), or lipids. Lipids have historically been relatively underutilized in the study of active microbial processes in the water column, however their analytical tractability and physiological role make them prime candidates for the study of microbial dynamics.

One of the most important roles of lipids, from a physiological standpoint, is forming the outer layer, or membrane of the cell (Figure 1). Membrane lipids have great promise as molecular tools to study microbes in the surface ocean due to their physiological and biochemical significance. On a per cell basis, membrane lipids are a substantial fraction of cellular material (Hagen et al., 1966; Suzumura and Ingall, 2001), 10-25% of cellular carbon in marine plankton (Wakeham et al., 1997). As one of the major cellular pools of phosphorus, the synthesis of phospholipids may consume up to 28% of cellular phosphate uptake (Van Mooy et al., 2006). Within the water column, membrane lipids are an abundant chemical component of particulate material, with total concentrations in the surface ocean typically on the order of 5 nM (Van Mooy and Fredricks, 2010; Figure 3). In particulate material exiting the euphotic zone, lipids have been shown to be 10-30% of the organic carbon (Wakeham et al., 1997). As a fraction of

total particulate phosphorus, one study found phospholipids to be 3-14% in surface coastal waters (Suzumura and Ingall, 2001). Given their absolute abundance, lipids play an important role in the biogeochemical cycling of carbon and phosphorus in the ocean. Furthermore, production of membrane lipids is obligate for both growth and replication of cells, giving membrane lipids a unique potential to be a proxy not only for stocks of microbial biomass but also for rates of microbial production (White et al., 1977). In addition to their important physiological and biogeochemical role, the structural diversity and analytical accessibility of membrane lipids make these compounds promising molecular tools for the study of microbes in the surface ocean (Sturt et al., 2004).

Through the analysis of intact polar membrane lipids, this thesis will explore two broad topics concerning microbial dynamics in the surface ocean: the microbial response to low nutrients, and heterotrophic bacterial production in the surface ocean. The particular questions I will endeavor to answer are:

1) What factors control microbial membrane lipid composition in the environment? Can the change in membrane lipid composition be used as an indicator of microbial nutrient stress?

2) Can phospholipid specific production rate be used as a measure of heterotrophic bacterial production rate?

Exploring both of these questions will rely on many quantitative measurements of membrane lipids from the environment. The first step towards answering these questions, therefore, is refining a method to quantify membrane lipid concentration in seawater samples that will be suitable for the analysis of large datasets. This will be the focus of Chapter 2. Chapters 3 and 4 will explore the factors controlling membrane lipid composition in the environment, and the potential of membrane lipids to be indicators of microbial nutrient stress. The applicability of phospholipid specific production rate to estimate heterotrophic bacterial production rate will be assessed in Chapter 5. The following sections will introduce the relevant background information and motivation for each of these topics, and will outline the work undertaken to answer these questions.

1.1 Measurement of membrane lipids in marine environmental samples

Chemical structure of intact polar membrane lipids

There are two key features to the lipids that form the bilayer membrane of cells: a polar, hydrophilic moiety—these are the headgroups which form the inner and outer surface of the membrane; and a nonpolar hydrophobic moiety—these are the fatty hydrocarbon chains that align themselves in the interior of the membrane (Figure 1). A vast array of intact polar membrane lipid molecular species exist, each of which is defined by the composition of the headgroup, the length and degree of unsaturation of the fatty hydrocarbon chains, and the structure of the backbone bonding the hydrophobic and hydrophilic moieties. The most common backbone structures are glycerols and long-chain bases (e.g. sphingosine, which includes both the backbone and a fatty alcohol). This thesis is focused on the study of intact polar diacylglycerolipids (IP-DAGs) in the ocean, lipids that have two fatty acid chains with ester bonds linking them to a glycerol backbone. These are the lipids that dominate the membranes of bacterial and eukaryotic microbial membranes (Van Mooy and Fredricks, 2010). Archael microbial membranes, in contrast, are dominated by intact polar dialkylglycerolipids (IP-DEGs), lipids with a glycerol backbone and ether linked fatty alcohol chains (DeLong et al., 1998; Schouten et al., 2008).

Within IP-DAGs, there are three main types of lipids, defined by the heteratoms in the headgroup: phospholipid headgroups contain a phosphate group; betaine lipid headgroups contain a quaternary amine group and do not contain phosphate; glycolipid headgroups contain a sugar and no phosphorus or nitrogen—within this type, one class contains sulfate bound to a sugar and is referred to as a sulfolipid (Figure 2). Within each of these types, lipid classes are defined by the chemical structure of the headgroup. There are nine IP-DAG headgroup classes that have been found to be most abundant in the ocean (Van Mooy and Fredricks, 2010; Figure 2): three classes of phospholipids, phosphatidylglycerol (PG), phosphatidylethanolamine (PE), and phosphatidylcholine (PC); three classes of betaine lipids, diacylglyceryl-trimethyl-homoserine (DGTS),

diacylglyceryl-hydroxymethyl-trimethyl-β-alanine (DGTA), and diacylglyceryl-carboxyhydroxy-methylcholine (DGCC); and three classes of glycolipids, monoglycosyldiacylglycerol (MGDG), diglycosyldiacylglycerol (DGDG), and sulfoquinovosyldiacylglycerol (SQDG). The biogeochemical significance of these class distinctions is that phosphorus and nitrogen are scarce in many areas of the ocean (Moore et al., 2004) and may be limiting for microbial production, thus the fraction of the membrane composed of phospholipids or betaine lipids may pose a significant cellular nutrient requirement.

Lipid analysis

Membrane lipids have been well-studied for over half a century, with treatises on the lipids of bacteria appearing in the 1960s and 1970s (Goldfine, 1972; Hagen et al., 1966; Kates, 1964; Oliver and Colwell, 1973; Shaw, 1974). A variety of methods for the extraction, separation and purification of lipids were developed by the 1970s, and many of these methods are still employed today. The Bligh and Dyer extraction method was introduced in 1959, and is routinely used today for lipid extraction from a variety of sample types including seawater, freshwater, sediments, tissue samples, and filters. A modified version of this method (Sturt et al., 2004) was employed for all of the IP-DAG samples in this thesis.

The key components of a "Bligh and Dyer solvent extraction" are the addition of organic and aqueous solvents in a ratio such that they form a single-phase solution in which the sample is extracted and lipids are dissolved, then further addition of solvents in a ratio such that the aqueous and organic phases separate, with lipids dissolved in the organic phase. The organic phase is typically dichlormethane or chloroform, while the aqueous solvents are methanol and a buffered saline solution (or the water sample of interest). Once the phases have been separated the organic phase can be easily collected by mechanical means (using a pipette or separation funnel) and the lipids can be concentrated or derivatized before analysis. While extraction methods have seen relatively little modification over the last several decades, the methods for detecting and

quantifying lipids have advanced tremendously in the last two decades, thanks in large part to advances in high pressures liquid chromatography (HPLC) and mass spectrometry (MS).

Prior to HPLC-MS techniques for lipid analysis, one of the most versatile methods of lipid detection was thin layer chromatography (TLC). TLC has been employed extensively and gives detailed information on the chemical composition of diverse lipids (Christie, 2003). It is excellent for resolving different classes of lipids, and is useful for presence-absence analysis. TLC can be coupled with a flame ionization detector (FID) for quantitative analysis of lipids, however it is not possible to get detailed structural and abundance information in a single analysis. Detailed structural analysis of lipids is possible with nuclear magnetic resonance (NMR) spectroscopy, though the relatively large sample size required (on the order of μg's for ^{13}C spectroscopy) severely limits the application of this method in environmental analysis. As HPLC became available for geochemical analyses, initially the most common detectors were UV-vis spectrophotometers, which are not amenable for IP-DAG analysis as most IP-DAGs are not UV absorbers. HPLC became a much more useful tool for lipid analysis with the development of the evaporative light scattering detector (ELSD). ELSD analysis is capable of sensitive quantification of IP-DAGs, given calibration to appropriate standards, however it measures only bulk properties and provides no information on the chemical properties of the lipids (Christie, 2003).

With extensive sample preparation or derivatization, TLC-FID or HPLC-ELSD can quantify lipids with more structural resolution, however, labortatory preparation time then limits sample throughput. One common type of derivatization for intact lipids is transesterifciation or saponification to transform the diacyl moities into fatty acid methyl esters (FAMEs). FAMEs can be readily analyzed with gas chromatrography (GC) linked to FID or MS, providing precise quantification as well as in-depth structural information. The analysis of FAMEs has been extensively employed in biogeochemical studies of sediments, estuaries, lakes, and oceans (Perry et al., 1979; Volkman et al., 1998; Yoshinaga et al., 2008). The FAMEs derived from intact polar lipids have proven to

have great utility as biomarkers for the study of microbes in the environment. However, with the loss of the headgroup in the derivitazation, potential biological and biogeochemical information also lost.

With the introduction of "soft ionization" techniques (e.g. electrospray ionization, ESI) in the mid 1990s (Kim et al., 1994) it became possible to study intact polar lipids using HPLC-MS. Using HPLC-ESI-MS analysis it is possible to characterize and quantify every molecular species present in a diverse assemblage of intact polar lipids from environmental samples (Koivusalo et al., 2001). This depth of information provides unprecedented potential to discern taxonomic and environmental information from lipid analyses. HPLC-ESI-MS analysis of samples from a variety of settings have demonstrated the utility of intact polar lipids as molecular tools to assess microbial presence, abundance, and diversity in the environment (Ertefai et al., 2008; Rütters et al., 2002; Sturt et al., 2004).

Quantification of IP-DAGs in the oceans

Since the introduction of HPLC-ESI-MS methods for IP-DAG analysis, intact polar lipids have been quantified in a relatively small, but growing, number of seawater samples from a range of marine settings. Van Mooy et al. (2006) measured the concentration of glycolipids and phospholipids in the surface waters of the North Pacific Subtropical Gyre at station ALOHA, and the concentration of glycolipids, phospholipids and betaine lipids at the BATS station in the Sargasso Sea (Van Mooy et al. 2009) and in depth profiles at four locations in the South Pacific (Van Mooy and Fredricks, 2010). The ratio of "substitute" lipids to phospholipids was measured in each of these locations (SQDG:PG and betaine lipids:PC) and it was found that the ratio was higher in locations with low phosphate (Van Mooy et al., 2009). In each of these locations phospholipid synthesis rate was also measured, and it was found that phospholipid synthesis, as a percent of total phosphate uptake, was correlated with phosphate concentration (Van Mooy et al. 2009). These studies motivated many of the questions addressed in this thesis.

Measurements of the absolute concentration of IP-DAGs in surface ocean particulate matter have also been made in the Black Sea and the North Sea. In the Black Sea, Schubotz et al. (2009) measured the concentration of IP-DAGs and IP-DEGs in a high-resolution depth profile and sediment samples, and did extensive analysis of the molecular species present and likely microbial sources. In the North Sea, Brandsma et al. (2012) measured the concentration of IP-DAGs in a year-long timeseries study at a coastal station, and found that there was little temporal variation in the relative abundance of different IP-DAG classes. Across all of these studies a relatively consistent picture has emerged of total IP-DAG concentration in surface waters and the most abundant classes of IP-DAGs.

Most of these measurements were made using HPLC-ESI-MS with an ion-trap mass spectrometer. This method relies on manual identification of the molecular ions associated with each IP-DAG class, based on retention time and diagnostic fragmentation patterns, followed by integration of a separate chromatogram for each molecular ion of interest. The concentration of an IP-DAG class is then determined by summing the peak areas of the relevant chromatograms (anywhere from 1 to 20 chromatograms for a typical marine sample, depending on the IP-DAG class), and using external standard curves to convert that peak area to a molar amount of IP-DAG. IP-DAG analysis using ion-trap mass spectrometry is excellent for characterization of new or unfamiliar compounds, and provides great characterization of the diversity of molecular ions across samples. However, the laborious data analysis process for each sample severely limits sample throughput and is prohibitive for the analysis of large transect datasets or timeseries measurements. The development of a more efficient mass spectrometry data collection and analysis method could greatly increase sample throughput and enable the measurement of datasets with greater temporal and geographic resolution.

Chapter 2 of this thesis develops a new, high throughput method for quantifying environmental IP-DAG samples using triple quadrupole MS. The subsequent chapters of this thesis apply this triple quadrupole MS method to quantify IP-DAGs in the surface waters of the North Atlantic, the North Pacific, and the Mediterranean Sea. In the North

Atlantic IP-DAGs were measured along a longitudinal transect, spanning a nutrient gradient from the phosphate-rich waters north of the Gulf Stream into the oligotrophic, phosphate-deplete Sargasso Sea. In the Mediterranean Sea IP-DAGs were sampled with unprecedented latitudinal and depth resolution across a transect from the oligotrophic western Algero-Provencal basin to the ultraoligotrophic eastern Levantine basin. This dataset roughly quadruples the number of published data points for IP-DAG concentration in seawater.

1.2 Microbial response to nutrient stress

Measuring microbial response to nutrient conditions

Many areas of the ocean have extremely low concentrations of dissolved phosphorus and nitrogen, key nutrients for microbial growth. The ambient concentration of dissolved nutrients is not, however, equivalent with the concentration of bioavailable nutrients, which in many cases is a fraction of the total dissolved pool (Björkman and Karl, 2003; Dyhrman et al., 2002). For phosphate, regions of the ocean with ambient concentrations in the tens of nmol per L, or less, are considered phosphate-depleted regions. The areas of the global ocean that are the most strongly phosphate depleted include the Sargasso Sea in the North Atlantic, and the Mediterranean Sea (Lomas et al., 2010; Pujo-Pay et al., 2011).

The ratio of bioavailable, dissolved nutrients (C:N:P, as well as trace elements including Si, Fe, Co, and more) is crucial in determining the productivity, and the community composition, of an ocean biome (Follows et al., 2007; Karl et al., 2001; Moore et al., 2004; Moutin et al., 2002). A biome is considered to be nutrient limited when addition of nutrients, or a particular nutrient (e.g. phosphate), leads to an increase in the productivity of the system, measured by the increase in microbial biomass, primary production, bacterial production, export production, or another parameter of interest (Moutin and Raimbault, 2002). In contrast to nutrient depletion, which is defined in

terms of chemical concentrations, nutrient limitation reflects the biological response to available nutrients.

Nutrient limitation is sometimes assessed by large-scale ocean fertilization experiments where nutrients are added directly to a patch of ocean and followed for a period of days to weeks (Boyd et al., 2007; Thingstad et al., 2005), and more often by small-scale "microcosm" bottle incubations where nutrients are added to bottles of whole seawater and incubated at conditions approximating *in situ* light and temperature for a period of days (or less commonly weeks) (Carlson et al., 2002; Tanaka et al., 2011). When ambient nutrients are limited, organisms employ a variety of cellular strategies to either be more effective at acquiring the nutrient (e.g. expression of alkaline phosphatase enzymes to access phosphorus from dissolved organic phosphorus, (Dyhrman et al., 2002)) or get by with lower per-cell quotas of the nutrient (e.g. substitution of phospholipids by non-phospholipids; Van Mooy et al., 2009). Nutrient stress is typically assayed by measuring the expression of these low-nutrient coping strategies. Nutrient stress may be defined in relation to one particular element, e.g. phosphorus, and in terms of one particular microbial group, e.g. *Trichodesmium*, or in terms of the microbial community at large depending on the assay method employed.

Lipids as indicators of nutrient stress

The particular mix of IP-DAGs that makes up the membrane varies across different types of microbes, with glycolipids being abundant in phytoplankton, phospholipids being abundant in heterotrophic bacteria, and betaine lipids being abundant in eukaryotic phytoplankton (Hagen et al., 1966; Kato et al., 1996; Van Mooy et al., 2009; Van Mooy et al., 2006). In cultures, the composition of the membrane has been shown to change in response to available nutrients—for some types of organisms, when phosphate concentration is low they will make more of their membrane from "substitute" sulfolipids and betaine lipids (Benning et al., 1993; Benning et al., 1995; Martin et al., 2011; Minnikin et al., 1974; Van Mooy et al., 2009; Van Mooy et al., 2006). In particular, SQDG is thought to substitute for PG, and betaine lipids (any one or a

combination of DGTS, DGTA and DGCC) substitute for PC—in both cases the substitute lipid and the phospholipid being replaced have the same ionic charge. Studies of marine microbial cultures and surveys of genomic information have indicated that this ability to alter membrane composition is not shared equally among different types of microbes. In particular, heterotrophic bacteria have not been found to have the genes for SQDG synthesis, and do not been observed to alter their phospholipid content in culture incubations (Van Mooy et al., 2009; Van Mooy et al., 2006).

Phosphorus is scarce in much of the ocean, and may be the limiting factor for microbial production in some areas (Mather et al., 2008; Moutin et al., 2008). It has been demonstrated that phosphate uptake into phospholipids, as a percent of total phosphate uptake, scales with phosphate concentration and can range from 1-28% of total phosphate uptake (Van Mooy et al., 2009). Given that phospholipid synthesis can represent a large portion of cellular phosphate needs, the ability to substitute non-phospholipids has the potential to provide a substantial advantage in low phosphorus conditions. Van Mooy et al. (2009) calculated that the replacement of phospholipids with glycolipids in cyanobacterial cells would spare phosphorus equivalent to 10-86% of the phosphorus in their genomic DNA.

From these studies it is clear that, in culture conditions, individual species are capable of adjusting their lipid composition in response to phosphate conditions, and in the environment phospholipids are a variable and significant part of the total lipid pool and phospholipid synthesis is a variable and significant part of total phosphate uptake. What has not been explored is whether the observed differences in total lipid composition in different environments are the result of individual organisms varying their physiology, as demonstrated in cultures, or, instead are the result of shifts in the community composition, with selection for low-phospholipid containing species in low-phosphorus environments. Additionally, it has yet to be tested whether mixed microbial communities in the environment will exhibit changes in membrane lipid composition in response to changes in nutrients, as has been shown for individual species in culture. If such changes were observed for a mixed microbial community in an environmental setting, this would

suggest that changes in membrane lipid composition might be an important microbial mechanism for coping with low nutrients in environmental settings, and that the measurement of lipid ratios in the environment might be a useful tool for assessing microbial nutrient stress.

To address these questions, in Chapter 3, I measured the membrane composition of different microbial groups in environmental samples from the North Atlantic, and examined the variation of membrane composition for heterotrophic bacteria and cyanobacteria across a natural phosphate gradient. In Chapter 4, I measured the concentrations of the nine major IP-DAGs across the oligotrophic Mediterranean Sea, and compared this to variations in nutrients and microbial populations across the basin. I used this data to assess the potential influence of changes in community and changes in physiology to explain the observed variations in IP-DAG ratios. Additionally, in the Mediterranean I conducted nutrient amendment incubations with whole seawater and measured the change in IP-DAG ratios to determine if changes in these ratios might be useful indicators of nutrient stress in mixed microbial communities.

1.3 Microbial production rate

Methods for measuring heterotrophic bacterial production rate

The importance of bacteria in the marine carbon cycle came to light more than thirty years ago (Azam et al., 1983; Ducklow, 1983; Pomeroy, 1974). As the significance of bacterial carbon fluxes was realized, methods were sought to quantify the rate of bacterial production. The primary methods that became established used the uptake rate of tritiated thymidine (^{3}H-TdR) (Fuhrman and Azam, 1980; Fuhrman and Azam, 1982; Karl, 1979; Kirchman et al., 1982) and uptake rate of tritiated leucine (^{3}H-Leu) (Kirchman et al., 1985; Kirchman, 1992; Simon and Azam, 1989; Smith and Azam, 1992). In the intervening decades these methods have been applied thousands of times in oceans around the globe. The bacterial production rates measured by these methods have established our collective paradigm that heterotrophic bacteria growth rate is slow, on the

order of 0.1 per day, compared to phytoplankton growth rate which is more commonly on the order of 1 per day (Ducklow, 2000).

Since the development of the ^{3}H-Leu and ^{3}H-TdR methods in the 1980s, much has been learned about the species diversity of heterotrophic bacteria (Giovannoni and Rappé, 2000; Rappé et al., 2002), the variation in substrate specificity (Alonso-Sáez and Gasol, 2007; Cottrell and Kirchman, 2000; Longnecker et al., 2010; Schwalbach et al., 2010) and the variation in production rate across bacterial clades (Lebaron et al., 2002; Longnecker et al., 2005; Van Wambeke et al., 2011). A study of clade-specific uptake of $^{33}PO_4$, ^{3}H-TdR, and ^{3}H-Leu showed that, in the North Atlantic, generally less than 10% of heterotrophic bacterial cells were active in the uptake of ^{3}H-Leu and ^{3}H-TdR, a fraction 2-10 times less than the number of cell active in the uptake of $^{33}PO_4$ (Longnecker et al., 2010). This suggests that heterotrophic bacterial production measured by uptake of ^{3}H-Leu and ^{3}H-TdR may be an underestimate of the true rate of bacterial production, perhaps by as much as a factor of 10. Given this finding, there is motivation to develop a new method to measure heterotrophic bacterial production, one which does not rely on the uptake of a substrate that is specific to a subset of open ocean heterotrophic bacteria. Development of such a method could provide new insights into the role of heterotrophic bacteria in the ocean carbon cycle.

I propose to use phosphate, as a more general substrate, and measure its uptake into phospholipids specific to heterotrophic bacteria as a method for measuring heterotrophic bacterial production. In order for this to be a valid and accurate method for measuring heterotrophic bacterial production, it is necessary to verify three criteria: 1) phosphate is a general substrate taken up by all heterotrophic bacteria and fulfills the majority of heterotrophic bacterial phosphorus demand; 2) the incorporation of phosphate into particular phospholipids is specific to heterotrophic bacteria amongst marine microbes; 3) there is a consistent, quantitative relationship between heterotrophic bacterial cell turnover rate and phospholipid turnover rate. The first criteria can be established by a review of existing literature, which will be done in chapter 5. The second criteria can be established by review of existing literature and evaluation of

results from chapters 3 and 4. The third criteria will be addressed through experiments in Chapter 5. An overview of existing literature on phospholipid production rates is presented below.

Lipids as indicators of microbial production

Surface area to volume constraints impose a minimum amount of membrane lipid per cell. In accordance with the high surface area to volume ratio expected of small marine microbial cells, it has been shown that lipids are a substantial fraction of cellular material (Wakeham et al., 1997). Given that membrane lipids play a non-negotiable physiological role, their production is obligate for the growth and replication of cells. Therefore it is reasonable to assume that there would be a quantitative relationship between cell growth and membrane lipid production. This idea was explored beginning in the 1970s, commensurate with the rising interest in measuring bacterial growth rates in the environment.

Many studies have been conducted measuring microbial phospholipid production rate (King et al., 1977; White et al., 1977; White and Tucker, 1969), and some studies have compared phospholipid production rate to the ^{3}H-thymidine uptake method for measuring bacterial production (Freeman and Lock, 1995; Moriarty et al., 1985; Van Mooy et al., 2008). Phospholipid production rates were found to be a useful measure of bacterial growth in biofilms and estuarine settings (Freeman and Lock, 1995; King et al., 1977; White et al., 1977), and provided insight into phosphorus cycling in the open ocean (Van Mooy et al., 2008). Early studies examined phospholipid metabolism in cultures of *Haemophilus parainfluenza* (White and Tucker, 1969) and found that cell doubling times were similar to phospholipid doubling times. White et al. (1977) and Moriarity et al. (1985) demonstrated in estuarine and marine settings (respectively) that phospholipid production rates were similar to other measures of microbial production, including uptake of ^{3}H-TdR in marine sediments.

However, no study has empirically established a quantitative relationship between phospholipid turnover rate and open ocean heterotrophic bacterial cell turnover rate. This

measurement is crucial to the validation of phospholipid production rate as a measure of heterotrophic bacterial production rate. The measurement of this relationship, and application of phospholipid production rate as a measure heterotrophic bacterial production rate, is the focus of Chapter 5.

1.4 Summary of work presented

Chapter 2 of this thesis is devoted to the development and validation of a new molecular ion-independent method for quantifying IP-DAGs in seawater samples using HPLC-ESI-triple quadrupole-MS. Using a molecular ion-independent quantitation method provides more efficient analysis of samples, enabling analysis of much larger datasets than were previously practical.

Chapter 3 assesses the microbial sources of IP-DAGs in environmental samples from the North Atlantic. Three experimental approaches were employed: stable isotope tracing, cell sorting flow cytometry, and selective incubations.

Chapter 4 explores the variability of IP-DAGs across a nutrient gradient in the Mediterranean Sea and assesses the relative contribution of changes in microbial community structure and physiological shifts to the observed gradients in IP-DAGs. Microcosm incubations were also conducted to assess the relevance of ratios of IP-DAGs as indicators of microbial nutrient stress.

Chapter 5 proposes, tests, and applies a new method for measuring heterotrophic bacterial production using phospholipid specific production rates. Regrowth incubations were conducted in the Sargasso Sea and the North Pacific to measure the quantitative relationship between phospholipid specific production rate and heterotrophic bacterial cell specific growth rate. Phospholipid specific production rate measurements were compared to established ^{3}H-Leu and ^{3}H-TdR-based measures of heterotrophic bacterial production rate in the North Pacific, the North Atlantic, and the Mediterranean Sea.

Cumulatively, this thesis explores the biogeochemical and physiological significance of IP-DAGs in the ocean, and the information that these biochemicals convey about microbial dynamics in the surface ocean.

References

Alonso-Sáez, L., Gasol, J.M., 2007. Seasonal Variations in the Contributions of Different Bacterial Groups to the Uptake of Low-Molecular-Weight Compounds in Northwestern Mediterranean Coastal Waters. Applied and Environmental Microbiology 73, 3528-3535.

Azam, F., Fenchel, T., Field, J.G., Gray, J.S., Meyer-Reil, L.A., Thingstad, F., 1983. The Ecologocial Role of Water-Column Microbes in the Sea. Marine Ecology Progress Series 10, 257-263.

Benning, C., Beatty, J.T., Prince, R.C., Somerville, C.R., 1993. The sulfolipid sulfoquinovosyldiacylglycerol is not required for photosynthetic electron transport in Rhodobacter sphaeroides but enhances growth under phosphate limitation. Proceedings of the National Academy of Sciences 90, 1561-1565.

Benning, C., Huang, Z.-H., Gage, D.A., 1995. Accumulation of a Novel Glycolipid and a Betaine Lipid in Cells of Rhodobacter sphaeroides Grown under Phosphate Limitation. Archives of Biochemistry and Biophysics 317, 103-111.

Björkman, K.M., Karl, D.M., 2003. Bioavailability of dissolved organic phosphorus in the euphotic zone at Station ALOHA, North Pacific Subtropical Gyre. Limnology and Oceanography 48, 1049-1057.

Bligh, E.G., Dyer, W.J., 1959. A Rapid Method of Total Lipid Extraction and Purification. Canadian Journal of Physiology and Pharmacology 37, 911-917.

Boyd, P.W., Jickells, T., Law, C.S., Blain, S., Boyle, E.A., Buesseler, K.O., Coale, K.H., Cullen, J.J., de Baar, H.J.W., Follows, M.J., Harvey, M., Lancelot, C., Levasseur, M., Owens, N.P.J., Pollard, R., Rivkin, R.B., Sarmiento, J., Schoemann, V., Smetacek, V., Takeda, S., Tsuda, A., Turner, S., Watson, A.J., 2007. Mesoscale iron enrichment experiments 1993-2005: synthesis and future directions. Science 315, 612-617.

Brandsma, J., Hopmans, E.C., Philippart, C.J.M., Veldhuis, M.J.W., Schouten, S., Damsté, J.S.S., 2012. Low temporal variation in the intact polar lipid composition of North Sea coastal marine water reveals limited chemotaxonomic value. Biogeosciences 9, 1073-1084.

Carlson, C.A., Giovannoni, S.J., Hansell, D.A., Goldberg, S.J., Parsons, R., Otero, M.P., Vergin, K., Wheeler, B.R., 2002. Effect of nutrient amendments on bacterioplankton production, community structure, and DOC utilization in the northwestern Sargasso Sea. Aquatic Microbial Ecology 30, 19-36.

Christie, W.W., 2003. Lipid Analysis, 3rd ed. The Oily Press, Bridgwater, England.

Cottrell, M.T., Kirchman, D.L., 2000. Natural Assemblages of Marine Proteobacteria and Members of the *Cytophaga-Flavobacter* Cluster Consuming Low- and High-Molecular-Weight Dissolved Organic Matter. Applied and Environmental Microbiology 66, 1692-1697.

DeLong, E.F., King, L.L., Massana, R., Cittone, H., Murray, A., Schleper, C., Wakeham, S.G., 1998. Diphytanyl ether lipids in nonthermophilic crenarchaeotes. Applied and Environmental Microbiology 64, 1133-1138.

Ducklow, H., 2000. Bacterial Production and Biomass in the Oceans, in: Kirchman, D.L. (Ed.), Microbial Ecology of the Oceans. Wiley-Liss, New York, pp. 85-120.

Ducklow, H.W., 1983. Production and fate of bacteria in the oceans. BioScience 33, 494-501.

Dyhrman, S.T., Webb, E.A., Anderson, D.M., Moffett, J.W., Waterbury, J.B., 2002. Cell-specific detection of phosphorus stress in Trichodesmium from the western North Atlantic. Limnology and Oceanography 47, 1832-1836.

Ertefai, T.F., Fisher, M.C., Fredricks, H.F., Lipp, J.S., Pearson, A., Birgel, D., Udert, K.M., Cavanaugh, C.M., Gschwend, P.M., Hinrichs, K.-U., 2008. Vertical distribution of microbial lipids and functional genes in chemically distinct layers of a highly polluted meromictic lake. Organic Geochemistry 39, 1572-1588.

Follows, M.J., Dutkiewicz, S., Grant, S., Chisholm, S.W., 2007. Emergent biogeography of microbial communities in a model ocean. Science 315, 1843-1846.

Freeman, C., Lock, M.A., 1995. Isotope dilution analysis and rates of 32P incorporation into phospholipids as a measure of microbial growth rates in biofilms. Water Research 29, 789-792.

Fuhrman, J.A., Azam, F., 1980. Bacterioplankton Secondary Production Estimates for Coastal Waters of British Columbia, Antarctica, and California. Applied and Environmental Microbiology 39, 1085-1095.

Fuhrman, J.A., Azam, F., 1982. Thymidine Incorporation as a Measure of Heterotrophic Bacterioplankton Production in Marine Surface Waters: Evaluation and Field Results. Marine Biology 66, 109-120.

Gasol, J.M., Pinhassi, J., Alonso-Sáez, L., Ducklow, H., Herndl, G.J., Koblízek, M., Labrenz, M., Luo, Y., Morán, X.A.G., Reinthaler, T., Simon, M., 2008. Towards better understanding of microbial carbon flux in the sea. Aquatic Microbial Ecology 53, 21-38.

Giovannoni, S.J., Rappé, M.S., 2000. Evolution, diversity, and molecular ecology of marine prokaryotes, in: Kirchman, D.L. (Ed.), Microbial Ecology of the Oceans. Wiley-Liss, New York, pp. 47-84.

Goldfine, H., 1972. Comparative Aspects of Bacterial Lipids. Advances in Microbial Physiology 8, 1-58.

Hagen, P.-O., Goldfine, H., Le B. Williams, P.J., 1966. Phospholipids of Bacteria with Extensive Intracytoplasmic Membranes. Science 151, 1543-1544.

Karl, D.M., 1979. Measurement of microbial activity and growth in the ocean by rates of stable ribonucleic acid synthesis. Applied and Environmental Microbiology 38, 850-860.

Karl, D.M., 2002. Hidden in a sea of microbes. Nature 415, 590-591.

Karl, D.M., Björkman, K.M., Dore, J.E., Fujieki, L., Hebel, D.V., Houlihan, T., Letelier, R.M., Tupas, L.M., 2001. Ecological nitrogen-to-phosphorus stoichiometry at station ALOHA. Deep-Sea Research II 48, 1529-1566.

Kates, M., 1964. Bacterial Lipids. Advances in Lipid Research 2, 17-90.

Kato, M., Sakai, M., Adachi, K., Ikemoto, H., Sano, H., 1996. Distribution of Betaine Lipids in Marine Algae. Phytochemistry 42, 1341-1345.

Kim, H.-Y., Wang, T.-C.L., Ma, Y.-C., 1994. Liquid chromatography/mass spectrometry of phospholipids using electrospray ionization. Analytical Chemistry 66, 3977-3982.

King, J.D., White, D.C., Taylor, C.W., 1977. Use of lipid composition and metabolism to examine structure and activity of estuarine detrital microflora. Applied and Environmental Microbiology 33, 1177-1183.

Kirchman, D., Ducklow, H., Mitchell, R., 1982. Estimates of Bacterial Growth from Changes in Uptake Rates and Biomass. Applied and Environmental Microbiology 44, 1296-1307.

Kirchman, D., K'nees, E., Hodson, R., 1985. Leucine Incorporation and Its Potential as a Measure of Protein Synthesis by Bacteria in Natural Aquatic Systems. Applied and Environmental Microbiology 1985, 3.

Kirchman, D.L., 1992. Incorporation of thymidine and leucine in the subarctic Pacific: application to estimating bacterial production. Marine Ecology Progress Series 82, 301-309.

Koivusalo, M., Haimi, P., Heikinheimo, L., Kostiainen, R., Somerharju, P., 2001. Quantitative determination of phospholipid compositions by ESI-MS: effects of acyl

chain length, unsaturation, and lipid concentration on instrument response. Journal of Lipid Research 42, 663-672.

Lebaron, P., Servais, P., Baudoux, A.-C., Bourrain, M., Courties, C., Parthuisot, N., 2002. Variations of bacterial-specific activity with cell size and nucleic acid content assessed by flow cytometry. Aquatic Microbial Ecology 28, 131-140.

Lomas, M.W., Burke, A.L., Lomas, D.A., Bell, D.W., Shen, C., Dyhrman, S.T., Ammerman, J.W., 2010. Sargasso Sea phosphorus biogeochemistry: an important role for dissolved organic phosphorus (DOP). Biogeosciences 7, 695-710.

Longnecker, K., Lomas, M.W., Van Mooy, B.A.S., 2010. Abundance and diversity of heterotrophic bacterial cells assimilating phosphate in the subtropical North Atlantic Ocean. Environmental Microbiology 12, 2773-2782.

Longnecker, K., Sherr, B.F., Sherr, E.B., 2005. Activity and Phylogenetic Diversity of Bacterial Cells with High and Low Nucleic Acid Content and Electron Transport System Activity in an Upwelling Ecosystem. Applied and Environmental Microbiology 71, 7737-7749.

Martin, P., Van Mooy, B.A.S., Heithoff, A., Dyhrman, S.T., 2011. Phosphorus supply drives rapid turnover of membrane phospholipids in the diatom Thalassiosira pseudonana. The ISME Journal 5, 1057-1060.

Mather, R.L., Reynolds, S.E., Wolff, G.A., Williams, R.G., Torres-Valdes, S., Woodward, E.M.S., Landolfi, A., Pan, X., Sanders, R., Achterberg, E.P., 2008. Phosphorus cycling in the North and South Atlantic Ocean subtropical gyres. Nature Geosciences 1, 439-443.

Minnikin, D.E., Abdolrahimzadeh, H., Baddiley, J., 1974. Replacement of acidic phospholipids by acidic glycolipids in Pseudomonas diminuta. Nature 249, 268.

Moore, J.K., Doney, S.C., Lindsay, K., 2004. Upper ocean ecosystem dynamics and iron cycling in a global three-dimensional model. Global Biogeochemical Cycles 18.

Moriarty, D.J.W., White, D.C., Wassenberg, T.J., 1985. A convenient method for measuring rates of phospholipid synthesis in seawater and sediments: its relevance to the determination of bacterial productivity and the distrubance artifacts introduced by measurements. Journal of Microbiological Methods 3, 321-330.

Moutin, T., Karl, D.M., Duhamel, S., Rimmelin, P., Raimbault, P., Van Mooy, B.A.S., Claustre, H., 2008. Phosphate availability and the ultimate control of new nitrogen input by nitrogen fixation in the tropical Pacific Ocean. Biogeosciences 5, 95-109.

Moutin, T., Raimbault, P., 2002. Primary production, carbon export and nutrients availability in western and eastern Mediterranean Sea in early summer 1996 (MINOS cruise). Journal of Marine Systems 33-34, 273-288.

Moutin, T., Thingstad, T.F., Van Wambeke, F., Marie, D., Raimbault, P., Slawyk, G., Claustre, H., 2002. Does competition for nanomolar phosphate supply explain the predominance of the cyanobacterium Synechococcus? Limnology and Oceanography 47, 1562-1567.

Oliver, J.D., Colwell, R.R., 1973. Extractable Lipids of Gram-Negative Marine Bacteria: Phospholipid Composition. Journal of Bacteriology 114, 897-908.

Perry, G.J., Volkman, J.K., Johns, R.B., 1979. Fatty acids of bacterial origin in contemporary marine sediments. Geochimica et Cosmochimica Acta 43, 1715-1725.

Pomeroy, L.R., 1974. The Ocean's Food Web, A Changing Paradigm. BioScience 24, 499-504.

Pujo-Pay, M., Conan, P., Oriol, L., Cornet-Barthaux, V., Falco, C., Ghiglione, J.-F., Goyet, C., Moutin, T., Prieur, L., 2011. Integrated survey of elemental stoichiometry (C,N,P) from the western to eastern Mediterranean Sea. Biogeosciences 8, 883-899.

Rappé, M.S., Connon, S.A., Vergin, K.L., Giovannoni, S.J., 2002. Cultivation of the ubiquitous SAR11 marine bacterioplankton clade. Nature 418, 630-633.

Rütters, H., Sass, H., Cypionka, H., Rullkötter, J., 2002. Phospholipid analysis as a tool to study complex microbial communities in marine sediments. Journal of Microbiological Methods 48, 149-160.

Schouten, S., Hopmans, E.C., Baas, M., Bourmann, H., Standfest, S., Könneke, M., Stahl, D.A., Sinninghe Damsté, J.S., 2008. Intact membrane lipids of "Candidatus Nitrosopumilus maritimus", a cultivated representative of the cosmopolitan mesophilic Group I Crenarachaeota. Applied and Environmental Microbiology 74, 2433-2440.

Schubotz, F., Wakeham, S.G., Lipp, J.S., Fredricks, H.F., Hinrichs, K.-U., 2009. Detection of microbial biomass by intact polar membrane lipid analysis in the water column and surface sediments of the Black Sea. Environmental Microbiology 11, 2720-2734.

Schwalbach, M.S., Tripp, H.J., Steindler, L., Smith, D.P., Giovannoni, S.J., 2010. The presence of the glycolysis operon in SAR11 genomes is positively correlated with ocean productivity. Environmental Microbiology 12, 490-500.

Shaw, N., 1974. Lipid composition as a guide to the classification of bacteria. Advances in Applied Microbiology 17, 63-108.

Simon, M., Azam, F., 1989. Protein content and protein synthesis rates of planktonic marine bacteria. Marine Ecology Progress Series 51, 201-213.

Smith, D.C., Azam, F., 1992. A simple, economical method for measuring bacterial protein synthesis rates in seawater using 3H-leucine. Marine Microbial Food Webs 6, 107-114.

Sturt, H.F., Summons, R.E., Smith, K., Elvert, M., Hinrichs, K.-U., 2004. Intact polar membrane lipids in prokaryotes and sediments deciphered by high-performance liquid chromatography/electrospray ionization multistage mass spectrometry--new biomarkers for biogeochemistry and microbial ecology. Rapid Communications in Mass Spectrometry 18, 617-628.

Suzumura, M., Ingall, E.D., 2001. Concentrations of lipid phosphorus and its abundance in dissolved and particulate organic phosphorus in coastal seawater. Marine Chemistry 75, 141-149.

Tanaka, T., Thingstad, T.F., Christaki, U., Colombet, J., Cornet-Barthaux, V., Courties, C., Grattenpache, J.-D., Lagaria, A., Nedoma, J., Oriol, L., Psarra, S., Pujo-Pay, M., Van Wambeke, F., 2011. Lack of P-limitation of phytoplankton and heterotrophic prokaryotes in surface waters of three anticyclonic eddies in the stratified Mediterranean Sea. Biogeosciences 8, 525-538.

Thingstad, T.F., Krom, M.D., Mantoura, R.F.C., Flaten, G.A.F., Groom, S., Herut, B., Kress, N., Law, C.S., Pasternak, A., Pitta, P., Psarra, S., Rassoulzadegan, F., Tanaka, T., Tselepides, A., Wassmann, P., Woodward, E.M.S., Riser, C.W., Zodiatis, G., Zohary, T., 2005. Nature of phosphorus limitation in the ultraoligotrophic eastern Mediterranean. Science 309, 1068-1071.

Van Mooy, B.A.S., Fredricks, H.F., 2010. Bacterial and eukaryotic intact polar lipids in the eastern subtropical South Pacific: Water-column distribution, planktonic sources, and fatty acid composition. Geochimica et Cosmochimica Acta 74, 6499-6516.

Van Mooy, B.A.S., Fredricks, H.F., Pedler, B.E., Dyhrman, S.T., Karl, D.M., Koblízek, M., Lomas, M.W., Mincer, T.J., Moore, L.R., Moutin, T., Rappé, M.S., Webb, E.A., 2009. Phytoplankton in the ocean substitute phospholipids in response to phosphorus scarcity. Nature 458, 69-72.

Van Mooy, B.A.S., Moutin, T., Duhamel, S., Rimmelin, P., Wambeke, F.V., 2008. Phospholipid synthesis rates in the eastern tropical South Pacific Ocean. Biogeosciences 5, 133-139.

Van Mooy, B.A.S., Rocap, G., Fredricks, H.F., Evans, C.T., Devol, A.H., 2006. Sulfolipids dramatically decrease phosphorus demand by picocyanobacteria in

oligotrophic environments. Proceedings of the National Academy of Sciences 103, 8607-8612.

Van Wambeke, F., Catala, P., Pujo-Pay, M., Lebaron, P., 2011. Vertical and longitudinal gradients in HNA-LNA cell abundances and cytometric characteristics in the Mediterranean Sea. Biogeosciences 8, 1853-1863.

Volkman, J.K., Barrett, S.M., Blackburn, S.I., Mansour, M.P., Sikes, E.L., Gelin, F., 1998. Microalgal biomarkers: A review of recent research developments. Organic Geochemistry 29, 1163-1179.

Wakeham, S.G., Hedges, J.I., Lee, C., Peterson, M.L., Hernes, P.J., 1997. Compositions and transport of lipid biomarkers through the water column surficial sediments of the equatorial Pacific Ocean. Deep-Sea Research II 44, 2131-2162.

White, D.C., Bobbie, R.J., Morrison, S.J., Oosterhof, D.K., Taylor, C.W., Meeter, D.A., 1977. Determination of Microbial Activity of Estuarine Detritus by Relative Rates of Lipid Biosynthesis. Limnology and Oceanography 22, 1089-1099.

White, D.C., Tucker, A.N., 1969. Phospholipid metabolism during bacterial growth. Journal of Lipid Research 10, 220-233.

Yoshinaga, M.Y., Sumida, P.Y.G., Wakeham, S.G., 2008. Lipid biomarkers in surface sediments from an unusual coastal upwelling area from the SW Atlantic Ocean. Organic Geochemistry 39, 1385-1399.

Figure 1

Membrane lipid bilayer

Schematic representation of a lipid bilayer forming a cell membrane. The green circle represent the hydrophilic lipid headgroups (shown in inset) that align themselves on the surface of the membrane, while the white squiggly lines represent hydrophobic fatty acid chains that orient towards the interior of the membrane. Illustration by Amy Caracappa-Qubeck, WHOI Graphics

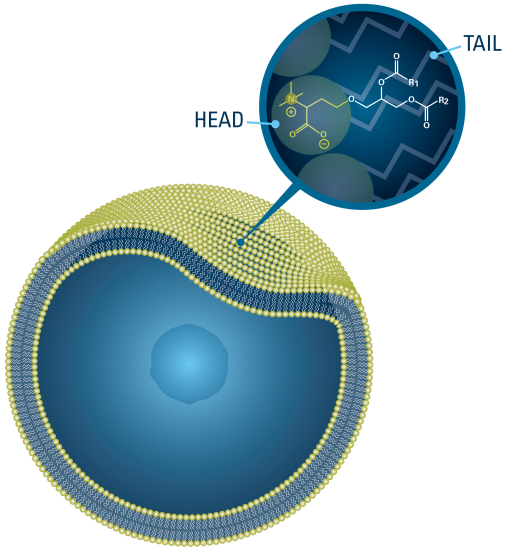

Figure 2

Major IP-DAG headgroup classes in marine microbes

The nine most common headgroup structures in marine bacterial and eukaryotic membranes. R1 and R2 represent fatty acid chains. Biogeochemically significant heteroatoms are highlighted, phosphorus (P) in orange, nitrogen (N) in blue, sulfur (S) in yellow.

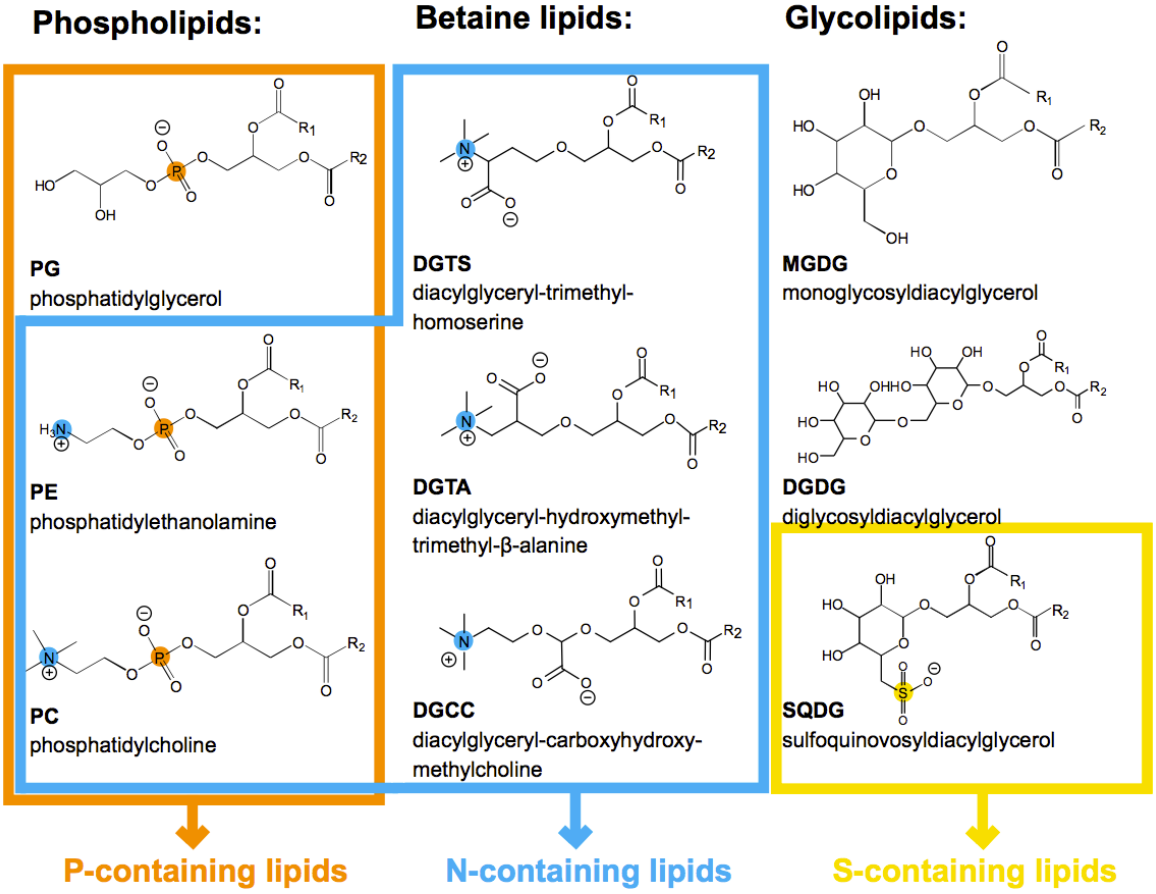

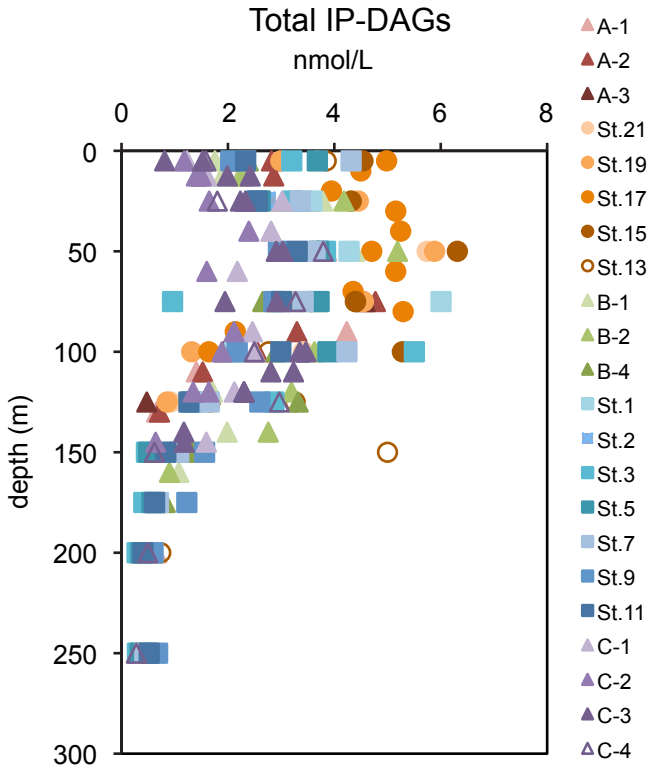

Figure 3

Representative depth profile of IP-DAG concentration in seawater

The sum of the nine most common headgroup classes of IP-DAGs in depth profiles in the upper 300 m of the water column. Profiles are from a transect across the Mediterranean Sea from the oligotrophic west (A-1, warm colored symbols) across a nutrient gradient to the ultraoligotrophic east (C-4, cool colored symbols). Concentration of individual IP-DAG classes reported in Popendorf et al., 2011b, Chapter 4.

Chapter 2

Molecular ion-independent quantitation of intact polar diacylglycerolipids in marine plankton using triple quadrupole mass spectrometry

Kimberly J. Popendorf, Helen F. Fredricks, Benjamin A.S. Van Mooy
Department of Marine Chemistry and Geochemistry, Woods Hole Oceanographic Institution, Woods Hole, MA

In review at *Lipids*

Abstract

Intact polar diacylglycerolipids (IP-DAG) are a diverse family of lipid molecules that form the bulk of bacterial and eukaryotic microbial membranes and have become the focus of a number of major research efforts. In a typical marine sample, there can be dozens of distinct species in each class of IP-DAG owing to the diversity of the two fatty acids contained within each IP-DAG. Current analytical approaches rely on laboriously quantifying the molecular ions of each of these species independently. Thus, we saw a need for a method for quantifying IP-DAG classes that was: i) selective for individual classes, ii) inclusive of all species within a class, iii) independent of foreknowledge of the molecular ions of the IP-DAG, and iv) amenable to automated, high-throughput data analysis methods. Our new HPLC-electrospray-ionization triple-quadrupole MS (HPLC-ESI-TQMS) method can be applied to quantify the nine major classes of IP-DAG in planktonic communities: the phospholipids phosphatidylglycerol (PG), phosphatidylethanolamine (PE), and phosphatidylcholine (PC); the glycolipids monoglycosyldiacylglycerol (MGDG), diglycosyldiacylglycerol (DGDG) and sulfoquinovosyldiacylglycerol (SQDG); and the betaine lipids diacylglyceryl trimethylhomoserine (DGTS), diacylglyceryl hydroxymethyltrimethyl-β-alanine (DGTA), and diacylglyceryl carboxyhydroxymethylcholine (DGCC). The analyses rely on neutral fragment and parent ion scan events that yield one chromatogram for each class of IP-DAG, simplifying downstream analysis and increasing sample throughput. Limits of detection for the IP-DAG classes ranged from 5 to 160 pmol on column, with at least one decade of linear response for all classes. The efficacy of the method was demonstrated by analyzing plankton community samples from a variety of marine environments.

1. Introduction

Intact polar diacylglycerols (IP-DAGs) are a diverse family of lipid molecules that dominate the cell membranes of bacterial and eukaryotic microbes. These microbes constitute the majority of biomass in the surface ocean (Cho and Azam, 1990), and, accordingly, IP-DAGs are the most abundant family of lipid molecules in the sea (Van Mooy and Fredricks, 2010) . IP-DAGs play a major role in the modern marine carbon cycle, and are an important molecular provenance for petroleum deposits in marine sedimentary basins. However, until very recently, IP-DAG molecular diversity was poorly understood; while measurements of the constituent fatty acids of IP-DAGs in marine environments have been made for decades (Farrington and Quinn, 1971; Wakeham and Canuel, 1988), the analytical procedures used to measure fatty acids do not distinguish between fatty acids derived from different IP-DAG classes.

Led by advances in high performance liquid chromatography/electrospray ionization ion-trap mass spectrometry (HPLC-ESI-ITMS) methods (Rütters et al., 2002; Sturt et al., 2004) we have established that IP-DAGs in the upper ocean are dominated by glycolipids, phospholipids, sulfolipids and betaine lipids (Popendorf et al., 2011b; Schubotz et al., 2009; Van Mooy and Fredricks, 2010; Van Mooy et al., 2009; Van Mooy et al., 2006) (SM Figure 1) . Phospholipids from marine microbes have been well studied (Oliver and Colwell, 1973; Suzumura and Ingall, 2001; Van Mooy et al., 2008; White, 1988), however the latter two classes of molecules, sulfolipids and betaine lipids, were largely unknown to chemical oceanography until recently (Schubotz et al., 2009; Van Mooy and Fredricks, 2010; Van Mooy et al., 2009; Van Mooy et al., 2006), and appear to be significantly more abundant in the surface ocean than phospholipids (Brandsma et al., 2012; Popendorf et al., 2011b; Schubotz et al., 2009; Van Mooy and Fredricks, 2010). In addition, sulfolipids and betaine lipids have shown utility as indicators of nutrient stress and stoichiometric flexibility (Bellinger and Van Mooy, 2012; Martin et al., 2011; Popendorf et al., 2011b; Van Mooy et al., 2009; Van Mooy et al., 2006). Quantification of IP-DAGs at the class level is of particular interest, as the heteroatoms that distinguish

headgroup classes (e.g. P and N) are often in short supply in the marine environment (Moore et al., 2004), and thus the abundance and distribution of these classes is both biogeochemically and physiologically significant. Given the biogeochemical and physiological significance of IP-DAGs, and the relative lack of information about the most abundant classes, there is clearly a need to identify and quantify IP-DAGs in the upper ocean.

Using HPLC-ESI-ITMS we have found that nearly all IP-DAG molecular diversity in the upper ocean can be accounted for by three classes of phospholipids, phosphatidylglycerol (PG), phosphatidylethanolamine (PE), and phosphatidylcholine (PC); three classes of betaine lipids diacylglyceryl trimethylhomoserine (DGTS), diacylglyceryl hydroxymethyltrimethyl-β-alanine (DGTA), and diacylglyceryl carboxyhydroxymethylcholine (DGCC); and three classes of glycolipids, monoglycosyldiacylglycerol (MGDG), diglycosyldiacylglycerol (DGDG) and sulfoquinovosyldiacylglycerol (SQDG) (SM Figure 1) (Van Mooy and Fredricks, 2010). Due to the diversity of fatty acids there are often more than a dozen distinct IP-DAG molecular species within each class (e.g. PG species with 16:0/16:1 fatty acids, 16:0/18:2 fatty acids, etc.) (Schubotz et al., 2009; Van Mooy and Fredricks, 2010). In a typical planktonic community sample from the upper ocean, these nine classes often encompass more than one hundred individual species.

Quantifying IP-DAGs with the original HPLC-ESI-ITMS method developed by one of us (Fredricks, née Sturt), in collaboration with a different research group, depended on collecting molecular ion chromatograms and integrating peak areas for individual IP-DAG species (Sturt et al., 2004). In samples collected from natural planktonic communities, this meant integrating a large number of molecular ion chromatograms for each sample (in many cases more than one hundred) and binning the quantitative results into the nine IP-DAG classes. This data analysis was time consuming, often many hours per sample, and represented a significant barrier to our analytical throughput. In addition, samples within a sample set often contained different molecular species of each class of IP-DAG, and thus a peak in any unfamiliar molecular

ion chromatogram demanded collection and inspection of MS^2 and MS^3 spectra for definitive identification. Even so, isobaric IP-DAG from different classes that elute near each other (e.g. PG with 16:0/18:2 vs. DGTS with 18:1/18:1, both m/z 764) often proved difficult to resolve in practice, and could contribute to the over or underestimation of IP-DAG class abundance. Thus, we saw a need for a method for simultaneously quantifying all species in each IP-DAG class, rather than quantifying each molecular ion separately and assigning it to an IP-DAG class.

In the ESI-ITMS method we identified molecular ions for each IP-DAG class in post-run analysis, based on retention time and the characteristic fragmentation of the different lipid headgroups. Rather than identifying these molecular ions in post-run analysis and manually integrating chromatograms for each molecular ion, this paper introduces a new method wherein these diagnostic fragmentation patterns can instead be used to define MS scans that will automatically identify all of the molecular ions associated with a particular IP-DAG class. The output of each scan will then be a single chromatogram of all molecular ions that matched the fragmentation pattern for a particular IP-DAG class. Integration of this single chromatogram will then be sufficient to quantify the IP-DAG class. Additionally, mass spectra across this chromatogram will identify the molecular ions present in the IP-DAG class, and can be used to compare the relative abundance of individual species across different samples.

We have developed a method for IP-DAG analysis using high performance liquid chromatography / electrospray ionization triple quadrupole mass spectrometry (HPLC-ESI-TQMS) that is quantitative and sensitive enough to measure IP-DAG in relatively small volumes of seawater (i.e. 10s of mL). The overarching philosophy is to monitor and quantify chromatograms based on a MS fragmentation pattern that is i) diagnostic for each IP-DAG class and ii) inclusive of all species within that class of IP-DAG. The versatility of the triple quadrupole mass spectrometer allows us to acquire data in two modes that satisfy these criteria, parent ion scans and neutral fragment scans. A parent ion scan involves scanning quadrupole 1 (Q1) within a fixed range (encompassing all reasonable molecular species within an IP-DAG class) whilst quadrupole 3 (Q3) stays

fixed at a particular product ion m/z value. A neutral fragment scan involves scanning both Q1 and Q3 at a precise, fixed m/z difference, where the offset is equal to the mass of a neutral fragment corresponding to the loss of the polar headgroup from an IP-DAG class. The 9 IP-DAG analytes we target show either a diagnostic product ion or neutral loss that is derived from the polar headgroup and as such is independent of the fatty acid moieties (Table 1).

This approach obviates the need for any foreknowledge of the fatty acids and thus the m/z of molecular ions for the quantification of IP-DAG classes. Quantifying IP-DAG classes through the integration of a single chromatogram drastically shortens the data analysis time and increases sample throughput, making it possible to quantify IP-DAGs from the environment with high spatial or temporal resolution.

2. Materials and Methods

2.1 Standards

Synthetic dipalmitoyl-PE, -PG, -PC and –DNP-PE (dinitrophenyl-phosphatidylethanolamine) were purchased from Avanti Polar Lipids, Inc. (Alabaster, AL). Purified natural MGDG and DGDG were purchased from Matreya LLC (Pleasant Gap, PA) or Sigma-Aldrich (St. Louis, MO). Purified natural SQDG was purchased from Lipid Products (South Nutfield, UK). None of the betaine lipids were available commercially, so batch cultures of several diatoms were grown and DGCC and DGTA were isolated and purified by preparative HPLC in-house. DGCC was isolated from *Thalassiosira pseudonana* and DGTA from *Chaetoceros affinis*. Structure and purity were confirmed by NMR (DGCC) and LCMS (DGCC and DGTA). The mass of DGCC and DGTA was confirmed by GC-FID of the fatty acid methyl esters (FAME) obtained after hydrolysis of the lipids with methanolic HCl (0.1M, heat @ 70 °C for 1 hour). Calibration curves of relevant FAME were constructed from dilutions of a mixed FAME standard (#47885-U, Sigma-Aldrich) that spanned the expected range microbial acyl chain lengths and a diversity of unsaturations. We have yet to obtain DGTS as a pure

standard. Since DGTS and DGTA are structural isomers (see Supplemental Material Fig. 1), it might be expected that the MS response factor for DGTA and DGTS are similar to one another. We have observed, however, that the response on the TQMS is less sensitive to DGTA than to DGTS, which we expect is due mostly to lower fragmentation efficiency for DGTA. While an authentic standard of DGTS is unavailable, we have calculated a response factor for DGTS using comparison of our DGTA standard and representative oceanic samples containing both DGTS and DGTA on the ion trap and triple quadrupole MS systems. This quantification should be re-evaluated when an authentic DGTS standard is available.

A mixed calibration standard was prepared to a final concentration of 16 μmol L^{-1} of each IP-DAG in 9:1 dichloromethane : methanol. Serial dilutions were prepared from 8 μmol L^{-1} to 30 nmol L^{-1} to cover the full dynamic range of all the lipid components. Internal recovery standard (dipalmitoyl-DNP-PE) was added to the initial 8 μmol L^{-1} mixed standard and subsequently diluted with the calibration standards to give a DNP-PE calibration curve by which the recovery of DNP-PE from samples could be calculated. A series of calibration standards (all 20 μL injections, see below), with DNP-PE, were run at the beginning of each batch of samples, and quality control standards (1 μmol L^{-1} final concentration) were run every 5 to 10 samples.

2.2 Sample collection and extraction

Plankton community samples were obtained in the South Atlantic Ocean and the Mediterranean Sea. One or two liter seawater samples were collected using a Niskin bottle mounted on a CTD rosette, and transferred to an acid-washed polycarbonate bottle for immediate filtration. Water was filtered through a 47 mm 0.2 μm poresize Durapore hydrophilic membrane filter (Whatman) using light vacuum (<200 mmHg). Filters were folded in half (sample-side in), wrapped in combusted aluminum foil, and stored in liquid nitrogen until extraction. Total lipids were extracted from each filter using a modified Bligh & Dyer method (Bligh and Dyer, 1959) by adding the sample filter, 2 mL methanol, 1 mL dichloromethane and 0.8 mL phosphate buffered saline (137 mmol L^{-1}

sodium chloride, 2.7 mmol L^{-1} potassium chloride, 11.9 mmol L^{-1} phosphate, pH = 7.4; Fisher Scientific) to a 12 mL glass centrifuge tube. After adding solvents, the internal recovery standard was added as 20 μL of 65.6 μmol L^{-1} DNP-PE in methanol. After disrupting the cells for 10 minutes in an ultrasonic bath, an additional 1 mL of dichloromethane and 1 mL phosphate buffer were added. The samples were then centrifuged for 5 min at 515 x *g*. The lower organic phase was transferred from the centrifuge tube to a 2 mL HPLC vial (2 mL screw cap borosilicate glass, Agilent) using a combusted glass pipette, and concentrated to 200 μL by drying under nitrogen. For analysis, 20 μL of this total lipid extract (equivalent to approximately 10% of the initial seawater sample) was injected on the HPLC-MS, yielding individual IP-DAG class concentrations on the order of 10-100 pmol on column.

We had observed that sensitivity could be improved for low concentrations of IP-DAG standards by adding a carrier compound to the HPLC vials prior to addition of IP-DAG. We experimented with a variety of molecules including tocopherol, butylated hydroxy toluene (BHT), dipalmitoyl-PC, and a mix of distearic-, stearic/palmitoyl-MGDG. Based on the observed increase in sensitivity at low IP-DAG concentrations, as well as its antioxidant properties, BHT was selected as a carrier compound. To each HPLC vial, 10 μL of a 1.5 mmol L^{-1} solution of BHT in methanol was added prior to addition of samples or IP-DAG standards. All samples were capped with argon to further limit oxidation and sample degradation, and were stored at -80º C until analysis. We have observed that under these conditions IP-DAG samples are stable for long periods of time, up to several years.

2.3 Chromatographic conditions

Chromatographic separation was performed on an Agilent 1200 HPLC system (Agilent Technologies) consisting of a binary pump, autosampler (with sample tray cooled to 4 °C), a column compartment at room temperature, and a photodiode-array detector (Thermo Finnigan), which then leads into the TQMS. A LiChrospher diol column (150 mm x 2.1 mm i.d., 100 Å, 5 μm packing material, Alltech) was used with a

gradient of 100% A to 50% B in 22.5 minutes with 7.5 minutes equilibration time. The flow rate was 0.4 mL min^{-1} for the first 25 minutes then 1 mL min^{-1} for 5 minutes for rapid column equilibration. Eluents were as follows (by volume): eluent A = 790:200:1.2:0.4 n-hexane: isopropanol: formic acid: 25% aqueous ammonium hydroxide; eluent B = 880:100:1.2:0.4 isopropanol: water: formic acid: 25% aqueous ammonium hydroxide. The photodiode-array was programmed to collect full scan data (200-800 nm) and also a single channel at 340 nm which is the wavelength of maximum absorption of the internal recovery standard DNP-PE. Eluents were made from LC/MS or GC Resolv grade solvents, formic acid and aqueous ammonium hydroxide from Fisher Scientific.

2.4 Mass spectrometry conditions

Mass spectrometry was performed on a Thermo TSQ Vantage TQMS operating in positive ionization mode with a heated electrospray source. Nitrogen was used for the sheath and auxiliary gas, argon was used in the collision cell. Source parameters were as follows: spray voltage 3 kV, vaporizer 100 °C, sheath gas pressure 30, auxiliary gas pressure 5 (gas pressures given in arbitrary units, approximate to psi), capillary 200 °C. The 'S-lens' values and collision energies for each lipid class were determined while directly infusing the relevant lipid (~2-8 nM in 9:1 DCM:MeOH) in an an isocratic mixture of eluents A and B.

The TSQ Vantage uses an 'S-lens' and exit lens rather than the more common tube lens and skimmer to optimize transport of the ions from the source into the ion optics. The S-lens is somewhat mass-selective, the radio-frequency amplitude of the S-lens is increased from 0 to a maximum of 300 to optimize passage of ions with increasing m/z ratios, with the amplitude set to plateau slightly in the IP-DAG m/z scan range, going from 136 at 600 m/z to 220 at 1000 m/z.

2.5 Quantification using parent ion and neutral fragment scans

The 9 classes of IP-DAG were quantified in a single analytical run where the TQMS cycles through constant neutral fragment scan and parent ion scan events that

effectively capture the molecular diversity of species in each IP-DAG class (Table 1). In contrast, the internal recovery standard, DNP-PE, is a single species (dipalmitoyl) and thus was quantified using selected reaction monitoring (SRM, the dipalmitoyl DNP-PE transition is 875.6 to 551.5 i.e. loss of the DNP-PE headgroup to give a diglyceride-type product ion). For the internal standard this SRM scan is also useful because it affords enhanced sensitivity, enabling detection to very low levels. Details of the scan events are given in Table 1. Collision gas pressure for all scan events was 1.0 mTorr. Neutral fragment scan ranges were kept as narrow as possible without excluding possible IP-DAG species to ensure that scan times were kept to a reasonable 0.5 s each. Parent ion scan times could be shorter at 0.1 s, and the SRM scan time for DNP-PE was 0.05 s. Peak width (FWHM) was set to 0.70 for both Q1 and Q3. Throughout the analytical run the TQMS continuously cycled through these nine scan events.

Each scan event produces a total ion current chromatogram for an IP-DAG class (Figure 4). The scan event is selective for a diagnostic fragmentation that is common to all species of a given IP-DAG class, therefore the peak area of each chromatogram represents the sum of the abundance of all molecular species within an IP-DAG class. Peaks were automatically integrated and manually verified (using QuanBrowser software in the Xcalibur package from Thermo Fisher Scientific). In the case of DGTS and DGTA, both classes are monitored in a single scan event, production of 236 m/z fragment, but the classes are chromatographically resolved and thus their peak areas can be integrated separately.

The response factor for each IP-DAG class was measured from standard curves of authentic standards, using a linear regression of pmol IP-DAG on column versus peak area (Figure 1). This response factor was used to convert the integrated peak area for each IP-DAG class in a sample to pmol IP-DAG on column. The abundance of the internal standard (DNP-PE) in each sample was similarly calculated using an external standard curve. Comparison of the amount of DNP-PE measured on column to the known amount added to the TLE was used to calculate the fraction of total sample measured on column, and thus calculate pmol IP-DAG per sample.

2. 6 Method adaptation to new chromatographic conditions

Since our method was developed, the commercial availability of the LiChrospher diol column has become undependable. The data presented here was collected using a LiChrospher diol column, however, as future investigators may not be able to acquire this material, we present an alternative. After extensive column exploration, PrincetonSpher diol packing material (Princeton Chromatography Inc., Cranbury, NJ) was found to have improved retention properties and we have adapted our chromatography methods to this column material. Minor modifications to the chromatography method were required as follows: a PrincetonSpher diol column (150 mm x 2.1 mm i.d., 100 Å, 5 μm packing material) was used with a gradient of 100% A to 52% B in 20 minutes, then to 71.5% B over 5 minutes, then held for 10 minutes at 71.5% B, followed by 10 minutes equilibration time at 100% A. The flow rate was 0.4 mL min^{-1} for the first 40 minutes then 1 mL min^{-1} for 5 minutes for rapid column equilibration. Eluents were as follows (by volume): eluent A = 800:200:1.0:0.4 n-hexane: isopropanol: formic acid: 25% aqueous ammonium hydroxide; eluent B = 900:100:1.0:0.4 isopropanol: water: formic acid: 25% aqueous ammonium hydroxide. These modifications have no impact on TQMS method performance.

3. Results and Discussion

3.1 Range of IP-DAG quantification using TQMS

All eight of our authentic IP-DAG calibration standards, as well as our internal recovery standard DNP-PE, demonstrated greater than one decade of continuous linear response (Figure 1). The response factor for each IP-DAG (peak area (pmol on column)$^{-1}$) is dependent on both its ionization efficiency in the ESI source and its fragmentation efficiency in the TQMS. The lower limit of quantification is defined by the smallest quantity of analyte on column for which the prediction intervals (similar to 95% confidence intervals) of the standard curve exceed "zero" peak area (Figure 1). The

upper limit of quantification is controlled largely by column loading capacity, chromatographic peak shapes deteriorate significantly at loading > 1 nmol on column. At higher IP-DAG concentrations, dimer formation may also become a more significant factor for instrument response. Each of the phospholipid classes exhibited a linear response across a range of 5-160 pmol on column. Variation in response was greater across the glycolipid classes. For MGDG, the limit of quantification was approximately 2.5 pmol on column, and the response was linear up to 80 pmol on column. At higher concentrations the response is continuous but nonlinear—MGDG is the least retained on the diol phase, and as such is most prone to column overloading at high concentrations. Relative to MGDG, the MS response was less sensitive for both DGDG and SQDG, but although the limit of quantification was higher, 20 and 10 pmol on column respectively, the response was linear to 160 pmol on column. Betaine lipids had a low limit of quantification, less than 5 pmol on column for both DGTA and DGCC. For DGTA the response was linear to 140 pmol on column, while for DGCC the linear range is slightly smaller to 55 pmol on column. Our internal recovery standard, DNP-PE, was measured by selected reaction monitoring, and the greater sensitivity afforded by this scan type enables quantification below 1 pmol on column. The response for DNP-PE is linear across two decades, up to 160 pmol on column. The lower limits of quantification for most IP-DAG classes are roughly half the molar amounts of our previous method using HPLC-ESI-ITMS and quantification of molecular ions (Van Mooy and Fredricks, 2010). Recent applications of HPLC-ESI-TQMS using molecular ion quantification may be even more sensitive (Brandsma et al., 2012); this demonstrates the trade-off in sensitivity for enhanced throughput and ease of data analysis.

Fortuitously, in the ocean the range in concentration of IP-DAG is relatively small, spanning approximately one order of magnitude on the order of hundreds to thousands of pmol L^{-1}. We have developed our lipid extraction procedures so that the range in sample concentrations generally falls within the range of linear response on the instrument, on the order of 10-100 pmol on column. This enables quantification of environmental IP-DAG concentrations using a single analytical run in most cases. On

occasion samples may need to be diluted to allow MGDG quantification, which is detected non-linearly at high concentrations and is generally relatively abundant in plankton communities.

3.2 Inclusiveness of scans for different species within a single class of IP-DAG

Although our method targets fragmentation patterns common to all IP-DAG species within a class, individual species of IP-DAG are defined by their variable fatty acids moieties, which introduces the possibility that the TQMS response within an IP-DAG class might vary as a function of fatty acid composition (Koivusalo et al., 2001). In a natural planktonic community, the fatty acid composition ranges from chain lengths of 14 to 24 carbons and unsaturations ranging from none to six, yielding IP-DAG molecular species with diacyl moiety carbon atoms ranging from 28 to 44, and acyl double bonds ranging from none to 12 (Van Mooy and Fredricks, 2010). We examined the relative response of a short-chain, fully saturated species (dipalmitoyl, 16:0) and a species with a long-chain, unsaturated fatty acid (palmitoyl/arachidonic, 16:0/20:4) for three classes of phospholipids (Figure 2). We found that the response of the saturated and unsaturated versions of PG and PC were slightly different, but only by about 20% (PG: slope of linear regression = 1.213, $R^2 = 0.998$, n = 18, $p < 0.001$; PC: slope of linear regression = 0.831, $R^2 = 0.995$, n=18, $p < 0.001$)). Until such time that standards are available for each of the one hundred or more IP-DAG species encountered in marine environments, inaccuracies of 20% will need to be tolerated; an alternative would be to model the relationship between response and fatty acid composition, but uncertainties in these models might not be substantially less than 20%. Clearly, caution is warranted in making oceanographic interpretations that hinge critically on the absolute concentrations of IP-DAG in marine environments.

Our analysis of PG and PC provide some assurances about the expected response of other IP-DAG classes, because the ionization and fragmentation of PG and PC are common to all of the glycolipids and betaine lipids respectively. PG forms an adduct with ammonium in positive ion mode ($[M+NH_4]^+$), and its diagnostic fragmentation is

loss of the neutral headgroup. These traits are shared by all three classes of glycolipids (MGDG, DGDG and SQDG; see Table 1), and it is thus reasonable to expect that the variation in response for the individual species of glycolipid would be captured by variation in PG response. Similarly, PC and all three classes of betaine lipid (DGTS, DGTA, DGCC) form an $[M]^+$ ion and their diagnostic fragmentation is production of a characteristic positive headgroup ion. In the case of betaine lipids and PC, because the charge on the parent ion is on the headgroup, as opposed to an adduct associated with the diacyl moiety, it might be expected that the MS response of these classes would be least impacted by variation in the fatty acid composition. Indeed we found that PC exhibits the least difference in response between the short-chain saturated and long-chain unsaturated species.

In contrast to PG and PC, PE has a unique ionization and fragmentation scheme, forming an $[M+H]^+$ ion that yields a diagnostic constant neutral fragment. This class of phospholipid exhibited the largest variation in response with different molecular species, a linear regression of saturated versus unsaturated species response estimated the variation to be more than 35% (regressing saturated against unsaturated peak area, the slope was 0.631, R^2=0.999, n=18, p<0.001). Given the unique ionization and fragmentation of PE we posit that PE provides less insight on the potential errors from fatty acid diversity in other IP-DAG classes. Nonetheless, even greater caution is warranted in the treatment of PE concentration data.

3.3 Comparison of quantification using ITMS and TQMS

IP-DAGs were quantified in three samples of South Atlantic surface seawater to compare the absolute concentrations calculated using the previously established ITMS method (Sturt et al., 2004; Van Mooy and Fredricks, 2010) and the TQMS method described in this paper (Figure 3, Table 2). The three samples analyzed spanned a wide geographic range across the South Atlantic, from the Benguela upwelling region west of Africa, across the western flank of the Mid-Atlantic Ridge, to the waters off the continental shelf of Uruguay. Given the diverse locations of these samples it is

unsurprising that the relative distribution of IP-DAGs varied across the three samples (Figure 3). IP-DAG concentrations calculated by the two methods were of the same order of magnitude for all six IP-DAG classes analyzed in all three samples, and were similar to published IP-DAG concentrations from other marine samples (Brandsma et al., 2012; Popendorf et al., 2011b; Van Mooy and Fredricks, 2010). Both methods found similar relative distributions of IP-DAGs in each sample, with phospholipids being relatively abundant in the Benguela upwelling sample, all IP-DAGs being at relatively low concentrations in the Mid-Atlantic sample, and glycolipids being relatively abundant in the Uruguayan coast (Figure 3).

The ratio of the IP-DAG concentration from the TQMS method versus the ITMS method (Table 2) across the three samples indicated that the different quantification methods may have some systematic bias for the quantification of some IP-DAG classes. Some of this bias can be explained by the different ways in which these molecules are detected in the two MS systems, and some by the way in which the chromatograms are integrated. In the ITMS method, the first step in quantification is to manually identify all of the dominant molecular ions in each IP-DAG class, using comparison to retention time of standards and MS^2 fragmentation data available for the most abundant base peak ions in each MS scan. Having identified the molecular ions of interest, base peak chromatograms are extracted for each molecular ion and peak areas integrated in each chromatogram. The list of molecular ions in Table 3 represents the individual base peak chromatograms that were integrated to quantify the IP-DAGs in these three samples (92 chromatograms in total, averaging 10 chromatograms per IP-DAG class). For each IP-DAG class, the peak areas of the relevant chromatograms are then summed (anywhere from 1 chromatogram for DGCC in the Benguela upwelling sample to 18 chromatograms for PE in the same sample, Table 3) to give the total IP-DAG class peak area. Response factors from standard curves (in which each IP-DAG class was represented by at most three molecular species in the authentic standards available) are then used to calculate IP-DAG concentration from these peak areas.

In contrast, for the TQMS method, each scan event produces one chromatogram (Figure 4), and this single chromatogram represents the abundance of all molecular ions whose fragmentation pattern matched that of a particular headgroup class. This single chromatogram is then integrated, and this peak area is compared to the peak area of standard curves (also one chromatogram per IP-DAG class) to calculate IP-DAG concentration. The summation of multiple chromatograms using the ITMS method may be contributing error in the calculation of IP-DAG concentrations. This is likely particularly true for IP-DAG classes that have many molecular ions all at low concentrations, such as DGDG, where each integrated peak has a relatively low signal to noise ratio and thus integration of each smoothed peak adds some amount of error. For DGDG, which is generally at low concentrations in the ocean (Table 4; Van Mooy and Fredricks, 2010; Popendorf et al. 2011b) the summation of seven chromatograms in the ITMS method seems to lead to highly variable results relative to the TQMS method. Given the low signal to noise of the peaks being integrated at these low concentrations it is likely that the single chromatogram integration in the TQMS method is most accurate.

The largest, most consistent systematic difference observed between the ITMS and TQMS methods was for MGDG, where the ITMS method gave MGDG concentrations that ranged from 20% to four-fold greater than TQMS concentrations. Using the diol column and normal phase chromatography (the same chromatography conditions for both MS methods), MGDG is the least retained of all the IP-DAG classes and generally has the widest, least Gaussian peak (Figure 4; Popendorf et al., 2011a). Peak smoothing is generally applied to the chromatograms from both MS methods prior integration, and it is possible that this smoothing of the wide, non-Gaussian peak for MGDG contributes to error in its calculation, again exacerbated by the summation of many chromatograms in the ITMS method (from 9 to 12 separate chromatograms for these samples). For both MGDG and DGDG, potential error in the ITMS quantification method likely stems from the summation of many chromatogram integrations, each of which contributes error. The absolute quantification of these glycolipids using ITMS could be further investigated using authentic standards with a diverse range of diacyl

moieties, so that the peak areas of the standard curves represent the summation of many chromatograms, each of a molecular ion with a known concentration.

The concentration of SQDG was systematically higher using the TQMS method (with difference ranging from 30% to two-fold greater). In this case the higher concentrations are likely due to the ability of the TQMS method to detect SQDG molecular ions that are co-eluting with other IP-DAG classes such as DGDG and DGCC (see Popendorf et al., 2011a for a representative chromatogram). Because the shoulders of the SQDG peak frequently co-elutes with DGDG and DGCC it is often difficult to distinguish the molecular ions in the ITMS method and we are thus likely missing or mis-assigning some of these molecular ion chromatograms and underestimating SQDG with the ITMS method.

The concentration of PC was also found to be systematically higher using the TQMS method (with differences between TQMS and ITMS ranging from 20 to 60%). In the TQMS method PC is detected using a parent ion scan, whereas the glycolipids and other phospholipids are detected using constant neutral fragment scans. Both of these scan types rely on fragmentation of the headgroup from the diacyl moiety, and the characteristic mass of this headgroup for the IP-DAG class of interest. The difference between these scan types is that for PC this fragmented headgroup is a charged ion, 184 m/z, and the abundance of this ion is measured in Q3, whereas for the other phospholipids and glycolipids this headgroup fragment is neutral and thus we rely on the detection of the intact diacyl moiety ion in Q3. By the nature of the relatively weak bond between the headgroup and the diacyl moieties, any fragmentation of the IP-DAGs is likely to produce headgroup fragments, which will be detected for PC, but only a fraction of the molecules that fragment will produce intact diacyl moieties, which will be detected by the constant neutral loss scans. Thus the parent ion scan used to quantify PC is more sensitive than the neutral fragment scans used to detect the glycolipids and the other phospholipids (note the 1-3 orders of magnitude greater peak areas for PC compared these other classes in Figure 1, as well as the higher peak areas for the betaine lipids also detected by parent ion scan). The detection of PC using production of the 184 m/z ion

should be specific for PC, and thus we expect quantification of PC using the TQMS method to be relatively accurate. According to the sensitivities of the scan types, the lower concentrations of PG and PE measured by the TQMS method versus the ITMS method may reflect underestimation of the true abundance of these molecules using the TQMS method, however these differences are not large enough to warrant significant concern relative to other sources of error and natural variability across samples.

For all IP-DAG classes the difference in absolute concentration was much less than an order of magnitude between the ITMS and TQMS quantification methods. Furthermore, with the exception of MGDG, quantification with either method would have led to the same representation of relative abundances for the different classes in these three samples (Figure 3), and the same broad conclusions about IP-DAGs in the environment would have been drawn. Thus we are confident that quantifying IP-DAGs using the TQMS method will give results that are comparable to the previously established ITMS method, and for many IP-DAG classes may be more accurate.

3.4 Diagnostic TQMS chromatograms for IP-DAGs in a natural planktonic community

We validated our HPLC-ESI-TQMS method with planktonic community samples from the Mediterranean Sea (Figure 4) (Popendorf et al., 2011b). As is typical of oligotrophic marine environments, phosphate concentrations in the Mediterranean Sea were < 40 nmol L^{-1} (Table 4). All nine IP-DAG classes were readily detected and peak shapes were remarkably Gaussian (Figure 4), especially considering that each IP-DAG peak is an amalgamation of a number of distinct species defined by variations in fatty acid composition. In some IP-DAG classes in our Mediterranean Sea sample, such as SQDG, the variety of molecular species was relatively limited (Figure 4); this observation agrees well with the data we collected using our HPLC-ESI-ITMS method from planktonic communities in the South Pacific (Van Mooy and Fredricks, 2010) and South Atlantic (Table 3), which also showed a limited diversity of SQDG molecules. However, in other IP-DAG classes, such as PE, the composition of fatty acids was extremely diverse and unexpected; the 662 m/z ion representing the diglyceride moiety

C30:1 (likely 14:0/16:1 fatty acids) was not observed in the South Pacific (Van Mooy and Fredricks, 2010). Other differences exist between the Mediterranean and South Atlantic samples, such as the abundance of the 908 m/z ion in DGDG (representing the diglyceride moiety C32:1) in the Mediterranean sample (Figure 4) and its absence in the South Atlantic samples (Table 3). The observed differences between our Mediterranean Sea sample (Figure 4), the South Atlantic samples (Table 3), and the South Pacific samples (Van Mooy and Fredricks, 2010) underscore the importance of a method that assumes no prior knowledge of the species present. Using an SRM approach would require a method containing over one hundred transitions to capture the majority of the IP-DAG signal present in this single Mediterranean Sea sample, and approximately 1,000 transitions to be inclusive of all potential fatty acid combinations (C14 to C24) that could be present across an oceanic transect.

Using our TQMS method we have analyzed IP-DAGs in depth profiles from transects across the Mediterranean Sea and the South Atlantic Ocean, revealing distinct patterns of lipid abundance. More than 100 IP-DAG samples were analyzed from each of these transects, providing a level of spatial and depth resolution that would have been impractical with the previous ITMS method. IP-DAG concentrations are presented in fifteen representative samples from six different locations, spanning the geographic range of each cruise transect and depths from 5 m to 175 m (Table 4).

In the Mediterranean Sea, there was an increase in total lipids at the deep chlorophyll maximum (DCM) relative to the surface, due to an increase in phospholipid and glycolipid concentrations (despite the decrease in betaine lipid concentration). This trend was more prominent in the west (Sicilian channel and Ionian basin) than in the east (Levantine basin). In contrast, in the South Atlantic Ocean total lipid concentrations were higher at the surface than at the DCM in all three locations. The gradients in these IP-DAG concentrations can be studied in relation to gradients in other biogeochemical parameters, and can potentially provide insight into the nutrient availability or nutrient stress experienced by plankton across diverse environments (Popendorf et al., 2011b). The increased ability to reliably and efficiently quantify IP-DAGs provided by this

method opens new possibilities for high spatial and temporal resolution sampling of these important molecules.

3.5 Application to other environmental settings

The analytical efficiency of this TQMS method makes it possible to quantify IP-DAGs in large numbers of samples from depth profiles, across environmental gradients, or at frequent timepoints in incubations or timeseries. With the previous ITMS method such large sample numbers would have been analytically impractical. While this TQMS method does not require identification or knowledge of the molecular ions, it is limited to detecting the IP-DAG classes defined by the MS scans (Table 1). Thus the TQMS method outlined here is most applicable for environments or cultures where other methods have been applied to verify the environmental significance of the IP-DAG classes being detected. For this method to be used to quantify total lipids in a sample, it must first be demonstrated that the IP-DAG classes determined in this method represent the majority of total lipids. Alternatively, the principles of the method outlined here can be adapted to detect and quantify other lipid classes, such as glycosphingolipids, that have been found to be biochemically significant but quantitatively minor lipids in the environment (Vardi et al., 2009). If a diagnostic fragmentation pattern can be established for a lipid class then a TQMS scan can be defined to quantify that lipid class, and this defined scanning method will enable quantification of compounds that would otherwise be lost in the noise of MS methods that only characterize the most abundant base peak ions. Given appropriate diagnostic fragmentation patterns, the principles of this TQMS method can be applied to develop MS scans that will enable the quantification of diverse lipids from a range of environments.

The nine classes of IP-DAG that our method was developed to detect and quantify compose the vast majority of IP-DAGs in the upper ocean and are ubiquitous across the globe (Brandsma et al., 2012; Edwards et al., 2011; Popendorf et al., 2011a; Schubotz et al., 2009; Van Mooy and Fredricks, 2010; Van Mooy et al., 2009; Van Mooy et al., 2006). The distribution of fatty acids in each class of IP-DAG tends to be distinct from

other classes of IP-DAG, but is otherwise remarkably diverse and unpredictable in the environment (Brandsma et al., 2012; Schubotz et al., 2009; Van Mooy and Fredricks, 2010). Despite the diversity of fatty acids in IP-DAG, the distribution of IP-DAG classes correlates only with broadly defined planktonic taxa. Thus IP-DAGs appear to have limited potential as true chemotaxonomic biomarkers (Brandsma et al., 2012; Edwards et al., 2011; Popendorf et al., 2011a; Schubotz et al., 2009; Van Mooy and Fredricks, 2010; Van Mooy et al., 2009; Van Mooy et al., 2006). However, it was shown some time ago that the relative proportions of IP-DAG in plankton appear to be sensitive to the scarcity of dissolved phosphate in culture medium; phospholipids tend to be relatively more abundant in plankton grown in phosphate-replete growth media, while glycolipids and betaine lipids tend to be relatively more abundant in phosphate-depleted growth media (Benning et al., 1993; Benning et al., 1995; Minnikin et al., 1974; Van Mooy et al., 2006).

Recently, predicted correlations between IP-DAG and phosphate concentrations have been confirmed in marine environments and wetlands, and experimentally validated under in situ conditions (Bellinger and Van Mooy, 2012; Longnecker et al., 2010; Popendorf et al., 2011a; Popendorf et al., 2011b; Van Mooy et al., 2009). Thus, we expect that interest in IP-DAGs as a physiological indicator of nutrient stress will continue to increase, and that the straightforward and reliable method we present here will be of use to a broad range of investigators working in diverse fields such as microbiology, oceanography, ecology, and biofuels technology.

4. Conclusions

The method we present significantly streamlines the analysis of IP-DAG classes in marine samples and enables their quantification. The method is distinct from other approaches because it does not require either analysis or foreknowledge of molecular ions and IP-DAG diversity. Data analysis is greatly simplified since the analysis of each sample yields nine chromatograms (one for each class of IP-DAG) versus previous approaches which demanded the analysis of many dozens of chromatograms (one for

each species of IP-DAG) (Van Mooy and Fredricks, 2010; Van Mooy et al., 2009; Van Mooy et al., 2006). Although the sensitivity and linearity of detection varies across IP-DAG classes, in practice the method can be used quantitatively in marine samples. The mass spectrometer response also varied significantly between classes. The response of IP-DAGs with different fatty acids were highly correlated based on our analysis of phospholipids. However, inaccuracies of 20% or more are possible; this inaccuracy could be overcome with the development of a representative calibration standard (composed of the dozens of different IP-DAG species), however we posit that these inaccuracies are tolerable at the present time because our knowledge of IP-DAGs in marine environments is still in its infancy. We have applied our method to marine samples the world over, and are able to reliably detect IP-DAGs from all nine major classes.

Acknowledgements

We would like to gratefully acknowledge the contributions of Patrick Martin for South Atlantic IP-DAG data as well as assistance extracting and purifying betaine standards; Laura Sofen for culturing phytoplankton as well as extraction and purification of betaine standards; Krista Longnecker and Sonya Dyhrman for assistance culturing phytoplankton for betaine standards; James Fulton and Suni Shah for work developing the PrincetonSpher diol chromatography method; and Catherine Carmichael and Daniel Montlucon for GC-FID analysis to quantify the betaine standards. This research was supported by the U.S. Office of Naval Research (N00014-08-0764 and N00014-09-0091) and the U.S. National Science Foundation (OCE-0646944 and OCE-1029687).

References

Bellinger, B.J., Van Mooy, B.A.S., 2012. Non-phosphorus lipids in periphyton reflect available nutrients in the Florida Everglades, USA. Journal of Phycology 48, 303-311.

Benning, C., Beatty, J.T., Prince, R.C., Somerville, C.R., 1993. The sulfolipid sulfoquinovosyldiacylglycerol is not required for photosynthetic electron transport in Rhodobacter sphaeroides but enhances growth under phosphate limitation. Proceedings of the National Academy of Sciences 90, 1561-1565.

Benning, C., Huang, Z.-H., Gage, D.A., 1995. Accumulation of a Novel Glycolipid and a Betaine Lipid in Cells of Rhodobacter sphaeroides Grown under Phosphate Limitation. Archives of Biochemistry and Biophysics 317, 103-111.

Bligh, E.G., Dyer, W.J., 1959. A Rapid Method of Total Lipid Extraction and Purification. Canadian Journal of Physiology and Pharmacology 37, 911-917.

Brandsma, J., Hopmans, E.C., Philippart, C.J.M., Veldhuis, M.J.W., Schouten, S., Damsté, J.S.S., 2012. Low temporal variation in the intact polar lipid composition of North Sea coastal marine water reveals limited chemotaxonomic value. Biogeosciences 9, 1073-1084.

Cho, B.C., Azam, F., 1990. Biogeochemical significance of bacterial biomass in the ocean's euphotic zone. Marine Ecology Progress Series 63, 253-259.

Edwards, B.R., Reddy, C.M., Camilli, R., Carmichael, C.A., Longnecker, K., Van Mooy, B.A.S., 2011. Rapid microbial respiration of oil from the Deepwater Horizon spill in offshore surface waters of the Gulf of Mexico. Environmental Research Letters 6.

Farrington, J.W., Quinn, J.G., 1971. Fatty acid diagensis in recent sediment from Narragansett Bay, Rhode Island. Nature 230, 67-69.

Koivusalo, M., Haimi, P., Heikinheimo, L., Kostiainen, R., Somerharju, P., 2001. Quantitative determination of phospholipid compositions by ESI-MS: effects of acyl chain length, unsaturation, and lipid concentration on instrument response. Journal of Lipid Research 42, 663-672.

Longnecker, K., Lomas, M.W., Van Mooy, B.A.S., 2010. Abundance and diversity of heterotrophic bacterial cells assimilating phosphate in the subtropical North Atlantic Ocean. Environmental Microbiology 12, 2773-2782.

Martin, P., Van Mooy, B.A.S., Heithoff, A., Dyhrman, S.T., 2011. Phosphorus supply drives rapid turnover of membrane phospholipids in the diatom Thalassiosira pseudonana. The ISME Journal 5, 1057-1060.

Minnikin, D.E., Abdolrahimzadeh, H., Baddiley, J., 1974. Replacement of acidic phospholipids by acidic glycolipids in Pseudomonas diminuta. Nature 249, 268.

Moore, J.K., Doney, S.C., Lindsay, K., 2004. Upper ocean ecosystem dynamics and iron cycling in a global three-dimensional model. Global Biogeochemical Cycles 18.

Oliver, J.D., Colwell, R.R., 1973. Extractable Lipids of Gram-Negative Marine Bacteria: Phospholipid Composition. Journal of Bacteriology 114, 897-908.

Popendorf, K.J., Lomas, M.W., Van Mooy, B.A.S., 2011a. Microbial sources of intact polar diacylglycerolipids in the Western North Atlantic Ocean. Organic Geochemistry 42, 803-811.

Popendorf, K.J., Tanaka, T., Pujo-Pay, M., Lagaria, A., Courties, C., Conan, P., Oriol, L., Sofen, L.E., Moutin, T., Van Mooy, B.A.S., 2011b. Gradients in intact polar diacylglycerolipids across the Mediterranean Sea are related to phosphate availability. Biogeosciences 8, 3733-3745.

Rütters, H., Sass, H., Cypionka, H., Rullkötter, J., 2002. Phospholipid analysis as a tool to study complex microbial communities in marine sediments. Journal of Microbiological Methods 48, 149-160.

Schubotz, F., Wakeham, S.G., Lipp, J.S., Fredricks, H.F., Hinrichs, K.-U., 2009. Detection of microbial biomass by intact polar membrane lipid analysis in the water column and surface sediments of the Black Sea. Environmental Microbiology 11, 2720-2734.

Sturt, H.F., Summons, R.E., Smith, K., Elvert, M., Hinrichs, K.-U., 2004. Intact polar membrane lipids in prokaryotes and sediments deciphered by high-performance liquid chromatography/electrospray ionization multistage mass spectrometry--new biomarkers for biogeochemistry and microbial ecology. Rapid Communications in Mass Spectrometry 18, 617-628.

Suzumura, M., Ingall, E.D., 2001. Concentrations of lipid phosphorus and its abundance in dissolved and particulate organic phosphorus in coastal seawater. Marine Chemistry 75, 141-149.

Van Mooy, B.A.S., Fredricks, H.F., 2010. Bacterial and eukaryotic intact polar lipids in the eastern subtropical South Pacific: Water-column distribution, planktonic sources, and fatty acid composition. Geochimica et Cosmochimica Acta 74, 6499-6516.

Van Mooy, B.A.S., Fredricks, H.F., Pedler, B.E., Dyhrman, S.T., Karl, D.M., Koblízek, M., Lomas, M.W., Mincer, T.J., Moore, L.R., Moutin, T., Rappé, M.S., Webb, E.A., 2009. Phytoplankton in the ocean substitute phospholipids in response to phosphorus scarcity. Nature 458, 69-72.

Van Mooy, B.A.S., Moutin, T., Duhamel, S., Rimmelin, P., Wambeke, F.V., 2008. Phospholipid synthesis rates in the eastern tropical South Pacific Ocean. Biogeosciences 5, 133-139.

Van Mooy, B.A.S., Rocap, G., Fredricks, H.F., Evans, C.T., Devol, A.H., 2006. Sulfolipids dramatically decrease phosphorus demand by picocyanobacteria in oligotrophic environments. Proceedings of the National Academy of Sciences 103, 8607-8612.

Vardi, A., Van Mooy, B.A.S., Fredricks, H.F., Popendorf, K.J., Ossolinski, J.E., Haramaty, L., Bidle, K.D., 2009. Viral glycosphingolipids induce lytic infection and cell death in marine phytoplankton. Science 326, 861-865.

Wakeham, S.G., Canuel, E.A., 1988. Organic geochemistry of particulate matter in the eastern tropical North Pacific Ocean: Implications for particle dynamics. Journal of Marine Research 46, 183-213.

White, D.C., 1988. Validation of quantitative analysis for microbial biomass, community structure, and metabolic activity. Arch. Hydrobiol. Beih. Ergebn. Limnol. 31, 1-18.

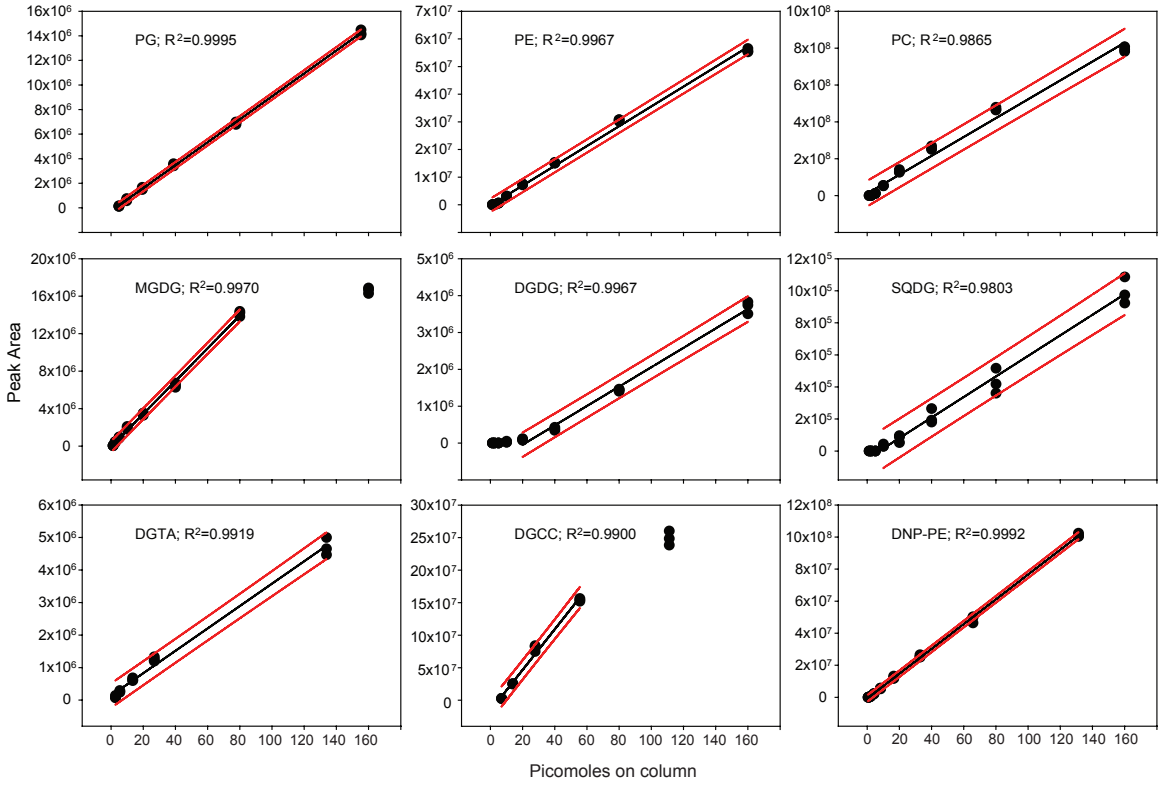

Figure 1
TQMS response for eight IP-DAG classes and an internal standard (DNP-PE) from 2.5 to 160 pmol on column. Each concentration of analyte (pmol on column) was measured in triplicate. The black line is a regression through all points in the range of linear response, the red lines are prediction intervals.

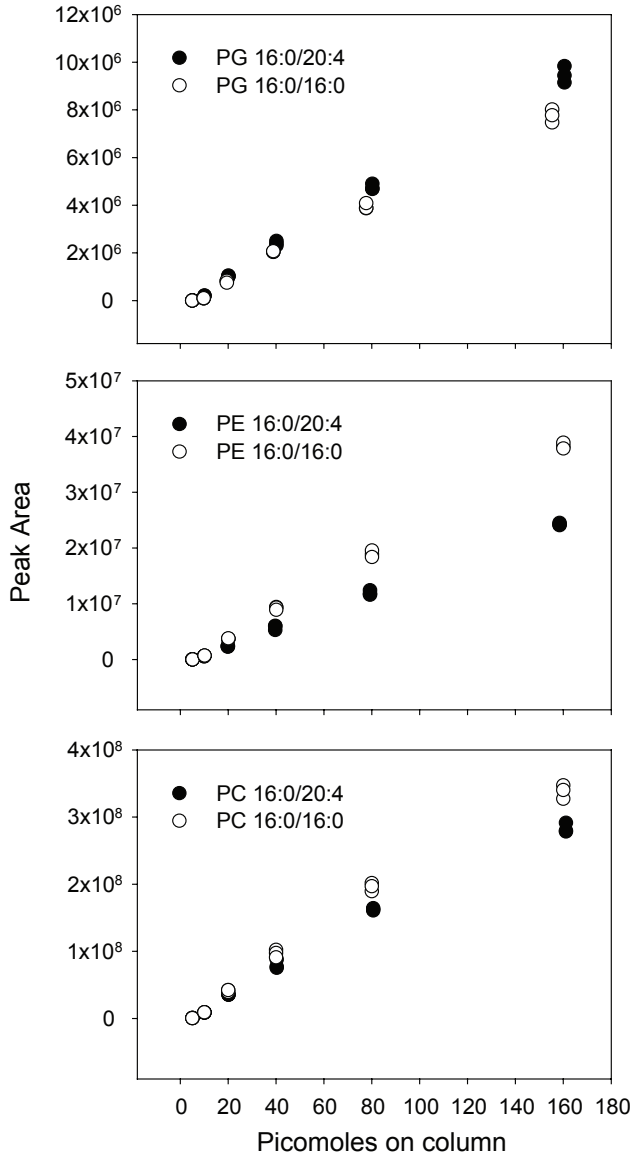

Figure 2
A mixed standard was made of three classes of phospholipids (PG, PE, and PC) with different molecular species of each class: a saturated species (16:0/16:0, dipalmitoyl—open circles), and an unsaturated species (16:0/20:4, palmitoyl/arachidonic—filled circles). Standard curves of each species are presented, ranging from 5 to 160 pmol on column. Each concentration of analyte (pmol on column) was measured in triplicate.

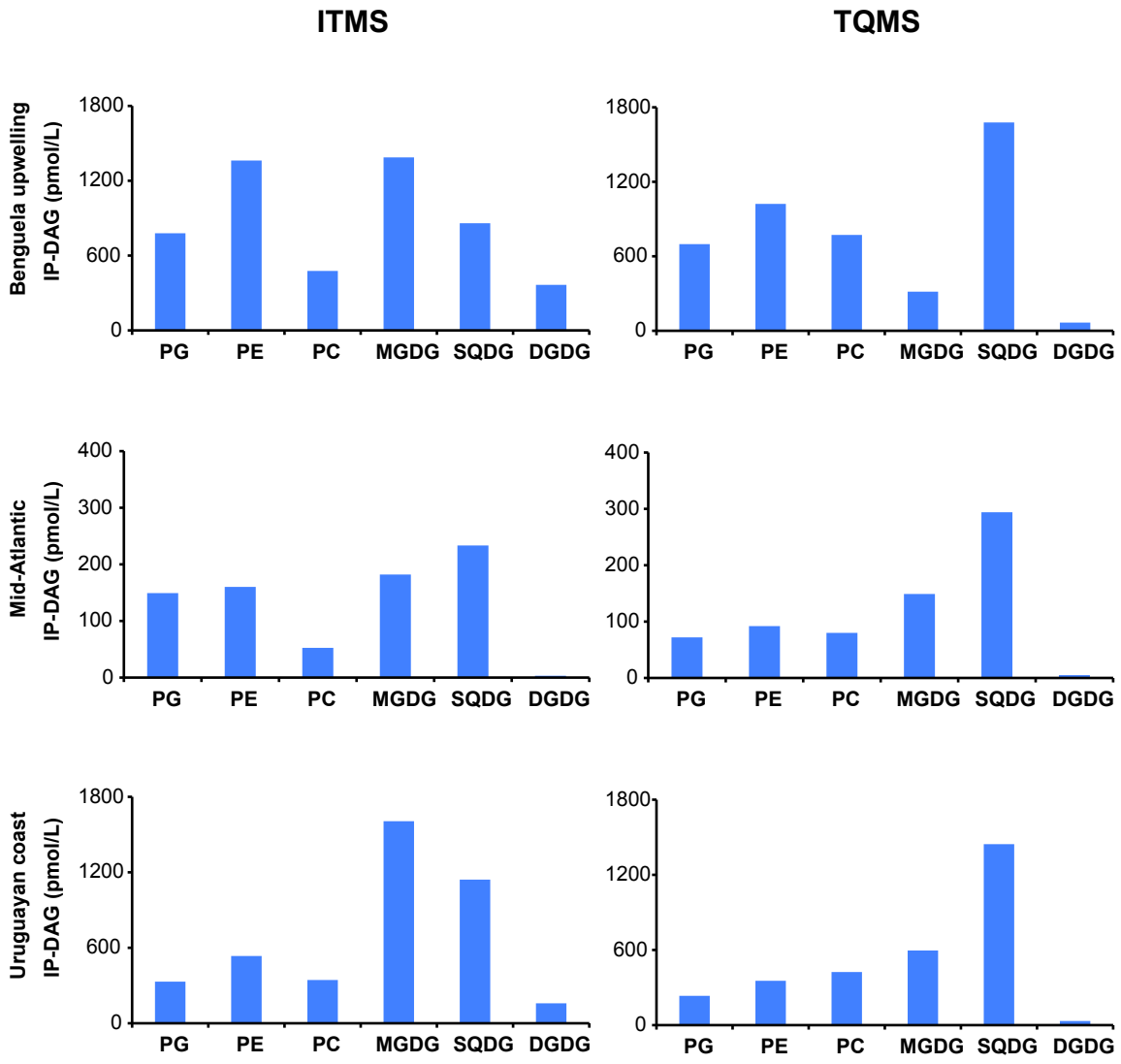

Figure 3

Comparison of IP-DAG quantification using HPLC-ESI-ITMS (plots in the left column) and HPLC-ESI-TQMS (plots in the right column). Six classes of IP-DAGs were quantified (PG, PE, PC, MGDG, SQDG and DGDG) in three surface seawater samples from across the South Atlantic, concentrations are pmol IP-DAG per L seawater.

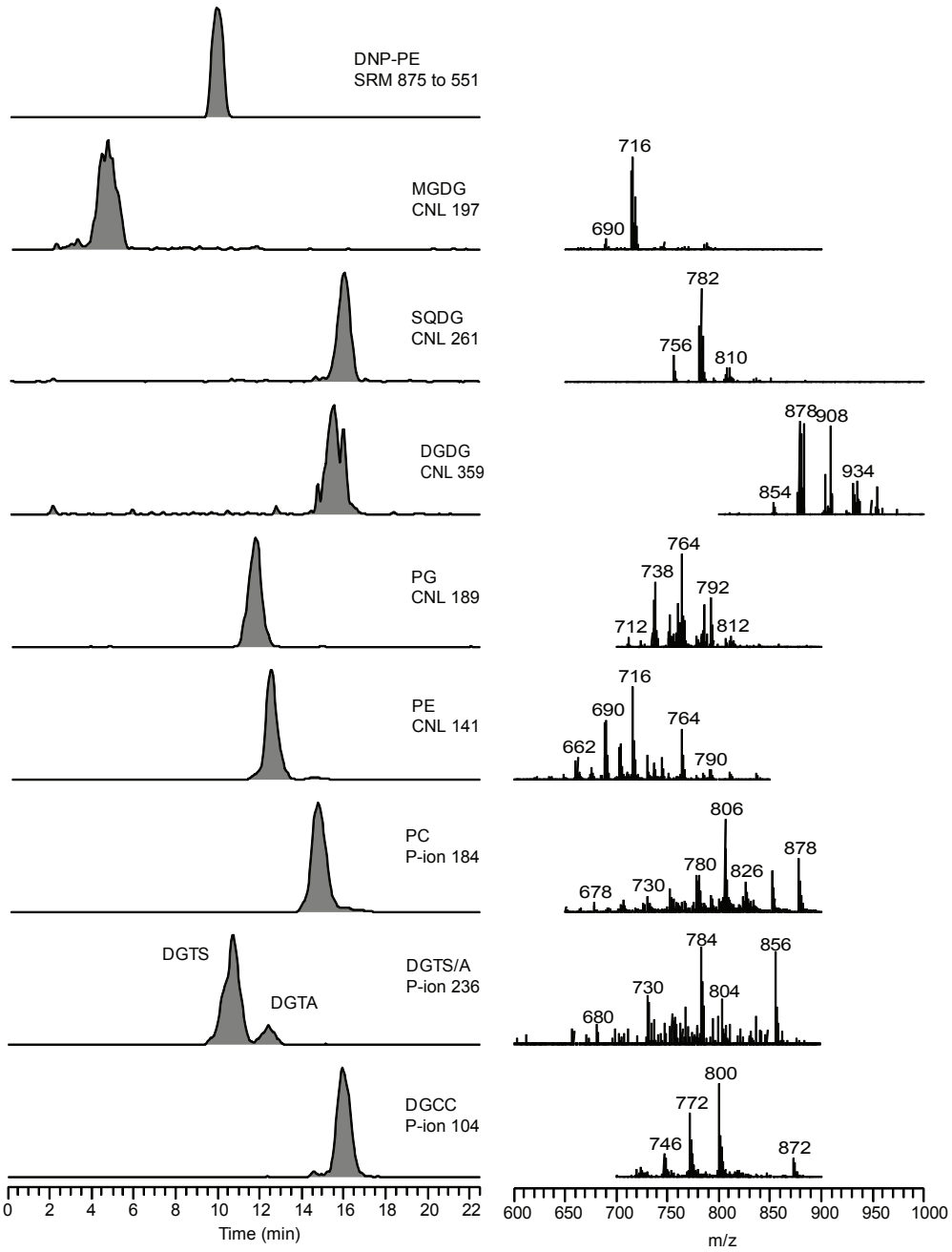

Figure 4

Total ion current chromatograms and mass spectra from a single chromatographic run of a representative sample from the Mediterranean Sea (39.102°N 5.204°E, 75 m depth). The chromatograms (left, individually normalized) show the total ion current of each scan event representing an IP-DAG class versus retention time. Each mass spectrum (right) shows the relative abundance of the molecular species of that IP-DAG class. The width of the baseline in each spectrum represents the m/z scan range for that scan event. Data for each IP-DAG class are generated by a separate scan event, either a selected reaction monitoring scan (SRM, for the internal standard DNP-PE), a constant neutral fragment loss scan (CNL, with the mass of neutral fragment), or a parent ion scan (P-ion, with the mass of the characteristic product ion). The abundance of DGTS and DGTA are monitored in the same scan event (parent ion scan for 236 m/z product ion), each peak is integrated separately for quantification; the spectrum shown is of DGTA.

Table 1

Mass spectrometry conditions for molecular-ion independent analysis of nine classes of IP-DAG and an internal standard (DNP-PE) in positive ion mode using a TQMS. Linear range of quantitation (pmol on column) is based on analysis of standard curves of authentic standards (see Figure 1).

	Lipid class	Molecular ion	Scan type	Neutral fragment or product ion mass	Neutral fragment or *product ion*	Scan range (m/z)	Collision energy (V)	Linear range of quantitation (pmol o.c.)
Phospholipids	PG	$[M+NH_4]^+$	Neutral fragment	189	-phosphoglycerol	700-900	18	5-160
	PE	$[M+H]^+$	Neutral fragment	141	-phosphoethanolamine	600-850	19	5-160
	PC	$[M]^+$	Parent ion scan	184	*phosphocholine*	650-900	32	5-160
Glycolipids	MGDG	$[M+NH_4]^+$	Neutral fragment	197	-glycosyl, $-H_2O$	650-900	22	2.5-80
	DGDG	$[M+NH_4]^+$	Neutral fragment	359	-glycosyl, $-H_2O$	800-1000	24	20-160
	SQDG	$[M+NH_4]^+$	Neutral fragment	261	-glycosyl, $-H_2O$	650-1000	24	10-160
Betaine lipids	DGTS & DGTA	$[M]^+$	Parent ion scan	236	*headgroup*	600-900	60	2.5-130
	DGCC	$[M]^+$	Parent ion scan	104	*choline*	700-900	40	5-55
Internal Std	DNP-PE	$[M+NH_4]^+$	Selected reaction monitoring	875 to 551	-headgroup	n/a	19	0.5-160

Table 2

Comparison of IP-DAG quantification using the ESI-ITMS method and ESI-TQMS method for three glycolipid classes and three phospholipid classes. Betaine lipid standards were not analyzed using the ITMS method, thus although betaine lipid molecular ions were detected and peak areas integrated (SM Table 1), response factors were not available to calculate betaine lipid concentrations using the ITMS method (TQMS betaine lipid quantification for these samples is given in Table 3). The three samples quantified were surface ocean water (5 m depth) from three locations across the South Atlantic, further sample information is given in Table 4.

		Uruguyan coast (A)		Mid-Atlantic (B)		Benguela upwelling (C)						
		ITMS	**TQMS**	**ITMS**	**TQMS**	**ITMS**	**TQMS**	**TQMS/ITMS**			**TQMS/ITMS**	
	IP-DAG class	pmol/L	pmol/L	pmol/L	pmol/L	pmol/L	pmol/L	(A)	(B)	(C)	**Average**	% st. dev.
Phospholipids	PG	331	234	149	72	779	698	0.7	0.5	0.9	**0.7**	30
	PE	535	354	160	92	1362	1022	0.7	0.6	0.8	**0.7**	13
	PC	344	424	53	80	477	772	1.2	1.5	1.6	**1.5**	14
Glycolipids	MGDG	1606	596	182	149	1387	315	0.4	0.8	0.2	**0.5**	65
	DGDG	159	33	3	5	365	66	0.2	1.6	0.2	**0.6**	121
	SQDG	1142	1445	233	294	859	1678	1.3	1.3	2.0	**1.5**	27

Table 3

Relative abundance of molecular ions per IP-DAG class using ESI-ITMS

Three IP-DAG samples from the South Atlantic Ocean were quantified using the ESI-ITMS method, for sample information see Table 3. Each of the molecular ions (MI) listed below was integrated in a separate base peak chromatogram, and peak areas were summed for each IP-DAG class to calculate the IP-DAG concentrations given in Table 2. For each sample, percent abundance of each MI was calculated as percent of total peak area per IP-DAG class. Dashes indicate MI was not detected.

		% abundance per IP-DAG class		
	MI	**Uruguayan coast**	**Mid-Atlantic**	**Benguela upwelling**
PG	710	-	-	16.0
	736	16.3	-	18.6
	738	32.7	22.3	27.9
	752	17.3	17.6	4.3
	764	18.5	24.3	24.6
	766	15.3	21.0	8.6
	778	-	6.8	-
	780	-	7.9	-
PE	636	-	-	2.9
	648	-	-	2.0
	650	-	-	1.1
	662	2.9	-	13.3
	676	-	-	3.7
	678	-	-	2.3
	688	9.8	6.2	14.2
	690	14.3	12.6	12.6
	702	2.8	-	2.6
	704	11.0	20.3	2.4
	716	23.5	13.3	17.3
	718	10.8	13.2	4.8
	730	8.4	9.7	1.7
	732	-	5.5	5.4
	744	10.1	19.3	-
	764	6.4	-	7.0
	766	-	-	2.4
	790	-	-	2.2
	792	-	-	2.0
PC	780	7.3	-	12.0
	786	8.2	-	6.7
	806	37.0	71.1	25.2
	808	9.0	-	10.7
	826	6.5	-	14.1
	852	13.0	-	20.5
	878	19.0	28.9	10.8

		% abundance per IP-DAG class		
	MI	**Uruguayan coast**	**Mid-Atlantic**	**Benguela upwelling**
MGDG	690	11.2	12.5	1.0
	692	8.9	16.0	3.9
	716	14.8	5.5	1.4
	718	30.3	27.2	20.4
	720	6.0	9.2	3.4
	738	1.3	-	3.5
	744	3.0	5.3	5.0
	746	4.9	8.0	8.7
	774	-	8.2	2.4
	784	6.2	-	17.4
	786	10.2	8.0	26.2
	788	3.1	-	6.7
DGDG	878	9.9	-	10.3
	880	22.9	-	11.9
	900	11.6	-	-
	924	21.5	-	-
	926	8.8	-	9.4
	946	-	-	14.8
	948	16.1	-	24.5
	950	9.3	-	9.7
	952	-	-	19.3
SQDG	746	5.5	-	-
	756	12.5	13.5	32.3
	780	17.5	9.7	-
	782	19.5	22.2	24.2
	784	39.1	47.3	10.5
	810	-	-	16.4
	812	5.9	7.2	9.6
	830	-	-	7.0
DGTA	756	7.4	-	-
	758	5.4	-	-
	784	34.3	29.7	-
	786	12.3	20.3	-
	830	11.0	-	26.6
	856	29.6	50.0	73.4
DGTS	642	-	-	4.3
	654	3.5	-	10.3
	656	14.9	17.1	17.3
	668	-	-	6.7
	670	4.2	-	10.6
	680	4.3	-	-
	682	10.5	-	12.7
	696	-	-	7.5
	704	14.7	11.1	5.3
	706	6.5	9.5	-
	708	5.9	8.6	5.6
	710	7.5	12.0	-
	724	-	-	9.6
	730	4.1	-	5.8
	732	4.5	9.1	4.3
	734	4.5	6.6	-
	736	5.3	11.7	-
	738	3.8	14.3	-
	758	5.9	-	-
DGCC	772	11.1	16.9	-
	774	12.7	-	-
	800	52.7	58.4	-
	872	23.5	24.6	100.0

Table 4

IP-DAG concentrations from three locations across the Mediterranean Sea and three locations across the South Atlantic, with multiple depths sampled at each location. The full dataset from the Mediterranean Sea is presented in Popendorf et al., Biogeosciences 2011. DCM is deep chlorophyll maximum; n.d. is not detected; *an authentic standard was not available for DGTS, therefore the quantification presented here is less certain than for other IP-DAGs.

		Latitude Longitude	depth (m)	PO_4 (nmol/L)	PG (pmol/L)	PE (pmol/L)	PC (pmol/L)	MGDG (pmol/L)	DGDG (pmol/L)	SQDG (pmol/L)	DGTA (pmol/L)	DGTS* (pmol/L)	DGCC (pmol/L)	Total IP-DAGs (nmol/L)
Mediterranean Sea	Levantine basin	33.580°N 31.934°E	surface 5	3	212	249	371	117	n.d.	547	473	181	183	2.33
			DCM 100	1	294	261	326	225	280	1443	165	n.d.	n.d.	3.00
			aphotic zone 150	9	202	245	202	n.d.	n.d.	183	n.d.	n.d.	n.d.	0.83
	Ionian basin	34.328°N 19.819°E	surface 5	n.d.	297	220	266	189	n.d.	432	490	206	232	2.33
			DCM 75	n.d.	588	588	815	468	395	2314	450	148	240	6.01
			aphotic zone 150	1	169	228	176	86	n.d.	297	n.d.	n.d.	n.d.	0.96
	Sicilian channel	39.102°N 5.204°E	surface 5	30	331	181	255	246	173	921	500	172	215	2.99
			DCM 75	43	591	532	627	365	242	1687	293	100	109	4.55
			aphotic zone 150	233	153	226	240	n.d.	n.d.	n.d.	n.d.	n.d.	n.d.	0.62
South Atlantic	Benguela upwelling	23.677°S 13.713°E	surface 5	781	698	1022	772	315	66	1678	309	764	116	5.74
			DCM 25	1025	581	1085	828	163	33	919	514	750	116	4.99
	Mid-Atlantic	24.000°S 26.321°W	surface 5	78	72	92	80	149	5	294	0	103	36	0.83
			DCM 175	224	5	61	69	41	0	0	0	13	4	0.19
	Uruguayan coast	37.105°S 52.413°W	surface 5	39	234	354	424	596	33	1445	440	977	278	4.78
			DCM 75	49	219	331	441	435	69	1849	262	320	166	4.09

Phospholipids:

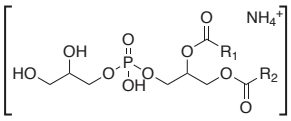

PG
phosphatidylglycerol

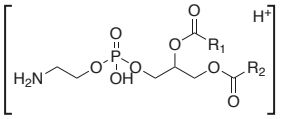

PE
phosphatidylethanolamine

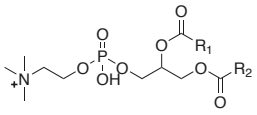

PC
phosphatidylcholine

Glycolipids:

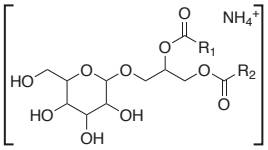

MGDG
monoglycosyldiacylglycerol

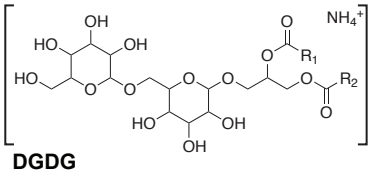

DGDG
diglycosyldiacylglycerol

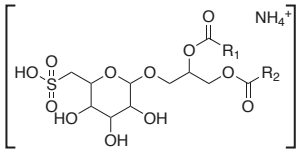

SQDG
sulfoquinovosyldiacylglycerol

Betaine lipids:

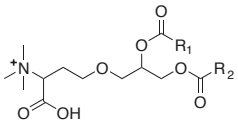

DGTS
diacylglyceryl-trimethyl-homoserine

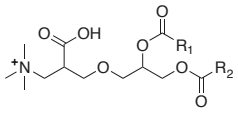

DGTA
diacylglyceryl-hydroxymethyl-trimethyl-β-alanine

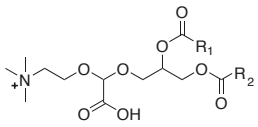

DGCC
diacylglyceryl-carboxyhydroxy-methylcholine

Supplemental Material Figure 1
Headgroups of the nine most abundant IP-DAG classes in marine environments. Chemical forms are presented as the molecular ions, with ammonium adducts (contributed by the HPLC eluents) associated with the relevant classes. R_1 and R_2 represent acyl chains that vary in composition.

Chapter 3

Microbial sources of intact polar diacylglycerolipids in the Western North Atlantic Ocean

Microbial sources of intact polar diacylglycerolipids in the Western North Atlantic Ocean. *Organic Geochemistry*. Kimberly J. Popendorf, Michael W. Lomas, Benjamin A.S. Van Mooy. 2011. 42, 803-811. doi: 10.1016/j.orggeochem.2011.05.003

Organic Geochemistry 42 (2011) 803–811

Contents lists available at ScienceDirect

Organic Geochemistry

journal homepage: www.elsevier.com/locate/orggeochem

Microbial sources of intact polar diacylglycerolipids in the Western North Atlantic Ocean

Kimberly J. Popendorf [a], Michael W. Lomas [b], Benjamin A.S. Van Mooy [a,*]

[a] Department of Marine Chemistry and Geochemistry, Woods Hole Oceanographic Institution, Woods Hole, MA 02543, USA
[b] Bermuda Institute of Ocean Sciences, St. George, Bermuda

ARTICLE INFO

Article history:
Received 22 December 2010
Received in revised form 11 April 2011
Accepted 7 May 2011
Available online 18 May 2011

ABSTRACT

Intact polar membrane lipids are essential components of microbial membranes and recent work has uncovered a diversity of them occurring in the ocean. While it has long been understood that lipid composition varies across microbial groups, the microbial origins of the intact polar lipids in the surface ocean remain to be fully explained. This study focused on identifying the microbial sources of intact polar diacylglycerolipids (IP-DAGs) in the surface waters of the western North Atlantic Ocean. We used three approaches to define these microbial sources: (i) ^{13}C tracing to identify photoautotrophic and heterotrophic production of the major classes of IP-DAGs, (ii) cell sorting flow cytometry of *Prochlorococcus*, *Synechococcus* and heterotrophic bacteria to determine IP-DAG composition and (iii) regrowth incubations targeting IP-DAG production by heterotrophic bacteria. Stable isotope tracing indicated that sulfoquinovosyldiacylglycerol (SQDG) and diacylglyceryl-trimethyl-homoserine (DGTS) were produced predominantly by photoautotrophs, while phosphatidylglycerol (PG) production was dominated by heterotrophic bacteria. Of the cells sorted with flow cytometry, *Prochlorococcus* and *Synechococcus* were found to have abundant glycolipids, while heterotrophic bacteria were dominated by phospholipids. The regrowth incubations showed that the growth of heterotrophic bacteria correlated with an increase in the concentration of PG, phosphatidylethanolamine (PE) and monoglycosyldiacylglycerol (MGDG). The finding of MGDG in heterotrophic bacteria differs from previous work, which had asserted that the membranes of heterotrophic bacteria in this environment were composed entirely of phospholipids. Overall, our findings indicate that phytoplankton are the primary source of SQDG and DGTS, while heterotrophic bacteria are the dominant source of PG, making these three compounds promising biomarkers for the study of microbes in the surface ocean.

1. Introduction

Membrane lipids are essential structural components of microbial cells. The particular mix of lipids forming the membrane defines its role in the microbial cell by affecting membrane fluidity, diffusive permeability and interaction with proteins (e.g. Zhang and Rock, 2008), among other properties. In the surface ocean, lipids comprise a substantial portion of cellular biomass (11–23% of the organic carbon in plankton; Wakeham et al., 1997) and cellular nutrient requirements (1–28% of plankton phosphate needs; Van Mooy et al., 2006). Production of membrane lipids is obligate for both growth and replication of cells, so membrane lipids are a significant cellular investment of resources and play a key role in the cycling of carbon and nutrients in the ocean.

Intact membrane lipids are attractive compounds for environmental microbial studies due to their structural diversity, which can be readily assessed using high performance liquid chromatography/mass spectrometry analysis (HPLC–MS; Rütters et al., 2002; Sturt et al., 2004; Ertefai et al., 2008; Schubotz et al., 2009). The structures, defined by the head group and fatty acid moiety composition, can provide information on both the phylogenetic source of the lipids and the environmental conditions under which they were produced (Schubotz et al., 2009; Van Mooy and Fredricks, 2010). In addition, synthesis of membrane lipids is fundamental for cell growth, so their production rate has the potential to reflect microbial production (White et al., 1977; Van Mooy et al., 2008). Our study aimed to identify the microbial sources of intact membrane lipids in the surface ocean in order to increase their utility as molecular tools for studying the role of microbes in biogeochemical cycles.

Microbial membranes contain diverse classes of intact polar lipids, including phospholipids, glycolipids and betaine lipids (Kates, 1964; White and Tucker, 1969; Oliver and Colwell, 1973; King et al., 1977; Kato et al., 1996). With the advancement of HPLC–MS methodology it has been demonstrated that many representatives of these classes of microbial lipids are present in the surface ocean (Van Mooy et al., 2006, 2009; Schubotz et al., 2009; Van Mooy and

* Corresponding author. Tel.: +1 508 289 2322; fax: +1 508 457 2164.
E-mail address: bvanmooy@whoi.edu (B.A.S. Van Mooy).

0146-6380/$ - see front matter © 2011 Elsevier Ltd. All rights reserved.
doi:10.1016/j.orggeochem.2011.05.003

Fredricks, 2010). Membranes of bacterial and eukaryotic plankton in the surface ocean are dominated by intact polar diacylglycerolipids (IP-DAGs). Deeper in the water column, the concentration of archaeal polar lipids with alkyl chains can be much more significant (Schubotz et al., 2009). This study focuses on the cohort of IP-DAGs common in open ocean environments (Van Mooy et al., 2009; Van Mooy and Fredricks, 2010), which includes (Fig. 1): (i) three classes of glycolipids – monoglycosyldiacylglycerol (MGDG), diglycosyldiacylglycerol (DGDG) and sulfoquinovosyldiacylglycerol (SQDG), (ii) three classes of phospholipids – phosphatidylglycerol (PG), phosphatidylethanolamine (PE) and phosphatidylcholine (PC) and (iii) three classes of betaine lipids – diacylglyceryl trimethylhomoserine (DGTS), diacylglyceryl hydroxymethyl-trimethyl-β-alanine (DGTA) and diacylglyceryl carboxyhydroxymethylcholine (DGCC).

Association between IP-DAG head groups and microbial groups has been established, such as that of the glycolipids MGDG, DGDG and SQDG with the thylakoid membranes of cyanobacteria and other phytoplankton (Wada and Murata, 1998; Sakurai et al., 2006) and that of betaine lipids with eukaryotic plankton (Vogel and Eichenberger, 1992; Kato et al., 1996; Guschina and Harwood, 2006; Van Mooy et al., 2009). These studies focused mainly on cultures, or demonstrated the co-occurrence of lipids and microbes in the ocean (e.g. Van Mooy and Fredricks, 2010). However, most marine microbes have not been cultured and little work has been carried out to directly link IP-DAGs with specific microbial groups in the surface ocean.

We have examined the microbial sources of membrane lipids from environmental samples using three distinct approaches: (i) ^{13}C-labeled substrates to trace lipid production by photoautotrophs and heterotrophic bacteria, (ii) cell sorting flow cytometry to separate cyanobacteria and heterotrophic bacteria for IP-DAG analysis and (iii) regrowth incubations to examine the production of IP-DAGs during growth of heterotrophic bacteria. Our results indicate that several classes of IP-DAGs have the potential to be useful biomarkers for studying microbial processes in the sea.

2. Methods

2.1. Cruises and sampling scheme

Samples were collected on two cruises in the North Atlantic (Fig. 2): (i) the BV39 cruise in October 2007 aboard the R/V Atlantic Explorer, which was a meridional transect from Bermuda to Puerto Rico and (ii) the Oc443 cruise in April 2008 aboard the R/V Oceanus, which comprised a leg from Woods Hole, Massachusetts northeast to 43°N 65°W and a second leg south along 65°W towards Bermuda. Samples were collected throughout both cruises for determination of soluble reactive phosphate and cell abundance. At five stations on the BV39 cruise and three stations on the Oc443 cruise, samples were collected for cell sorting flow cytometry. In the southern, oligotrophic portion of the Oc443 cruise water was collected for stable isotope incubations and in the northern portion of the BV39 cruise water for regrowth incubation. Water for all samples was collected using Niskin bottles mounted on a rosette equipped with conductivity, temperature and pressure sensors.

2.2. Phosphate concentration

For both cruises, samples were collected at multiple depths at each station or cast for determination of soluble reactive phosphorus (SRP). Seawater samples (ca. 200 ml) were collected directly from the Niskin bottles into high density polypropylene bottles and frozen at −20 °C until analysis. SRP was measured using the MAGIC method (Karl and Tien, 1992).

2.3. Stable isotope incubations

2.3.1. Experimental design

The study used incubations of whole seawater with ^{13}C-labeled substrates to identify IP-DAGs produced by autotrophs, organisms

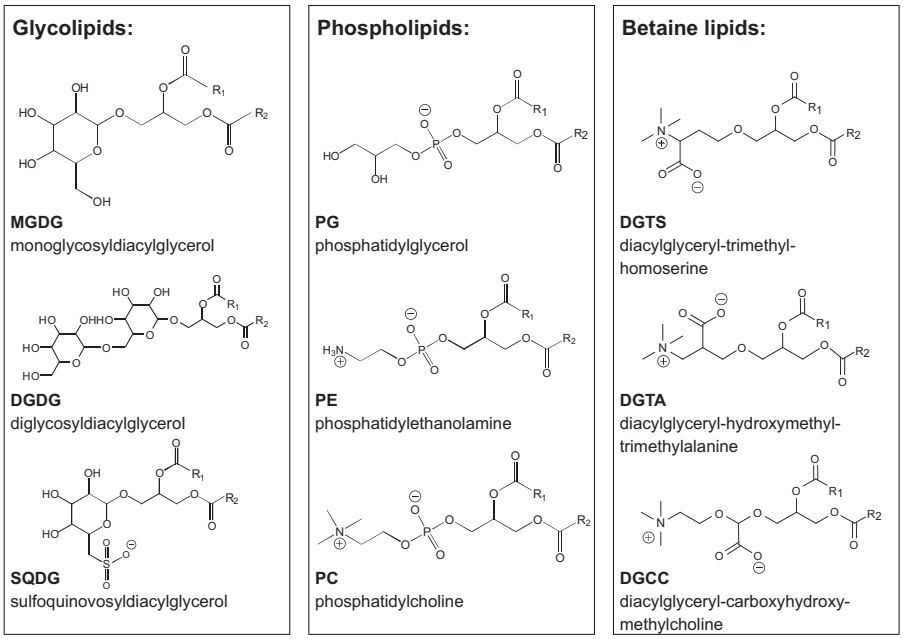

Fig. 1. IP-DAGs dominating plankton membranes in the surface ocean (R_1 and R_2 represent FA moieties).

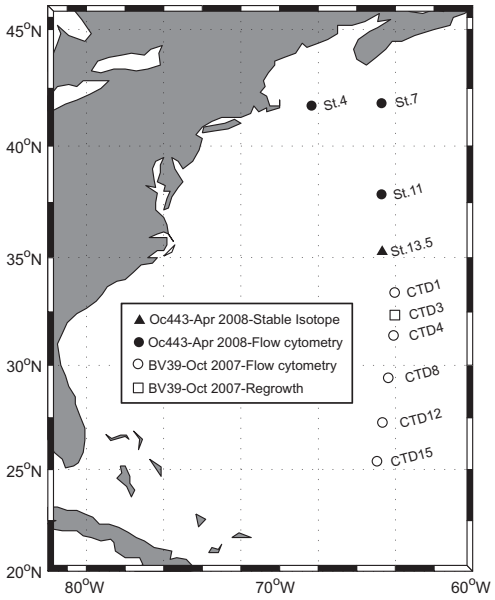

Fig. 2. Sampling locations during two cruises in the North Atlantic Ocean.

that use inorganic carbon as carbon source (here ^{13}C-labeled bicarbonate) and heterotrophs, organisms that use organic carbon as their carbon source (here ^{13}C-labeled glucose). Incubations were conducted in the light and the dark, with the ^{13}C–bicarbonate incubation in the light (denoted as ^{13}C–bicarbonate light), targeting IP-DAG production by photoautotrophs, and the ^{13}C–glucose incubation in the dark (^{13}C–glucose dark) the most targeted for production by heterotrophic bacteria. Incubations were conducted aboard the R/V Oceanus during the Oc443 cruise in April 2008. Water was collected at Station 13.5 at 35.5°N, 65.0°W (Fig. 2). Seawater from 20 m was collected using Niskin bottles and transferred immediately to three acid-washed clear polycarbonate carboys using acid-washed Tygon tubing. There were three conditions for the three carboys: (i) addition of ^{13}C-labeled glucose to a final concentration of ca. 100 nM (2-^{13}C D-glucose; Cambridge Isotope Laboratories, Inc.), (ii) addition of ^{13}C-labeled bicarbonate to a final concentration of ca. 20 μM (Cambridge Isotope Laboratories, Inc.) and (iii) a control with no substrate addition. Immediately following addition of ^{13}C-labeled substrate, the carboys were placed in on-deck flow through incubators at surface seawater temperature. Incubation in the dark used 20 l carboys and an opaque incubator, while the experiment in the light used 10 l carboys and a clear plexiglass incubator covered with neutral density screen which blocked ca. 50% of the surface irradiance. All incubations lasted 24 h. At the end of incubation the entire contents of the carboys were filtered onto 0.2 μm Anodisc filters (Whatman) using vacuum filtration (ca. −200 mm Hg), ca. 1 l per filter. Filters were wrapped in combusted Al foil and stored in liquid N_2 until extraction.

2.3.2. Lipid extraction and analysis

Lipids were extracted from the filters using a modified Bligh and Dyer protocol (Bligh and Dyer, 1959), as described by Van Mooy and Fredricks (2010). Phosphatidylethanolamine-N-(2,4-dinitrophenyl) (DNP-PE; Avanti Polar Lipids) was added with the initial solvent as an internal recovery standard. Total extracts were analyzed using HPLC–MS with a Hewlett Packard 1100 HPLC instrument and Thermo-Finnigan LCQ Deca XP ion trap mass spectrometer with electrospray ionization (ESI) interface. Full HPLC and MS methods are provided by Van Mooy and Fredricks (2010), as updated from Sturt et al. (2004). Eight IP-DAG classes were identified: MGDG, SQDG, PG, and PE were identified by characteristic neutral fragment loss in positive ion mode, while PC, DGTS, DGTA and DGCC were identified by characteristic fragment ions in positive ion mode (Sturt et al., 2004; Van Mooy and Fredricks, 2010). Once molecular ions had been established for each IP-DAG class, the eight classes were purified using preparative HPLC with an Agilent 1200 HPLC instrument equipped with a UV/visible variable wavelength detector, a fraction collector, and an Agilent LC/MSD SL mass spectrometer. Retention times were established by way of MSD detection in positive ion full scan mode of the previously assigned molecular ion of each IP-DAG, and these were used to set conservative time-based fraction collection windows for each IP-DAG (Fig. 3).

2.3.3. Fatty acid (FA) processing and analysis

Each IP-DAG fraction was transesterified to produce FA methyl esters (FAMEs). The intact lipids were reacted (ca. 2 h) with methanolic HCl under N_2 at 70 °C. FAMEs were analyzed using gas chromatography isotope ratio mass spectrometry (GC-IRMS) to determine relative abundance and δ^{13}C values (‰) relative to Peedee Belemnite. FAMEs were identified by comparison of retention times with a standard (Sigma–Aldrich, Supelco 37-component FAME Mix 47885-U). Samples for GC-IRMS (gas chromatography-isotope ratio mass spectrometry) were injected from hexane/CH_2Cl_2 via a programmable temperature vaporizing inlet (Gerstel PTV CIS-4), operated in solvent venting mode, to a Hewlett Packard 6890 GC instrument with Varian CP-Sil 5 CB LB column (60 m × 0.25 mm id × 0.25 μm phase) with a 1 m guard column and He flow of 1 ml/min. Combustion was with a Finnigan-MAT GC Combustion III interface coupled to a DeltaPlus stable isotope ratio mass spectrometer, where the interface had been modified to an integral fused silica design (Goodman, 1998). Data were acquired and manipulated with the Finnigan-MAT IsodatNT software package. To compare the enrichment of the IP-DAGs under the different incubation conditions, the average enrichment of each purified IP-DAG was expressed as the weighted average enrichment of the composite FAs for that sample. This was calculated as the sum of the enrichment of each FA multiplied by its abundance, divided by the total abundance of FAs. The control incubations with no ^{13}C-labeled substrate were used to determine an average δ^{13}C value of −27.6‰ (st. dev. 1.0‰) for FAs with no isotopic

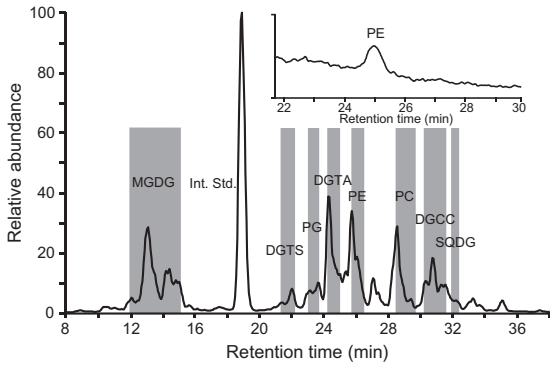

Fig. 3. Base peak ion chromatogram of a representative total lipid extract from the stable isotope incubations showing major IP-DAG classes. Grey bars indicate time-based fraction collection windows for each IP-DAG class. Inset is an example total ion chromatogram for a PE fraction after separation, showing the purity of the fractions after collection.

enrichment and all other $\delta^{13}C$ values are given as enrichment relative to this baseline.

2.4. Cell sorting flow cytometry

2.4.1. Sampling and flow cytometry

Samples for cell sorting flow cytometry were collected at three locations on the Oc443 cruise in April 2008 and at five locations on the BV39 cruise in October 2007; at each location three to six depths were sampled in the upper 120 m of the water column. Each sample (1–2 l) was collected in Niskin bottles and transferred to an acid-washed polycarbonate bottle before filtration. Samples were filtered using vacuum filtration (ca. −200 mm Hg) onto 47 mm diameter 0.2 μm polycarbonate filters (Whatman) for BV39 samples or 47 mm diameter 0.2 μm hydrophilic Durapore filters (Millipore) for Oc443 samples. Filtration was stopped when ca. 1 ml liquid remained on the filter to avoid directly exposing live unfixed cells to air; the remaining volume and filter were gently transferred to 5 ml cryovials, diluted to 5 ml with 0.2 μm filtered low nutrient seawater and fixed with paraformaldehyde to a concentration of 1%. Samples were fixed (15 min) at room temperature and then at 4 °C (several h) before being flash frozen in liquid N_2. They were kept frozen in liquid N_2 until being thawed for flow cytometry sorting at the Bermuda Institute of Ocean Sciences. Cyanobacteria were sorted according to methods given by Casey et al. (2009). Heterotrophic bacteria were sorted as follows: 1 ml aliquots of homogenized sample were transferred to 5 ml polypropylene Falcon tubes (BD Biosciences, San Jose, CA). Cell suspension was stained (10 min) with 1 μl nucleic acid dye SYTO-13 (0.2 μm filter-sterilized; 5 mM in dimethyl sulfoxide; Invitrogen, Carlsbad, CA) at room temperature in the dark. After laser noise and bubble exclusion with FSC pulse height and width, panels and gating hierarchy were adapted from Guindulain et al. (1997) to exclude *Prochlorococcus* and *Synechococcus* from heterotrophic bacteria by SSC (pulse height), FITC (pulse area 530/40 nm), PE (pulse height 580/30 nm) and "Chlorophyll" (pulse height 692/40 nm) fluorescence. Cells were sorted at 27.5 PSI and rate was maintained below 20,000 s^{-1}. Recovery and purity for heterotrophic bacterial sorts were 96 ± 3% and 98 ± 6%, respectively ($n = 7$). Mean abort rates were consistently <5%. Sorted cells were deposited into 5 ml polypropylene Falcon tubes, flash frozen in liquid N_2 and stored at −80 °C until extraction.

2.4.2. Extraction and analysis

Thawed samples were combined before extraction as follows: Oc443 samples from each station (St. 4, St. 7 and St. 11) all depths were combined; for BV39 samples, all depths from CTD4 were combined, and for casts CTD1, CTD8, CTD12 and CTD15 samples from the same depth were combined to give samples from 5 m, 20 m, 40 m, and the deep chlorophyll maximum (80 m, 115 m, 120 m and 110 m at the respective casts; see Supplementary material Table 1). After combining samples, lipids were extracted using a modified Bligh and Dyer extraction protocol as above with the following adjustment: for samples BV39-CTD4 and BV39-40 m, the total liquid volume of the cell sorts was used in place of phosphate buffer; for all other samples the cell sorted samples were combined and vacuum filtered (ca. −200 mm Hg) onto 47 mm 0.02 μm Anodisc filters (Whatman) and the filters extracted as for stable isotope samples. HPLC–MS analysis of the extract used an Agilent 1200 HPLC instrument coupled to a Thermo Scientific TSQ Vantage triple quadrupole mass spectrometer with heated ESI interface using HPLC conditions as in Section 2.3.2. IP-DAG classes were quantified in positive ion mode by integrating the total ion current of either the constant neutral loss scan, parent ion scan, or selected reaction monitoring (SRM) scan as follows: MGDG neutral loss of 197 da; SQDG neutral loss of 261 da; DGDG neutral loss of 359 da; PG neutral loss of 189 da; PE neutral loss of 141 da; PC product ion of m/z 184; DNP-PE (internal standard) SRM for the transition of m/z 875 to m/z 551. Response factors for each IP-DAG were established by analyzing standard curves prepared with synthetic PG, PE, PC, and DNP-PE (Avanti Polar Lipids Inc., Alabaster, AL), natural MGDG and DGDG standards (Matreya, LLC, Pleasant Gap, PA) and natural SQDG (Lipid Products, South Nutfield, UK). One sample of *Prochlorococcus* (BV39-CTD4) had an anomalously high concentration of PC, most likely due to low specificity of cell sorting at this location, possibly because of high numbers of conjoint *Prochlorococcus* and heterotrophic bacteria (Malfatti and Azam, 2009). It was not included in calculations of average IP-DAG composition of *Prochlorococcus*.

2.5. Regrowth incubation

2.5.1. Experimental design and analysis

Incubations were conducted on board the R/V Atlantic Explorer during the BV39 cruise in October 2007. Seawater was collected at 32.610°N 64.100°W at 5 m depth and transferred from Niskin bottles to acid-washed 20 l polycarbonate carboys using acid-washed Tygon tubing. Triplicate carboys were prepared with 2 l whole seawater and 18 l seawater gravity-filtered through an acid-cleaned 0.2 μm Polycap 36 TC filter (hydrophilic polyethersulfone membrane, Whatman). Carboys were incubated (72 h) in a dark temperature controlled room (within 2 °C of surface water temperature) and sampled every 12 h for cell counts and IP-DAG concentration. For IP-DAG concentration, 1 l of water was filtered onto a 47 mm 0.2 μm Anodisc filter (Whatman) using vacuum filtration (ca. −200 mm Hg). Filters were wrapped in Al foil and stored in liquid N_2. For flow cytometry cell counts, 1.5 ml water was added to a 2.0 ml cryovial and fixed with paraformaldehyde for a final concentration of 1%. Samples were stored at −80 °C until analysis. Extraction and analysis of glycolipids and phospholipids were conducted as above for the flow cytometry sorted samples. Betaine lipids were not analyzed.

3. Results

3.1. Phosphate concentration

On the Oc443 cruise, Stations 4 and 7 were north of the Gulf Stream and phosphate concentration ranged from 350 nM to 500 nM in the upper 100 m (Supplementary material, Table 1), while Stations 11 and 13.5 were south of the Gulf Stream where phosphate concentration in the upper 100 m was consistently <40 nM. The BV39 transect, from Bermuda to Puerto Rico, was entirely in the oligotrophic waters of the Sargasso Sea, and phosphate concentration in the upper 100 m was consistently <20 nM and often <10 nM.

3.2. Planktonic sources of IP-DAGs probed via stable isotope tracing

In the ^{13}C–bicarbonate light incubation, each IP-DAG class showed substantial isotopic enrichment above the controls, except for PG. The most enriched lipid in the ^{13}C–bicarbonate light incubation was MGDG, with a weighted average composite FA enrichment of 188‰ above the controls (Fig. 4). The average enrichment of SQDG was 52‰, the second highest enrichment in the ^{13}C–bicarbonate light incubation. The other IP-DAG classes – PE, PC, DGTA and DGCC – showed enrichment ranging from 20‰ to 40‰ in the ^{13}C–bicarbonate light incubation. The enrichment of DGTS was comparatively low at 15‰. In the ^{13}C–bicarbonate dark incubation, none of the IP-DAGs showed substantial enrichment.

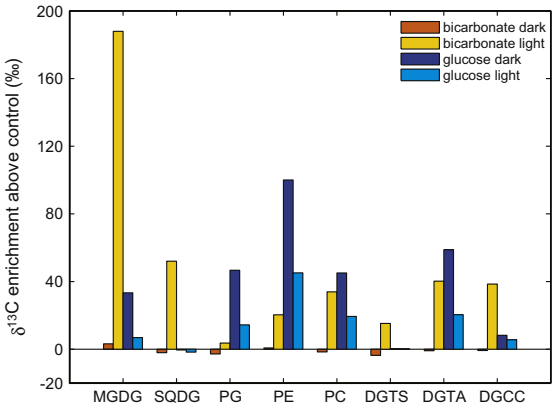

Fig. 4. Average isotopic enrichment of eight IP-DAGs from whole seawater incubated with ^{13}C-labeled substrates under light and dark conditions. Data are presented as enrichment above 27.6‰, the average δ^{13}C of the control samples with no isotope addition.

In the ^{13}C–glucose dark incubation, most IP-DAG classes showed substantial ^{13}C enrichment, with the exception of SQDG and DGTS (Fig. 4). The most enriched IP-DAG class was PE at 100‰, while enrichment of PG was 47‰. The other four IP-DAGs enriched in the ^{13}C–glucose incubations (MGDG, PC, DGTA and DGCC) had enrichment ranging from 8‰ to 59‰ in the ^{13}C–glucose dark incubation. For every IP-DAG class that showed enrichment in the ^{13}C–glucose dark incubation, it also showed enrichment in the ^{13}C–glucose light incubation but to a lesser extent. The six IP-DAGs isotopically enriched in the ^{13}C–glucose incubations were 2.8 ± 1.2 times more enriched in the dark incubation than in the light incubation.

In summary, three IP-DAGs showed ^{13}C enrichment exclusively with one substrate: SQDG and DGTS were enriched only in the ^{13}C–bicarbonate light incubation and PG was enriched only in the ^{13}C–glucose incubations. The other classes of IP-DAGs – MGDG, PE, PC, DGTA and DGCC – were enriched whether incubated with ^{13}C–bicarbonate or ^{13}C–glucose.

3.3. Planktonic sources of IP-DAGs probed by way of cell sorting flow cytometry

Samples were collected for cell sorting flow cytometry at two locations where phosphate concentration was high (Stations 4 and 7) and at six where phosphate concentration was low. Though *Prochlorococcus* was more abundant than *Synechococcus* at the stations with low phosphate, *Synechococcus* was present in a wider geographic range, extending to the nutrient-rich waters in the north. Heterotrophic bacteria were abundant throughout the transect, averaging 3.0×10^5 cells/ml, and showed no consistent correlation with geography or depth (Supplementary material, Table 1). Phospholipids and glycolipids were abundant in the extracts from the sorted cells, but betaine lipids were below the level of quantification and so were not included in the subsequent data analysis.

Five samples of *Prochlorococcus* were analyzed, all from the oligotrophic sampling sites, and on average 86% of the membrane lipids were glycolipids (Fig. 5). The most abundant IP-DAG was MGDG, averaging 50% of the membrane lipids, followed by SQDG (36%); the other glycolipid, DGDG, was <1%. Phospholipids comprised 14% of the membrane lipids on average; the most abundant was PG (9%), followed by PE (4%) and PC (<1%).

Seven samples of *Synechococcus* were analyzed; glycolipids composed an average of 82% of the membrane lipids and were dominated by MGDG at 55%, followed by SQDG at 20% (Fig. 5). In contrast to *Prochlorococcus*, most of the *Synechococcus* samples contained the glycolipid DGDG, averaging 7% of the detected lipids. The phospholipid contribution to the membrane was roughly split between PG and PE (avg. 9% and 8% of the total membrane lipids) with PC contributing <1% (Fig. 5).

The membrane composition of the cyanobacteria (average of five samples of *Prochlorococcus* and seven of *Synechococcus*) averaged 16% phospholipids and 84% glycolipids for all locations (Fig. 6a). For *Synechococcus*, the difference in membrane composition between the samples from high and low phosphate stations was striking, the two samples from high phosphate locations having an average of 50% glycolipids (Fig. 6), and the five from low phosphate locations having an average of 94% glycolipids. Combining the data from all ten samples of cyanobacteria (*Prochlorococcus* and *Synechococcus*) for low phosphate locations, glycolipids comprised 90% of the membrane lipids (Fig. 6).

Over the eight samples of heterotrophic bacteria, the average membrane composition was 70% phospholipids and 30% glycolipids (Figs. 5 and 6). The phospholipids in the heterotrophic bacteria were roughly equally distributed between PG, PE, and PC (25%, 19% and 26%), while glycolipids were almost exclusively MGDG (27%). The membrane composition of heterotrophic bacteria was quite different between the high and low phosphate locations, with phospholipids averaging 97% of the membrane in the two samples from high phosphate locations and 62% in the six samples from low phosphate locations (Fig. 6).

In summary, the extracts from *Prochlorococcus*, *Synechococcus* and heterotrophic bacteria sorted by way of flow cytometry demonstrated broad differences in the membrane composition between the cyanobacteria and the heterotrophic bacteria, as well as differences in membrane composition between samples from locations with low or high phosphate concentration.

3.4. Heterotrophic bacterial sources of IP-DAGs probed by way of regrowth incubations

In order to directly examine the link between the growth of heterotrophic bacteria and the production of IP-DAGs, a "regrowth" experiment was set up with 90% filtered (0.2 μm) seawater and

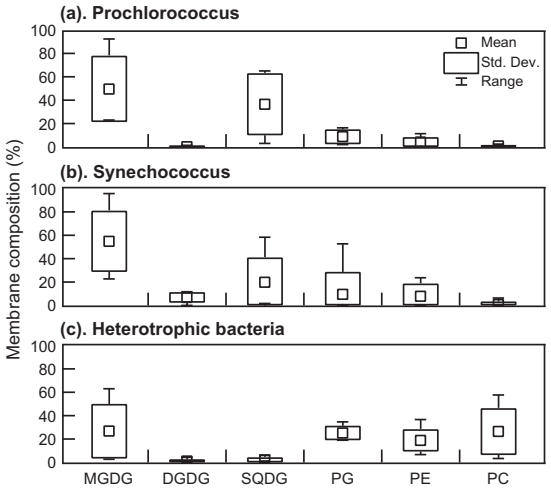

Fig. 5. Average IP-DAG content of *Prochlorococcus* (a), *Synechococcus* (b) and heterotrophic bacteria (c) from samples collected across the North Atlantic and sorted by way of flow cytometry prior to lipid extraction.

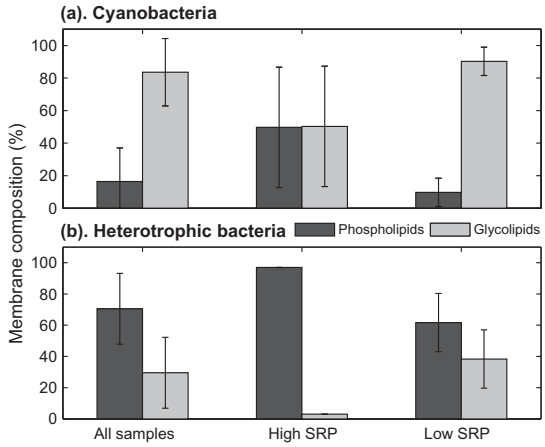

Fig. 6. Relative amounts of glycolipids and phospholipids in cyanobacteria (a) and heterotrophic bacteria (b), as an average of all samples ($n = 12$ for cyanobacteria, $n = 8$ for heterotrophic bacteria), locations with high SRP (>250 nM, $n = 2$, $n = 2$) and locations with low SRP (<40 nM, $n = 10$, $n = 6$). Error bars are ± one standard deviation.

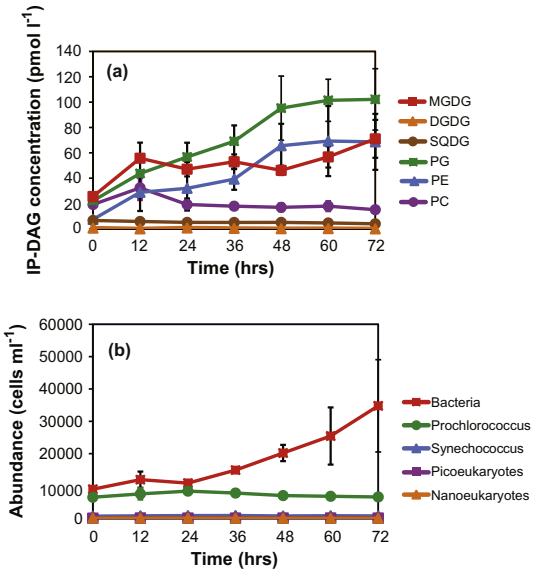

Fig. 7. IP-DAG concentration (a) and cell abundance (b) over a 72 h regrowth incubation. Error bars are standard deviation of single analyses from triplicate incubations.

10% whole sea, which were incubated in the dark to target growth of heterotrophic bacteria. With reduced grazing pressure and unaltered ambient nutrients, the heterotrophic bacterial abundance increased from 9.0×10^3 cells/ml to 3.5×10^4 cells/ml over 3 days, while the abundance of *Prochlorococcus*, *Synechococcus* and eukaryotes remained very low and constant (Fig. 7). Concurrent analysis of IP-DAGs from the whole community (all cells >0.2 μm) showed that the abundance of PC, DGDG and SQDG also remained relatively constant, while MGDG, PG and PE increased (Fig. 7). Heterotrophic bacteria abundance was significantly positively correlated with MGDG, PG and PE concentration (R^2 0.45, 0.44 and 0.53 respectively, $p < 0.05$).

4. Discussion

Our goal was to determine the microbial sources of the most abundant classes of IP-DAGs in the North Atlantic. Any class of IP-DAG shown to be unique to a microbial group offers the promise of being applied in future studies as a biomarker for that group. However, it is important to note that the three approaches we applied, while complementary, yield information on the sources of IP-DAGs from operationally defined groups of plankton whose definitions vary according to the sampling method. In addition, the study spanned a range of locations. Thus some disagreement in the sources of IP-DAGs identified using the different approaches was expected. For example, the organisms that incorporated ^{13}C into IP-DAGs from ^{13}C–glucose were not necessarily identical to the heterotrophic bacteria isolated via cell sorting flow cytometry. Indeed, some phytoplankton species are known to take up glucose, while some heterotrophic bacteria cannot (Neilson and Lewin, 1974; Alonso-Sáez and Gasol, 2007; Schwalbach et al., 2010). Similarly, the heterotrophic bacteria isolated via flow cytometry were not necessarily identical to those heterotrophic bacteria that grew in the regrowth incubations; it has been reported that the communities of heterotrophic bacteria that emerge in these types of incubations may differ from the initial inoculums (Fuchs et al., 2000; Carlson et al., 2002; Yokokawa et al., 2004). With these qualifications in mind, we drew on the data provided by these different approaches in order to form a consensus, where possible, on sources of classes of IP-DAGs.

4.1. Microbial sources of IP-DAGs

4.1.1. SQDG

The ^{13}C enrichment of SQDG from incubations amended with ^{13}C–bicarbonate in the light, along with the absence of ^{13}C enrichment in the ^{13}C–glucose incubations, suggests that this class of IP-DAG was produced primarily by photoautotrophs (Fig. 4). This is supported by the abundance of SQDG in cyanobacteria and lack of SQDG in heterotrophic bacteria collected via cell sorting flow cytometry (Fig. 5). Furthermore, SQDG was found not to increase with the abundance of heterotrophic bacteria in the regrowth incubations, as observed by Van Mooy et al. (2009). Previous studies have shown SQDG to be a significant fraction of the membrane lipids in cyanobacteria cultures (Benning, 1998; Wada and Murata, 1998; Van Mooy et al., 2006) and have identified a close association between SQDG abundance and cyanobacterial abundance in the ocean (Van Mooy and Fredricks, 2010). A survey of shotgun genomic sequences from the Sargasso Sea did not place gene sequences for SQDG synthesis (sqdB; Benning, 1998) in known heterotrophic clades (Van Mooy et al., 2006). Together, published work and our data support the conclusion that photoautotrophs are the nearly exclusive source of SQDG in the surface ocean.

4.1.2. DGTS

The betaine lipid DGTS was also isotopically enriched only in the ^{13}C–bicarbonate light incubation (Fig. 4), indicating that it too was produced exclusively by photoautotrophs. The ^{13}C enrichment of classes of IP-DAGs is indicative of the proportional rate at which the IP-DAG is turned over during biosynthesis (e.g. the quotient of the synthesis rate and the cellular concentration). The lower ^{13}C enrichment of DGTS than SQDG may be because DGTS turns over more slowly in the cell than SQDG as cellular maintenance repairs and replaces membrane lipids (White and Tucker, 1969; Zhang and Rock, 2008). Alternatively, DGTS could have been produced by a different set of photoautotrophs than SQDG and these organisms may have been turning over more slowly than those that dominate production of SQDG. The association of betaine lipids

with eukaryotic phytoplankton in previous studies (Kato et al., 1996; Van Mooy and Fredricks, 2010) supports the latter hypothesis, as eukaryotic phytoplankton likely have a lower growth rate than prokaryotic cyanobacteria (Furnas, 1990; Veldhuis et al., 1993). In addition, DGTS abundance was below our limit of quantification in both *Prochlorococcus* and *Synechococcus*. Betaine lipids were not measured in the regrowth incubation, but in a similar incubation conducted in the Sargasso Sea betaines were shown not to increase with increasing abundance of heterotrophic bacteria (Van Mooy et al., 2009). We therefore posit that eukaryotic phytoplankton are the primary source of DGTS in the surface ocean. Little is known of the functional role of DGTS in marine microbial cells, but the substantial difference in enrichment between DGTS and DGTA, with very similar structures (Fig. 1), indicates that these betaine lipids may be produced by distinct clades of phytoplankton. Indeed, few marine organisms are known to produce both compounds (Harwood, 1998; Van Mooy et al., 2006).

4.1.3. PG and PE

The phospholipid PG was substantially enriched only in the ^{13}C–glucose incubations (Fig. 4), indicating that it was probably produced primarily by heterotrophic bacteria. Importantly, it is the only IP-DAG that showed no appreciable enrichment in the ^{13}C–bicarbonate light incubation, precluding substantial synthesis of PG by photoautotrophs. In the heterotrophic bacteria isolated via flow cytometry, PG was a major lipid (Fig. 5), whereas in the cyanobacteria PG accounted for only a small fraction of the total IP-DAGs, particularly in low phosphate samples (Fig. 6); the average percentage of PG in cyanobacteria membranes was less than half that in heterotrophic bacteria membranes. This is consistent with previous work that established that, although PG is present in both heterotrophic bacteria (Oliver and Colwell, 1973; Van Mooy et al., 2006) and cyanobacteria (Wada and Murata, 1998; Sato et al., 2000a,b; Sato, 2004; Van Mooy et al., 2006), cyanobacteria contain little PG in environments were phosphate is scarce (Van Mooy et al., 2009). Given that heterotrophic bacteria generally outnumber cyanobacteria by an order of magnitude in the western North Atlantic (Cavender-Bares et al., 2001; Supplementary material, Table 1) we conclude that the vast majority of PG in the low phosphate waters of the Sargasso Sea originates from heterotrophic bacteria despite their somewhat smaller size. The increase in PG concentration, correlated with the increase in heterotrophic bacterial cells in the regrowth experiment (Fig. 7), lends further support to heterotrophic bacteria being the major source of PG.

Previous studies of cultures found that PE is absent from cyanobacteria membranes, but is abundant in heterotrophic bacteria membranes (Oliver and Colwell, 1973; Wada and Murata, 1998; Van Mooy et al., 2006). The membrane of *Pelagibacter ubique*, the most abundant heterotrophic bacterium in the Sargasso Sea, was shown to be composed solely of PE and PG (Van Mooy et al., 2009). Like these culture results, the flow cytometry sorted samples showed only minor amounts of PE in cyanobacteria and much more abundant PE in heterotrophic bacteria. Since PE has not been observed in any axenic culture of cyanobacteria (Wada and Murata, 1998), we suggest that the PE in the sorted *Prochlorococcus* and *Synechococcus* cells indicates that they might be contaminated with small amounts of heterotrophic bacteria, either due to nonspecific sorting inherent in our flow cytometry methods (sort purity ca. 98%; Section 2.4.1) or possibly due to misassignment of cells in the sorting process because of aggregation of cyanobacteria and heterotrophic bacteria (Malfatti and Azam, 2009). If so, this would also suggest that at least some of the PG in the sorted *Synechococcus* and *Prochlorococcus* could also have originated from heterotrophic bacteria.

The results of the 3 day regrowth incubation corroborate a heterotrophic bacterial source of PE: the increase in heterotrophic bacterial cells correlated with an increase in PE abundance (Fig. 7). This, along with data from flow cytometry sorted cells (Fig. 5), suggests that production of PE may be dominated by heterotrophic bacteria. However, despite the relative lack of PE in cyanobacteria, PE was isotopically enriched in both the ^{13}C–glucose incubations and the ^{13}C–bicarbonate light incubations (Fig. 4), consistent with production by both heterotrophic bacteria and photoautotrophs. However, in comparing the results of the flow cytometry sorted samples and stable isotope incubations, it is important to note that the sorted *Prochlorococcus*, *Synechococcus* and heterotrophic bacteria cells do not represent the full microbial community in the environment. In contrast, the isotopic enrichments in the stable isotope incubations represent production by all the microbes (>0.2 μm) in the environment, which includes pico- and nano-eukaryotes and larger organisms from which lipids were not sampled in the cell sorting flow cytometry. Therefore, the isotopic enrichment of PE in the ^{13}C–bicarbonate light incubation may represent production of PE by eukaryotic phytoplankton. Alternatively, it may represent secondary enrichment, whereby autotrophic organisms took up the ^{13}C–bicarbonate and produced ^{13}C-labeled dissolved organic carbon that was subsequently taken up by heterotrophic bacteria and incorporated into PE.

4.1.4. MGDG

In the ^{13}C–bicarbonate light incubation, MGDG was the most enriched class of IP-DAG. However, it was also enriched in the ^{13}C–glucose incubations, suggesting that it was produced by both photoautotrophs and heterotrophic bacteria. Indeed, the flow cytometry sorted samples demonstrated that MGDG was abundant in both cyanobacteria and heterotrophic bacteria. In the regrowth incubation MGDG abundance increased with increasing heterotrophic bacterial cells, reinforcing the idea that MGDG was a substantial component of heterotrophic bacteria membranes in the oligotrophic Sargasso Sea. These results differ from culture studies, mostly conducted with phosphate-replete media, which have found heterotrophic bacteria membranes to be exclusively phospholipids (Kates, 1964; Oliver and Colwell, 1973; Van Mooy et al., 2006, 2009).

4.1.5. Other IP-DAGs

In the flow cytometry sorted samples, PC was abundant in heterotrophic bacteria and not in cyanobacteria (Fig. 5), in agreement with previous culture studies (Goldfine, 1972; Wada and Murata, 1998; Van Mooy et al., 2006). However, the regrowth incubations suggested that PC was not a major component of heterotrophic bacteria (Fig. 7). Yet PC is also known to be present in eukaryotic phytoplankton (Kato et al., 1996; Guschina and Harwood, 2006; Van Mooy et al., 2009), so it was not surprising that the PC was enriched in incubations with both ^{13}C–bicarbonate and ^{13}C–glucose (Fig. 4). Thus, we reach the same conclusion as Van Mooy and Fredricks (2010): potential planktonic origins of PC in the surface ocean are diverse, although eukaryotic phytoplankton is likely to be a dominant source.

The glycolipid DGDG was scarce in the flow cytometry sorted samples and regrowth incubation, and its abundance was too low to be measured in the stable isotope incubations, indicating it makes a minimal contribution to the membranes of marine microbes. This is in accord with studies that have found low concentrations of DGDG in surface seawater relative to the other glycolipids and phospholipids (Van Mooy and Fredricks, 2010).

In the flow cytometry sorted samples, betaine lipid levels were below our level of quantification in the prokaryotic groups collected; previous work would suggest that betaine lipids are not abundant in either *Prochlorococcus*, *Synechococcus* or heterotrophic bacteria (Van Mooy et al., 2009; Van Mooy and Fredricks, 2010). However, betaine lipids have been shown to have similar concentrations to glycolipids in seawater (Van Mooy and Fredricks, 2010), and presumably originate from a eukaryotic source (Kato et al., 1996; Van Mooy et al., 2009). The enrichment in incubations with

both ^{13}C–glucose and ^{13}C–bicarbonate indicate that DGTA and DGCC were probably produced by both heterotrophic bacteria and autotrophs. Therefore, based on the available information, we conclude that these two betaine lipids are unlikely to originate from any single group of plankton.

4.2. Stable isotope enrichment for light vs. dark incubation

The ^{13}C–bicarbonate dark incubation showed no isotopic enrichment of any of the lipids (Fig. 4), despite recent findings that heterotrophic bacteria can be responsible for substantial uptake of bicarbonate in the dark under some conditions (Alonso-Sáez et al., 2010). Recently several studies have focused on the uptake of dissolved inorganic carbon in the deep sea (Jost et al., 2008; Hansman et al., 2009; Varela et al., 2011). However, these studies were conducted with seawater rich in reduced inorganic nutrients (e.g. NH_4^+, H_2S), whereas our incubations were conducted with nutrient-depleted surface waters where highly oxidizing conditions prevail. If chemolithoautotrophs were present in our incubations, we suggest that other resident heterotrophic bacteria and phytoplankton would outcompete prokaryotic chemolithoautotrophs for nutrients, limiting their ability to take up bicarbonate in our dark incubations. Given the lack of ^{13}C enrichment of IP-DAGs in the ^{13}C–bicarbonate dark incubation, we can reasonably conclude that photoautotrophs were responsible for the observed uptake of ^{13}C–bicarbonate in our light incubation.

For every IP-DAG isotopically enriched in the ^{13}C–glucose incubations (MGDG, PG, PE, PC, DGTA, and DGCC), the ^{13}C enrichment in the dark incubation was roughly twofold more than in the light. There are two potential mechanisms to explain this pattern: (i) in the light, the photoautotrophs produced organic compounds that diluted the ^{13}C-labeled glucose in a broader pool of bioavailable organic carbon or (ii) in the light, the active photoautotrophs outcompeted the heterotrophic bacteria for nutrients (phosphate, NH_3, etc.), which caused the heterotrophic bacteria to grow more slowly and incorporate less ^{13}C–glucose. Although this isotopic discrepancy is surprisingly uniform across all these classes of IP-DAGs, at this time we do not have evidence to support or refute either of these two mechanisms.

4.3. Influence of phosphate concentration on membrane composition

It has recently been shown that the ability to substitute non-phosphorus membrane lipids for phospholipids may provide an advantage to organisms in phosphorus-limited environments, and that this ability may be confined to specific microbial groups (Van Mooy et al., 2009). Cyanobacteria and eukaryotic plankton have been shown to be capable of lipid substitution (Benning et al., 1995; Van Mooy et al., 2009), while heterotrophic bacteria have been hypothesized to be incapable of substitution. It would therefore be expected that in low phosphate environments, such as the Sargasso Sea, cyanobacteria would produce non-phosphorus lipids, while heterotrophic bacteria would produce primarily phospholipids. While it was demonstrated here that heterotrophic bacteria almost certainly dominate the production of the phospholipids PG and PE, it was also shown that the fraction of phospholipids varied with phosphate concentration for both cyanobacteria and heterotrophic bacteria. The IP-DAGs of heterotrophic bacteria in the high phosphate samples were almost exclusively phospholipids, whereas in the low phosphate samples MGDG composed more than one third of the total measured lipids (Fig. 6). Furthermore, the regrowth incubations also suggested that heterotrophic bacteria were a source of MGDG (Fig. 7). These results might indicate that heterotrophic bacteria are capable of substituting MGDG for phospholipids in oligotrophic surface waters as a low phosphorus adaptive strategy in a fashion similar to the substitution of SQDG for PG in cyanobacteria and betaine lipids for PC in eukaryotic plankton (Benning, 1998; Sato et al., 2000a,b; Van Mooy et al., 2009). In contrast to the other proposed lipid substitutions, the ionic charge of MGDG is not similar to the phospholipids it seems to be replacing; in the pH range of seawater, MGDG is neutral, while PG is anionic and PE and PC are zwitterionic. The ionic charge of IP-DAGs is thought to be important for maintaining membrane function. Whether or not a "substitution" mechanism is at work, it seems clear that MGDG can be a significant component of heterotrophic bacteria membranes in phosphorus-limited surface ocean environments, in contrast to previous work (Van Mooy et al., 2009; Van Mooy and Fredricks, 2010).

In high phosphate locations, north of the Gulf Stream, *Prochlorococcus* was not abundant enough for collection by cell-sorting flow cytometry, so the composition of cyanobacterial membranes in the high phosphate region could only be assessed for *Synechococcus*; this distribution of *Prochlorococcus* and *Synechococcus* is similar to previous observations (Cavender-Bares et al., 2001). The IP-DAGs of *Synechococcus* in the high phosphate locations were roughly half glycolipids and half phospholipids, while in the low phosphate locations the IP-DAGs were almost entirely glycolipids. In accord with the established sulfolipid substitution hypothesis (Benning, 1998; Yu et al., 2002; Van Mooy et al., 2006), the SQDG fraction of cyanobacterial membranes in the low phosphate samples was more than fivefold greater than in the high phosphate samples, reinforcing the conditions of phosphate limitation in the Sargasso Sea and the utility of IP-DAGs as indicators of the concomitant physiological response.

5. Conclusions

There are significant differences in the membrane composition between cyanobacteria and heterotrophic bacteria in the western North Atlantic. The membranes of cyanobacteria were predominantly glycolipids, while those of heterotrophic bacteria were predominantly, though not exclusively, phospholipids. Specifically, the production of the phospholipid PG, and potentially also PE, was dominated by heterotrophic bacteria, while production of the glycolipid SQDG was dominated by photoautotrophs. Production of the betaine lipid DGTS was also dominated by photoautotrophs, though apparently not *Prochlorococcus* or *Synechococcus*. These findings indicate that these classes of IP-DAG molecules could be important biomarkers for different groups of plankton. In particular, by more thoroughly constraining the dominant planktonic sources of IP-DAGs, our findings provide additional support for combining isotope tracing methods and IP-DAG analysis to determine growth rates of different groups of plankton in the upper ocean (e.g. Van Mooy et al., 2008).

Acknowledgments

We thank K. Longnecker and J. Ossolinski for contributions to the experiments conducted at sea. Likewise, we thank the crews of the R/V Oceanus and R/V Atlantic Explorer. We are also extremely grateful to J. Casey for diligence and dedication in the course of optimizing the cell-sorting flow cytometry methods. Finally, we thank C. Johnson and H. Fredricks for assistance with lipid analysis and two anonymous reviewers for helpful comments.

Appendix A. Supplementary material

Supplementary data associated with this article can be found, in the online version, at doi:10.1016/j.orggeochem.2011.05.003.

Associate Editor—**K.-U. Hinrichs**

References

Alonso-Sáez, L., Gasol, J.M., 2007. Seasonal variations in the contributions of different bacterial groups to the uptake of low-molecular-weight compounds in Northwestern Mediterranean Coastal Waters. Applied and Environmental Microbiology 73, 3528–3535.

Alonso-Sáez, L., Galand, P.E., Casamayor, E.O., Pedrós-Alió, C., 2010. High bicarbonate assimilation in the dark by Arctic bacteria. The ISME Journal 4, 1581–1590.

Benning, C., 1998. Biosynthesis and function of the sulfolipid sulfoquinovosyl diacylglycerol. Annual Review of Plant Physiology and Plant Molecular Biology 49, 53–75.

Benning, C., Huang, Z.-H., Gage, D.A., 1995. Accumulation of a novel glycolipid and a betaine lipid in cells of *Rhodobacter sphaeroides* grown under phosphate limitation. Archives of Biochemistry and Biophysics 317, 103–111.

Bligh, E.G., Dyer, W.J., 1959. A rapid method of total lipid extraction and purification. Canadian Journal of Physiology and Pharmacology 37, 911–917.

Carlson, C.A., Giovannoni, S.J., Hansell, D.A., Goldberg, S.J., Parsons, R., Otero, M.P., Vergin, K., Wheeler, B.R., 2002. Effect of nutrient amendments on bacterioplankton production, community structure, and DOC utilization in the northwestern Sargasso Sea. Aquatic Microbial Ecology 30, 19–36.

Casey, J.R., Lomas, M.W., Michelou, V.K., Dyhrman, S.T., Orchard, E.D., Ammerman, J.W., Sylvan, J.B., 2009. Phytoplankton taxon-specific orthophosphate (Pi) and ATP utilization in the western subtropical North Atlantic. Aquatic Microbial Ecology 58, 31–44.

Cavender-Bares, K.K., Karl, D.M., Chisholm, S.W., 2001. Nutrient gradients in the western North Atlantic Ocean: relationship to microbial community structure and comparison to patterns in the Pacific Ocean. Deep-Sea Research I 48, 2373–2395.

Ertefai, T.F., Fisher, M.C., Fredricks, H.F., Lipp, J.S., Pearson, A., Birgel, D., Udert, K.M., Cavanaugh, C.M., Gschwend, P.M., Hinrichs, K.-U., 2008. Vertical distribution of microbial lipids and functional genes in chemically distinct layers of a highly polluted meromictic lake. Organic Geochemistry 39, 1572–1588.

Fuchs, B.M., Zubkov, M.V., Sahm, K., Burkill, P.H., Amann, R., 2000. Changes in community composition during dilution cultures of marine bacterioplankton as assessed by flow cytometric and molecular biological techniques. Environmental Microbiology 2, 191–201.

Furnas, M.J., 1990. In situ growth rates of marine phytoplankton: approaches to measurement, community and species growth rates. Journal of Plankton Research 12, 1117–1151.

Goldfine, H., 1972. Comparative aspects of bacterial lipids. Advances in Microbial Physiology 8, 1–58.

Goodman, K., 1998. Hardware modifications to an isotope ratio mass spectrometer continuous-flow interface yielding improved signal, resolution, and maintenance. Analytical Chemistry 70, 833–837.

Guindulain, T., Comas, J., Vives-Rego, J., 1997. Use of nucleic acid dyes SYTO-13, TOTO-1, and YOYO-1 in the study of *Escherichia coli* and marine prokaryotic populations by flow cytometry. Applied and Environmental Microbiology 63, 4608–4611.

Guschina, I.A., Harwood, J.L., 2006. Lipids and lipid metabolism in eukaryotic algae. Progress in Lipid Research 45, 160–186.

Hansman, R.L., Griffin, S., Watson, J.T., Druffel, E.R.M., Ingalls, A.E., Pearson, A., Aluwihare, L., 2009. The radiocarbon signature of microorganims in the mesopelagic ocean. Proceedings of the National Academy of Sciences USA 106, 6513–6518.

Harwood, J.L., 1998. Membrane lipids in algae. In: Siegenthaler, P.-A., Murata, N. (Eds.), Lipids in Photosynthesis: Structure, Function and Genetics. Kluwer Academic Publishers, Netherlands, pp. 53–64.

Jost, G., Zubkov, M.V., Yakushev, E., Labrenz, M., Jürgens, K., 2008. High abundance and dark CO_2 fixation of chemolithoautotrophic prokaryotes in anoxic waters of the Baltic Sea. Limnology and Oceanography 53, 14–22.

Karl, D.M., Tien, G., 1992. MAGIC: a sensitive and precise method for measuring dissolved phosphorus in aquatic environments. Limnology and Oceanography 37, 105–116.

Kates, M., 1964. Bacterial lipids. Advances in Lipid Research 2, 17–90.

Kato, M., Sakai, M., Adachi, K., Ikemoto, H., Sano, H., 1996. Distribution of betaine lipids in marine algae. Phytochemistry 42, 1341–1345.

King, J.D., White, D.C., Taylor, C.W., 1977. Use of lipid composition and metabolism to examine structure and activity of estuarine detrital microflora. Applied and Environmental Microbiology 33, 1177–1183.

Malfatti, F., Azam, F., 2009. Atomic force microscopy reveals microscale networks and possible symbioses among pelagic marine bacteria. Aquatic Microbial Ecology 58, 1–14.

Neilson, A.H., Lewin, R.A., 1974. The uptake and utilization of organic carbon by algae: an essay in comparative biochemistry. Phycologia 13, 227–264.

Oliver, J.D., Colwell, R.R., 1973. Extractable lipids of gram-negative marine bacteria: phospholipid composition. Journal of Bacteriology 114, 897–908.

Rütters, H., Sass, H., Cypionka, H., Rullkötter, J., 2002. Phospholipid analysis as a tool to study complex microbial communities in marine sediments. Journal of Microbiological Methods 48, 149–160.

Sakurai, I., Shen, J.-R., Leng, J., Ohashi, S., Kobayashi, M., Wada, H., 2006. Lipids in oxygen-evolving photosystem II complexes of cyanobacteria and higher plants. Journal of Biochemistry 140, 201–209.

Sato, N., 2004. Roles of the acidic lipids sulfoquinovosyl diacylglycerol and phosphatidylglycerol in photosynthesis: their specificity and evolution. Journal of Plant Research 117, 495–505.

Sato, N., Hagio, M., Wada, H., Tsuzuki, M., 2000a. Environmental effects on acidic lipids of thylakoid membranes. In: Harwood, J.L., Quinn, P.J. (Eds.), Recent Advances in the Biochemistry of Plant Lipids. Portland Press, London, pp. 912–914.

Sato, N., Hagio, M., Wada, H., Tsuzuki, M., 2000b. Requirement of phosphatidylglycerol for photosynthetic function in thylakoid membranes. Proceedings of the National Academy of Sciences USA 97, 10655–10660.

Schubotz, F., Wakeham, S.G., Lipp, J.S., Fredricks, H.F., Hinrichs, K.-U., 2009. Detection of microbial biomass by intact polar membrane lipid analysis in the water column and surface sediments of the Black Sea. Environmental Microbiology 11, 2720–2734.

Schwalbach, M.S., Tripp, H.J., Steindler, L., Smith, D.P., Giovannoni, S.J., 2010. The presence of the glycolysis operon in SAR11 genomes is positively correlated with ocean productivity. Environmental Microbiology 12, 490–500.

Sturt, H.F., Summons, R.E., Smith, K., Elvert, M., Hinrichs, K.-U., 2004. Intact plar membrane lipids in prokaryotes and sediments deciphered by high-performance liquid chromatography/electrospray ionization multistage mass spectrometry – new biomarkers for biogeochemistry and microbial ecology. Rapid Communications in Mass Spectrometry 18, 617–628.

Van Mooy, B.A.S., Rocap, G., Fredricks, H.F., Evans, C.T., Devol, A.H., 2006. Sulfolipids dramatically decrease phosphorus demand by picocyanobacteria in oligotrophic environments. Proceedings of the National Academy of Sciences USA 103, 8607–8612.

Van Mooy, B.A.S., Moutin, T., Duhamel, S., Rimmelin, P., Van Wambeke, F., 2008. Phospholipid synthesis rates in the eastern subtropical South Pacific Ocean. Biogeosciences 5, 133–139.

Van Mooy, B.A.S., Fredricks, H.F., Pedler, B.E., Dyhrman, S.T., Karl, D.M., Koblízek, M., Lomas, M.W., Mincer, T.J., Moore, L.R., Moutin, T., Rappé, M.S., Webb, E.A., 2009. Phytoplankton in the ocean substitute phospholipids in response to phosphorus scarcity. Nature 458, 69–72.

Van Mooy, B.A.S., Fredricks, H.F., 2010. Bacterial and eukaryotic intact polar lipids in the eastern subtropical South Pacific: water-column distribution, planktonic sources, and fatty acid composition. Geochimica Cosmochimica Acta 74, 6499–6516.

Varela, M.M., van Aken, H.M., Sintes, E., Reinthaler, T., Herndl, G.J., 2011. Contribution of *Crenarchaeota* and *Bacteria* to autotrophy in the North Atlantic interior. Environmental Microbiology. doi:10.1111/j.1462-2920.2011.02457.x.

Veldhuis, M.J.W., Kraay, G.W., Gieskes, W.W.C., 1993. Growth and fluorescence characteristics of ultraplankton on a north-south transect in the eastern North Atlantic. Deep-Sea Research II 40, 609–626.

Vogel, G., Eichenberger, W., 1992. Betaine lipids in lower plants. Biosynthesis of DGTS and DGTA in *Ochromonas danica* (Chrysophyceae) and the possible role of DGTS in lipid metabolism. Plant Cell Physiology 33, 427–436.

Wada, H., Murata, N., 1998. Membrane lipids in cyanobacteria. In: Siegenthaler, P.-A., Murata, N. (Eds.), Lipids in Photosynthesis: Structure, Function and Genetics. Kluwer Academic Publishers, Netherlands, pp. 65–81.

Wakeham, S.G., Hedges, J.I., Lee, C., Peterson, M.L., Hernes, P.J., 1997. Compositions and transport of lipid biomarkers through the water column surficial sediments of the equatorial Pacific Ocean. Deep-Sea Research II 44, 2131–2162.

White, D.C., Tucker, A.N., 1969. Phospholipid metabolism during bacterial growth. Journal of Lipid Research 10, 220–233.

White, D.C., Bobbie, R.J., Morrison, S.J., Oosterhof, D.K., Taylor, C.W., Meeter, D.A., 1977. Determination of microbial activity of estuarine detritus by relative rates of lipid biosymthesis. Limnology and Oceanography 22, 1089–1099.

Yokokawa, T., Nagata, T., Cottrell, M.T., Kirchman, D.L., 2004. Growth rate of the major phylogenetic bacterial groups in the Delaware estuary. Limnology and Oceanography 49, 1620–1629.

Yu, B., Xu, C., Benning, C., 2002. Arabidopsis disrupted in SQD2 encoding sulfolipid synthase is impaired in phosphate-limited growth. Proceedings of the National Academy of Sciences USA 99, 5732–5737.

Zhang, Y.-M., Rock, C.O., 2008. Membrane lipid homeostatis in bacteria. Nature Reviews Microbiology 6, 222–233.

Supplementary Material
Table 1

Cruise	Experiment	Station/ CTD cast #	Latitude (°N)	Longitude (°W)	Date	Depth (m)	SRP (nM)	Heterotrophic bacteria (cells/mL)	*Prochlorococcus* (cells/mL)	*Synechococcus* (cells/mL)	Picoeukaryotes (cells/mL)	Nanoeukaryotes (cells/mL)
Oc443	**Flow cytometry**	St.4*	41.896	68.626	Apr 4 2008	5	400	294126	n.d.	5108	7653	59
						10	500	288102	n.d.	5187	8025	0
						15	400	273595	n.d.	4954	7443	8
						20	400	233120	n.d.	5271	7639	55
						30	400	209496	n.d.	4317	6568	24
						120	700	97474	n.d.	664	307	0
	Flow cytometry	St.7*	42	65	Apr 6 2008	5	376.6	345651	n.d.	2843	10493	86
						10	362.9	345513	n.d.	7709	9119	85
						15	365.5	353768	n.d.	2896	9028	46
						20	374.1	360808	n.d.	2625	9256	69
						30	382.0	336512	n.d.	3035	9604	15
						120	444.6	143765	n.d.	353	425	0
	Flow cytometry	St.11*	38	65	Apr 8 2008	5	13.0	112518	21849	19141	4483	0
						20†	6.5	856790	24138	19942	4399	19
						60	36.3	1001141	21633	26164	6935	29
						100‡	12.3	572683	8251	16042	6661	21
						200†	30.5	818746	2658	7243	3649	0
	Stbl. isotope incubation	St.13.5	35.5	65	Apr 9 2008	20	4.7	473996	64540	37695	3903	59
BV39	**Flow cytometry**	CTD1**	33.657	64.144	Oct 21 2007	5	2.05	298175	70672	6413	465	36
						20	4.68	371086	70533	6520	740	153
						40	0.07	298699	71964	7220	485	61
						80	0.07	139620	147519	1857	1250	109
	Flow cytometry	CTD4*	31.665	64.165	Oct 22 2007	5	0.50	299257	60528	8180	557	106
						20	0.50	288530	59059	8148	493	21
						40	0.50	301444	58481	7649	576	102
	Flow cytometry	CTD8**	29.668	64.470	Oct 22 2007	5	1.13	134988	7131	8101	548	72
						20	1.05	148887	6728	8707	490	109
						40	0.50	313682	59513	3830	614	63
						115	1.29	70122	40694	9	1140	117
	Flow cytometry	CTD12**	27.673	64.773	Oct 23 2007	5	1.21	177983	12545	7519	398	96
						20	0.50	178785	9965	7581	367	62
						40	1.69	239306	26421	7655	474	96
						120	4.57	80006	49331	0	944	52
	Flow cytometry	CTD15**	25.673	65.060	Oct 24 2007	5	7.06	177663	10304	7636	370	110
						20	3.77	179491	9621	8172	464	147
						40	3.69	177597	9609	7715	406	76
						110	16.19	108056	86781	4660	545	86
	Regrowth incubation	CTD3	32.610	64.100	Oct 21 2007	5		314127	64601	6893	763	249

*samples from all depths were combined at each of these stations to be flow cytometry samples Oc443-St.4, Oc443-St.7, Oc443-St.11, and BV39-CTD4

**these locations were combined by depth to be flow cytometry samples BV39-5m, BV39-20m, BV39-40m and BV39-deep chlorophyll maximum

†depths given are for flow cytometry sorted samples, cell counts were measured at 40 and 160m respectively

‡depth given is for flow cytometry sorted samples, SRP and cell counts were measured at 120m

n.d.=cells were not detected, SRP=soluble reactive phosphorus

Chapter 4

Gradients in intact polar diacylglycerolipids across the Mediterranean Sea are related to phosphate availability

This chapter was originally published in Biogeosciences by Copernicus Publications and is reproduced here with their permission

Gradients in intact polar diacylglycerolipids across the Mediterranean Sea are related to phosphate availability. *Biogeosciences*. K.J. Popendorf, T. Tanaka, M. Pujo-Pay, A. Lagaria, C. Courties, P. Conan, L. Oriol, L.E. Sofen, T. Moutin, B.A.S. Van Mooy. 2011. 8, 3733-3745. doi: 10.5194/bg-8-3733-2011

Biogeosciences, 8, 3733–3745, 2011
www.biogeosciences.net/8/3733/2011/
doi:10.5194/bg-8-3733-2011

Biogeosciences

Gradients in intact polar diacylglycerolipids across the Mediterranean Sea are related to phosphate availability

K. J. Popendorf[1], T. Tanaka[2,*,], M. Pujo-Pay[3,4], A. Lagaria[5,6], C. Courties[7,8], P. Conan[3,4], L. Oriol[3,4], L. E. Sofen[1], T. Moutin[2], and B. A. S. Van Mooy[1]**

[1]Dept. of Marine Chemistry and Geochemistry, Woods Hole Oceanographic Institution, MS #4, Woods Hole, MA 02543, USA
[2]Université de la Méditerranée, CNRS, Laboratoire d'Océanographie Physique et Biogéochimique, UMR 6535, Centre d'Océanologie de Marseille, Campus de Luminy, Case 901, 13288 Marseille cedex 09, France
[3]CNRS, UMR 7621, LOMIC, Observatoire Océanologique, 66651 Banyuls/mer, France
[4]UPMC Univ Paris 06, UMR 7621, LOMIC, Observatoire Océanologique, 66651 Banyuls/mer, France
[5]INSU-CNRS, Laboratoire d'Océanologie et des Géosciences, UMR 8187, Université Lille Nord de France, ULCO, 62930 Wimereux, France
[6]Hellenic Centre for Marine Research, Inst. of Oceanography, 71003 Heraklion, Crete, Greece
[7]CNRS, UMS 2348, Observatoire Océanologique, 66651 Banyuls/mer, France
[8]UPMC Univ Paris 06, Laboratoire ARAGO, Observatoire Océanologique, 66651 Banyuls/mer, France
[*]now at: INSU-CNRS, Laboratoire d'Océanographie de Villefranche, UMR 7093, 06230 Villefranche-sur-Mer, France
[**]now at: Université Pierre et Marie Curie-Paris VI, Laboratoire d'Océanographie de Villefranche, UMR 7093, 06230 Villefranche-sur-Mer, France

Received: 31 July 2011 – Published in Biogeosciences Discuss.: 8 August 2011
Revised: 1 December 2011 – Accepted: 2 December 2011 – Published: 20 December 2011

Abstract. Intact polar membrane lipids compose a significant fraction of cellular material in plankton and their synthesis imposes a substantial constraint on planktonic nutrient requirements. As a part of the Biogeochemistry from the Oligotrophic to the Ultraoligotrophic Mediterranean (BOUM) cruise we examined the distribution of several classes of intact polar diacylglycerolipids (IP-DAGs) across the Mediterranean, and found that phospholipid concentration as a percent of total lipids correlated with phosphate concentration. In addition, the ratios of non-phosphorus lipids to phospholipids – sulfoquinovosyldiacylglycerol (SQDG) to phosphatidylglycerol (PG), and betaine lipids to phosphatidylcholine (PC) – were also found to increase from west to east across the Mediterranean. Additionally, microcosm incubations from across the Mediterranean were amended with phosphate and ammonium, and in the course of several days nutrient amendments elicited a shift in the ratios of IP-DAGs. These experiments were used to assess the relative contribution of community shifts and physiological response to the observed change in IP-DAGs across the Mediterranean. The ratio of SQDG to chlorophyll-*a* was also explored as an indicator of phytoplankton response to nitrogen availability. This study is the first to demonstrate the dynamic response of membrane lipid composition to changes in nutrients in a natural, mixed planktonic community.

Correspondence to: K. J. Popendorf (kpopendorf@whoi.edu)

1 Introduction

Lipids form the membranes of cells and comprise a substantial fraction of planktonic carbon and phosphorus (Wakeham et al., 1997; Van Mooy and Fredricks, 2010). As such, lipids play key roles in the biogeochemical cycles of carbon and phosphorus in the ocean (Suzumura and Ingall 2001), and their synthesis poses a significant cellular nutrient requirement (Van Mooy et al., 2008, 2009). Bacterial and eukaryotic marine membranes are composed mainly of intact polar diacylglycerolipids (IP-DAGs) and these compounds are valuable tools for the study of microbes in the environment (Rütters et al., 2002; Sturt et al., 2004). These IP-DAGs are classified by the structure of their headgroups, which are differentiated by containing phosphorus, nitrogen, sulfur, sugars, or some combination of these (Guschina and Harwood, 2006; Kato et al., 1996; Oliver and Colwell, 1973; Sato,

Published by Copernicus Publications on behalf of the European Geosciences Union.

1992; Van Mooy and Fredricks, 2010). The relative abundance of different headgroups within a membrane contributes to the cellular demand for limiting nutrients. Because phosphorus is in low supply in much of the ocean and is in high cellular demand, the constraint imposed by production of phospholipids is nontrivial for marine microbes (Van Mooy et al., 2006, 2008, 2009).

Different groups of plankton contain different arrays of IP-DAG headgroups (Popendorf et al., 2011; Van Mooy et al., 2006), such that a community dominated by phytoplankton could be expected to have a different total IP-DAG composition than a community dominated by heterotrophic bacteria. Some types of plankton have been shown to be capable of substituting non-phosphorus lipids for phospholipids in conditions of phosphorus stress (Benning et al., 1993, 1995; Martin et al., 2011; Minnikin et al., 1974; Van Mooy et al., 2009), adjusting the composition of their membrane as a physiological response to nutrient conditions. This physiological response has been demonstrated in culture, but has not previously been observed in a natural, mixed planktonic community. It has been observed that the ratios of non-phosphorus lipids to phospholipids in the water column were lower in the phosphate-replete South Pacific and higher in the phosphate-depleted Sargasso Sea (Van Mooy et al., 2009), but we posit that this difference in IP-DAG ratio could be attributed to either differences in planktonic community structure or differences in the physiological adaptation of plankton to low nutrients. Deconvolving the contribution of these two mechanisms would provide deeper insights on the ecological and oceanographic meaning of IP-DAG ratios in the environment.

The Mediterranean Sea is well suited for a study of the influence of phosphate depletion on IP-DAG distribution, as it is characterized by exceptionally low concentrations of phosphate and high ratios of dissolved N:P (Krom et al., 1991; Moutin and Raimbault, 2002; Pujo-Pay et al., 2011). In the Biogeochemistry from the Oligotrophic to the Ultraoligotrophic Mediterranean (BOUM) cruise the ratio of nitrate plus nitrite to phosphate ranged from 24.5 at the surface in the west to 32.4 in the east (Pujo-Pay et al., 2011), far exceeding the canonical Redfield ratio of 16 and distinguishing the Mediterranean Sea as one of the most phosphorus-depleted bodies of water in the world. The major input of water to the Mediterranean is over the shallow sill of the Strait of Gibraltar, bringing in nutrient-depleted surface water from the Atlantic and establishing the oligotrophic nature of the Sea (Krom et al., 1991). The bathymetry and circulation lead to distinctly different water masses in the eastern and western basins with a gradient of nutrients, primary production, and planktonic community structure from west to east (Moutin and Raimbault, 2002; Moutin et al., 2002). During the summer months intense stratification develops in the Mediterranean, leading to a shallow mixed layer that is downwelled in some areas by anticyclonic eddies (Siokou-Fragou et al., 2010; Moutin et al., 2011). Thus the Mediterranean Sea, as a contained, highly oligotrophic water mass with a longitudinal gradient of phosphate, provides an excellent study site for the response of IP-DAGs to nutrient limitation.

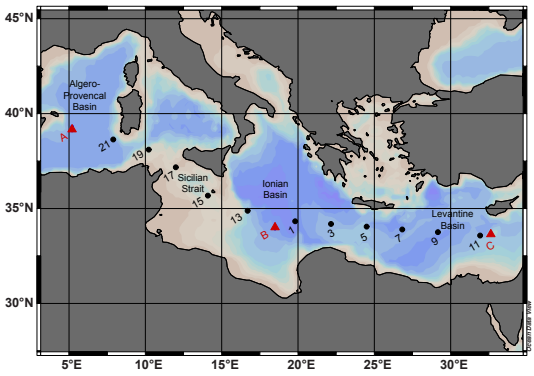

Fig. 1. Map of the Mediterranean Sea, colored to indicate bathymetry, with locations of sampling on the BOUM cruise. Numbered stations (black circles) denote locations where a single depth profile was sampled; lettered stations (red triangles) denote locations where multiple profiles were sampled in near proximity, and where microcosm incubations were conducted.

In this study we set out to see if the phosphorus gradient across the Mediterranean Sea (Krom et al., 1991, Pujo-Pay et al., 2011) leads to a shift in the membrane lipids of marine microbes, where we would expect the oligotrophic conditions in the west to correspond with proportionally more abundant phospholipids than the ultraoligotrophic conditions in the east. In addition, we performed microcosm incubations with nutrient amendments to test whether changes in the available nutrients would elicit a measurable change in IP-DAG composition in a natural, mixed planktonic community on short timescales. These controlled incubations allowed us to assess the relative contribution of physiological response and changes in community composition to the observed changes in IP-DAGs.

2 Methods

2.1 Sampling sites

This study was conducted as a part of the Biogeochemistry from the Oligotrophic to the Ultraoligotrophic Mediterranean (BOUM) cruise in June–July of 2008 aboard the R/V *L'Atalante*. Samples were collected for IP-DAG quantification along a transect from the Algero-Provencal basin (39.1° N, 5.2° E) to the eastern Levantine basin near Cyprus (33.7° N, 32.7° W; Fig. 1). At 11 stations samples for IP-DAG depth profiles were collected (numbered stations, 1–21). Each depth profile was composed of nine or ten samples taken between 5 m and 250 m. At three additional stations

(lettered stations, station A in the Algero-Provencal basin, station B in the Ionian basin, and station C in the Levantine basin), located near the center of anticyclonic eddies, multiple depth profiles were collected in close proximity (10 profiles in total). At each of these stations single profiles were taken to greater depths: 2700 m, 2500 m, and 900 m respectively at stations A, B and C. Microcosm incubations with nutrient amendments were also conducted at these stations.

2.2 Microcosm incubation set up and sampling

Water for the microcosm incubation was collected with Niskin bottles at 8 m depth. Each microcosm incubation consisted of triplicate 20 L carboys for each of four conditions: control (C) no nutrient addition; nitrogen addition (N) with 1600 nM NH_4Cl at stations A and B, 3200 nM at station C; phosphorus addition (P) with 100 nM KH_2PO_4 at all stations; nitrogen and phosphorus addition (NP) with 1600 nM NH_4Cl, 100 nM KH_2PO_4 at stations A and B, 3200 nM NH_4Cl, 100 nM KH_2PO_4 at station C. Carboys were incubated in on-deck incubators flushed with surface seawater to maintain ambient temperature, and outfitted with screens to reduce incident light by ca. 50 %. Samples were taken daily for a range of biogeochemical parameters (see Tanaka et al., 2011 for full results). Samples were taken for IP-DAGs at the initiation of the experiments and termination, at station A at the end of three days, at stations B and C at the end of four days.

2.3 IP-DAG sample collection and extraction

Samples for depth profiles were collected using Niskin bottles mounted on a rosette equipped with sensors for conductivity, temperature, pressure, oxygen, photosynthetically available radiation (PAR), and chlorophyll fluorescence. All samples for IP-DAGs were 1 L, transferred from CTD casts (depth profiles) or incubation carboys (microcosm) to filtration using polycarbonate bottles. Seawater was filtered onto 47 mm 0.2 μm poresize hydrophilic Durapore filters (Millipore) using gentle vacuum filtration (<200 mm Hg). Filters were folded in half, cell side in, wrapped in combusted aluminum foil and stored in liquid nitrogen until extraction. Extraction was conducted using a modified Bligh and Dyer solvent extraction method with phosphatidylethanolamine-N-(2,4-dinitrophenyl) (DNP-PE; Avanti Polar Lipids) as an internal recovery standard (Bligh and Dyer, 1959; Popendorf et al., 2011).

2.4 IP-DAG quantification

Total lipid extracts were analyzed using high performance liquid chromatography/mass spectrometry (HPLC-MS) with an Agilent 1200 HPLC and Thermo Scientific TSQ Vantage triple quadrupole MS with a heated electrospray ionization (ESI) interface following Popendorf et al. (2011). HPLC methods are given in Sturt et al. (2004). Nine IP-DAGs were quantified: three phospholipids, phosphatidylglycerol (PG), phosphatidylethanolamine (PE), phosphatidylcholine (PC); three glycolipids, sulfoquinovosyldiacylglycerol (SQDG), monoglycosyldiacylglycerol (MGDG), diglycosyldiacylglycerol (DGDG); and three betaine lipids, diacylglyceryl hydroxymethyl-trimethyl-β-alanine (DGTA), diacylglyceryl trimethylhomoserine (DGTS), and diacylglyceryl carboxyhydroxymethylcholine (DGCC). MS detection and quantification of phospholipids and glycolipids followed the methods given in Popendorf et al. (2011). Additionally, betaine lipids were analyzed. Detection of the betaine lipids was by positive ion mode parent ion scans, for DGTS and DGTA product ion *m/z* 236; for DGCC product ion *m/z* 104. Quantification of DGCC used an external standard curve prepared with natural DGCC extracted from *Thalassiosira pseudonana* grown in the Van Mooy lab, purified by preparative HPLC and then quantified by gas chromatography flame-ionization detector (GC-FID) analysis of transesterified fatty acid methyl esters. The response factor of DGTA on the TSQ MS was established previously using standard curves of DGCC and DGTA prepared in a similar fashion. MS response of DGTS and DGTA were compared on a Thermo-Finnigan LCQ Deca XP ion trap MS and the TSQ MS to calculate a response factor for DGTS.

2.5 Nutrients

Dissolved nitrate (NO_3^-), nitrite (NO_2^-) and phosphate (PO_4^{3-}) were measured on board using the automated colorimetric technique on a segmented flow Bran Luebbe autoanalyser II; ammonium (NH_4) determinations were performed on board by fluorometry on a Jasco FP-2020 fluorometer. For full method description see Pujo-Pay et al. (2011). Particulate phosphorus and particulate nitrogen were collected simultaneously on precombusted GF/F filters (Whatman), and were analyzed using the wet-oxidation procedure of Pujo-Pay and Raimbault (1994).

2.6 Microbial cell abundance

Abundances of the following microbial populations were assessed using flow cytometry: heterotrophic bacteria, *Synechococcus*, *Prochlorococcus*, picoeukaryotic phytoplankton, and nanoeukaryotic phytoplankton. Total cells are presented as a sum of these groups. Full methods for flow cytometry enumeration of both autotrophic and heterotrophic cells are provided in Talarmin et al. (2011) and Tanaka et al. (2011).

2.7 Chlorophyll

Depth profiles across the transect were sampled for pigments by filtering 2 L of seawater onto 25 mm GF/F filters, which were frozen until extraction. HPLC analysis was used to quantify pigments, see Ras et al. (2008) for full analytical methods. Total chlorophyll-*a* (chl-*a*) for the transect depth profiles is reported as a sum of chlorophyll-*a*, divinyl

chlorophyll-*a*, and chlorophyllide-*a*. For the microcosm incubations, chlorophyll-*a* was measured fluorometrically, see Tanaka et al. (2011) for complete methods.

2.8 Statistical treatment of data

Averages are reported ± one standard deviation. All reported correlation coefficients are from linear regression analysis. Significant differences in total IP-DAGs and IP-DAG ratios across different nutrient amendments in the microcosm incubations (Fig. 6) were identified by ANOVA and post-hoc Tukey-Kramer HSD tests using MatLab software (version R2009b), at a confidence level of 95 %. Principal component analysis (PCA) was conducted using MatLab software (version R2009b) following procedures and code outlined in Glover et al. (2011). The purpose of the PCA was to determine if the variability of individual IP-DAGs was similar to the variability of nutrients (PO_4, NO_3, NH_4), pigments (chl-*a*), or microbial groups (*Prochlorococcus*, *Synechococcus*, heterotrophic bacteria, picoeukaryotic phytoplankton, nanoeukaryotic phytoplankton). Accordingly a covariance matrix was constructed as the minor product of eighteen standardized parameters; 76 samples were included where each parameter was measured at the same depth from the same CTD cast. Two principal component factors were selected which captured the greatest variability in the data, and the loading of each parameter on the varimax rotation of these two factors is presented. Loadings were considered notable when their absolute values were greater than 0.6.

3 Results

3.1 Environmental conditions across the Mediterranean

The surface waters of the Mediterranean basins were distinguished by their variation of salinity (Figs. 1 and 2a): relatively low salinity in the Algero-Provencal basin in the west (stations A, 21), and across the Sicilian channel (stations 19 and 15) and the Sicilian strait (station 17), increasing salinity through the Ionian basin (stations 13, B, 1, 3), and highest salinity in the Levantine basin in the east (stations 5, 7, 9, 11, C). Intense summer stratification was apparent in the potential density (σ_θ, Fig. 2b), which also displayed downwelling at anticyclonic eddies near stations A, B, 9 and C. There was a west-east gradient in phosphate concentration with high phosphate in the west. The phosphocline was shallowest through the Sicilian channel (Fig. 2c) and deepened to the east (Pujo-Pay et al., 2011). Further discussion of the oceanographic conditions during the BOUM campaign are described by Moutin et al. (2011).

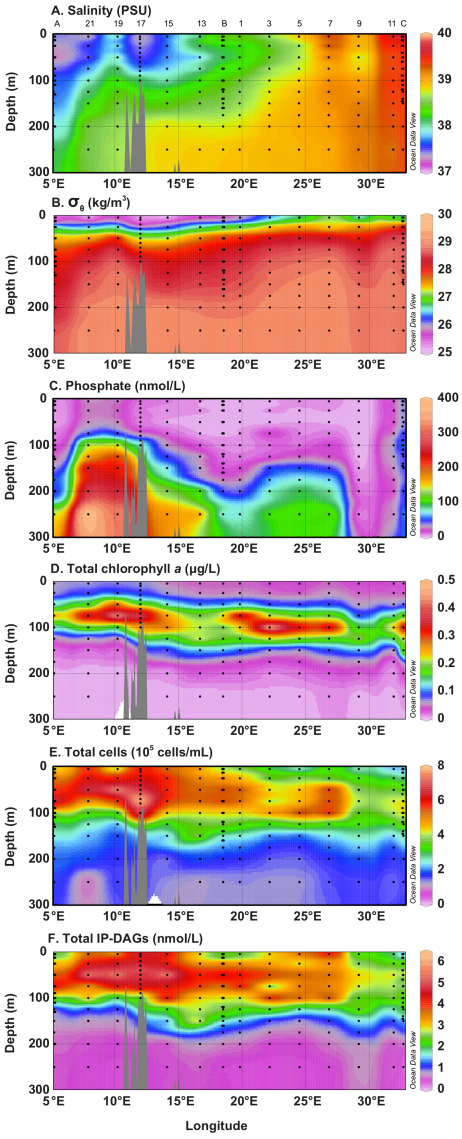

Fig. 2. Distribution of several parameters measured in the upper water column (300 m) from west to east across the Mediterranean Sea. Salinity **(A)** and potential density (σ_θ; **B**) were measured with the CTD sensors; phosphate **(C)** is soluble reactive phosphorus as measured by an autoanalyzer instrument; total chlorophyll-*a* **(D)** is the sum of chlorophyll-*a*, divinyl chlorophyll-*a* and chlorophyllide-*a*; total cells **(E)** is the sum of *Prochlorococcus*, *Synechococcus*, heterotrophic bacteria, picoeukaryotic phytoplankton, and nanoeukaryotic phytoplankton; total IP-DAGs **(F)** is the sum of the nine most abundant classes of IP-DAGs found in the water column. Numbers across the top panel indicate station labels; black dots indicate individual samples, colored contours indicate interpolated gradients.

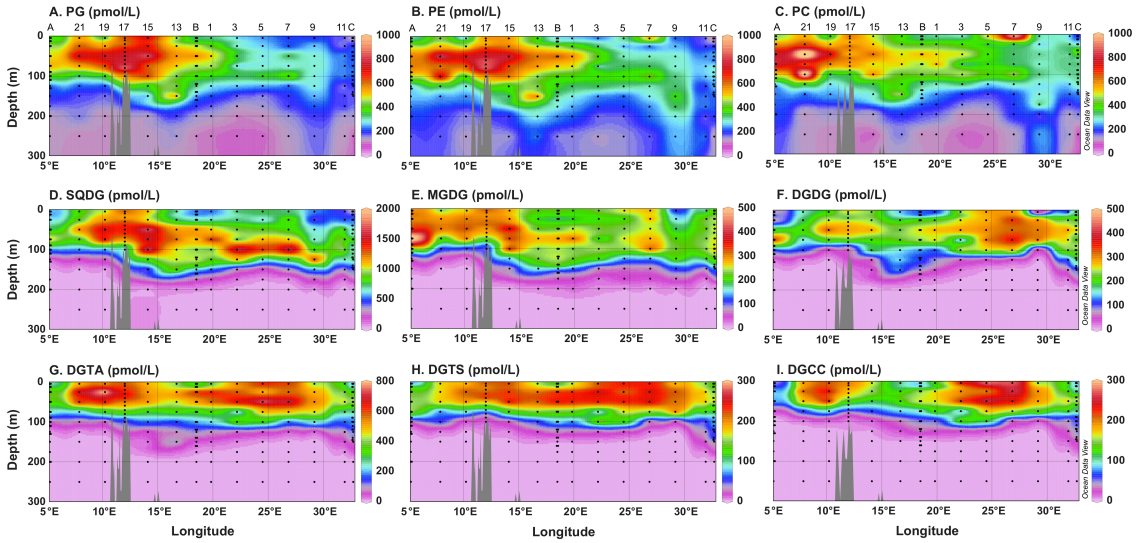

Fig. 3. Distribution of the nine most abundant IP-DAGs in the upper water column (300 m), each panel showing the concentration of a single class of IP-DAG from west to east across the Mediterranean Sea. The first row **(A–C)** is phospholipids; the second row **(D–F)** is glycolipids; the third row **(G–I)** is betaine lipids. Numbers across the top panels indicate station labels; black dots indicate individual samples, colored contours indicate interpolated gradients.

3.2 Distribution of IP-DAGs across the Mediterranean

The IP-DAG membrane lipid composition of particulate material was analyzed at 14 stations across the Mediterranean. In each sample the nine most abundant classes of marine IP-DAGs (Van Mooy and Fredricks, 2010) were quantified: three phospholipids, PG, PE, PC; three glycolipids, SQDG, MGDG, DGDG; and three betaine lipids, DGTA, DGTS, DGCC (Fig. 3). Total IP-DAG concentration, as the sum of these nine classes, averaged 2.4 ± 1.5 nM in the upper 250 m of the Mediterranean. The general distribution of total IP-DAGs paralleled that of total cells (Fig. 2), with a significant positive linear correlation ($R^2 = 0.64$, $n = 159$, $p < 0.01$). The average IP-DAG content per cell was found to be 6.6 ± 2.4 amol/cell, or approximately 3.7 ± 1.3 fg lipid C/cell (assuming an average IP-DAG molecular weight of 800 g mol^{-1} and 70 % w/w C). Total lipid concentration was highest in the western Mediterranean with a maximum of 6.3 nM at approximately 50 m in the Sicilian channel at station 15. The depth of the total IP-DAG maximum deepened from west to east, reaching 100 m in parts of the Levantine basin and a maximum concentration of only 4.3 nM in the east. The distribution of the total IP-DAGs by depth showed low concentration in the surface (1.0–5.0 nM), a maximum around 50–100 m (2.5–6.0 nM), and decreasing concentration down to 150 m (1.0–3.0 nM), then relatively low and constant down to 250 m (0.3–0.7 nM; Fig. 2). Near the surface, total IP-DAGs were dominated by the glycolipids (Fig. 3), closely followed by phospholipids. Averaging across the whole transect, from the surface to 150 m depth the most abundant IP-DAG was the glycolipid SQDG, roughly 30 % of the total IP-DAGs at many depths, with a maximum of 2.5 nM at 50 m in the Sicilian strait. Below 150 m the phospholipid PE was most abundant. The distribution of each lipid class varied both longitudinally and with depth, however the classes within each type of IP-DAG (phospholipids, glycolipids, betaine lipids) tended to have similar characteristics. This was particularly clear in the trends with depth: at depths below approximately 100 m betaine lipid concentrations decreased sharply; at depths below 150 m glycolipid concentrations decreased steeply, thus at depths greater than 150 m phospholipids dominated the reservoir of IP-DAGs (Fig. 3).

3.3 Variation within types of lipids

3.3.1 Phospholipids

Phospholipids demonstrated a strong longitudinal gradient, with a clear maximum in the west and decreasing concentrations to the east (Fig. 3a, b, c). The phosphate concentration was also higher in the west and decreased to the east (Fig. 2c). As a fraction of total IP-DAGs, total phospholipid concentration (the sum of PG, PE and PC; Fig. 4a) was significantly positively correlated with phosphate concentration ($R^2 = 0.30$, $n = 198$, $p < 0.01$). The longitudinal and

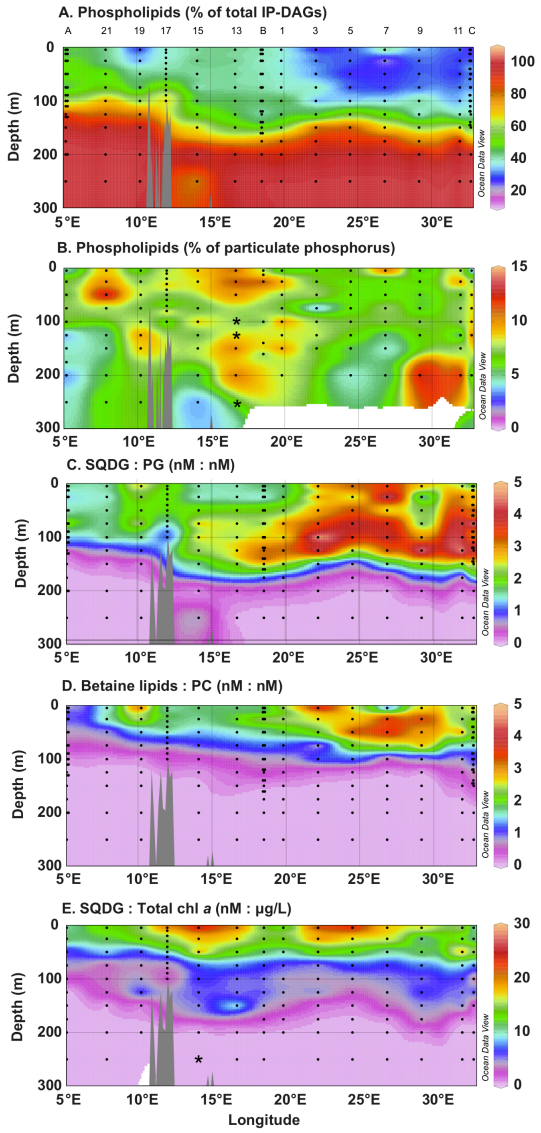

Fig. 4. Distribution of the ratios of lipids each shown in the upper 300 m from west to east across the Mediterranean Sea. Total phospholipids (the sum of the concentrations of PG, PE and PC) are shown as a percent of total IP-DAGs **(A)**, and as a percent of total particulate phosphorus **(B)**. The ratios of the concentration of non-phosphorus lipids to phospholipids are shown as the ratio of the sulfolipid SQDG to the phospholipid PG **(C)**, and the ratio of the sum of the betaine lipids (DGTA, DGTS and DGCC) to the phospholipid PC **(D)**. Also shown is the ratio of SQDG to total chlorophyll-*a* **(E)**. Numbers across the top panel indicate station labels; black dots indicate individual samples, colored contours indicate interpolated gradients; * indicates outlier values not plotted.

depth distribution of the three phospholipids, PG, PE, and PC, was quite similar (Fig. 3a, b, c). By depth, each phospholipid class was approximately 200–600 pM in the surface, increasing to 200–800 pM at 50–75 m, then decreasing to 100–200 pM at 250 m. Though the basin-wide distribution of the three phospholipids was similar, their relative abundance varied with depth. From 5 m to 100 m, PC was the most abundant phospholipid, and in many places the second most abundant IP-DAG after SQDG. At depths below 100 m PE was the most abundant phospholipid; and below 150 m PE was the most abundant IP-DAG. Maxima occurred at station 17 for PG and PE; station 21 for PC; at station 9 high concentrations of all three phospholipids persisted much deeper than the surrounding areas consistent with downwelling seen in isolines (Fig. 2). At several locations samples were taken from 250 m down to 2500 m (data not shown); below approximately 175 m all of the detectable IP-DAGS were phospholipids, which persisted in measurable quantities down to 2700 m (the deepest depth sampled). At 500 m and deeper, each phospholipid was roughly 50–100 pM, with PE being most abundant (40 % of total IP-DAGs).

3.3.2 Glycolipids

In contrast to the phospholipids, the glycolipids did not display a strong longitudinal gradient, nor was their distribution as similar across the three classes of IP-DAGs (Fig. 3d, e, f). By far the most abundant glycolipid was SQDG (Fig. 3d). Its vertical distribution showed a distinct minimum in concentration near the surface, an increase at 50–100 m, and a sharp decrease at 100 m in the Algero-Provencal basin in the west, a slightly deeper decline at 150 m to the east. The distributions of MGDG and DGDG were more similar to each other than to SQDG, being less abundant overall (∼200 pM near the surface), and having less pronounced minimums near the surface. DGDG was a little less abundant than MGDG, though MGDG and DGDG both had maxima at 75 m at station A, roughly 600 and 400 pM, respectively.

3.3.3 Betaine lipids

The three betaine lipids had similar patterns of distribution (Fig. 3g, h, i), but their absolute concentrations were quite different with DGTA having the highest concentration by a factor of 2 at most locations, a maximum of almost 900 pM compared to roughly 300 pM for DGTS and DGCC. For all three betaine lipids the highest concentration was in the Sicilian channel (stations 19 and 17), with a second maximum in the eastern Mediterranean at the boundary of the Ionian and Levantine basins (stations 3, 5 and 7). Depth profiles of the betaine lipids were different from the phospholipids and glycolipids in several ways: they did not exhibit a pronounced minimum near the surface; the maximum was slightly shallower, 50–75 m as opposed to 50–100 m; and their concentration decreased more steeply with increasing depth than either

glycolipids or phospholipids, by 100 m depth their concentration was near undetectable.

3.4 Ratio of IP-DAGs

From west to east across the Mediterranean, the strong gradient of the phospholipids from high to low led to a gradient in the ratio of non-phosphorus lipids to phospholipids (Fig. 4). As a percent of total IP-DAGs, phospholipids averaged 44.3 % ($\pm$ 10.7 %; Fig. 4a) in the upper 100 m of the Algero-Provencal through the Ionian basins, and 30.0 % ($\pm$ 7.4 %) in the upper 100 m of the Levantine basin. Across the Mediterranean, phospholipids were 76.0 % ($\pm$ 25.7 %) of total IP-DAGs below 100 m down to 250 m. As a fraction of particulate phosphorus, phospholipids represented 7.1 % ($\pm$ 2.5 %) of the phosphorus pool (Fig. 4b), with higher values in the west and typically lower values in the surface waters in the east. The fraction of particulate nitrogen represented by N-containing lipids (the sum of PE, PC, DGTA, DGTS and DGCC) was also calculated and found to be 0.4 % ($\pm$ 0.2 %, data not shown) though there was no notable west to east trend.

The ratio of the sulfolipid SQDG to the phospholipid PG (SQDG:PG; Fig. 4a) was low in the western Algero-Provencal basin (1.6 ± 0.3 in the upper 100 m), began to increase across the Sicilian channel (1.9 ± 0.7 in the upper 100 m) into the Ionian basin (2.5 ± 1.3 in the upper 150 m), and was highest in the eastern Levantine basin (3.1 ± 1.6 in the upper 150 m). The maximum deepened from west to east, from 75 m in the Algero-Provencal basin to 125 m in the Levantine basin.

The ratio of the betaine lipids to PC also exhibited a longitudinal gradient (betaine lipids:PC; Fig. 4b), being lowest in the west (1.0 ± 0.5 in the upper 50 m in the Algero-Provencal basin) and highest in the east (2.7 ± 0.9 in the upper 75 m in the Levantine basin). The ratio approached zero at a much shallower depth than SQDG:PG, due to the shallower depths of the betaine lipids relative to SQDG (Fig. 3). The maximum also deepened from west to east, more steeply than SQDG:PG, from near 5m in the Sicilian channel to 50 m in the Levantine basin.

Across the Mediterranean there was a strong positive correlation between SQDG and total chlorophyll-*a* ($R^2 = 0.50$, $n = 135$, $p < 0.01$). The maxima of both SQDG and chl-*a* occurred at depth (Figs. 2 and 3), between 50 and 100 m (shallower in the western basin, deeper in the eastern basins), however the ratio of SQDG to chl-*a* was highest near the surface (Fig. 4c). The deep chlorophyll maximum paralleled the abundance of *Prochlorococcus* (see Mella-Flores et al. (2011) for cyanobacteria abundance), and while the maximum of SQDG also followed the *Prochlorococcus* abundance, SQDG was also relatively abundant near the surface (Fig. 3d). There was not a longitudinal gradient in SQDG:chl-*a*, with the maxima of the ratio in the Sicilian strait (station 15) and across the boundary of the Ionian and Levantine basins (stations 3 and 5).

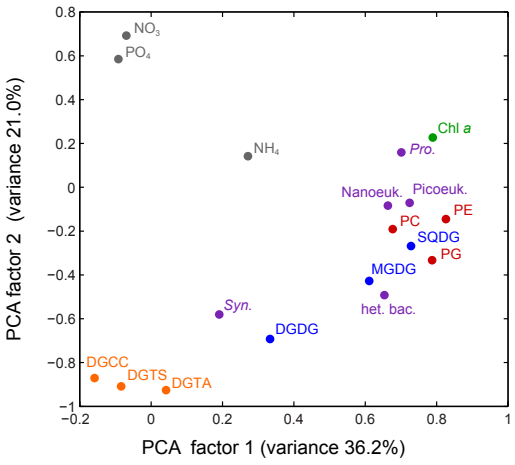

Fig. 5. Principal component analysis was applied to 18 parameters: concentration of three phospholipids (PG, PE, PC; red circles); concentration of three glycolipids (SQDG, MGDG, DGDG; blue circles); concentration of three betaine lipids (DGTA, DGTS, DGCC; orange circles); abundance of five plankton populations (purple circles): *Synechococcus* (*Syn.*), *Prochlorococcus* (*Pro.*), nanoeukaryotic phytoplankton (nanoeuk.), picoeukaryotic phytoplankton (picoeuk.), heterotrophic bacteria (het. bac.); concentration of three nutrients (grey circles); and concentration of total chlorophyll-*a* (Chl-*a*; green circle). Each parameter is plotted as its loading on the two principal component factors that captured the greatest amount of variance in the data.

3.5 Relationship between IP-DAGs and other biogeochemical parameters

Principal component analysis (PCA) showed that almost all of the phospholipids and glycolipids had similar loadings on the principal component factor which captured the greatest amount of variance in the data (factor 1, Fig. 5), except for DGDG which loaded heavily on factor 2. Additionally most of the microbial populations loaded closely to the glycolipids and phospholipids on factor 1, including heterotrophic bacteria, *Prochlorococcus*, nanoeukaryotic phytoplankton and picoeukaryotic phytoplankton. *Synechococcus* did not load closely to the other microbial populations on factor 1, though its loadings on both factors 1 and 2 were similar to DGDG. Total chlorophyll-*a* had similar loading to *Prochlorococcus*. The nutrients NH_4, NO_3, and PO_4 did not have loadings similar to any of the cells, chl-*a*, glycolipids or phospholipids in this analysis. However, NO_3 and PO_4 had heavy positive loadings on factor 2, while the three betaine lipids had a heavy negative loading on factor 2, and both nutrients and betaine lipids had similarly little loading on factor 1.

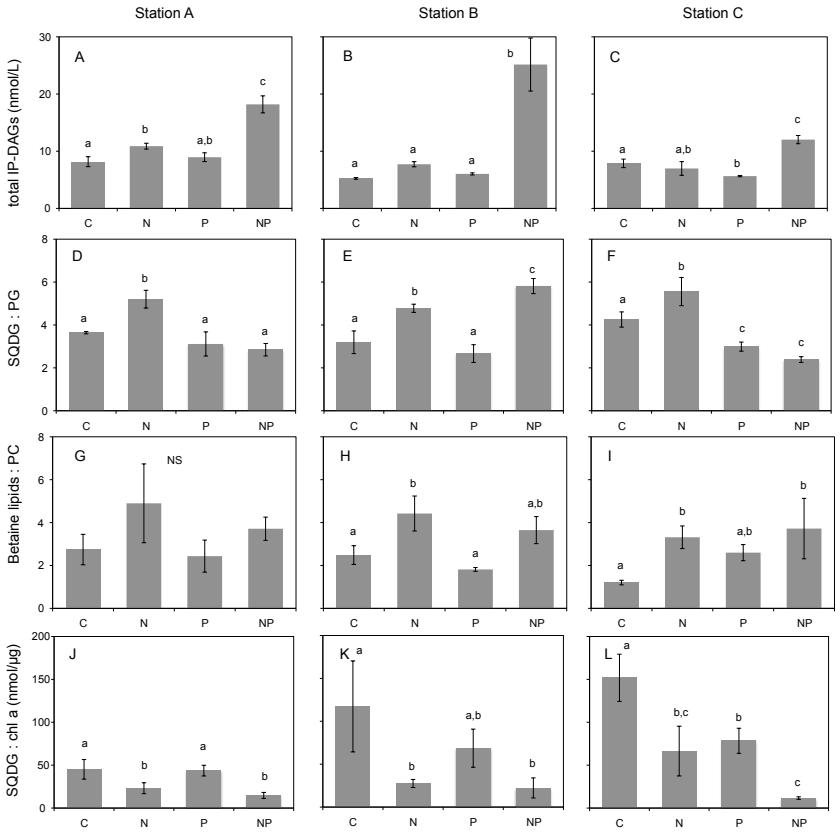

Fig. 6. Total IP-DAG concentration **(A–C)**, SQDG:PG ratio **(D–F)**, betaine lipid:PC ratio **(G–I)**, and SQDG:chlorophyll-*a* ratio **(J–L)** on the final day of incubations from three locations, stations A, B, and C (organized by column) with nutrient amendments: C is control (no amendment), N is addition of ammonium, P is addition of phosphate, NP is addition of ammonium and phosphate. Error bars are the standard deviation of triplicate carboys. In each plot, lowercase letters (a, b, c) indicate statistical post-hoc comparisons: bars labeled with different letters are significantly different ($p < 0.05$); NS indicates no significant difference.

3.6 Response of IP-DAGs to nutrient amendments in microcosm incubations

Microcosm incubations were conducted at three locations (stations A, B, and C) in the Mediterranean to determine the response of the biological community to changes in nutrient availability, specifically an increase in available ammonium (N condition), phosphate (P condition), or an increase in both ammonium and phosphate (NP condition). Over three or four days an array of biogeochemical parameters were measured to assess community response (see Tanaka 2011 for a full description of results). Comparison of IP-DAGs in the different nutrient amendments on the final day of the incubation showed that within the space of a few days the membrane lipid composition had changed dramatically.

Total IP-DAG concentration increased dramatically in the NP condition in all three experiments (stations A, B and C) relative to the control. With the addition of only ammonium or only phosphate there was a small increase in total IP-DAGs relative to the control at station A in the N condition, and a small decrease at station C in the P condition (Fig. 6a–c). In contrast to the change in total IP-DAG concentration, the ratio of SQDG to PG increased in the N condition at all three stations. At station B there was also a large increase in SQDG:PG in the NP condition. At station C there was a small decrease in SQDG:PG in the P condition as well as the NP condition. Shifts in betaine lipid:PC ratio in the N conditions were similar to those observed in SQDG:PG, with an increase relative to the control at stations B and C (changes were not significant at station A). In contrast to SQDG:PG there also appeared to be an increase in betaine

lipids:PC in the NP condition at all stations, however the variability across the three triplicates was slightly larger for the betaine:PC ratios than for SQDG:PG and thus the increase in the NP condition was only significant at station C. In the P condition there were no significant differences in betaine lipids:PC relative to the control.

The ratio of SQDG to chlorophyll-*a* also changed with nutrient additions, with a decrease in the ratio in both the N and NP conditions relative to the control at all stations. At station C there was also a decrease in the P condition, and no significant change in the P condition at the other two stations.

4 Discussion

Membrane lipids have a rich history of being applied as a proxy for microbial biomass in the environment (Balkwill et al., 1988, White et al., 1979), and recent work has shown that they may also be applied as indicators of community structure and physiology (Popendorf et al., 2011; Van Mooy et al., 2006, 2009). In this study, across the Mediterranean total cell abundance was highest in the west (Fig. 2) as expected from previous studies (Siokou-Frangou et al., 2010 and references therein), and total IP-DAG concentration was significantly positively correlated with total cell abundance. Though the distribution of cell size has also been observed to vary across the Mediterranean (Christaki et al., 2011; Siokou-Frangou et al., 2010), and could contribute to the variation in IP-DAG content per cell, apparently the variation in cell size has a smaller influence on IP-DAG concentration than cell abundance. Among the different IP-DAGs the strongest west to east gradient was seen in the phospholipids. When normalized to total IP-DAGs, the gradient of phospholipids was positively correlated with phosphate concentration, with phospholipids making up less of the membrane lipids in the surface waters of the ultraoligotrophic east. This aligns with the hypothesis that microbes will direct less of their cellular phosphate towards phospholipid production when the nutrient is increasingly scarce (Van Mooy et al., 2006, 2009). Indeed, phospholipids were generally a higher percent of particulate phosphorus in the west and lower in the east. With less phospholipids in the membrane, the balance of IP-DAGs is expected to come from glycolipids and betaine lipids. The particular substitutions that have been observed in cultures are SQDG substituting for PG, and betaine lipids substituting for PC (Benning et al., 1993, 1995; Martin et al., 2011; Van Mooy et al., 2006, 2009). Across the Mediterranean, the ratios of SQDG:PG and betaine lipids:PC were both highest in the east. This gradient in membrane composition corresponded with the change in nutrients across the Mediterranean (Pujo-Pay et al., 2011), however there are two potential mechanisms that could contribute to this variation in IP-DAGs: (1) physiological shifts within organisms, leading to increased non-phosphorus lipids per cell, or (2) changes in the composition of the microbial community leading to more abundant low-phospholipid containing organisms (for example *Synechococcus*; Popendorf et al., 2011; Van Mooy et al., 2006) when phosphorus is scarce. By combining measurements of IP-DAGs across the Mediterranean with measurements in microcosm incubations we were able to deconvolve the relative contribution of these two mechanisms.

4.1 Factors influencing IP-DAG ratios

The relative influence of community composition and physiological response to nutrients was assessed by principal component analysis (Fig. 5), comparing the variability in IP-DAG concentrations to the variability in nutrients and variability in the abundances of different planktonic groups. All of the microbial groups, except for *Synechococcus*, loaded heavily on factor 1 and only minimally on factor 2, thus factor 1 loads heavily on parameters representing community structure. Additionally, all of the phospholipids and glycolipids, except DGDG, load heavily on factor 1 and not heavily on factor 2, indicating that much of the variability in phospholipids and glycolipids across the transect might be associated with the variability in the planktonic community. *Synechococcus* and DGDG did not load heavily on factor 1, but they loaded closely to each other on factor 2. Previous studies have shown that DGDG is a significant component of *Synechococcus* membranes and is not as abundant in other cyanobacterial or heterotrophic bacterial membranes (Popendorf et al., 2011). Furthermore, the distribution across the transect showed that maxima of both DGDG and MGDG corresponded with high abundances of *Synechococcus* and *Prochlorococcus* respectively (see Mella-Flores et al. (2011) for the distribution of cyanobacteria). The similar loading of *Prochlorococcus* and chl-*a* in the PCA also corresponded with the observed co-occurrence of the deep chlorophyll maximum and *Prochlorococcus* maximum across the Mediterranean, further affirming the utility of the PCA. Similar associations between *Prochlorococcus* and chlorophyll-*a* were previously observed in the South Pacific (Van Mooy and Fredricks, 2010).

The other parameters that did not load heavily on factor 1 were nutrient concentrations and betaine lipid concentrations, which instead loaded heavily on factor 2. This may indicate that across the Mediterranean the concentration of betaine lipids was heavily influenced by the concentration of nutrients, implying a stronger signal of physiological response as opposed to variation in community structure. Though principal component analysis is a useful tool for indicating potential connections it cannot determine if community or physiology are causal in the variability of IP-DAGs. The variation of IP-DAGs with different microbial groups has been well studied in cultures (Oliver and Colwell, 1973; Guschina and Harwood, 2006; Kato et al., 1996; Van Mooy et al., 2006), and some work has also been done measuring the diversity of IP-DAGs in microbial groups from environmental samples (Popendorf et al., 2011). The physiological

response has also been well studied in monocultures (Benning et al., 1993, 1995; Martin et al., 2011; Van Mooy et al., 2009), however it remains to be shown whether the influence of changes in physiology can be detected in changes in IP-DAGs in a natural, mixed planktonic community.

4.2 Influence of physiology vs. community on IP-DAGs assessed in microcosm incubations

The microcosm incubations with nutrient amendments conducted on the BOUM cruise provided a unique opportunity for assessing the relative contributions of community composition and physiological response to the changes in IP-DAGs. Within the microcosms, we could account for changes in the community composition, enabling an examination of the changes in IP-DAGs that resulted from solely physiological adaptation. The addition of nitrogen and phosphorus to the oligotrophic, phosphate-depleted waters of the Mediterranean elicited a diverse array of both community and physiologic shifts in the microbial community.

With the addition of phosphate (P condition) in the microcosms no significant changes were observed in the abundance of various microbial groups (Tanaka et al., 2011). With the lack of change in community composition, the observed change of IP-DAGs in this condition would be expected to be primarily due to physiological response. However, primary production, bacterial production, and alkaline phosphatase activity did not change in response to the P amendment (Tanaka et al., 2011; Lagaria et al., 2011), which indicates that this system was not phosphate limited despite the low ambient phosphate concentration and high N:P at all three stations (Pujo-Pay et al., 2011). Relative to the control, phosphate addition elicited a change in the ratio of IP-DAGs at only one station: a small decrease in SQDG:PG at station C, as would be expected of a physiological response to increased phosphate. At all other stations there were no significant changes in the ratio of SQDG:PG or betaine lipids:PC. This lack of strong response to phosphorus addition is consistent with the observations of a previous phosphate addition experiment in the Mediterranean (Thingstad et al., 2005), which found that increased phosphate did not elicit a change in the phytoplankton community despite the expectation of phosphate limitation. The lack of observed shifts in IP-DAG ratios simply reflects a community that was not P-limited.

The addition of ammonium (N condition), on the other hand, elicited a strong physiological response. In the N condition alone there was a significant increase in alkaline phosphatase activity at all three stations (Tanaka et al., 2011), demonstrating clear enhancement of phosphorus stress (Lomas et al., 2010). The changes in IP-DAG ratios that were observed are what would be expected from a physiologic response to increased phosphorus stress: at all three stations the ratio of SQDG:PG increased, and at two stations the ratio of betaine lipids:PC increased relative to the control (changes were not significant at station A, although the mean was higher). These changes were consistent across the stations, despite inconsistent changes in the community structure which were generally small relative to changes observed in the NP condition (Tanaka et al., 2011). Thus these changes in IP-DAG ratios indicate that the increase in phosphorus stress led to a dynamic, physiologic cellular response resulting in IP-DAG substitution in a natural, mixed planktonic community. This is the first observation of a change in membrane composition as a physiological response in the environment, and it indicates that elevated ratios of these IP-DAGs observed in other phosphate depleted environments could be an indicator of phosphorus stress.

The increase of the betaine lipid:PC ratio in the N condition provided validation of the lipid substitution expected from observations in culture (Benning et al., 1995; Martin et al., 2011). This was particularly notable since betaine lipids in marine environments are not well understood (Van Mooy and Fredricks, 2010; Popendorf et al., 2011) and therefore mechanistic explanations for the observed trends are more limited. In all of the amendment conditions the change in betaine lipids:PC was more variable within the triplicate measurements than the change in SQDG:PG. The PCA indicated that betaine lipids might be more strongly influenced by physiological response than the glycolipids or phospholipids (Fig. 5), and the longitudinal trend in the betaine:PC ratio showed an increase in the ultraoligotrophic eastern Mediterranean Sea (Fig. 4), indicating an increase in response to low phosphate conditions as expected. However the sharp decrease in betaine lipid abundance with depth, relative to glycolipids and phospholipids, indicates that the abundance of these IP-DAGs may be controlled by unique factors, related either to physiology or community, which are thus far unidentified. The microcosm incubations support the conclusion that physiological response contributes to the observed trends in betaine lipid concentration, but future studies could further refine our understanding of betaine lipid sources and the factors that influence them.

In the NP condition there was a significant change in both the community composition and metabolic activity at all three stations. These changes included an increase in primary production at all three stations, an increase in bacterial production at stations B and C, and an increase in the abundance of many microbial groups including *Synechococcus* (all stations), autotrophic nanoplankton (stations B and C), and ciliates (stations A and C; Tanaka et al., 2011; Lagaria et al., 2011). The total IP-DAG concentration increased significantly at all three stations, as would be expected from the large increase in microbial abundance. The significant shifts in community structure, however, meant that little insight on physiology could be drawn from the observed changes in IP-DAG ratios.

4.3 Relationship between SQDG and chlorophyll-*a*

Previous studies have suggested that SQDG originates solely in photoautotrophic organisms (Popendorf et al., 2011; Van Mooy et al., 2006, 2009) and is associated with the organelles of photosynthesis (Sakurai et al., 2006; Sato, 2004; Wada and Murata 1998). Thus we would predict that across the Mediterranean there would be a strong correlation between SQDG and chlorophyll-*a*, and indeed this was observed. The maxima of both SQDG and chlorophyll-*a* occurred at depth, however the ratio of SQDG to chlorophyll-*a* was highest near the surface. While the maximum of SQDG paralleled the maximum in *Prochlorococcus* abundance (Mella-Flores et al., 2011), SQDG is known to also occur in other phytoplankton including *Synechococcus* and pico- and nanoeukaryotic phytoplankton (Popendorf et al., 2011; Sato, 2004; Van Mooy et al., 2006, 2009), which were more abundant near the surface than at the deep chlorophyll maximum (Mella-Flores et al., 2011). The increase in the ratio of SQDG to chlorophyll-*a* near the surface therefore indicates that though both molecules correlate with phytoplankton abundance, their ratio varies with depth. This may be due to a combination of both photoacclimation, decreasing cellular chlorophyll content with high surface irradiance (MacIntyre et al., 2002), or higher cellular SQDG content in the phytoplankton species that are more abundant near the surface.

Though no longitudinal gradient was observed in SQDG:chl-*a*, the change in the ratio in the microcosm incubations demonstrated a response to changes in nutrients. In the N and NP conditions at all stations the ratio of SQDG to chlorophyll-*a* decreased significantly relative to the control (at station C the ratio decreased relative to the control in all amendment conditions). This change in the N condition is likely representative of a physiological response (as previously discussed the changes in the NP condition are likely due to a combination of community changes and physiological response). Chlorophyll has a high nitrogen content, and is known to increase proportionally more than phytoplankton abundance when nitrogen is added to an N-starved system (Zohary et al., 2005). The addition of ammonium in these incubations led to an increase in chlorophyll-*a* in the N condition relative to the control at stations A and B (Tanaka et al., 2011), and, though the ratio of SQDG:PG was seen to increase in these conditions, the ratio of SQDG:chl-*a* decreased, indicating that this ratio is sensitive to nitrogen abundance. Thus the ratios of SQDG:chl-*a*, as an indicator of nitrogen availability, and SQDG:PG, as an indicator of phosphorus stress, may be complementary indicators of planktonic nutrient stress in oligotrophic marine environments.

5 Conclusions

We observed gradients in IP-DAGs that correlated with the phosphate gradient across the Mediterranean, which is consistent with the hypothesis that nutrient availability controls the relative abundance of IP-DAGs. Gradients in community structure undoubtedly contributed to this gradient, but our microcosm incubations showed that physiological shifts likely also contribute to the observed changes. The phospholipid concentration as a percent of total lipids was positively correlated with phosphate concentration across the Mediterranean, both phospholipids and phosphate concentration being higher in the west and lower in the east. Glycolipids and betaine lipids did not show a strong west to east gradient, however the ratio of non-phosphorus lipids to phospholipids varied across the Mediterranean, with SQDG:PG and betaine lipids:PC being higher in the ultraoligotrophic eastern Mediterranean. Throughout the Mediterranean, total IP-DAGs in the upper 250 m were correlated with cell abundance, reaffirming their direct representation of microbial biomass in the ocean. Comparison of the variation in IP-DAGs to variations in microbial groups and nutrients across the Mediterranean was used to examine the relative influence of microbial community composition changes and cellular physiology changes on the observed IP-DAG changes. Microcosm incubations of whole seawater with nutrient amendments provided further insight on these two mechanisms, and provided direct evidence from a mixed community under in situ conditions that shifts in IP-DAG ratios are part of a physiologic response to changes in nutrients. Additionally, the microcosm incubations demonstrated that an increase in ammonium led to a decrease in the ratio of SQDG to chl-*a*, indicating that this ratio may be an indicator of nitrogen availability. With knowledge of the factors influencing the variation of IP-DAGs in the environment, IP-DAGs can be molecular tools for the study of the microbes in the ocean and their role in biogeochemical cycles.

Acknowledgements. The authors would like to thank the captain and crew of the R/V *L'Atalante*, Josephine Ras and Hervé Claustre for the chlorophyll data (HPLC method), Stella Psarra for contributions to chlorophyll data (fluorometry method) and helpful comments on the manuscript, Helen Fredricks for HPLC-MS guidance, Krista Longnecker for assistance culturing *T. pseudonana* for the DGCC standard, Catherine Carmichael for her aid in quantifying the DGCC standard, Patrick Martin for his work with MS betaine comparisons, James Fulton for helpful discussions, and all of the scientists who participated in and contributed to the BOUM cruise. Additional thanks to two anonymous reviewers for helpful suggestions during the open review process. Funding for this work was provided by a grant from the National Science Foundation (OCE-0646944 and OCE-1031143).

Edited by: C. Jeanthon

References

Balkwill, D. L., Leach, F. R., Wilson, J. T., McNabb, J. F., and White, D. C.: Equivalence of microbial biomass measures based on membrane lipid and cell wall components, adenosine triphosphate, and direct counts in subsurface aquifer sediments, Microbial Ecol., 16, 73–84, 1988.

Benning, C., Beatty, J. T., Prince, R. C., and Somerville, C. R.: The sulfolipid sulfoquinovosyldiacylglycerol is not required for photosynthetic electron transport in Rhodobacter sphaeroides but enhances growth under phosphate limitation, Proc. Natl. Acad. Sci., 90, 1561–1565, 1993.

Benning, C., Huang, Z.-H., and Gage, D. A.: Accumulation of a Novel Glycolipid and a Betaine Lipid in Cells of Rhodobacter sphaeroides Grown under Phosphate Limitation, Arch. Biochem. Biophys., 317, 103–111, 1995.

Bligh, E. G. and Dyer, W. J.: A Rapid Method of Total Lipid Extraction and Purification, Canad. J. Physiol. Pharmacol., 37, 911–917, 1959.

Christaki, U., Van Wambeke, F., Lefèvre, D., Lagaria, A., Prieur, L., Pujo-Pay, M., Grattepanche, J.-D., Colombet, J., Psarra, S., Dolan, J. R., Sime-Ngando, T., Conan, P., Weinbauer, M. G., Moutin, T.: Microbial food webs and metabolic state across oligotrophic waters of the Mediterranean Sea during summer, Biogeosciences, 8, 1839–1852, doi:10.5194/bg-8-1839-2011, 2011.

Glover, D. M., Jenkins, W. J., and Doney, S. C.: Principal Component and Factor Analysis, in: Modeling Methods for Marine Science, Cambridge University Press, London, UK, 571, 2011.

Guschina, I. A. and Harwood, J. L.: Lipids and lipid metabolism in eukaryotic algae, Progress in Lipid Research, 45, 160–186, 2006.

Kato, M., Sakai, M., Adachi, K., Ikemoto, H., and Sano, H.: Distribution of Betaine Lipids in Marine Algae, Phytochemistry, 42, 1341–1345, 1996.

Krom, M. D., Kress, N., Brenner, S., and Gordon, L. I.: Phosphorus limitation of primary production in the eastern Mediterranean Sea, Limnol. Oceanogr., 36, 424–432, 1991.

Lagaria, A., Psarra, S., Lefèvre, D., Van Wambeke, F., Courties, C., Pujo-Pay, M., Oriol, L., Tanaka, T., and Christaki, U.: The effects of nutrient additions on particulate and dissolved primary production and metabolic state in surface waters of three Mediterranean eddies, Biogeosciences, 8, 2595–2607, doi:10.5194/bg-8-2595-2011, 2011.

Lomas, M. W., Burke, A. L., Lomas, D. A., Bell, D. W., Shen, C., Dyhrman, S. T., and Ammerman, J. W.: Sargasso Sea phosphorus biogeochemistry: an important role for dissolved organic phosphorus (DOP), Biogeosciences, 7, 695–710, doi:10.5194/bg-7-695-2010, 2010.

MacIntyre, H. L., Kana, T. M., Anning, T., and Geider, R. J.: Photoacclimation of photosynthesis irradiance response curves and photosynthetic pigments in microalgae and cyanobacteria, J. Phycol., 38, 17–38, 2002.

Martin, P., Van Mooy, B. A. S., Heithoff, A., and Dyhrman, S. T.: Phosphorus supply drives rapid turnover of membrane phospholipids in the diatom *Thalassiosira pseudonana*, The ISME Journal, 5, 1057–1060, 2011.

Mella-Flores, D., Mazard, S., Humily, F., Partensky, 5 F., Mahé, F., Bariat, L., Courties, C., Marie, D., Ras, J., Mauriac, R., Jeanthon, C., Bendif, E. M., Ostrowski, M., Scanlan, D. J., and Garczarek, L.: Is the distribution of Prochlorococcus and Synechococcus ecotypes in the Mediterranean Sea affected by global warming?, Biogeosciences Discuss., 8, 4281–4330, doi:10.5194/bgd-8-4281-2011, 2011.

Minnikin, D. E., Abdolrahimzadeh, H., and Baddiley, J.: Replacement of acidic phospholipids by acidic glycolipids in *Pseudomonas diminuta*, Nature, 249, 268, 1974.

Moutin, T. and Raimbault, P.: Primary production, carbon export and nutrients availability in western and eastern Mediterranean Sea in early summer 1996 (MINOS cruise), J. Mar. Syst., 33–34, 273–288, 2002.

Moutin, T., Thingstad, T. F., Van Wambeke, F., Marie, D., Raimbault, P., Slawyk, G., and Claustre, H.: Does competition for nanomolar phosphate supply explain the predominance of the cyanobacterium Synechococcus?, Limnol. Oceanogr., 47, 1562–1567, 2002.

Moutin, T., Van Wambeke, F., and Prieur, L.: The Biogeochemistry from the Oligotrophic to the Ultraoligotrophic Mediterranean (BOUM) experiment, Biogeosciences Discuss. 8, 8091-8160, doi:10.5194/bgd-8-8091-2011, 2011.

Oliver, J. D. and Colwell, R. R.: Extractable Lipids of Gram-Negative Marine Bacteria: Phospholipid Composition, J. Bacteriol., 114, 897–908, 1973.

Popendorf, K. J., Lomas, M. W., and Van Mooy, B. A. S.: Microbial sources of intact polar diacylglycerolipids in the Western North Atlantic Ocean, Org. Geochem., 42, 803–811, 2011.

Pujo-Pay, M., Raimbault, P.: Improvement of the wet-oxidation procedure for simultaneous determination of particulate organic nitrogen and phosphorus collected on filters, Mar. Ecol. Press Ser., 105, 203–207, 1994.

Pujo-Pay, M., Conan, P., Oriol, L., Cornet-Barthaux, V., Falco, C., Ghiglione, J.-F., Goyet, C., Moutin, T., and Prieur, L.: Integrated survey of elemental stoichiometry (C, N, P) from the western to eastern Mediterranean Sea, Biogeosciences, 8, 883–899, doi:10.5194/bg-8-883-2011, 2011.

Ras, J., Claustre, H., and Uitz, J.: Spatial variability of phytoplankton pigment distributions in the Subtropical South Pacific Ocean: comparison between in situ and predicted data, Biogeosciences, 5, 353–369, doi:10.5194/bg-5-353-2008, 2008.

Rütters, H., Sass, H., Cypionka, H., and Rullkötter, J.: Phospholipid analysis as a tool to study complex microbial communities in marine sediments, J. Microbiol. Meth., 48, 149–160, 2002.

Sakurai, I., Shen, J.-R., Leng, J., Ohashi, S., Kobayashi, M., and Wada, H.: Lipids in Oxygen-Evolving Photosystem II Complexes of Cyanobacteria and Higher Plants, J. Biochem., 140, 201–209, 2006.

Sato, N.: Betaine Lipids, The Botanical Magazine, Tokyo, 105, 185–197, 1992.

Sato, N.: Roles of the acidic lipids sulfoquinovosyl diacylglycerol and phosphatidylglycerol in photosynthesis: their specificity and evolution, J. Plant Res., 117, 495–505, 2004.

Siokou-Frangou, I., Christaki, U., Mazzocchi, M. G., Montresor, M., d'Alcalá, M. R., Vaqué, D., and Zingone, A.: Plankton in the open Mediterranean Sea: a review, Biogeosciences, 7, 1543–1586, doi:10.5194/bg-7-1543-2010, 2010.

Sturt, H. F., Summons, R. E., Smith, K., Elvert, M., and Hinrichs, K.-U.: Intact polar membrane lipids in prokaryotes and sediments deciphered by high-performance liquid chromatography/electrospray ionization multistage mass spectrometry–new biomarkers for biogeochemistry and microbial ecology, Rapid Comm. Mass Spectrom., 18, 617–628, 2004.

Suzumura, M. and Ingall, E. D.: Concentrations of lipid phosphorus and its abundance in dissolved and particulate organic phosphorus in coastal seawater, Mar. Chem., 75, 141–149, 2001.

Talarmin, A., Van Wambeke, F., Catala, P., Courties, C., and Lebaron, P.: Flow cytometric assessment of specific leucine incorporation in the open Mediterranean, Biogeosciences, 8, 253–265, doi:10.5194/bg-8-253-2011, 2011.

Tanaka, T., Thingstad, T. F., Christaki, U., Colombet, J., Cornet-Barthaux, V., Courties, C., Grattenpache, J.-D., Lagaria, A., Nedoma, J., Oriol, L., Psarra, S., Pujo-Pay, M., and Van Wambeke, F.: Lack of P-limitation of phytoplankton and heterotrophic prokaryotes in surface waters of three anticyclonic eddies in the stratified Mediterranean Sea, Biogeosciences, 8, 525–538, doi:10.5194/bg-8-525-2011, 2011.

Thingstad, T. F., Krom, M. D., Mantoura, R. F. C., Flaten, G. A. F., Groom, S., Herut, B., Kress, N., Law, C. S., Pasternak, A., Pitta, P., Psarra, S., Rassoulzadegan, F., Tanaka, T., Tselepides, A., Wassmann, P., Woodward, E. M. S., Riser, C. W., Zodiatis, G., and Zohary, T.: Nature of phosphorus limitation in the ultraoligotrophic eastern Mediterranean, Science, 309, 1068–1071, 2005.

Van Mooy, B. A. S., Rocap, G., Fredricks, H. F., Evans, C. T., and Devol, A. H.: Sulfolipids dramatically decrease phosphorus demand by picocyanobacteria in oligotrophic environments, P. Natl. A. Sci., 103, 8607–8612, 2006.

Van Mooy, B. A. S., Moutin, T., Duhamel, S., Rimmelin, P., and Wambeke, F. V.: Phospholipid synthesis rates in the eastern tropical South Pacific Ocean, Biogeosciences, 5, 133–139, http://www.biogeosciences.net/5/133/2008/, 2008.

Van Mooy, B. A. S., Fredricks, H. F., Pedler, B. E., Dyhrman, S. T., Karl, D. M., Koblížek, M., Lomas, M. W., Mincer, T. J., Moore, L. R., Moutin, T., Rappé, M. S., and Webb, E. A.: Phytoplankton in the ocean substitute phospholipids in response to phosphorus scarcity, Nature, 458, 69–72, 2009.

Van Mooy, B. A. S. and Fredricks, H. F.: Bacterial and eukaryotic intact polar lipids in the eastern subtropical South Pacific: Water-column distribution, planktonic sources, and fatty acid composition, Geochim. Cosmochim. Ac., 74, 6499–6516, 2010.

Wada, H. and Murata, N.: Membrane Lipids in Cyanobacteria, in: Lipids in Photosynthesis: Structure, Function and Genetics, edited by: Siegenthaler, P.-A. and Murata, N., Kluwer Academic Publishers, The Netherlands, 65–81, 1998.

Wakeham, S. G., Hedges, J. I., Lee, C., Peterson, M. L., and Hernes, P. J.: Compositions and transport of lipid biomarkers through the water column surficial sediments of the equatorial Pacific Ocean, Deep-Sea Res. Pt. II, 44, 2131–2162, 1997.

White, D. C., Davis, W. M., Nickels, J. S., King, J. D., and Bobbie, R. J.: Determination of the Sedimentary Microbial Biomass by Extractible Lipid Phosphate, Oecologia, 40, 51–62, 1979.

Zohary, T., Herut, B., Krom, M. D., Mantoura, R. F. C., Pitta, P., Psarra, S., Rassoulzadegan, F., Stambler, N., Tanaka, T., Thingstad, T. F., and Woodward, E. M. S.: P-limited bacteria but N and P co-limited phytoplankton in the Eastern Mediterranean – a microcosm experiment, Deep-Sea Res. Pt. II, 52, 3011–3023, 2005.

Chapter 5

Growth rate of marine microbes assessed by phospholipid specific production rate

1. Introduction

The importance of the microbial loop in the marine carbon cycle has been recognized for more than three decades (Pomeroy, 1974; Azam et al., 1983; Cho and Azam, 1988; Cole et al., 1988; Cho and Azam, 1990). Heterotrophic bacteria are responsible for large fluxes of carbon in the surface ocean through their uptake of dissolved organic carbon, which may either be converted to heterotrophic bacterial biomass, a flux measured as bacterial production, or may be respired and returned to the dissolved inorganic carbon pool through bacterial respiration. In the time since the microbial loop has been recognized as an important part of the carbon cycle, the methods for assessing heterotrophic bacterial stocks and processes have changed relatively little: bacterial abundance has been enumerated by microscopy and more recently by flow cytometry (Campbell et al., 1997; discussion in Ducklow, 2000), and bacterial production has been assessed by uptake of tritiated thymidine (^{3}H-TdR; Karl, 1979; Fuhrman and Azam, 1980, 1982; Kirchman et al., 1982) and uptake of tritiated leucine (^{3}H-Leu; Kirchman et al., 1985; Simon and Azam, 1989; Smith and Azam, 1992; Kirchman, 1992). Heterotrophic bacterial turnover rates based on these measures are generally on the order of 0.1 per day for open ocean sites worldwide (Ducklow, 2000 and references therein).

Since the inception of the ^{3}H-Leu and ^{3}H-TdR uptake methods there have been many advances in microbiological methods that have enabled new insights into heterotrophic bacterial diversity (Rappé et al., 1997, 2002), substrate specificity (Alonso-Sáez et al., 2007; Cottrell and Kirchman, 2000; Longnecker et al., 2010; Schwalbach et al., 2010), and cell activity (Lebaron et al., 2002; Longnecker et al., 2005; Van Wambeke et al., 2011). These insights in turn have led to increased understanding of the potential errors associated with the standard methods for measuring bacterial production. We now know that in many open ocean environments a relatively small fraction of heterotrophic bacteria take up exogenous Leu and TdR relative to uptake of other more ubiquitous substrates such as phosphate (Longnecker et al., 2010). Indeed, even at the inception of the ^{3}H-TdR method for marine samples, Fuhrman and Azam (1982) noted that uptake

rates of radiolabeled phosphate into DNA predicted bacterial production rates on the order of 2-7 times higher than rates of ^{3}H-TdR uptake into DNA, with the difference in rates being largest in open ocean sites. With the emergence of studies such as Longnecker et al. (2010), it has become increasingly apparent that measurement of bacterial production using uptake of ^{3}H-TdR or ^{3}H-Leu is likely to be an underestimate of true production rates in open ocean sites. In this study we propose, test, and apply a new method for measuring heterotrophic bacterial production rate in the ocean.

The current methods for measuring heterotrophic bacterial production use the uptake of ^{3}H-Leu or ^{3}H-TdR. When these materials are taken up the radioactive label is incorporated into biochemicals, proteins and DNA respectively, that are produced by all types of microbes. Therefore measuring heterotrophic bacterial production rate by the uptake rate of ^{3}H-Leu or ^{3}H-TdR relies on the uptake of exogenous leucine and thymidine being specific to heterotrophic bacteria. Rather than measuring the uptake of a specific substrate into a general biochemical, we instead propose a method for measuring heterotrophic bacterial production that relies on the uptake of a general substrate, available to broad array of microbes, and its incorporation into a biochemical specific to heterotrophic bacteria. Phosphate is a more ubiquitous substrate for heterotrophic bacteria than leucine or thymidine, and it is also taken up by a wide variety of other plankton. Thus in order for phosphate uptake to be a viable tracer for heterotrophic bacterial production, the incorporation of radiolabeled phosphate must be traced into biochemicals unique to heterotrophic bacteria.

Membrane lipids are a promising class of biochemicals for tracing microbial production due to their abundance (11-23% of cellular carbon, Wakeham et al. 1997), structural diversity (Van Mooy and Fredricks, 2010), and the fact that membrane production, and thus lipid production, is obligate for both growth and replication of cells. It has been shown that a wide variety of types of intact polar diacylglycerolipids (IP-DAGs) compose the membranes of marine microbes (Van Mooy et al., 2006, 2009; Van Mooy and Fredricks, 2010; Popendorf et al. 2011a, 2011b) including phospholipids, glycolipids, sulfolipids and betaine lipids.

The composition of microbial membranes varies across different functional and taxonomic groups (Van Mooy et al. 2006, 2009; Popendorf et al. 2011a). Heterotrophic bacterial membranes have been shown to be dominated by phospholipids (Oliver and Colwell, 1973; Van Mooy et al., 2006, 2009; Popendorf et al., 2011a), even in phosphorus depleted environments where the other abundant picoplankton, cyanobacteria, make their membranes almost entirely of glycolipids (Popendorf et al., 2011a). Surveys of the lipid composition of a wide array of planktonic cultures have shown that the phospholipid phosphatidylethanolamine (PE) is abundant in heterotrophic bacteria (Oliver and Colwell 1973; Van Mooy 2006, 2009) and is absent in all axenic cultures of cyanobacteria sampled thus far (Sakurai, et al. 2006; Van Mooy et al., 2006). The specificity of PE for heterotrophic bacteria was further supported by analysis of microbial membrane composition from environmental samples carried out by Popendorf et al. (2011a). This study employed a variety of experimental approaches to measure the membrane composition of operationally defined groups of microbes. In particular, the membrane composition of cyanobacteria versus heterotrophic bacteria, separated by cell sorting flow cytometry, indicate that the majority of PE and phosphatidylglycerol (PG) in the water column come from heterotrophic bacteria. Based on the lack of PE observed in cyanobacteria cultures, and the abundance of PG and PE in heterotrophic bacteria from both cultures and the environment, we calculate that the production of PE and PG in the environment is dominated by heterotrophic bacteria. Given the generality of phosphate as a substrate for all microbes, and the specificity of its incorporation into the phospholipids PE and PG as a tracer heterotrophic bacteria, we hypothesize that the production rate of PE and PG is representative of heterotrophic bacterial production rate.

When a method was being sought to quantify the role of heterotrophic bacteria in the marine carbon cycle in the 1980's, phospholipid production rate had been measured in bacterial culture (White and Tucker, 1969) and in environmental samples (White et al., 1977; Moriarty et al., 1985). However, both methdologicial limitations (e.g. the laborious process for lipid separation and quantification) and lack of critical measurements (e.g. quantitative measurement of membrane lipid turnover rate versus cell

turnover rate in the environment) prevented phospholipid production rate from being broadly adopted as a measure of bacterial production. With the development of new analytical techniques to measure the concentration of individual classes of phospholipids in environmental samples (Sturt et al., 2004; Chapter 2), and more detailed information on the sources of phospholipids in the ocean (Popendorf et al. 2011a), the tools and knowledge are available to reassess the potential of phospholipid production rate as a measure of heterotrophic bacterial production rate.

For phospholipid production rate to be a viable measure of heterotrophic bacterial production rate in the ocean, the outstanding factor to be addressed is the relationship between phospholipid turnover rate and cell turnover rate. In this chapter we will address this with canonical "regrowth" experiments, where we reduce grazing pressure and incubate in the dark to select for growth of heterotrophic bacteria. In these conditions we are able to measure the increase in heterotrophic bacterial cell concentration and use this as a definitive measure of heterotrophic bacterial production rate. We then compare this to the production rate of phospholipids (measured both by increase in the concentration of lipids over time, and by measurement of instantaneous production rate using uptake of radioactive phosphate) and traditional measures of bacterial production rate using uptake of ^{3}H-Leu and ^{3}H-TdR. From these data we can compare the relationship between specific growth rate of heterotrophic bacterial cells and specific production rate of phospholipids. If a quantitative relationship can be derived between the specific growth rate of cells and the specific production rate of lipids, then phospholipid specific production rate may be a new tool to measure heterotrophic bacteria production rate in the open ocean.

2. Methods

2.1 Study sites and sample collection

Samples were collected on four cruises: two cruises in the North Atlantic (BV39 and Oc443), one cruise in the Mediterranean Sea (BOUM), and one cruise in the North

Pacific (KM1013). The BV39 cruise was in October 2007 aboard the R/V *Atlantic Explorer*; data is presented from four stations throughout a meridional transect from Bermuda to Puerto Rico (samples from 32.610°N 64.100°W to 25.673°N 65.060°W). The Oc443 cruise was in April 2008 aboard the R/V *Oceanus*, and comprised a leg from Woods Hole, Massachusetts northeast to 43°N 65°W and a second leg south along 65°W towards Bermuda; data is presented from two stations north of the Gulf Stream, and three stations south of the Gulf Stream in the phosphorus depleted Sargasso Sea. the Biogeochemistry from the Oligotrophic to the Ultraoligotrophic Mediterranean (BOUM) cruise was in June–July of 2008 aboard the R/V *L'Atalante*; data is presented from ten stations along a transect from the Algero-Provencal basin (39.1°N 5.2°E) to the eastern Levantine basin near Cyprus (33.7°N 32.7°W). The KM1013 cruise was in July 2010 aboard the R/V *Kilo Moana*; data is presented from one station at 22.756°N 157.988°W. Water for all samples was collected using Niskin bottles mounted on a rosette equipped with conductivity, temperature and pressure sensors (CTD). At each station samples were collected for heterotrophic bacteria cell counts, phosphate concentration, membrane lipid concentration, phospholipid production rate, and ^{3}H-Leu and ^{3}H-TdR uptake rates. Regrowth experiments were conducted at one location in the Sargasso Sea in the North Atlantic, and one location in the North Pacific.

2.2 Regrowth experimental set-up

Seawater was collected using Niskin bottles mounted on a CTD rosette, then transferred to acid-washed 20 L polycarbonate carboys using acid-washed Tygon tubing. Triplicate carboys were prepared with 2 L whole seawater and 18 L seawater gravity-filtered through an acid-cleaned 0.2 μm Polycap 36 TC filter (hydrophilic polyethersulfone membrane, Whatman). Carboys were incubated in the dark, and sampled every 12-24 hours for cell counts, phosphate concentration, lipid concentration, phospholipid production rate, and ^{3}H-Leu and ^{3}H-TdR uptake rate. For the regrowth in the Sargasso Sea, the experiment was conducted on board the R/V *Atlantic Explorer* during the BV39 cruise in October 2007. Seawater was collected at 32.610°N 64.100°W at 5 m depth, and

the carboys were incubated in a dark, temperature-controlled room (within 2°C of surface water temperature). For the regrowth in the North Pacific, the experiment was conducted on board the R/V *Kilo Moana* during the KM1013 cruise in July 2010. Seawater was collected at 22.756°N 157.988°W at 25 m depth, and the carboys were incubated in on-deck flow-through incubators at ambient surface temperature, covered in foil and two layers of black plastic to maintain darkness.

2.3 Cell counts

Samples for cell counts were 1.5-2.0 mL seawater fixed with a final concentration of 1-2% formaldehyde (1.5 mL with 1% PFA for North Atlantic cruises BV39 and Oc443; 1.8 mL with 2% PFA for the Mediterranean Sea cruise BOUM; 2.0 mL with 1% filtered concentrated formaldehyde for North Pacific cruise KM1013). All samples were stored in 2.0 mL cryovials, allowed to fix at 4°C for 30 minutes to an hour, then flash frozen in liquid nitrogen and stored at -80°C until analysis. North Atlantic samples were analyzed at the Bermuda Institute of Ocean Sciences (BIOS) using a Becton Dickinson InFlux flow cytometer. Heterotrophic bacteria were discriminated from small phytoplankton (i.e. *Prochlorococcus* and *Synechococcus*) using side scatter, phycoerythrin (orange) and chlorophyll (red) fluorescence, and protein-binding stain (FITC) fluorescence; for full methods see Popendorf et al., 2011a. Mediterranean Sea samples were analyzed at the Observatoire Océanologique in Banyuls sur mer, France using a Becton Dickinson FacsCalibur flow cytometer. Heterotrophic bacteria were discriminated from small phytoplankton based on chlorophyll fluorescence; for full methods see Van Wambeke et al., 2011. North Pacific samples were analyzed at the Woods Hole Oceanographic Institution (WHOI) using a Millipore Guava easyCyte HT flow cytometer. Cells were stained with SYBR green (Lonza) (1% final concentration of 20x solution) for 45 minutes at room temperature in the dark. Cells were excited with a 488 nm 20 mW laser, then discriminated and enumerated based on side scatter (related to cell size) and green fluorescence (525/30 nm). Flow speed was set to 0.59 μL/s, approximately 100 μL was analyzed per sample. Each sample was counted in triplicate. Gates were set and samples

were analyzed using the guave InCyte software (Millipore). It was not possible to discriminate heterotrophic bacterial cells from small phytoplankton cells with similar DNA content. Based on other flow cytometry analyses from this cruise (Bjorkman et al., 2012) it is likely that approximately 75% of the counted cells in the t0 measurements of the regrowth were heterotrophic bacteria and the remainder were *Prochlorococcus*. Over the course of the 72 hour incubation in the dark we attributed the increase in cell concentration solely to increase in heterotrophic bacteria, based on observed population changes in similar regrowth experiments (Popendorf et al., 2011a).

2.4 Soluble reactive phosphorus (SRP) concentration

In the North Atlantic and North Pacific (BV39, Oc443, and KM1013), 200 mL samples of whole seawater were stored in HDPE bottles and frozen at -20 °C until analysis in lab. Samples from the North Atlantic (BV39 and Oc443, except for the regrowth samples) were analyzed at BIOS using the MAGIC method (Karl and Tien, 1992), see Lomas et al. (2010) for full methods. Samples from the Mediterranean Sea (BOUM) were analyzed at sea using a modified MAGIC method, see Rimmelin and Moutin (2005) for full methods. Samples for both sets of regrowth experiments and other North Pacific samples were analyzed at WHOI using MAGIC, more specifically: duplicate samples of 50 mL were concentrated to 6 mL using magnesium induced co-precipitation (Karl and Tien, 1992), then analyzed using arsenate correction (Johnson, 1971) and molybdenum blue (Strickland and Parsons, 1972), on a Nicolet evolution 300 spectrophotometer (Thermo Electron Corporation) measuring absorbance at 880/4 nm. For the Sargasso Sea regrowth experiment (BV39), SRP was measured over the course of the incubation from one carboy and these concentrations were applied for replicate carboys.

2.5 Intact polar diacylglycerolipids (IP-DAG) concentration

Samples for IP-DAG quantification were 1-2 L of whole seawater filtered using light vacuum filtration (<200 mm Hg) onto 47 mm diameter 0.2 μm poresize Anodisc filters (Whatman) for BV39 and Oc443, and hydrophilic Durapore filters (Millipore) for BOUM

and KM1013. Filters were wrapped in combusted aluminum foil and frozen in liquid nitrogen until analysis in lab. IP-DAGs were extracted using a modified Bligh and Dyer method and analyzed using high pressure liquid chromatography electrospray ionization triple quadrupole mass spectrometry (HPLC-ESI-TQMS) on an Agilent 1200 HPLC and Thermo Scientific TSQ Vantage TQMS. For full extraction, HPLC, MS, and quantitation methods see Chapter 2.

2.6 $^{33}PO_4$ uptake into phospholipids

Samples from depth profiles along transects, and at each timepoint in the regrowth experiments, were 50-200 mL seawater in acid-cleaned polycarbonate bottles or sterile, untreated polypropylene centrifuge tubes, spiked with 0.2-20 μCi $^{33}PO_4^{3-}$ (Perkin Elmer), incubated in the dark at ambient seawater temperature for 0.5-10 hours, then filtered onto 47 mm diameter 0.2 μm poresize filters using light vacuum filtration (<200 mm Hg). Details for incubations and extractions varied by cruise, and are outlined in the Table 1 below. For samples from the BV39, Oc443, and KM1013 cruises filters were wrapped in combusted aluminum foil and frozen in liquid nitrogen until extraction in lab; for samples from the BOUM cruise filters were transferred immediately to vials with solvents for Bligh and Dyer extraction and processed shipboard.

Table 1

	BV39	**Oc443**	**BOUM**	**KM1013**
filter type	Anodisc	Anodisc	Durapore	Durapore
seawater incubation (mL)	100	100	50	200
incubation length (hrs)	0.5-2	1-3/8-10*	1-2	8-11
$^{33}PO_4$ spike (μCi)	4	0.2	10-20	10
TLE vol (mL)	2	2	1.5	2
DNP-PE int std (μL)	20	20	n/a	n/a
final TLE vol (μL)	200	200	1500	2000
HPLC injection vol (μL)	20	20	100	100
fraction collector system	HP1050	MSD	HP1050	HP1050

*Oc443: incubations at high phosphate locations were 8-10 hrs, low phosphate locations were 1-3 hrs

IP-DAGs were extracted using the same extraction protocol as for IP-DAG quantification (see Chapter 2). The volume of the total lipid extract (TLE) was equal to the volume of dichloromethane used in the Bligh and Dyer extraction. For BV39 and Oc443, TLE was concentrated down to 200 μL by drying under nitrogen. Phospholipid classes were then separated and purified from the TLE using preparative HPLC. HPLC conditions were the same as for IP-DAG quantification (see Chapter 2). Time-based windows were used to collect purified fractions of three phospholipid classes: phosphatidylglycerol (PG), phosphatidylethanolamine (PE), and phosphatidylcholine (PC). Retention times were established by analyzing repeated injections of dipalmitoyl synthetic standards of PG, PE, and PC (Avanti Polar Lipids, Inc.). During fraction collection the outlet from the HPLC column was redirected to a fraction collector, bypassing the detector. Stability of retention times was monitored by running standards every 10-20 samples. For BV39, BOUM and KM1013 samples a Hewlett Packard 1050 HPLC (HP1050) was used with an ISCO Foxy Jr. fraction collector, retention times were established using a Sedere Evaporative Light Scattering Detector (ELSD); for Oc443 samples an Agilent 1200 HPLC was used with an Agilent 1200 fraction collector, retention times were established using an Agilent mass selective detector (MSD). Following fraction collection, each fraction (1-2 mL HPLC eluents, a mixture of hexane, isopropanol and water) was transferred to a 20 mL polyethylene scintillation vial with 15 mL Ultima Gold scintillation cocktail (Perkin Elmer). The ^{33}P radioactivity was determined on a Tricarb liquid scintillation counter, count times were 20 minutes for dpm in the 5-250 keV range. Phospholipid production rate was calculated as:

$$P_{lipid} = \frac{A}{s} * \frac{1}{t} \qquad \text{(eq. 1)}$$

where P_{lipid} is the phospholipid production rate (pmol P L^{-1} hr^{-1}), A is the ^{33}P radioactivity of the phospholipid fraction (dpm L^{-1}, accounting for the volume of the incubation and the fraction of TLE injected for preparative HPLC), s is the specific activity of $^{33}PO_4^{3-}$ in the incubations (dpm of spike (L^{-1}) (pmol SRP L^{-1})$^{-1}$), and t is the length of the incubation (hr).

2.7 ^{3}H-Leu and ^{3}H-TdR uptake

For BV39, Oc443, and KM1013, uptake of ^{3}H-Leu and ^{3}H-TdR were measured using the filtration method (Fuhrman and Azam, 1982; Kirchman et al., 1982; Simon and Azam, 1989). Samples were 30 mL (BV39, Oc443) or 50 mL (KM1013) seawater in acid-washed polycarbonate bottles, incubated with ^{3}H-Leu (20 nM final concentration, mixture of cold Leu and [4,5-^{3}H] L-Leucine, MP Biomedicals) or ^{3}H-TdR (10 nM, methyl-^{3}H thymidine, MP Biomedicals) for 1-10 hours (incubation times were the same as for phospholipid production rates, see Table 1) in the dark at ambient seawater temperature. Killed controls (1% formaldehyde added before ^{3}H spike) were run in parallel. Samples were killed with formaldehyde (1% final concentration), then filtered onto 25 mm 0.2 μm cellulose nitrate filters (Whatman), rinsed four times with ice-cold trichloroacetic acid (TCA), then with ice-cold 80% ethanol. Filters were stored dry in 20 mL polypropylene scintillation vials and brought back to lab. Filters were dissolved in 1 mL ethyl acetate, then 6 mL Ultima Gold LLT scintillation cocktail (Perkin Elmer) was added. Samples were allowed to sit in the dark for 24 hours before counting on Tri-carb 2770 TR/SL liquid scintillation analyzer (Packard; BV39 and Oc443) or Beckman Coulter LS6500 multipurpose scintillation counter (KM1013). Measured cpm were converted to dpm using commercial ^{3}H-toluene quenched standards in Ultima Gold scintillation cocktail (Perkin Elmer). For BOUM, uptake of ^{3}H-Leu was measured using the centrifugation method (Smith and Azam, 1992). Samples were 1.5 mL incubated with 23 nM ^{3}H-Leu (mixture of cold Leu and [4,5-^{3}H] L-Leucine, Perkin Elmer). For full methods see Van Wambeke et al. (2011). To convert ^{3}H-TdR uptake rates (pmol L^{-1} hr^{-1}) to heterotrophic bacterial production (cells L^{-1} hr^{-1}) a conversion factor of $1.0x10^{18}$ cells mol^{-1} was used (BV39, Oc443, KM1013). To convert ^{3}H-Leu uptake rates (pmol L^{-1} hr^{-1}) to heterotrophic bacterial production a conversion factor of $1.0x10^{17}$ cells mol^{-1} was used (BV39, Oc443, KM1013), or conversion factors of 1.5 kgC $(mol\ Leu)^{-1}$ and 20 fgC $cell^{-1}$, equivalent to $7.5x10^{16}$ cells $(mol\ Leu)^{-1}$ (BOUM).

2.8 Calculation of coefficients and statistical analysis

Exponential curves were fit for the regrowth experiment data using the Curve Fitting Toolbox in Matlab (R2012a). Standard deviations of the exponential coefficients were calculated using the normal distribution of errors created by the curve fitting model. Measurements were considered within error when pairwise comparisons of the coefficients from fits or averages from replicate analyses were within +/- 1 standard deviation of each other.

3. Results

3.1 Heterotrophic bacterial cell specific growth rate in regrowth experiments

The specific production rate of any given material (cells, biomass, or biochemicals) can be generically defined as μ:

$$\mu = \frac{P_N}{N(t)} \text{ (eq. 2)}$$

where P_N is the production rate of the material (mol L^{-1} d^{-1}, or cells L^{-1} d^{-1}), and $N(t)$ is the abundance of the material at time t (mol L^{-1}, or cells L^{-1}), thus the specific production rate, μ, has units of per time (d^{-1}). If a system is at steady state then the production of the material is balanced by losses, and the abundance of the material is not changing with time:

$$dN/dt = P_N - S_N = 0 \text{ (eq. 3)}$$

where dN/dt is the rate of change of abundance of the material, P_N is the production rate of the material, and S_N is the rate of loss of the material. In the case of a system at steady state, the specific production rate, μ, can be described as the turnover rate.

In the regrowth experiments, the incubation conditions were designed such that the concentration of heterotrophic bacterial cells was not at steady state, and instead the population was increasing. The concentration of cells, $C(t)$, was measured at roughly 12 hour time points over the course of 72 hours. During this time the heterotrophic bacterial cell concentration increased three-fold in the Sargasso Sea, from 1.0×10^4 cells mL^{-1} to 3.0×10^4 cells mL^{-1} (average of experiments A, B, and C, Fig. 1a), and almost four-fold in

the North Pacific, from $1.3x10^5$ cells mL^{-1} to $4.8x10^5$ cells mL^{-1} (average of experiments A, B, and C, Fig. 2a). During the period of log phase growth, where the increase in cell concentration was exponential over time, it follows that the change in cell concentration, *dC/dt*, can be modeled as a linear function of cell concentration:

$$dC/dt = \mu_{cell} C(t) \quad \text{(eq. 4)}$$

And it was thus possible to calculate μ_{cell} by fitting an exponential curve to the cell concentration data over time:

$$C(t) = C_0 e^{\mu_{cell} t} \quad \text{(eq. 5)}$$

where *C(t)* is the concentration of cells (mL^{-1}) at time *t*, C_0 is the initial concentration of cells at the beginning of log phase growth, and μ_{cell} is the specific growth rate of cells with units per time (d^{-1}). In this way we used the increase in cell concentration over time to provide a direct measure of heterotrophic bacterial cell specific growth rate.

In both of these experiments a 24 hour lag phase was observed, and log phase growth occurred from 24-72 hours in the Sargasso Sea and from 24-48 hours in the North Pacific. Fitting an exponential curve to the cell concentration during log phase growth (eq. 5), we calculated that μ_{cell} was about 0.5 per day in the Sargasso Sea regrowth experiment (s.d. 0.04; exponential curve fit to measures from three replicates A, B, and C for five timepoints, 24-72 hours; Fig. 3a) and μ_{cell} was about 1.3 per day in the North Pacific regrowth experiment (s.d. 0.3; exponential curve fit to measures from three replicates A, B, and C for three timepoints, 24-48 hours; Fig. 3b).

3.2 Phospholipid specific production rate in regrowth experiments

In these same regrowth experiments the concentration of membrane lipids was also measured at roughly 12 hour timepoints over 72 hours. The absolute concentration (pmol L^{-1}) of nine classes of IP-DAGs was quantified in each sample. During the period of log phase cell growth, in the Sargasso Sea three classes of IP-DAGs increased in concentration: the phospholipids phosphatidylglycerol (PG) and phosphatidylethanolamine (PE; Fig. 1b), and the glycolipid monoglycosyldiacylglycerol (MGDG; see Popendorf et al., 2011a for full IP-DAG concentration data). In the North

Pacific only PG and PE increased in concentration (Fig. 2b; other IP-DAG data not shown). Following the same model as cell specific growth rate described above, we calculated the specific production rate of the phospholipids, λ_{accum}, from the increase in phospholipid concentration over time during the period of log phase growth using an exponential fit:

$$L(t) = L_0 e^{\lambda_{accum} t} \quad \text{(eq. 6)}$$

where *L(t)* is the concentration of a particular IP-DAG class (e.g. PG or PE, pmol L^{-1}) at time *t*, L_0 is the IP-DAG concentration at the start of log phase growth, and λ_{accum} is the IP-DAG specific production rate in units d^{-1}. Fitting an exponential curve to the IP-DAG concentrations in the Sargasso Sea regrowth experiment (fit to the measures of A, B, and C for five timepoints 24-72 hours, Fig. 1b) we calculated that λ_{accum} was about 0.3 per day for PG and 0.3 per day for PE (s.d. 0.1 for both PG and PE; Fig. 3a). In the North Pacific regrowth experiment lipid data was only available through 36 hours. Fitting an exponential curve to the available data (fit to the measures of A, B, and C for three timepoints 12-36 hours, Fig. 2b) we calculated that λ_{accum} was about 1.7 per day for both PG and PE (s.d. 0.8 and 1.2 respectively; Fig. 3b).

In addition to measuring the accumulation of phospholipids over time, we were also able to measure the "instantaneous" production rate of phospholipids (pmol L^{-1} d^{-1}) by measuring the incorporation of radioactive phosphate ($^{33}PO_4^{3-}$) into individual phospholipid classes during brief incubations (Figs. 1c and 2c). This provided a different way to the calculate the phospholipid specific production rate, $\lambda_{instant}$, at individual timpeoints using the equation:

$$\lambda_{instant} = \frac{P_{lipid}}{L(t)} \quad \text{(eq. 7)}$$

where P_{lipid} is phospholipid production rate measured by the amount of $^{33}PO_4^{3-}$ incorporated into a particular phospholipid class (PG or PE) during a brief incubation (pmol L^{-1} d^{-1}), and *L(t)* is the concentration of the phospholipid class (PG or PE) at the start of the brief incubation (pmol L^{-1}). We measured the instantaneous production rate of PG and PE over the course of the regrowth experiments (Figs. 1c and 2c), and used

this to calculate $\lambda_{instant}$PG and $\lambda_{instant}$PE during log phase growth (Fig. 3). In the Sargasso Sea regrowth experiment we calculated that $\lambda_{instant}$PG was about 0.6 per day (s.d. 0.3) and $\lambda_{instant}$PE was 0.8 per day (s.d. 0.6; average of replicates A, B, and C from 24-72 hours; Fig. 3a). In the North Pacific regrowth experiment we calculated that $\lambda_{instant}$ of both PG and PE was 1.0 per day (s.d. 0.3 and 0.6 respectively; average of replicates A, B, and C from 24-36 hours; Fig. 3b).

3.3 Uptake of leucine and thymidine in regrowth experiments

In the regrowth experiments, in addition to measuring cell concentration, phospholipid concentration and phospholipid production rate, we also measured the uptake rates of ^{3}H-Leu and ^{3}H-TdR (Fig. 1d and 2d). This data was used two different ways: 1) using conversion factors of Leu/cell and TdR/cell from published literature we were able to calculate ^{3}H-Leu- and ^{3}H-TdR-based heterotrophic bacterial cell specific growth rates, μ_{Leu} and μ_{TdR} respectively; and 2) we calculated conversion factors of Leu/cell and TdR/cell using the ^{3}H-Leu and ^{3}H-TdR uptake rates over time and the change in cell concentration over time.

Heterotrophic bacterial cell specific growth rate was calculated at individual timepoints from the uptake rates of ^{3}H-TdR and ^{3}H-Leu using the following equation:

$$\mu_{TdR} = \frac{P_{TdR} * CF}{C(t)} \quad \text{(eq. 8)}$$

where P_{TdR} is the uptake rate of TdR (mol TdR L^{-1} d^{-1}) into cold TCA-insoluble cellular material, which we measured using the standard filtration method (Kirchman, 1992), *C(t)* is the concentration of heterotrophic bacterial cells (cell L^{-1}), and *CF* is a conversion factor (cell (mol TdR)$^{-1}$) which we took from published literature (substituting Leu for TdR throughout for the calculation of μ_{Leu}). Using average reported conversion factors of $1.0x10^{17}$ cells (mol Leu)$^{-1}$ and $1.0x10^{18}$ cells (mol TdR)$^{-1}$ (Steinberg et al., 2008; Ducklow, 2000), in the Sargasso Sea regrowth experiment we calculated μ_{Leu} to be about 0.7 per day (s.d. 0.2) and μ_{TdR} to be about 0.8 per day (s.d. 0.3; average of replicates A, B, and C from 24-72 hours; Fig. 3a). In the North Pacific regrowth experiment we

calculated μ_{Leu} to be about 1.6 per day (s.d. 1.1) and μ_{TdR} to be about 1.3 per day (s.d. 0.9; average of replicates A, B, and C from 24-36 hours; Fig. 3b).

Mathematical methods for calculating conversion factors vary, several approaches are outlined in Ducklow, 2000. There are two general approaches, a "derivative" method using the slope of a linear regression of ln(^{3}H-uptake) versus time and intercepts of ^{3}H-uptake/time and cells/time (Kirchman et al., 1982), and a "cumulative" method using cumulative cell production and integrated ^{3}H-uptake, effectively a point to point calculation of changes in cells and uptake of ^{3}H between each timepoint (Fuhrman and Azam, 1982). While these methods are based on sound mathematical theory that should yield similar results for idealized exponential growth of bacteria, the reality of most datasets is that in practice calculation by different methods can yield substantially different results. Two variations of each of these methods were applied to the regrowth data, with results that varied by as much as an order of magnitude (Table 2). Using the "cumulative" method, applied as a point-to-point calculation of the change from the start to the end of the exponential growth phase, yielded conversion factors in the middle of the range for each regrowth: for the Sargasso Sea regrowth experiment, a ^{3}H-Leu conversion factor of 2.3×10^{17} cells/mol and a ^{3}H-TdR conversion factor of 9.7×10^{17} cells/mol; for the North Pacific regrowth experiment a ^{3}H-Leu conversion factor of 1.0×10^{17} cells mol^{-1} and a ^{3}H-TdR conversion factor of 1.0×10^{18} cells mol^{-1}. In the Sargasso Sea these conversion factors are very close to those we applied from the literature, and in the North Pacific the calculated conversion factors are identical to those we applied from the literature.

3.4 Comparison of specific production rates in regrowth experiments

In summary, in these regrowth experiments, specific production rates were measured four different ways: by increase in heterotrophic bacterial cell concentration over time (μ_{cell}), by increase in phospholipid concentration over time (λ_{accum} for PG and PE), by instantaneous production rate of phospholipids divided by phospholipid concentration ($\lambda_{instant}$ for PG and PE), and by uptake rates of ^{3}H-TdR and ^{3}H-Leu (μ_{Leu} and

μ_{TdR}). The measurement of μ_{cell} does not rely on the measurement of any biochemical proxies and is the most direct measurement of heterotrophic bacterial specific growth rate. Therefore μ_{cell} is the value to which we compared our other measurements of specific production rate to assess their validity as methods for measuring heterotophic bacterial production. In the North Pacific regrowth experiment all of our other measurements of specific production rate (λ_{accum}PG, λ_{accum}PE, $\lambda_{instant}$PG, $\lambda_{instant}$PE, μ_{Leu}, and μ_{TdR}) were within error of μ_{cell}, with an average specific production rate of about 1.6 per day. In the Sargasso Sea regrowth experiment all measures of specific production rate except for λ_{accum}PG were also within error of μ_{cell}, and the average specific production rate was about 0.6 per day.

3.5 Specific growth rate in the ocean

The specific production rate of phospholipids, $\lambda_{instant}$PG and $\lambda_{instant}$PE, and heterotrophic bacterial cell specific growth rate based on uptake rates of ^{3}H-Leu and ^{3}H-TdR, μ_{Leu} and μ_{TdR}, were measured throughout the North Atlantic, across the Mediterranean Sea, and at one location in the North Pacific. To make these calculations, at each sampling site individual measurements were made of phosphate concentration (SRP), IP-DAG concentrations, instantaneous phospholipid production rates (P_{lipid}), heterotrophic bacterial cell concentration, and uptake rates of ^{3}H-Leu (all locations) and ^{3}H-TdR (except in the Mediterranean Sea). At most sampling locations multiple depths were sampled, and data are presented for the average of samples from the upper 40 m (Fig. 4).

In the North Pacific subtropical gyre, measurements were made at the same site as the regrowth experiment (Table 3). In the water column we found $\lambda_{instant}$PG to be 0.6 per day and $\lambda_{instant}$PE to be 0.8 per day (Fig. 4a), while μ_{Leu} and μ_{TdR} were both 0.1 per day (Fig. 4b). In the North Atlantic, measurements were made across a transect from phosphate-rich waters north of the Gulf Stream (samples from two locations) south into the phosphate-depleted waters of the Sargasso Sea (samples at three locations on the Oc443 cruise, and four locations on the BV39 cruise; Table 3). In the phosphate-replete

waters north of the Gulf Stream, $\lambda_{instant}$PG was 0.3 per day and $\lambda_{instant}$PE was 0.7 per day, and μ_{Leu} and μ_{TdR} were again 0.1 per day. In the phosphate-deplete Sargasso Sea during the spring cruise (Oc443) phospholipid specific production rates were higher, 2.7 and 1.9 per day for $\lambda_{instant}$PG and $\lambda_{instant}$PE respectively, while μ_{Leu} and μ_{TdR} were 0.1 per day. During the fall cruise in the Sargasso Sea (BV39), phospholipid specific production rates were 0.7 and 0.5 per day for $\lambda_{instant}$PG and $\lambda_{instant}$PE, and 0.1 per day for μ_{Leu} and 0.2 per day for μ_{TdR}. Excluding the spring cruise in the Sargasso Sea, across the North Pacific and North Atlantic $\lambda_{instant}$PG averaged fives times greater than ^{3}H-based rates, and $\lambda_{instant}$PE averaged six times greater. During the spring cruise in the Sargasso Sea, $\lambda_{instant}$PG was roughly 35 greater than ^{3}H-based rates, and $\lambda_{instant}$PE was 25 times greater than ^{3}H-based rates.

In the Mediterranean Sea samples were collected across a transect from the oligotrophic west (Algero-Provencal basin/Sicilian channel) to the ultraoligotrophic east (Levantine basin). Across the Algero-Provencal basin through the Ionian basin, phospholipid specific production rates were similar to those measured in the Sargasso Sea in the spring, about 3.6 per day for $\lambda_{instant}$PG and 2.6 per day for $\lambda_{instant}$PE. In the eastern Levantine basin rates were much higher, 11.0 per day for $\lambda_{instant}$PG and 5.4 per day for $\lambda_{instant}$PE. Across all basins μ_{Leu} was 0.1 per day, giving a steeply increasing ratio of $\lambda_{instant}$ to μ_{Leu} from the west to the eastern Mediterranean.

4. Discussion

4.1 Evaluation of current methods

To refine our understanding of the role that heterotrophic bacteria play in the ocean carbon cycle, the question we want to answer is: what is the rate of heterotrophic bacterial production in the surface ocean?

The ultimate goal of measuring bacterial production is an accurate determination of the rate of conversion of dissolved organic matter into biomass. In the ocean, the stock of bacterial biomass is often at steady state on the timescale of days to weeks, with production of bacterial biomass balanced by loss processes including viral lysis, grazing,

and cell death. This negates the possibility of measuring bacterial production by direct assessment of changes in cell concentration or changes in heterotrophic bacterial biomass as we were able to do in the regrowth experiments. Thus it is necessary to employ some form of chemical tracer whose incorporation is a good proxy for the production of heterotrophic bacterial biomass. The difficulty in measuring heterotrophic bacterial production stems in part from the nature of heterotrophy: heterotrophs are defined by their reliance on organic carbon as a carbon source, but the pool of dissolved organic carbon in the marine environment is a diverse, complex mixture of a vast array of molecules (Repeta et al., 2002) whose biological accessibility is hard to assess (Hullar et al., 1996). Thus measurements that rely on the uptake of an organic carbon tracer may be heavily biased by the selection of a particular substrate to serve as a proxy for organic carbon uptake. Wright and Hobbie (1965) established the utility of radiolabeled organic solutes in the determination of microbial processes in aquatic systems, and later work assessed the specificity of ^{3}H-TdR and ^{3}H-Leu uptake as a tracer for heterotrophic bacterial uptake (Karl, 1979; Fuhrman and Azam, 1980, 1982; Kirchman et al., 1982, 1985).

Many of the establishing papers for the ^{3}H-Leu and ^{3}H-TdR methods clearly lay out the criteria for an accurate method of measuring bacterial production (Fuhrman and Azam, 1982; Moriarty, 1986 and references therein), which can be summarized as the following: that the labeled substrate be available to the whole population of interest, that the labeled material be specific to the population of interest, and that the ratio of incorporated material to cell biomass production be measurable and consistent.

When the ^{3}H-TdR and ^{3}H-Leu uptakes methods were established it was determined that uptake of exogenous thymidine and leucine was unique to heterotrophic bacteria among plankton, within the resolution of available tools for assessment, thus the production of ^{3}H labeled DNA or protein (defined as particulate material insoluble in cold trichloroacetic acid) was deemed to be specific to heterotrophic bacteria (Fuhrman and Azam, 1980, 1982; Kirchman et al., 1982). Recent work has demonstrated that, in addition to heterotrophic bacteria, phototrophic cyanobacteria, particularly

Prochlorococcus, also incorporate ^{3}H-TdR and ^{3}H-Leu in dark incubations (Michelou et al., 2007; Talarmin et al. 2011). Therefore the tritiated material produced in the incubations is not specific to heterotrophic bacteria.

For ^{3}H-TdR and ^{3}H-Leu uptake to accurately represent heterotrophic bacterial production the uptake of the labeled substrate needs to be ubiquitous for all heterotrophic bacteria. This was challenged early on when Fuhrman and Azam (1982) found that uptake of radiolabeled phosphate into DNA gave synthesis rates that were 3 to 7 times greater than the uptake of ^{3}H-TdR into DNA. In a more recent study, Longnecker et al. (2010) found that 2 to 10 times more heterotrophic bacterial cells are active in the uptake of $^{33}PO_4$ compared to the uptake of ^{3}H-TdR or ^{3}H-Leu.

Given that Longnecker et al. (2010) found that less than 20% of DAPI-stained cells in the North Atlantic were active in the uptake of ^{3}H-Leu and ^{3}H-TdR, we expect that uptake rates of ^{3}H-Leu and ^{3}H-TdR underestimate bacterial production rate in the open ocean. Therefore we have proposed and applied a new method for measuring heterotrophic bacterial production rate that relies on the uptake of a more ubiquitous substrate, phosphate, into phospholipids specific for heterotrophic bacteria, PG and PE. In order for this new method to be an accurate measure of heterotrophic bacterial production rate, it is necessary that: 1) phosphate uptake be ubiquitous for all heterotrophic bacteria and that it be the dominant source of phosphorus for heterotrophic bacteria; 2) the phospholipids PG and PE be specific to heterotrophic bacteria; and 3) there is a consistent, quantitative relationship between phospholipid specific production rate and cell specific growth rate. The first two of these criteria have been demonstrated to be true in published literature, and the third in this study—all three will be discussed in more detail below.

4.2 Conversion factors from bottle incubations

To convert measures of ^{3}H-TdR or ^{3}H-Leu uptake rate to estimates of cell growth rate, conversion factors of TdR/cell and Leu/cell have been calculated using regrowth experiments like those employed in this study (Fuhrman and Azam, 1982; Kirchman et

al., 1982; Simon and Azam, 1989; Kirchman, 1992; Carlson et al., 1996). These conversion factors are generally difficult and time consuming to measure. Thus, for reasons of practicality most published bacterial production rates have been calculated using values from the literature for the most similar environment available. This enables the measurement of bacterial production rate across transects, in depth profiles, and in timeseries—important information for understanding ocean biogeochemical cycles, and inaccessible data if measurements are limited to the specific parcels of water where regrowth experiments have been conducted. Nonetheless, even in sequential regrowth experiments in the same environment the conversion factors measured sometimes cover a 5-fold (Carlson et al., 1996) or greater than 10-fold range (Kirchman, 1992), and the error introduced by these conversion factors may be large (Ducklow, 2000 and references therein).

The power of being able to measure heterotrophic bacterial specific growth rate using phospholipid specific production rate is that this method obviates the need for any conversion factor. The method requires the measurement of three parameters: instantaneous phospholipid production rate, phospholipid concentration, and phosphate concentration. All three of these parameters can be readily measured in the water column, giving a measure of $\lambda_{instant}$ *in situ*, without the introduction of any conversion factors measured in multi-day bottle incubations.

Studies have shown that in multi-day bottle incubations of mixed microbial communities, similar to the regrowth experiments employed here, the community composition at the end of 24 or 48 hours may be quite different from the original community in the inoculating seawater (Fuchs et al., 2000; Eilers et al., 2000). Changes in community composition have the potential to influence the conversion factors measured because community composition is likely to affect both the growth rate of the community and the percent of heterotrophic bacterial cells active in the uptake of ^{3}H-TdR and ^{3}H-Leu. The growth rate of different clades of proteobacteria has been shown to vary by a factor of two (Yokokawa and Nagata, 2005) or up to 10-fold in some settings (Yokokawa et al., 2004). The fraction of cells active in the uptake of amino acids has

been shown to vary as much as 10-fold across different clades of proteobacteria (Alonso-Sáez and Gasol, 2007; Cottrell and Kirchman, 2000). More particularly, in traditional heterotrophic bacterial production incubations with ^{3}H-TdR and ^{3}H-Leu, Longnecker et al. (2010) found that in different bacterial clades different percentages of cells were active in the uptake of Leu and TdR. Given this variation across clades, changes in the relative abundance of different bacterial clades in regrowth incubations may influence the conversion factors measured in these incubations. Applying these conversion factors to calculations of μ_{TdR} and μ_{Leu} in the water column, where a significantly different microbial community may be present, is likely to lead to inaccuraces in the estimated heterotrophic bacterial growth rate.

Indeed, when we measured μ_{TdR} and μ_{Leu} in the water column, at the same locations where we conducted the regrowth experiments and applying the same conversion factors, the specific growth rates we estimated in the water column were 1/10 or less than the rates in the regrowth experiments after 24 hours in the bottle incubations. However, the rates we measured in the water column were very similar to published rates for these locations, and the conversion factors we calculated were very similar to average conversion factors from the literature (Ducklow, 2000 and references therein). In contrast, we found that $\lambda_{instant}$PG and $\lambda_{instant}$PE rates measured in the regrowth experiments and in the water column at the same location gave values within error of each other. These measurements of $\lambda_{instant}$ in the water column do not rely on any parameters measured in the regrowth experiments, thus alleviating potential errors from changes in the community composition in multi-day bottle incubations.

4.3 Phosphate as a general substrate for heterotrophic bacteria

Phosphorus is a universal building block for life, and the uptake of some form of phosphorus is therefore obligate for all microbes. Across the western North Atlantic subtropical gyre the dissolved phosphorus pool is often upwards of 90% dissolved organic phosphorus (DOP), and dissolved inorganic phosphate is generally low nM concentrations (Lomas et al., 2010). Across the North Pacific subtropical gyre the

concentration of phosphate is generally higher, in the range of 50-100 nM, though in certain locations and seasons it can also be below 10 nM, and DOP is often greater than 80% of total dissolved phosphorus (Björkman et al., 2000, 2012). In the North Atlantic, Zubkov et al. (2007) found that bacterioplankton (heterotrophic bacteria plus cyanobacteria) are responsible for the majority of planktonic phosphate uptake. Using ATP as a model compound for DOP they calculated that DOP uptake rate was roughly 13% of phosphate uptake rate, and DOP uptake was thus playing a secondary role as a phosphorus source for plankton. In the North Pacific, Björkman and Karl (2003) found that biologically available phosphorus exceeded dissolved inorganic phosphate (SRP) concentrations in the surface waters by a factor of 1.4-2.8. Their measurements of SRP uptake rates and biologically available phosphorus uptake rates indicated that DOP might be as much as 50% of total phosphorus uptake.

While a variety of organisms are capable of accessing dissolved organic phosphorus (Hoppe, 2003 and references therein), the biological availability and uptake rate of dissolved organic phosphorus is difficult to assess (Dyhrman et al., 2007). Based on enzyme expression and genetic information, DOP uptake has been thought to be more significant as a source of phosphorus for phytoplankton than bacteria (Hoppe, 2003; Dyhrman and Ruttenberg, 2006; Dyhrman et al. 2007; Lomas et al. 2010). Duhamel et al. (2008) found less than 3% of marine bacteria cells stained for alkaline phosphatase activity in the Mediterranean Sea. However, recent studies employing cell-specific measurement of radiolabeled ATP uptake as a proxy for DOP found that, of the abundant microbes in the North Pacific (i.e. comparing heterotrophic bacteria and *Prochlorococcus*; Björkman et al., 2012) and the Sargasso Sea (i.e. comparing heterotrophic bacteria, *Prochlorococcus*, and *Synechococcus*; Michelou et al., 2007), heterotrophic bacteria were responsible for the majority of ATP uptake due to their abundance. Though this indicates that on a community level heterotrophic bacteria are the major microbial consumers of ATP, the cell-specific uptake rates indicated that this still supplies only a small fraction of heterotrophic bacterial phosphorus needs, with cell-specific ATP uptake rates (amol cell^{-1} d^{-1}) less 3% of phosphate uptake rates for

heterotrophic bacteria in the North Pacific (Björkman et al., 2012), and less than 23% for heterotrophic bacteria in the Sargasso Sea (Michelou et al., 2011). Indirect estimates from data in Casey et al. (2009) suggest bacteria may acquire roughly 10% of their phosphorus from organic sources, based on ^{33}P-ATP uptake as a proxy for DOP and $^{33}PO_4$ uptake in whole seawater and cell-sorted groups of phytoplankton.

Given the data currently available, it seems reasonable to assume that the majority (conservatively 80-90%) of heterotrophic bacterial phosphorus need is being met by uptake of dissolved inorganic phosphate, and therefore tracing the uptake of $^{33}PO_4$ should be quantitatively representative of phosphorus uptake by active heterotrophic bacteria. However, this assumption should be revisited as new data on organic phosphorus utilization becomes available. If it comes to light that dissolved organic phosphorus is a significant source of phosphorus for heterotrophic bacteria, then the measurements made here using uptake of inorganic phosphate would in fact be underestimating true phospholipid production rate, and thus underestimating true heterotrophic bacterial production rate. If this is the case, it further broadens the offset between the current paradigm of slow bacterial production rates based on ^{3}H-TdR and ^{3}H-Leu methods and our estimate of higher bacterial production rate based on phospholipid production rates.

The concept of what constitutes an "active" cell continues to evolve with the methodology for assessing single cell activity (Lebaron et al., 2002; Longnecker et al., 2005; Larsen et al., 2008; Duhamel et al., 2008; Van Wambeke et al., 2008). As the definition of an active cell, or indeed a live cell, continues to evolve so has our understanding of the implications of variable cell activity for rate measurements in the environment. To say that phosphate is accessible for all heterotrophic bacteria does not mean that all live cells in the environment are actively taking up phosphate at a given point in time. The objective, however, is to use a labeled substrate which is as broadly representative as possible for heterotrophic uptake of material in the environment. Longnecker et al. (2010) demonstrated that, for broad assemblages of heterotrophic bacteria in the North Atlantic Ocean, 2 to 10 times more heterotrophic bacterial cells are active in the uptake of $^{33}PO_4$ compared to uptake of ^{3}H-Leu or ^{3}H-TdR, and therefore

uptake rate of $^{33}PO_4$ should be a more accurate representation of heterotrophic bacterial production and should predict a faster rate of growth.

4.4 Phospholipids as a specific product for heterotrophic bacteria

Early studies of the membrane lipid composition of bacteria found that bacterial membranes are composed largely of phospholipids (Kates, 1964; Hagen et al., 1966; Golfine, 1972). With more advanced lipid analysis techniques, quantitative analysis of a diversity of marine microbial cultures has confirmed that marine heterotrophic bacteria lipids are dominated by phospholipids: Van Mooy et al. (2006) measured the lipid composition of three strains of cultured marine heterotrophic bacteria and found them to be exclusively composed of the phospholipids PG, PE and PC. Van Mooy et al. (2009) measured the membrane composition of the heterotrophic bacteria *Pelagibacter ubique*, a representative species of the ubiquitous SAR11 clade that dominates the heterotrophic bacterial community in the Sargasso Sea, and found the membrane to be composed exclusively of PG and PE.

In contrast, studies of cultures of phytoplankton have found PG and PE to contribute relatively little to total lipids (Harwood, 1998; Wada and Murata, 1998; Van Mooy et al., 2006). In particular, PE has never been observed in axenic cyanobacteria cultures (Van Mooy et al., 2006) and only in very low abundance in non-axenic cyanobacteria cultures and other phytoplankton (Harwood, 1998; Van Mooy et al., 2006; Martin et al., 2011). PG is known to be a part of thylakoid membranes (Douce et al., 1973) and a necessary component for the functioning of photosystem II (Sato et al., 2000; Sakurai et al., 2006), and therefore occurs in phytoplankton membranes. However, surveys of phytoplankton cultures have found it to be a relatively small fraction of the total lipids in both eukaryotic phytoplankton (Harwood, 1998) and cyanobacteria (Sakurai et al., 2006; Wada and Murata, 1998), comprising less than 10% of the total lipids in multiple strains of *Prochloroccus* and *Synechococcus* (Van Mooy et al. 2006), the most abundant cyanobacteria in open ocean environments.

To determine if the lipid composition of microbes in the environment is similar to that observed in cultures, Popendorf et al. (2011a) employed several experimental approaches to compare the membrane lipids of phytoplankton versus heterotrophic bacteria from open ocean seawater samples. The study used cell sorting flow cytometry to separate heterotrophic bacteria, *Prochloroccus*, and *Synechoccus* from several sites across the North Atlantic (including the same location and time as the Sargasso Sea regrowth experiment in this study), and found that results in the environment are similar to cultures. The lipids of heterotrophic bacteria were found to be dominated by the phospholipids PG, PE and PC, while the lipids of *Synechococcus* and *Prochlorococcus* were dominated by glycolipids and contained minimal amounts of PG (<10% of total lipids). In these flow sorted samples small amounts of PE were also observed in *Synechococcus* and *Prochlorococcus*, although the occurrence of PE in cyanobacteria is at odds with a wealth of culture data (Wada and Murata, 1998; Sakurai et al., 2006; Van Mooy et al., 2006). It is likely that non-specific cell sorting contributed small amounts of heterotrophic bacteria, and thus PE, to the *Prochlorococcus* and *Synechoccocus* samples, possibly due to robust cell assemblages of cyanobacteria with heterotrophic bacteria (Malfatti and Azam, 2009). However, the PE, irrespective of source, was still minimal in the cyanobacteria sorted fractions relative to heterotrophic bacteria. Given that heterotrophic bacteria are an order of magnitude more abundant than cyanobacteria in the North Atlantic (Carlson et al., 1996; Cavender-Bares et al., 2001; Popendorf et al., 2011a supplemental material), and the high PG and PE content in heterotrophic bacteria (25% and 19% of total lipids respectively; Popendorf et al., 2011a) and low PG and PE content in cyanobacteria (9% and 4% in *Prochlorococcus*, 9% and 8% in *Synechococcus*; Popendorf et al., 2011a), we estimate that the majority of PG and PE in the water column (greater than 80%) is produced by heterotrophic bacteria.

Additional experiments in Popendorf et al. (2011a) employed stable isotope tracing with ^{13}C-labeled bicarbonate and ^{13}C-labeled glucose to differentiate production of membrane lipids by autotrophs versus heterotrophs. The experiments were done with 24-hour incubations in the Sargasso Sea. The results showed that PG incorporated

significant ^{13}C in incubations with ^{13}C-glucose and almost none with ^{13}C-bicarbonate, indicating that in the Sargasso Sea PG is produced almost exclusively by heterotrophic bacteria, further confirming evidence from culture studies and the environment that PG production in the ocean is dominated by heterotrophic bacteria. This experiment found that PE was enriched in ^{13}C in incubations with both ^{13}C-glucose and ^{13}C-bicarbonate. It was unclear from the results if this was due to production by both autotrophs and heterotrophs, or if this instead was the result of secondary production wherein autotrophic microbes took up ^{13}C-labeled bicarbonate and released dissolved ^{13}C-labeled organic carbon that was subsequently taken up by heterotrophic bacteria and incorporated into PE. Given that our present study has measured heterotrophic bacterial production rates, using $\lambda_{instant}$PG and $\lambda_{instant}$PE, of about 2 per day in this area, it seems likely that secondary production contributed to the ^{13}C enrichment of PE during 24 hour incubations with ^{13}C-bicarbonate.

The region of the North Atlantic that was sampled by the Popendorf et al. (2011a) environmental study covered a nutrient gradient from high phosphate concentrations in the north (>400 nM SRP) to very low concentrations in the Sargasso Sea (<1 nM SRP, Popendorf et al., 2011a supplemental material). Based on the lipid data from cell sorting flow cytometry, we calculate that heterotrophic bacteria were the dominant source of PG and PE in both the high phosphate areas and the low phosphate areas. This is significant because it has been demonstrated that the phospholipid content of phytoplankton is influenced by phosphate conditions, with phospholipids composing a larger fraction of total lipids in high phosphate conditions (Minnikin et al., 1974; Benning et al., 1993, 1995; Van Mooy et al., 2006, 2009; Martin et al., 2011). Therefore the contribution of phytoplankton to PG and PE production is likely to be greater in high phosphate areas. Given that phytoplankton specific growth rates are often on the order of 1 per day (Ducklow, 2000), while current ^{3}H-Leu and ^{3}H-TdR-based measures of heterotrophic specific growth estimate rates of roughly 0.1 per day, a higher contribution of PG and PE from phytoplankton could lead to an overestimation of heterotrophic specific growth rate using phospholipid specific production rates.

However, data from published culture and environmental studies indicate that phytoplankton are not likely to be producing more than about one-fifth of the PG and PE in the water column. Thus the potential contribution of phytoplankton to the phospholipid production rates that we measured is unlikely to account for the order of magnitude difference that we observed between our estimates of heterotrophic bacterial production rate and those based on uptake rates of ^{3}H-Leu and ^{3}H-TdR. Based on data from cultures and from environmental samples from the North Atlantic, both PG and PE should be sufficiently specific for heterotrophic bacteria such that their production is representative of heterotrophic bacterial production in the open ocean.

4.5 Relationship between phospholipid specific production rate and cell specific growth rate

Phospholipid production rate has been measured many times before, in cultures, sediment, and aquatic samples (White and Tucker, 1969; White et al. 1977; Moriarty et al. 1985; Freeman and Lock, 1995; Van Mooy et al., 2008). Comparisons have been made in the past between phospholipid production rate and other measures of bacterial production, including uptake of ^{3}H-TdR (Moriarty et al., 1985; Freeman and Lock, 1995), and one study recently explored the relationship between the rates of bacterial production, primary production, and phospholipid synthesis (Van Mooy et al., 2008). At the introduction of these measurements in the 1970's, one potential setback to the broad adoption of phospholipid production rates as measures of microbial activity was that, at the time, the separation and quantification of individual phospholipid classes (i.e. PE and PG) was laborious and time-consuming. Since then, the advancement of preparative high pressure liquid chromatography (HPLC) techniques has provided an efficient, robust and reliable method for the separation of individual lipid classes, and mass spectrometry (MS) has provided unprecedented ability to quantify lipids. The calculation of phospholipid specific production rate in the ocean has been made possible only relatively recently by advances in HPLC-MS analytical techniques that enable the quantification of

absolute concentrations of IP-DAGs from seawater samples (Rütters et al., 2002; Sturt et al., 2004; Chapter 2).

To be able to interpret phospholipid production rate in the environment as a meaningful measure of microbial activity it is necessary to know the relationship between cell turnover rate and phospholipid turnover rate. The relationship between cell growth and phospholipid metabolism was first addressed in culture experiments by White and Tucker (1969). They conducted detailed experiments to study phospholipid metabolism using cultures of *Haemophilus parainfluenza*, a gram-negative bacteria that contains the lipids PG, PE, PC, cardiolipin, phosphatidylserine, and phosphatidic acid. Incubations demonstrated that the concentration of bacteria scaled with total lipid concentration. Furthermore, based on the increase in cells over time and PE over time they found that both had the same doubling time (42 minutes). They performed incubations with $H_3{}^{32}PO_4$ and a variety of ^{14}C-labeled organic compounds to study to the turnover rate of various components of the phospholipids, including the phosphate headgroup, the glycerol backbone, and the fatty acid chains. For all of the different phospholipid classes, pulse-chase experiments indicated that ^{14}C turned over more slowly than ^{32}P in the headgroup and glycerol unit, although ^{32}P did not seem to turnover more quickly than the cells. This was expanded to an environmental setting by White et al. (1977) who measured phospholipid synthesis rate in incubations of leaf detritus in an estuary. Using incubations with $H_3{}^{32}PO_4$ and ^{14}C-acetate they found that total phospholipid synthesis rate was correlated with other measures of microbial activity. Furthermore they hypothesized that the uptake of $^{32}PO_4$ into phospholipids in brief incubations should represent primarily prokaryotic microbial activity. Moriarty et al. (1985) reinforced this idea in incubations of marine sediment slurries, where they measured lipid synthesis rates using the uptake of $H_3{}^{32}PO_4$ into phospholipids and $H_2{}^{35}SO_4$ into sulfolipids and compared this to the uptake rate of ^{3}H-TdR. They found that phospholipid synthesis rates and ^{3}H-TdR uptake rates gave very similar estimates of bacterial production, and that cycloheximide, which inhibits eukaryotic growth, did not affect phospholipid synthesis in the first twenty minutes of the incubations. These results supported the idea that phospholipid synthesis

rate could represent bacterial production rate in environmental samples, but, prior to our study, no experiments had examined the quantitative relationship between heterotrophic bacterial specific growth rate and phospholipid specific production rate in an open ocean setting.

At the outset of this study we hypothesized that marine microbial prokaryotic membrane is not significantly recycled during cell life, and using regrowth experiments we have shown that indeed μ_{cell} is within error of λ_{accum} and $\lambda_{instant}$ for heterotrophic bacteria in the open ocean. Given the error in our current measurements, from a combination of both methodological and biological variability, we cannot resolve differences smaller than roughly 40% between μ_{cell} and λ, so it is possible that some amount of membrane recycling does occur within the cell. This may contribute to the observed variations between μ_{cell} versus λ_{accum} and $\lambda_{instant}$ in the Sargasso Sea compared to the North Pacific regrowth experiments. However, within the error of our measurements, even if true λ were 40% greater than true μ_{cell}, this is not sufficient to account for the order of magnitude difference that we observed between $\lambda_{instant}$ and μ_{Leu} in the water column. In summary, we have demonstrated that phospholipid specific production rate is sufficiently similar to heterotrophic bacterial specific growth rate such that $\lambda_{instant}$ provides a good measure of heterotrophic bacterial specific growth rate in the ocean.

4.6 Significance of phospholipid turnover rate in the ocean

Ultimately we would like to know the role that heterotrophic bacteria play in the marine carbon cycle, and how variable this role is in different biomes of the ocean. Through the results of our regrowth experiment and examination of existing literature, we have shown that the measurement of phospholipid specific production rate in the water column is a good measure of heterotrophic bacteria specific growth rate. The phospholipid specific production rates we measured in the North Pacific and the North Atlantic estimate heterotrophic bacterial specific growth rates on the order of 1 per day, or, if we assume steady state, a bacterial turnover rate of 1 per day. In comparison, our ^{3}H-Leu and ^{3}H-TdR based specific growth rate estimates were on the order of 0.1 per day,

an order of magnitude less. These ^{3}H-Leu and ^{3}H-TdR values are typical of measurements in these areas (Carlson et al., 1996; Ducklow et al., 2000; Steinberg et al., 2001), and therefore heterotrophic bacterial growth has generally been assumed to be slow. Though faster than the current paradigm, our phospholipid specific production rates predict heterotrophic bacterial specific growth rates that are akin to phytoplankton specific growth rates measured in these gyres (Ducklow, 2000) and are therefore not beyond the reasonable realm for microbial activity in the ocean. Based on our measurement of phospholipid specific production rate, we posit that true bacterial turnover rates in the North Atlantic and North Pacific subtropical gyres are on the order of 1 day, roughly an order of magnitude greater than previously thought.

The phospholipid specific production rates measured in the Mediterranean Sea were higher than in the North Atlantic and North Pacific, ranging from about 2.5 to 11 per day. Though the highest rates in the eastern Mediterranean were two orders of magnitude greater than μ_{Leu} in those locations, these phospholipid specific production rates translate to bacterial turnover times of roughly 2 hours which is physiologically conceivable (White and Tucker, 1969). The surface ocean of the Mediterranean Sea is a unique environment with exceptionally low phosphate concentrations and extremely high dissolved inorganic N:P ratios far in exceedance of Redfield stoichiometry (Krom et al., 1991; Moutin and Raimbault, 2002), with dissolved N:P values ranging from 24 in the western Mediterranean up to 32 in the eastern Mediterranean (Pujo-Pay et al., 2011). In this unique environment it is possible that these phospholipid specific production rates, though high, are real. However, the extremely low phosphate concentrations also pose methodological challenges as the SRP concentration is often on the edge of the available method limit of detection, and uncertainties in SRP contribute to errors in $\lambda_{instant}$. The methods used to measure SRP in the Mediterranean in this study were slightly different from those on the cruises in the North Pacific and North Atlantic, and the measurements of SRP and instantaneous phospholipid production rate (P_{lipid}) were also made shipboard, as opposed to in the lab for the other cruises. Potentially these factors could have contributed to the difference in $\lambda_{instant}$ in these locations.

Irrespective of the high rates measured in the Mediterranean Sea, the $\lambda_{instant}$ rates measured in the North Atlantic and North Pacific were 5-10 times greater than μ_{TdR} and μ_{Leu}. In these locations we conducted regrowth experiments to verify that phospholipid specific production rate was within error of heterotrophic bacterial growth rate. For these gyres, published literature supports our assertion that phosphate is a sufficiently general substrate for heterotrophic bacteria and PG and PE are sufficiently specific products such that phospholipid specific production rate is a good measure of heterotrophic bacterial specific growth rate. Given the phospholipid specific production rates that we measured in the North Atlantic and North Pacific, a conservative estimate of heterotrophic bacterial specific growth rate is a minimum of three times and an average of ten times greater than the current paradigm based on measurements of μ_{Leu} and μ_{TdR}.

The role of heterotrophic bacteria in the ocean carbon cycle is defined not only by the rate of bacterial production, but also by the rate of bacterial respiration. The sum of these two fluxes is the total bacterial carbon demand, representing the total amount of dissolved organic carbon taken up by heterotrophic bacteria. Current measurements of bacterial production and bacterial respiration estimate that bacterial production is only responsible for roughly 10% of bacterial carbon demand in the open ocean (del Giorgio and Cole, 2000). Given the magnitude of bacterial respiration, an order of magnitude greater rate of bacterial production would only double the total bacterial carbon demand.

A two-times higher bacterial carbon demand flux has significant implications for the marine carbon cycle, indicating that more carbon goes through the microbial loop than previously thought. This carbon demand may be met by a larger fraction of primary production being converted to secondary production (heterotrophic biomass) than currently assumed. Fuhrman and Azam (1982) estimated that bacterial production consumed between 10 and 50% of local particulate primary production in the Southern California Bight, and a 1988 review by Cole et al. estimated that bacterial production was an average of 30% of particulate primary production based on many measurements in nearshore and offshore regions. Later studies in pelagic systems have found much lower values, with bacterial production as a percent of particulate primary production ranging

from 1-23% in the Sargasso Sea (Carlson et al., 1996; Steinberg et al., 2001). In the equatorial Pacific, Ducklow et al. (1995) found a range of 12-22%, and in the eastern South Pacific Van Wambeke et al. (2008) observed a highly variable relationship ranging from 19% to bacterial production exceeding particulate primary production.

These studies looked at particulate primary production, though heterotrophic bacterial production is supported by the uptake of dissolved organic carbon and thus bacterial carbon demand may be met by dissolved organic carbon released through phytoplankton exudation, viral lysis, and other processes not measured in particulate primary production (Lagaria et al., 2011). The production of dissolved organic matter is estimated to 10-20% of total primary production across a range of environments (reviewed in Nagata, 2000), but direct measurements of dissolved primary production are not common and the range in values is large within individual studies. Lagaria et al. (2011) measured dissolved primary production, particulate primary production, and bacterial production across the Mediterranean Sea and found that dissolved primary production ranged from 9 to 18% of total primary production, and bacterial production (the same μ_{Leu} measuements used in this study) ranged from 6 to 11% of total primary production, though they concluded that primary production and heterotrophic bacterial carbon demand were relatively decoupled in this system.

A second mechanism to meet higher bacterial carbon demand is that cycling of organic carbon in the surface ocean may involve more *re*-cycling than previously thought. Once inorganic carbon has been fixed by phytoplankton and taken up by bacteria it may be returned to the dissolved organic matter pool through exudation or viral lysis, and consumed again by other bacteria without passing through primary producers (Fuhrman, 2000). If a process, such as viral lysis, rapidly returns bacterial biomass to the dissolved organic pool then it is not necessary for total primary production to support the entirety of bacterial carbon demand on short timescales. Viral lysis is known to be an important process in the cycling of dissolved organic carbon (Fuhrman, 1999) but the rates of viral regeneration of dissolved organic carbon are not well constrained (Brussard et al., 2008). Higher rates of bacterial production may be

accommodated by the dissolved organic carbon cog of the ocean carbon cycle spinning faster than previously thought, potentially fueled by viral lysis.

Either scenario, of greater recycling of dissolved organic carbon or greater bacterial uptake of total primary production, could reasonably supply sufficient carbon to heterotrophic bacteria for the higher bacterial carbon demand estimated from the fast turnover rate of phospholipids. Both scenarios would modify our understanding of the role of heterotrophic bacteria in surface ocean carbon fluxes.

4.7 Future research

The applicability of this method in phosphorus-replete open ocean areas should be further evaluated, as well as its potential applicability in coastal areas that have significantly different microbial communities. For this method to be applicable outside of blue-water, open-ocean settings, work must first be done to evaluate the specificity of PG and PE to heterotrophic bacteria in different environments. Thus far only a limited amount of work has explored membrane lipid variability across oceanic nutrient gradients (Van Mooy et al., 2006, 2009; Popendorf et al. 2011a, 2011b), and even less is known about the distribution of lipids and their variability in coastal or freshwater settings (Bellinger et al., 2012). Given the importance of heterotrophic bacterial production in coastal and estuarine settings it would be valuable to explore the applicability of this method in these environments.

The interpretation of these results should be revisited as more is learned about the basin-scale and clade-level variability in heterotrophic bacterial utilization of dissolved organic phosphorus. Since this method measures the uptake of radiolabeled inorganic phosphorus, heterotrophic bacterial uptake of dissolved organic phosphorus could be leading to underestimation of phospholipid production rates using this method. This again may be particularly relevant to explore in coastal settings where phosphorus dynamics are significantly different from open ocean settings.

5. Conclusions

In regrowth experiments, we have measured the specific growth rate of heterotrophic bacterial cells and specific production rate of phospholipids and found them to be approximately the same in both the Sargasso Sea and the North Pacific. These specific production rates were also equal to cell specific growth rate calculated from uptake of ^{3}H-Leu and ^{3}H-TdR in the regrowth experiments. We calculated specific production rate of heterotrophic bacteria using the increase in direct counts of bacterial cells over time (by flow cytometry), and calculated specific production rate of phospholipids by both accumulation of phospholipids over time and measurement of instantaneous production rate (by brief incubation with $^{33}PO_4$ and purification of individual phospholipids). It is significant that phospholipid specific production rate in the regrowth experiments was within error when measured by both accumulation of phospholipids and by instantaneous production rate, which indicates that there was not significant internal recycling of phospholipids. Both methods of measuring phospholipid specific production rate were within error of direct measurement of cell specific growth rate using the increase in heterotrophic bacterial cells over time. Thus we showed that phospholipid specific production rate can be measured in the ocean and used as a proxy for heterotrophic bacterial specific growth rate. This measurement can be made without the use of conversion factors for lipid/cell content, and is amenable to routine sampling in depth profiles across transects or in timeseries settings.

We measured phospholipid specific production rate across the North Atlantic, across the Mediterranean Sea, and at one location in the North Pacific. Phospholipid specific production rates ranged from 0.3 per day in the North Atlantic to greater than 10 per day in the Mediterranean Sea. In the North Atlantic and North Pacific, average phospholipid specific production rates were approximately 1 per day. This specific production rate is significantly higher than the rate estimated by traditional ^{3}H-Leu and ^{3}H-TdR uptake methods measured at these same locations, which averaged 0.1 per day with little variation across different locations.

We posit that true heterotrophic bacterial turnover rate in the subtropical gyres of the North Atlantic and North Pacific may be on the order of 1-3 per day, vastly faster than most estimates based on ^{3}H-based measurements which suggest turnover rates on the order of 0.05-0.3 per day (Ducklow, 2000). A faster turnover rate on this magnitude would have profound implications for the role that heterotrophic bacteria are playing in the cycling of carbon in the ocean, suggesting that larger fluxes of carbon move through the bacterial loop than previously assumed, and modifying our understanding of the role of these abundant, cosmopolitan organisms.

Acknowledgments

The authors would like to gratefully acknowledge data contributions from collaborators, Krista Longnecker for the ^{3}H-Leu and ^{3}H-TdR measurements on the Oc443 cruise, and France Van Wambeke for ^{3}H-Leu measurements on the BOUM cruise. Additionally we would like to thank Justin Ossolinski, Karin Nordkvist, Agathe Talarmin, and Isabel Ferrera for assistance on cruises, and the captains and crews of the *R/V Atlantic Explorer*, the *R/V Oceanus*, the *R/V L'Atalante*, and the *R/V Kilo Moana*.

References

Alonso-Sáez, L., Gasol, J.M., 2007. Seasonal Variations in the Contributions of Different Bacterial Groups to the Uptake of Low-Molecular-Weight Compounds in Northwestern Mediterranean Coastal Waters. Applied and Environmental Microbiology 73, 3528-3535.

Alonso-Sáez, L., Gasol, J.M., Arístegui, J., Vilas, J.C., Vaqué, D., Duarte, C.M., Agustí, S., 2007. Large-scale variability in surface bacterial carbon demand and growth in the subtropical northeast Atlantic Ocean. Limnology and Oceanography 52, 533-546.

Azam, F., Fenchel, T., Field, J.G., Gray, J.S., Meyer-Reil, L.A., Thingstad, F., 1983. The Ecologocial Role of Water-Column Microbes in the Sea. Marine Ecology Progress Series 10, 257-263.

Bellinger, B.J., Van Mooy, B.A.S., 2012. Non-phosphorus lipids in periphyton reflect available nutrients in the Florida Everglades, USA. Journal of Phycology 48, 303-311.

Benning, C., Beatty, J.T., Prince, R.C., Somerville, C.R., 1993. The sulfolipid sulfoquinovosyldiacylglycerol is not required for photosynthetic electron transport in Rhodobacter sphaeroides but enhances growth under phosphate limitation. Proceedings of the National Academy of Sciences 90, 1561-1565.

Benning, C., Huang, Z.-H., Gage, D.A., 1995. Accumulation of a Novel Glycolipid and a Betaine Lipid in Cells of Rhodobacter sphaeroides Grown under Phosphate Limitation. Archives of Biochemistry and Biophysics 317, 103-111.

Björkman, K., Duhamel, S., Karl, D.M., 2012. Microbial group specific uptake kinetics of inorganic phosphate and adenosine-5'-triphosphate (ATP) in the North Pacific Subtropical Gyre. Frontiers in Microbiology 3, 1-17.

Björkman, K., Thomson-Bulldis, A.L., Karl, D.M., 2000. Phosphorus dynamics in the North Pacific subtropical gyre. Aquatic Microbial Ecology 22, 185-198.

Björkman, K.M., Karl, D.M., 2003. Bioavailability of dissolved organic phosphorus in the euphotic zone at Station ALOHA, North Pacific Subtropical Gyre. Limnology and Oceanography 48, 1049-1057.

Brussard, C.P.D., Wilhelm, S.W., Thingstad, T.F., Weinbauer, M.G., Bratbak, G., Heldal, M., Kimmance, S.A., Middelboe, M., Nagasaki, K., Paul, J.H., Schroeder, D.C., Suttle, C.A., Vaqué, D., Wommack, K.E., 2008. Global-scale processes with a nanoscale drive: the role of marine viruses. The ISME Journal 2, 575-578.

Campbell, L., Liu, H., Nolla, H.A., Vaulot, D., 1997. Annual variability of phytoplankton and bacteria in the subtropical North Pacific Ocean at Station ALOHA during the 1991-1994 ENSO event. Deep-Sea Research I 44, 167-192.

Carlson, C.A., Ducklow, H.W., Sleeter, T.D., 1996. Stocks and dynamics of bacterioplankton in the northwestern Sargasso Sea. Deep-Sea Research II 43, 491-515.

Casey, J.R., Lomas, M.W., Michelou, V.K., Dyhrman, S.T., Orchard, E.D., Ammerman, J.W., Sylvan, J.B., 2009. Phytoplankton taxon-specific orthophosphate (Pi) and ATP utilization in the western subtropical North Atlantic. Aquatic Microbial Ecology 58, 31-44.

Cavender-Bares, K.K., Karl, D.M., Chisholm, S.W., 2001. Nutrient gradients in the western North Atlantic Ocean: Relationship to microbial community structure and comparison to patterns in the Pacific Ocean. Deep-Sea Research I 48, 2373-2395.

Cho, B.C., Azam, F., 1988. Major role of bacteria in biogeochemical fluxes in the ocean's interior. Nature 332, 441-443.

Cho, B.C., Azam, F., 1990. Biogeochemical significance of bacterial biomass in the ocean's euphotic zone. Marine Ecology Progress Series 63, 253-259.

Cole, J.J., Findlay, S., Pace, M.L., 1988. Bacterial production in fresh and saltwater ecosystems: a cross-system overview. Marine Ecology Progress Series 43, 1-10.

Cottrell, M.T., Kirchman, D.L., 2000. Natural Assemblages of Marine Proteobacteria and Members of the *Cytophaga-Flavobacter* Cluster Consuming Low- and High-Molecular-Weight Dissolved Organic Matter. Applied and Environmental Microbiology 66, 1692-1697.

del Giorgio, P.A., Cole, J.J., 2000. Bacterial energetics and growth efficiency, in: Kirchman, D.L. (Ed.), Microbial Ecology of the Oceans. Wiley-Liss, New York, pp. 289-325.

Douce, R., Holtz, B., Benson, A.A., 1973. Isolation and properties of the envelope of spinach chloroplasts. The Journal of Biological Chemistry 248, 7215-7222.

Ducklow, H., 2000. Bacterial Production and Biomass in the Oceans, in: Kirchman, D.L. (Ed.), Microbial Ecology of the Oceans. Wiley-Liss, New York, pp. 85-120.

Ducklow, H.W., Quinby, H.L., Carlson, C.A., 1995. Bacterioplankton dynamics in the equatorial Pacific during the 1992 El Niño. Deep-Sea Research II 42, 621-638.

Duhamel, S., Gregori, G., Van Wambeke, F., Mauriac, R., Nedoma, J., 2008. A method for analysying phosphatase activity in aquatic bacteria at the single cell level using flow cytometry. Journal of Microbiological Methods 75, 269-278.

Dyhrman, S.T., Ammerman, J.W., Van Mooy, B.A.S., 2007. Microbes and the marine phosphorus cycle. Oceanography 20, 110-116.

Dyhrman, S.T., Ruttenberg, K.C., 2006. Presence and regulation of alkaline phosphatase activity in eukaryotic phytoplankton from the coastal ocean: Implications for dissolved organic phosphorus remineralization. Limnology and Oceanography 51, 1381-1390.

Eilers, H., Pernthaler, J., Amann, R., 2000. Succession of pelagic marine bacteria during enrichment: a close look at cultivation-induced shifts. Applied and Environmental Microbiology 66, 4634-4640.

Freeman, C., Lock, M.A., 1995. Isotope dilution analysis and rates of 32P incorporation into phospholipids as a measure of microbial growth rates in biofilms. Water Research 29, 789-792.

Fuchs, B.M., Zubkov, M.V., Sahm, K., H., B.P., Amann, R., 2000. Changes in community composition during dilution cultures of marine bacterioplankton as assessed by flow cytometric and molecular biological techniques. Environmental Microbiology 2, 191-201.

Fuhrman, J., 2000. Impact of viruses on bacterial processes, in: Kirchman, D.L. (Ed.), Microbial Ecology of the Oceans. Wiley-Liss, New York, pp. 327-350.

Fuhrman, J.A., 1999. Marine viruses and their biogeochemical and ecological effects. Nature 399, 541-548.

Fuhrman, J.A., Azam, F., 1980. Bacterioplankton Secondary Production Estimates for Coastal Waters of British Columbia, Antarctica, and California. Applied and Environmental Microbiology 39, 1085-1095.

Fuhrman, J.A., Azam, F., 1982. Thymidine Incorporation as a Measure of Heterotrophic Bacterioplankton Production in Marine Surface Waters: Evaluation and Field Results. Marine Biology 66, 109-120.

Goldfine, H., 1972. Comparative Aspects of Bacterial Lipids. Advances in Microbial Physiology 8, 1-58.

Hagen, P.-O., Goldfine, H., Le B. Williams, P.J., 1966. Phospholipids of Bacteria with Extensive Intracytoplasmic Membranes. Science 151, 1543-1544.

Harwood, J.L., 1998. Membrane Lipids in Algae, in: Siegenthaler, P.-A., Murata, N. (Eds.), Lipids in Photosynthesis: Structure, Function and Genetics. Kluwer Academic Publishers, Netherlands, pp. 53-64.

Hoppe, H.-G., 2003. Phosphatase activity in the sea. Hydrobiologia 493, 187-200.

Hullar, M.A., Fry, B., Peterson, B.J., Wright, R.T., 1996. Microbial utilization of estuarine dissolved organic carbon: a stable isotope tracer approach tested by mass balance. Applied and Environmental Microbiology 62, 2489-2493.

Johnson, D.L., 1971. Simultaneous Determination of Arsenate and Phosphate in Natural Waters. Environmental Science & Technology 8, 411-414.

Karl, D.M., 1979. Measurement of microbial activity and growth in the ocean by rates of stable ribonucleic acid synthesis. Applied and Environmental Microbiology 38, 850-860.

Karl, D.M., Tien, G., 1992. MAGIC: A sensitive and precise method for measuring dissolved phosphorus in aquatic environments. Limnology and Oceanography 37, 105-116.

Kates, M., 1964. Bacterial Lipids. Advances in Lipid Research 2, 17-90.

Kirchman, D., Ducklow, H., Mitchell, R., 1982. Estimates of Bacterial Growth from Changes in Uptake Rates and Biomass. Applied and Environmental Microbiology 44, 1296-1307.

Kirchman, D., K'nees, E., Hodson, R., 1985. Leucine Incorporation and Its Potential as a Measure of Protein Synthesis by Bacteria in Natural Aquatic Systems. Applied and Environmental Microbiology 1985, 3.

Kirchman, D.L., 1992. Incorporation of thymidine and leucine in the subarctic Pacific: application to estimating bacterial production. Marine Ecology Progress Series 82, 301-309.

Kirchman, D.L., Ducklow, H.W., 1993. Estimating conversion factors for the thymidine and leucine methods for measuring bacterial production, in: Kemp, P.F., Sherr, B., Sherr, E., Cole, J.J. (Eds.), Handbook of Methods in Microbial Ecology. Lewis Publishers, Boca Raton, FL, pp. 513-518.

Krom, M.D., Kress, N., Brenner, S., Gordon, L.I., 1991. Phosphorus limitation of primary production in the eastern Mediterranean Sea. Limnology and Oceanography 36, 424-432.

Lagaria, A., Psarra, S., Lef èvre, D., Van Wambeke, F., Courties, C., Pujo-Pay, M., Oriol, L., Tanaka, T., Christaki, U., 2011. The effects of nutrient additions on particulate and dissolved primary production in surface waters of three Mediterranean eddies. Biogeosciences Discussion 2010, 8919-8952.

Larsen, A., Tanaka, T., Zubkov, M.V., Thingstad, T.F., 2008. P-affinity measurements of specific osmotroph populations using cell-sorting flow cytometry. Limnology and Oceanography: Methods 6, 355-363.

Lebaron, P., Servais, P., Baudoux, A.-C., Bourrain, M., Courties, C., Parthuisot, N., 2002. Variations of bacterial-specific activity with cell size and nucleic acid content assessed by flow cytometry. Aquatic Microbial Ecology 28, 131-140.

Lomas, M.W., Burke, A.L., Lomas, D.A., Bell, D.W., Shen, C., Dyhrman, S.T., Ammerman, J.W., 2010. Sargasso Sea phosphorus biogeochemistry: an important role for dissolved organic phosphorus (DOP). Biogeosciences 7, 695-710.

Longnecker, K., Lomas, M.W., Van Mooy, B.A.S., 2010. Abundance and diversity of heterotrophic bacterial cells assimilating phosphate in the subtropical North Atlantic Ocean. Environmental Microbiology 12, 2773-2782.

Longnecker, K., Sherr, B.F., Sherr, E.B., 2005. Activity and Phylogenetic Diversity of Bacterial Cells with High and Low Nucleic Acid Content and Electron Transport System Activity in an Upwelling Ecosystem. Applied and Environmental Microbiology 71, 7737-7749.

Malfatti, F., Azam, F., 2009. Atomic force microscopy reveals microscale networks and possible symbioses among pelagic marine bacteria. Aquatic Microbial Ecology 58, 1-14.

Martin, P., Van Mooy, B.A.S., Heithoff, A., Dyhrman, S.T., 2011. Phosphorus supply drives rapid turnover of membrane phospholipids in the diatom Thalassiosira pseudonana. The ISME Journal 5, 1057-1060.

Michelou, V.K., Cottrell, M.T., Kirchman, D.L., 2007. Light-stimulated bacterial production and amino acid assimilation by cyanobacteria and other microbes in the North Atlantic Ocean. Applied and Environmental Microbiology 73, 5539-5546.

Michelou, V.K., Lomas, M.W., Kirchman, D.L., 2011. Phosphate and adenosine-5'-triphosphate uptake by cyanobacteria and heterotrophic bacteria in the Sargasso Sea. Limnology and Oceanography 56, 323-332.

Minnikin, D.E., Abdolrahimzadeh, H., Baddiley, J., 1974. Replacement of acidic phospholipids by acidic glycolipids in Pseudomonas diminuta. Nature 249, 268.

Moriarty, D.J.W., 1986. Measurements of bacterial growth rates in aquatic systems from rates of nucleic acid synthesis. Advances in Microbial Ecology 9, 245-292.

Moriarty, D.J.W., White, D.C., Wassenberg, T.J., 1985. A convenient method for measuring rates of phospholipid synthesis in seawater and sediments: its relevance to the determination of bacterial productivity and the distrubance artifacts introduced by measurements. Journal of Microbiological Methods 3, 321-330.

Moutin, T., Raimbault, P., 2002. Primary production, carbon export and nutrients availability in western and eastern Mediterranean Sea in early summer 1996 (MINOS cruise). Journal of Marine Systems 33-34, 273-288.

Nagata, T., 2000. Production mechanisms of dissolved organic matter, in: Kirchman, D.L. (Ed.), Microbial Ecology of the Oceans. Wiley-Liss, New York, pp. 121-152.

Oliver, J.D., Colwell, R.R., 1973. Extractable Lipids of Gram-Negative Marine Bacteria: Phospholipid Composition. Journal of Bacteriology 114, 897-908.

Pomeroy, L.R., 1974. The Ocean's Food Web, A Changing Paradigm. BioScience 24, 499-504.

Popendorf, K.J., Lomas, M.W., Van Mooy, B.A.S., 2011a. Microbial sources of intact polar diacylglycerolipids in the Western North Atlantic Ocean. Organic Geochemistry 42, 803-811.

Popendorf, K.J., Tanaka, T., Pujo-Pay, M., Lagaria, A., Courties, C., Conan, P., Oriol, L., Sofen, L.E., Moutin, T., Van Mooy, B.A.S., 2011b. Gradients in intact polar diacylglycerolipids across the Mediterranean Sea are related to phosphate availability. Biogeosciences 8, 3733-3745.

Pujo-Pay, M., Conan, P., Oriol, L., Cornet-Barthaux, V., Falco, C., Ghiglione, J.-F., Goyet, C., Moutin, T., Prieur, L., 2011. Integrated survey of elemental stoichiometry (C,N,P) from the western to eastern Mediterranean Sea. Biogeosciences 8, 883-899.

Rappé, M.S., Connon, S.A., Vergin, K.L., Giovannoni, S.J., 2002. Cultivation of the ubiquitous SAR11 marine bacterioplankton clade. Nature 418, 630-633.

Rappé, M.S., Kemp, P.F., Giovannoni, S.J., 1997. Phylogenetic diversity of marine coastal picoplankton 16S rRNA genes cloned from the continental shelf off Cape Hatteras, North Carolina. Limnology and Oceanography 42, 811-826.

Repeta, D.J., Quan, T.M., Aluwihare, L.I., Accardi, A., 2002. Chemical characterization of high molecular weight dissolved organic matter in fresh and marine waters. Geochimica Cosmochimica Acta 66, 955-962.

Rimmelin, P., Moutin, T., 2005. Re-examination of the MAGIC method to detect low orthophosphate concentration in seawater. Analytica Chimica Acta 548, 174-182.

Rütters, H., Sass, H., Cypionka, H., Rullkötter, J., 2002. Phospholipid analysis as a tool to study complex microbial communities in marine sediments. Journal of Microbiological Methods 48, 149-160.

Sakurai, I., Shen, J.-R., Leng, J., Ohashi, S., Kobayashi, M., Wada, H., 2006. Lipids in Oxygen-Evolving Photosystem II Complexes of Cyanobacteria and Higher Plants. Journal of Biochemistry 140, 201-209.

Sato, N., Hagio, M., Wada, H., Tsuzuki, M., 2000. Requirement of phosphatidylglycerol for photosynthetic function in thylakoid membranes. Proceedings of the National Academy of Sciences 97, 10655-10660.

Schwalbach, M.S., Tripp, H.J., Steindler, L., Smith, D.P., Giovannoni, S.J., 2010. The presence of the glycolysis operon in SAR11 genomes is positively correlated with ocean productivity. Environmental Microbiology 12, 490-500.

Simon, M., Azam, F., 1989. Protein content and protein synthesis rates of planktonic marine bacteria. Marine Ecology Press Series 51, 201-213.

Smith, D.C., Azam, F., 1992. A simple, economical method for measuring bacterial protein synthesis rates in seawater using 3H-leucine. Marine Microbial Food Webs 6, 107-114.

Steinberg, D.K., Carlson, C.A., Bates, N.R., Johnson, R.J., Michaels, A.F., Knap, A.H., 2001. Overview of the US JGOFS Bermuda Atlantic Time-series Study (BATS): a decade-scale look at ocean biology and biogeochemistry. Deep-Sea Research II 48, 1405-1447.

Steinberg, D.K., Mooy, B.A.S.V., Buesseler, K.O., Boyd, P.W., Kobari, T., Karl, D.M., 2008. Bacterial vs. zooplankton control of sinking particle flux in the ocean's twilight zone. Limnology and Oceanography 53, 1327-1338.

Strickland, Parsons, 1972. A Practical Handbook of Seawater Analysis.

Sturt, H.F., Summons, R.E., Smith, K., Elvert, M., Hinrichs, K.-U., 2004. Intact polar membrane lipids in prokaryotes and sediments deciphered by high-performance liquid chromatography/electrospray ionization multistage mass spectrometry--new biomarkers for biogeochemistry and microbial ecology. Rapid Communications in Mass Spectrometry 18, 617-628.

Talarmin, A., Van Wambeke, F., Catala, P., Courties, C., Lebaron, P., 2011. Flow cytometric assessment of specific leucine incorporation in the open Mediterranean. Biogeosciences 8, 253-265.

Van Mooy, B.A.S., Fredricks, H.F., 2010. Bacterial and eukaryotic intact polar lipids in the eastern subtropical South Pacific: Water-column distribution, planktonic sources, and fatty acid composition. Geochimica et Cosmochimica Acta 74, 6499-6516.

Van Mooy, B.A.S., Fredricks, H.F., Pedler, B.E., Dyhrman, S.T., Karl, D.M., Koblízek, M., Lomas, M.W., Mincer, T.J., Moore, L.R., Moutin, T., Rappé, M.S., Webb, E.A., 2009. Phytoplankton in the ocean substitute phospholipids in response to phosphorus scarcity. Nature 458, 69-72.

Van Mooy, B.A.S., Moutin, T., Duhamel, S., Rimmelin, P., Wambeke, F.V., 2008. Phospholipid synthesis rates in the eastern tropical South Pacific Ocean. Biogeosciences 5, 133-139.

Van Mooy, B.A.S., Rocap, G., Fredricks, H.F., Evans, C.T., Devol, A.H., 2006. Sulfolipids dramatically decrease phosphorus demand by picocyanobacteria in

oligotrophic environments. Proceedings of the National Academy of Sciences 103, 8607-8612.

Van Wambeke, F., Catala, P., Pujo-Pay, M., Lebaron, P., 2011. Vertical and longitudinal gradients in HNA-LNA cell abundances and cytometric characteristics in the Mediterranean Sea. Biogeosciences 8, 1853-1863.

Van Wambeke, F., Obernosterer, I., Moutin, T., Ulloa, O., Claustre, H., 2008. Heterotrophic bacterial production in the eastern South Pacific: longitudinal trends and coupling with primary production. Biogeosciences 5, 157-169.

Wada, H., Murata, N., 1998. Membrane Lipids in Cyanobacteria, in: Siegenthaler, P.-A., Murata, N. (Eds.), Lipids in Photosynthesis: Structure, Function and Genetics. Kluwer Academic Publishers, Netherlands, pp. 65-81.

Wakeham, S.G., Hedges, J.I., Lee, C., Peterson, M.L., Hernes, P.J., 1997. Compositions and transport of lipid biomarkers through the water column surficial sediments of the equatorial Pacific Ocean. Deep-Sea Research II 44, 2131-2162.

White, D.C., Bobbie, R.J., Morrison, S.J., Oosterhof, D.K., Taylor, C.W., Meeter, D.A., 1977. Determination of Microbial Activity of Estuarine Detritus by Relative Rates of Lipid Biosynthesis. Limnology and Oceanography 22, 1089-1099.

White, D.C., Tucker, A.N., 1969. Phospholipid metabolism during bacterial growth. Journal of Lipid Research 10, 220-233.

Wright, R.T., Hobbie, J.E., 1965. The uptake of organic solutes in lake water. Limnology and Oceanography 10, 22-28.

Yokokawa, T., Nagata, T., 2005. Growth and Grazing Mortality Rates of Phylogenetic Groups of Bacterioplankton in Coastal Marine Environments. Applied and Environmental Microbiology 71, 6799-6807.

Yokokawa, T., Nagata, T., Cottrell, M.T., Kirchman, D.L., 2004. Growth rate of the major phylogenetic bacterial groups in the Delaware estuary. Limnology and Oceanography 49, 1620-1629.

Zubkov, M.V., Mary, I., Woodward, E.M.S., Warwick, P.E., Fuchs, B.M., Scanlan, D.J., Burkill, P.H., 2007. Microbial control of phosphate in the nutrient-depleted North Atlantic subtropical gyre. Environmental Microbiology 9, 2079-2089.

Figure 1
Sargasso Sea
Regrowth Experiment

Triplicate 20 L carboys (A, red circles, B, green triangles, and C, blue squares) were filled with 90% filtered seawater and 10% whole seawater from 5 m depth and incubated in the dark for 72 hours. Measurements were made every 12 hours for (A) heterotrophic bacterial cell concentration, (B) concentration of the phospholipid phosphatidylglycerol (PG, filled markers) and phosphatidylethanolamine (PE, open markers), (C) production rate of the phospholipids PG (filled markers) and PE (open markers), and (D) uptake rate of 3H-leucine (Leu, filled markers) and 3H-thymidine (TdR, open markers). Incubations were conducted shipboard in the North Atlantic Sargasso Sea during the BV39 cruise in October 2007.

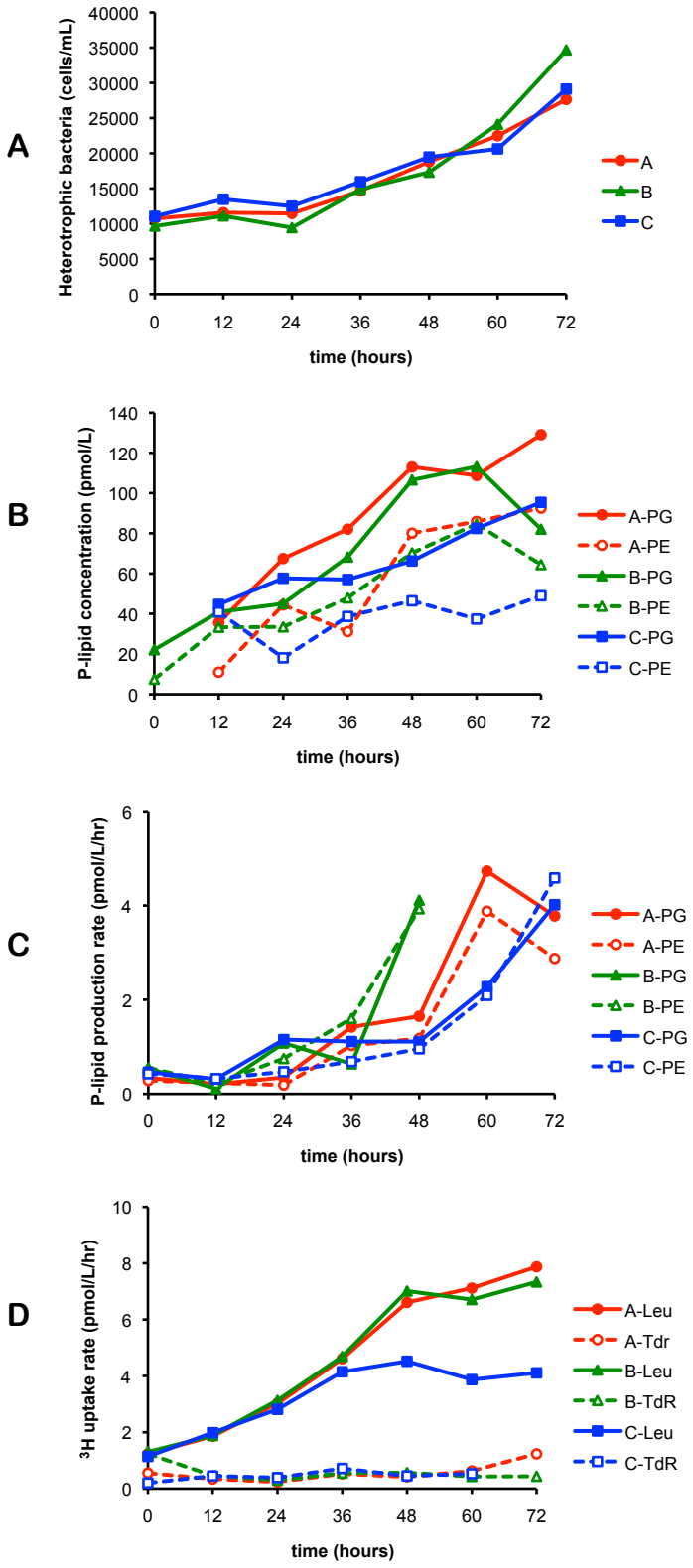

Figure 2
North Pacific
Regrowth Experiment

Triplicate 20 L carboys (A, red circles, B, green triangles, and C, blue squares) were filled with 90% filtered seawater and 10% whole seawater from 25 m depth and incubated in the dark for 72 hours. Measurements were made every 12 hours for (A) cell concentration of small plankton (heterotrophic bacteria plus *Prochlorococcus*), (B) concentration of the phospholipid phosphatidylglycerol (PG, filled markers) and phosphatidylethanolamine (PE, open markers), (C) production rate of the phospholipids PG (filled markers) and PE (open markers), and (D) uptake rate of ^{3}H-leucine (Leu, filled markers) and ^{3}H-thymidine (TdR, open markers). Incubations were conducted shipboard in the North Pacific subtropical gyre during the KM1013 cruise in July 2010.

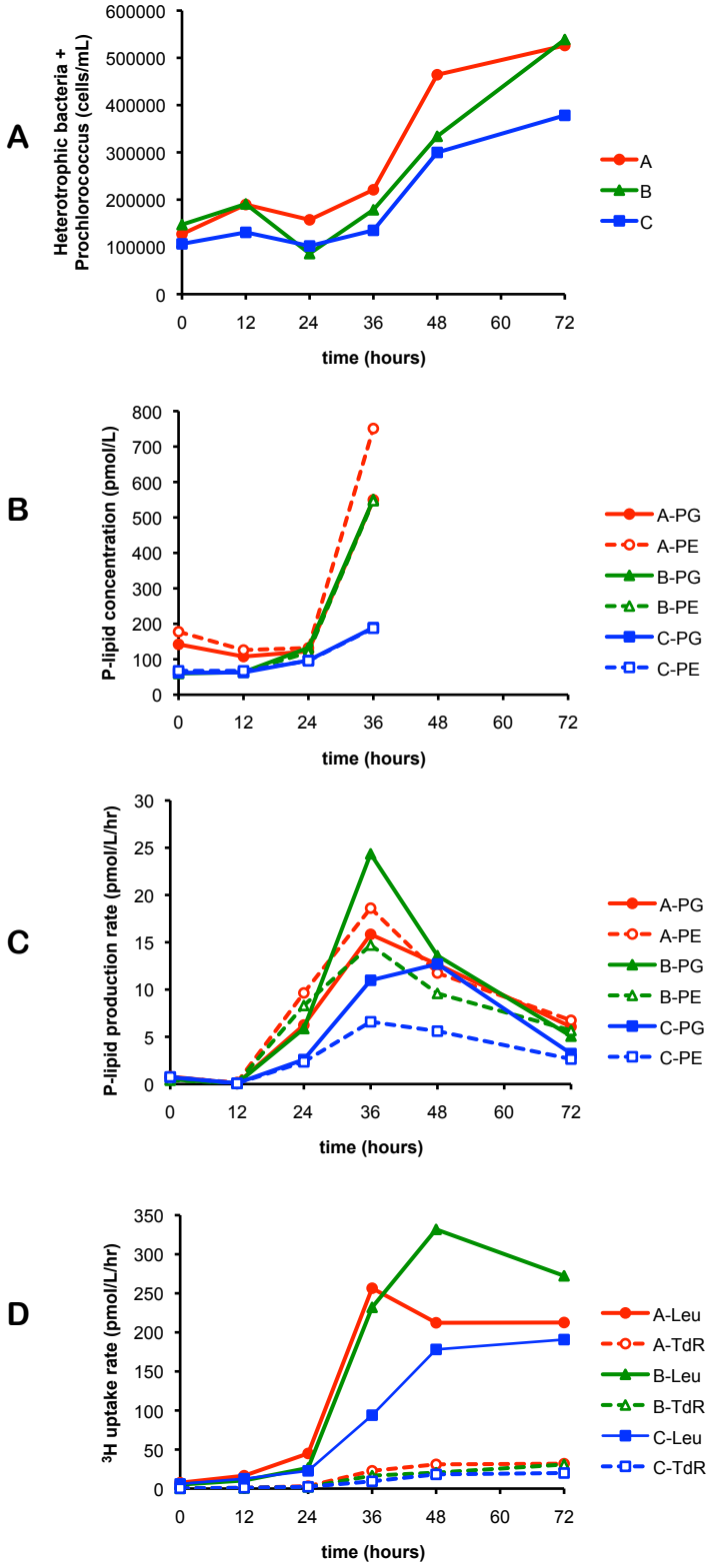

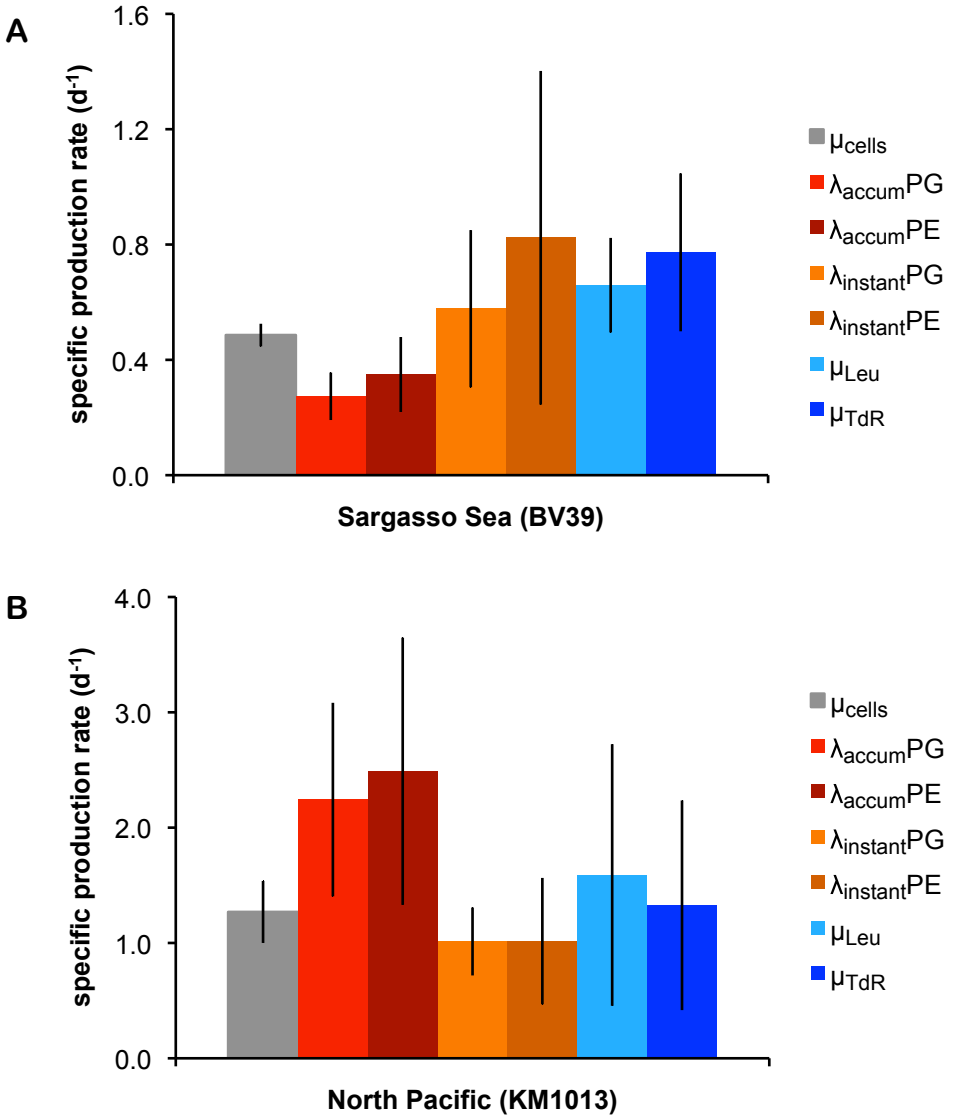

Figure 3
Specific growth rate in regrowth experiments
Specific production rate in regrowth experiments in (A) the Sargasso Sea (BV39, October 2007) and (B) the North Pacific Subtropical Gyre near station ALOHA (KM1013, July 2010). Specific production rate was calculated four different ways: exponential fit to the change in cell concentration over time (μ_{cells}, grey bar); exponential fit to the change in phospholipid (PG and PE) concentration over time (λ_{accum}, red bars); average of timepoints during exponential growth of instantaneous phospholipid production rate divided by phospholipid concentration ($\lambda_{instant}$, orange bars); average of timepoints during exponential growth of ^{3}H-Leu and ^{3}H-TdR uptake rate multiplied by a conversion factor and divided by cell concentration (μ_{Leu} and μ_{TdR}, blue bars). Error bars (black lines) represent +/- 1 standard deviation. All experiments were performed in triplicate.

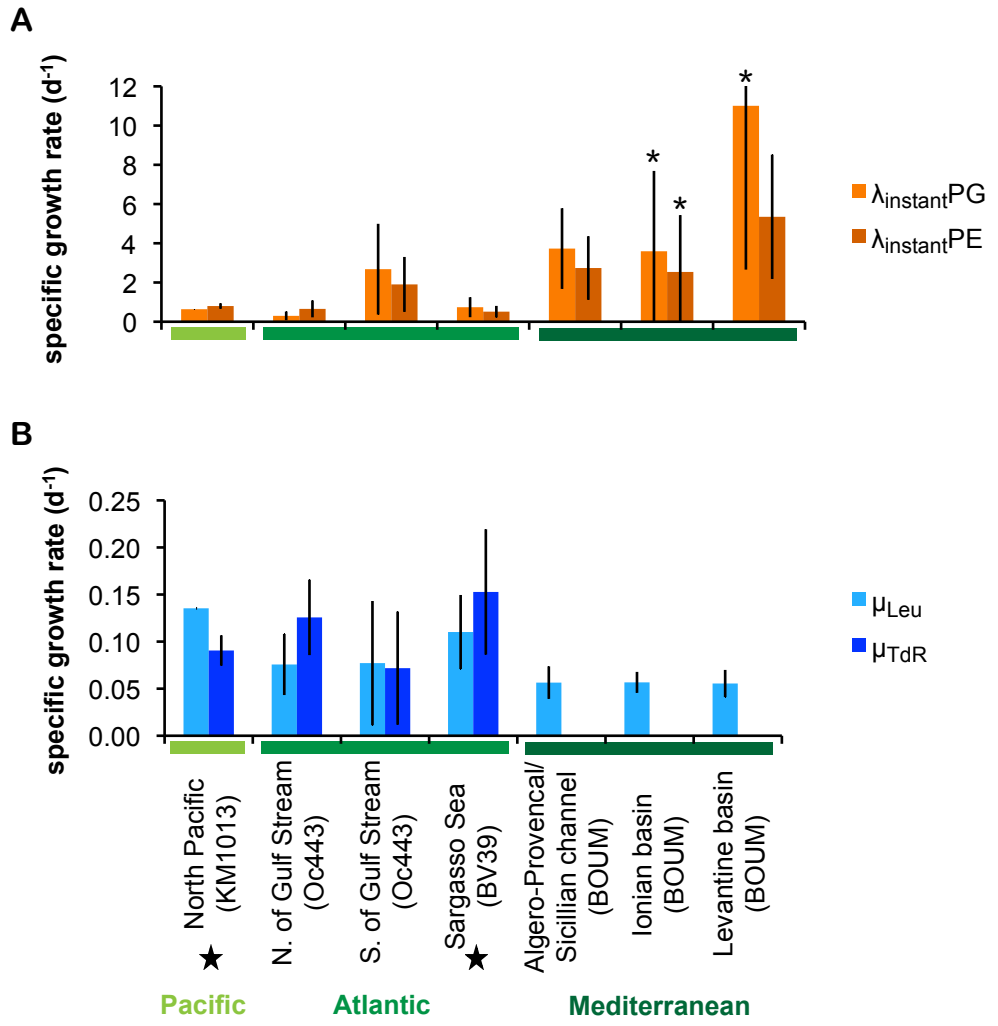

Figure 4
Specific growth rate in the ocean
Specific growth rate of heterotrophic bacteria calculated by (A) phospholipid specific production rate ($\lambda_{instant}$PG and $\lambda_{instant}$PE), and by (B) uptake rate of ^{3}H-Leu and ^{3}H-TdR (μ_{Leu} and μ_{TdR}). Regrowth experiments were performed at locations marked with a star (★). Error bars are standard deviation, asterisk indicates error bars beyond the plotted range. Cruise numbers are given in parentheses, for number of samples and depths see Table 3.

Table 2

Reference	Calculation method	Sargasso Sea cell/mol Leu	Sargasso Sea cell/mol TdR	North Pacific cell/mol Leu	North Pacific cell/mol TdR
Kirchman et al., 1982	"derivative" method	6.4×10^{16}	7.3×10^{17}	2.0×10^{18}	3.1×10^{19}
Kirchman and Ducklow, 1993	modified "derivative" method	5.7×10^{16}	5.6×10^{17}	3.2×10^{17}	4.7×10^{18}
Fuhrman and Azam, 1982	cumulative method, point-to-point	5.7×10^{17}	1.2×10^{18}	8.2×10^{16}	1.0×10^{18}
this study	cumulative method, t_0-t_{final}	2.3×10^{17}	9.7×10^{17}	1.0×10^{17}	1.0×10^{18}

Table 3

Location	Cruise	# of samples	depths (m)	SRP (nM)	heterotrophic bacteria (cells/mL)	Specific production rate (d^{-1})			
						PG instant.	PE instant.	^{3}H-Leu	^{3}H-TdR
North Pacific Subtropical Gyre	KM1013	3	25	53	639837	0.64	0.80	0.14	0.09
North Atlantic - north of Gulf Stream	Oc443	6	5-30	391	342813	0.30	0.65	0.08	0.13
North Atlantic - south of Gulf Stream	Oc443	5	5-40	5	564557	2.68	1.90	0.08	0.07
North Atlantic - Sargasso Sea	BV39	8	5-40	3	193755	0.74	0.51	0.11	0.15
Mediterranean Sea - Algero-Provencal basin/Sicillian channel	BOUM	5	5-25	10	568731	3.73	2.74	0.06	n.d.
Mediterranean Sea - Ionian basin	BOUM	4	5-25	5	458830	3.59	2.54	0.06	n.d.
Mediterranean Sea - Levantine basin	BOUM	10	5-25	12	290083	11.01	5.35	0.06	n.d.

n.d.=not determined

Chapter 6

Conclusions

Conclusions

In a single drop of seawater there are hundreds of thousands of individual organisms, each cell a minute chemical factory churning through reactions that transform the material within and around the cell. The cumulative action of these tiny, abundant organisms results in major fluxes moving material from the surface ocean to the deep, and contributing to the exchange of material between land, air, and sea. To understand the complex interactions between biology, geology and chemistry on globally important scales, we need to be able to measure the magnitude and rate of these microbially mediated transformations. This thesis has endeavored to address this challenge by demonstrating that membrane lipids, intact polar diacylglycerolipids (IP-DAGs), provide valuable information about microbial dynamics in the surface ocean, and using this information to study bacterial production and microbial response to nutrient stress.

Major findings

Microbial sources of IP-DAGs

In the North Atlantic I employed three different experimental approaches to determine the microbial sources of the most abundant IP-DAG headgroup classes. The consensus among the three experimental approaches indicated that, in the phosphorus depleted Sargasso Sea, the sulfolipid SQDG and the betaine lipid DGTS are produced exclusively by photoautotrophs, and heterotrophic bacteria dominate the production of the phospholipids PG and PE. Using cell sorting flow cytometry, it was shown that both heterotrophic bacteria and *Synechoccocus* contain significantly less phospholipids, as a fraction of total lipids, in low phosphate locations compared to high phosphate locations. The finding that heterotrophic bacteria have proportionally less phospholipids in low phosphate locations was novel, as heterotrophic bacteria have never been shown to be capable of lipid substitution in culture experiments, and the gene for synthesis of the canonical substitute glycolipid, SQDG, has not been found in any genetic surveys of heterotrophic bacteria (Van Mooy et al., 2006). While SQDG was not observed in

environmental samples of heterotrophic bacteria, multiple experimental approaches confirmed that heterotrophic bacteria contain the glycolipid MGDG in low phosphate locations.

Microbial response to nutrient stress

Previous studies have shown that physiologic shifts occur in monocultures in response to changes in nutrients, resulting in lower phospholipid content in the membrane when phosphate is low (Van Mooy et al., 2009). For the first time, in the Mediterranean Sea it was demonstrated that a similar phenomenon occurs in a mixed community, environmental sample: the ratio of IP-DAGs changed rapidly (over the course of several days) in response to altered nutrients, without significant changes in the microbial community composition. This indicates that the physiological shift in membrane composition can be measured in a mixed microbial community, and that this change in IP-DAG ratios in response to altered nutrients can be a useful indicator of nutrient stress.

Though this effect was demonstrated in microcosm incubations, it was determined that variations in IP-DAG ratios observed across the Mediterranean transect were likely representative of the combined effect of changes in both microbial community and cellular physiology. The average SQDG:PG ratio observed across the phosphorus-deplete Mediterranean Sea was 2.5 (s.d. 1.4), and the betaine lipid:PC ratio was 1.7 (s.d. 1.1). These values are less than the ratios measured in either the phosphorus-replete South Pacific (3.6 and 3.6 respectively) or phosphorus-deplete Sargasso Sea (4.5 and 13.1 respectively; Van Mooy et al., 2009). This variation in the absolute value of these ratios is unsurprising, given that this study across the Mediterranean Sea suggests that the total IP-DAG composition at any one location is a function of both the phosphate concentration and the microbial community composition. Considering the range of SQDG:PG and betaine lipid:PC ratios measured in phosphorus-deplete and phosphorus-replete locations thus far, it is unlikely that the absolute value of these ratios at a single timepoint or single location is a useful indicator of microbial community nutrient stress. However, the *relative* change in this ratio in nutrient amendment incubations, timeseries

measurements, or across transects of relatively consistent microbial communities can provide new insights on the microbial response to nutrient stress.

In the Mediterranean Sea, I calculated that phospholipids ranged from 1-14% of particulate phosphorus, and that this fraction trended with the phosphate concentration: phospholipids were a larger fraction of the particulate pool where dissolved phosphate concentrations were higher. The fact that phospholipids could be up to 14% of particulate phosphorus speaks to their importance in the marine phosphorus cycle, but more significantly the wide range of values indicates that membrane lipids are likely the most flexible cellular pool of phosphorus, and variation in membrane lipids may be a significant mechanism for microbes to alter their cellular C:N:P ratios, ultimately influencing particulate C:N:P ratios on basin-wide scales.

Heterotrophic bacterial production

In the phosphorus-deplete Sargasso Sea, and in the more phosphorus-replete North Pacific subtropical gyre, I conducted regrowth experiments and determined that, in both locations, phospholipid specific production rate for both PG and PE was within error of heterotrophic bacterial cell specific growth rate determined by direct measurement of the increase in cell concentration. The results of these regrowth experiments, in combination with my results from North Atlantic experiments (chapter 3) and other published literature, confirm these three criteria: 1) phosphate is a general substrate taken up by all heterotrophic bacteria and fulfills the majority of heterotrophic bacterial phosphorus demand; 2) the incorporation of phosphate into particular phospholipids is specific to heterotrophic bacteria amongst marine microbes; 3) there is a consistent, quantitative relationship between heterotrophic bacterial cell turnover rate and phospholipid turnover rate. These results validate the measurement of phospholipid specific production rates in the water column as a method to represent heterotrophic bacterial cell specific growth rates.

Applying this method to surface seawater samples on multiple cruises found that heterotrophic bacteria specific growth rate in the North Pacific was 0.7 per day, across

the North Atlantic it ranged from 0.3 to 2.7 per day, and across the Mediterranean Sea it ranged from 2.5 to 11.0 per day. These growth rates were 3 times to two orders of magnitude greater than heterotrophic bacterial specific growth rate measured by traditional ^{3}H-Leu and ^{3}H-TdR uptake methods. Across the North Atlantic and the North Pacific, phospholipid specific production rate estimated an average heterotrophic bacterial specific growth rate of 1 per day.

Heterotrophic bacterial growth rates on the order of 1 per day are an order of magnitude faster than the global average rates estimated by the established ^{3}H-Leu and ^{3}H-TdR uptake methods, which give rates of approximately 0.1 per day (Ducklow, 2000). This challenges the traditional paradigm of slow growing heterotrophic bacteria in the open ocean. An order of magnitude faster bacterial production rate suggests a two-fold greater total bacterial carbon demand. This greater bacterial carbon demand could be met either by heterotrophic bacteria consuming a larger fraction of total primary production than is currently estimated, or by more rapid recycling of organic carbon within the surface ocean microbial loop, potentially fueled by viral lysis.

Methodological advances

These insights into microbial dynamics in the surface ocean were enabled by the development of an improved method for IP-DAG quantification. High sample throughput was achieved by developing a molecular ion-independent method of quantification on an HPLC-ESI-TQMS system. This analytical approach will hopefully open the doors for increased exploration of IP-DAGs in the ocean, and further understanding of the microbial role in biogeochemical cycles.

Future research

In the exploration of microbial sources of IP-DAGs, the origin of betaine lipids in the water column is something of a mystery. The results of stable isotope tracing studies in Chapter 3 indicated that DGTS is produced exclusively by photoautotrophs, which is commensurate with lipid analysis of phytoplankton cultures that have found DGTS to be

abundant in some eukaryotic phytoplankton (Kato et al., 1996; Martin et al., 2011; Van Mooy et al., 2009). Based on cultures studies it seems that the betaine lipids DGTS, DGTA, and DGCC are abundant in eukaryotic phytoplankton (though few phytoplankton have an abundance of more than one type of betaine) (Kato et al., 1996; Martin et al., 2011; Van Mooy et al., 2009; Van Mooy et al., 2006), and betaine lipids have only been observed in a very limited number of bacterial species (Benning et al., 1995; Van Mooy and Fredricks, 2010). Thus we expect that eukaryotic phytoplankton would be the major source of betaine lipids in the water column. However, in Chapter 4, the concentration of betaine lipids in the Mediterranean Sea was not strongly correlated with the abundance of eukaryotic phytoplankton, and principal component analysis did not indicate that their distributions were closely related. In depth profiles across the Mediterranean, betaine lipids had a unique profile relative to phospholipids and glycolipids, and seemed to be restricted to the upper 100 m of the water column. In summary, the organisms producing betaine lipids in the ocean and the factors controlling the profile of betaine lipids in the water column are not well understood. Future studies could potentially employ isotope tracing studies with different ^{15}N and ^{13}C labeled compounds, similar to those conducted in Chapter 3, to further constrain the microbial source of betaine lipids.

Microcosm incubations in the Mediterranean Sea demonstrated that, in a mixed microbial community, a change in nutrients can elicit a change in the ratio of IP-DAGs on short timescales. This shift in membrane composition has been observed many times in culture studies, and is hypothesized to be a cellular phosphorus-saving mechanism (Van Mooy et al., 2006, 2009). However, it has yet to be shown in culture or mixed community incubations that this change in membrane lipid C:N:P translates to a commensurate shift in total cellular C:N:P. This could be tested in nutrient amendment incubations where the concentrations of IP-DAGs and particulate C, N, and P are measured over several days. These results would confirm if this change in membrane composition is a microbial phosphorus-saving mechanism, or if instead it allows for a re-allocation of cellular phosphorus but does not decrease total cellular phosphorus need.

The potential to measure heterotrophic bacterial specific growth rate using phospholipid specific production rate opens tantalizing possibilities for re-evaluating the role of heterotrophic bacteria in the surface ocean carbon cycle. However, the method validation conducted in Chapter 5 was focused on oligotrophic open ocean environments. Before this method can be applied to measure heterotrophic bacterial specific growth rate in other settings the three method criteria described above must first be verified. Particularly in high phosphorus environments, such as coastal oceans or estuaries, the specificity of PG and PE for heterotrophic bacteria should be evaluated. One approach to do this would be to combine radiolabeled phosphate incubations with cell sorting flow cytometry, and subsequent analysis of the radioactivity of the phospholipid classes from the different flow sorted cell groups to determine if heterotrophic bacteria alone produce ^{33}P-labeled PG or PE. In addition, the microbial utilization of dissolved organic phosphorus needs to be considered in new environments, and re-evaluated for oligotrophic environments as new data becomes available. If heterotrophic bacteria are found to acquire a significant amount of their cellular phosphorus from organic sources then this method could be underestimating true heterotrophic bacterial production rates. Adjusting for this would create an even larger difference between heterotrophic bacterial production rates estimated by phospholipid specific production rate and ^{3}H-Leu and ^{3}H-TdR uptake methods, predicting an even faster role for heterotrophic bacteria in the ocean carbon cycle.

References

Benning, C., Huang, Z.-H., Gage, D.A., 1995. Accumulation of a Novel Glycolipid and a Betaine Lipid in Cells of Rhodobacter sphaeroides Grown under Phosphate Limitation. Archives of Biochemistry and Biophysics 317, 103-111.

Ducklow, H., 2000. Bacterial Production and Biomass in the Oceans, in: Kirchman, D.L. (Ed.), Microbial Ecology of the Oceans. Wiley-Liss, New York, pp. 85-120.

Kato, M., Sakai, M., Adachi, K., Ikemoto, H., Sano, H., 1996. Distribution of Betaine Lipids in Marine Algae. Phytochemistry 42, 1341-1345.

Martin, P., Van Mooy, B.A.S., Heithoff, A., Dyhrman, S.T., 2011. Phosphorus supply drives rapid turnover of membrane phospholipids in the diatom Thalassiosira pseudonana. The ISME Journal 5, 1057-1060.

Van Mooy, B.A.S., Fredricks, H.F., 2010. Bacterial and eukaryotic intact polar lipids in the eastern subtropical South Pacific: Water-column distribution, planktonic sources, and fatty acid composition. Geochimica et Cosmochimica Acta 74, 6499-6516.

Van Mooy, B.A.S., Fredricks, H.F., Pedler, B.E., Dyhrman, S.T., Karl, D.M., Koblízek, M., Lomas, M.W., Mincer, T.J., Moore, L.R., Moutin, T., Rappé, M.S., Webb, E.A., 2009. Phytoplankton in the ocean substitute phospholipids in response to phosphorus scarcity. Nature 458, 69-72.

Van Mooy, B.A.S., Rocap, G., Fredricks, H.F., Evans, C.T., Devol, A.H., 2006. Sulfolipids dramatically decrease phosphorus demand by picocyanobacteria in oligotrophic environments. Proceedings of the National Academy of Sciences 103, 8607-8612.

Appendix A

Fatty acid abundance within IP-DAG headgroup classes

In the course of the stable isotope tracing work conducted in Chapter 3, the abundance of fatty acids in each headgroup class was analyzed using GC-IRMS. Fatty acids were binned according to carbon chain length, and data is presented for the relative abundance of chain lengths within each IP-DAG headgroup class. Data presented are the average of six incubaion conditions (see Chapter 3 for methods), error bars are 1 standard deviation. The FAME standard used to identify fatty acids did not contain C17 fatty acids, thus these fatty acids could not be positively identified and are listed as "C17".

Figure 1. Fatty acid abundance plotted by headgroup class

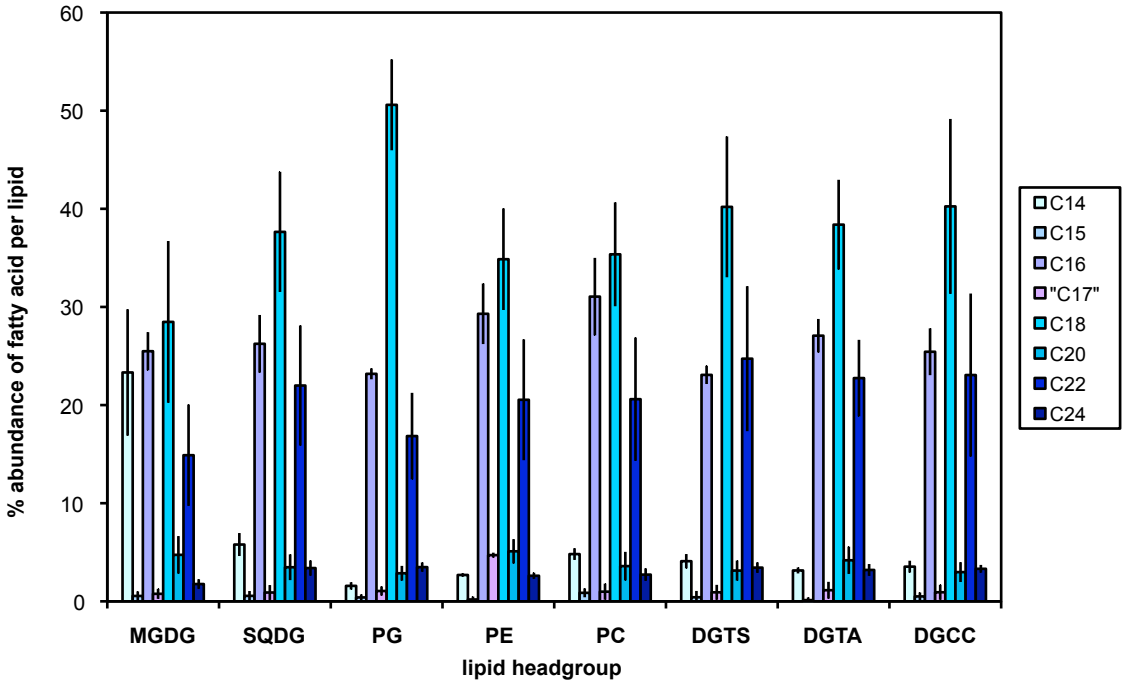

Figure 2. Fatty acid abundance plotted carbon chain length

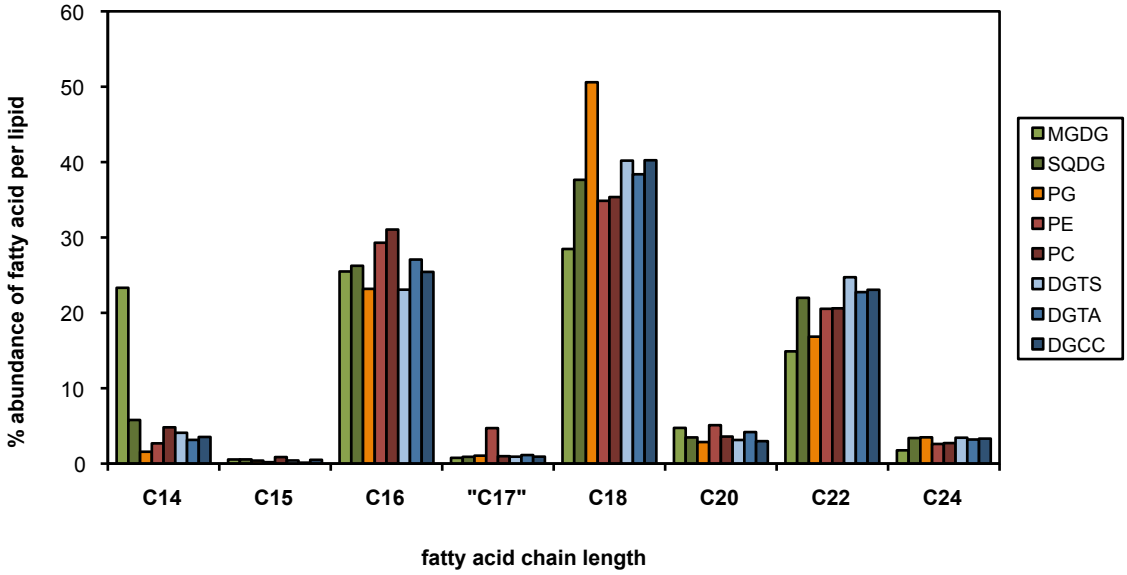

Fatty acid abundance and $\delta^{13}C$ of fatty acids per IP-DAG headgroup class, binned by carbon chain length. IP-DAG headgroup classes were separated using preparative HPLC, IP-DAGs were tranesterified and fatty acid methyl esters were analyzed for abundance and $\delta^{13}C$ using GC-IRMS. $\delta^{13}C$ (‰) values are relative to PeeDee Belemnite and are not corrected for ^{13}C contribution from methanol during transesterification; values presented are the weighted average enrichment of the composite fatty acids (the enrichment of each fatty acid multiplied by its abundance, summed, and divided by the total fatty acid abundance). Samples are from six different incubation conditions (averages presented in Figures 1 and 2): control with no amendment, bicarbonate with ^{13}C-labeled bicarbonate, glucose with ^{13}C-labeled glucose, each amendment incubatd in both the light and the dark for 24 hours. Incubations were conducted in the Sargasso Sea. For full methods see Chapter 3 (Popendorf et al., Organic Geochemistry, 2011).

Table 1

		C14		C15		C16		C17		C18		C20		C22		C24	
		% abund	$\delta^{13}C$	% abund	$\delta^{13}C$	% abund	$\delta^{13}C$	% abund	$\delta^{13}C$	% abund	$\delta^{13}C$	% abund	$\delta^{13}C$	% abund	$\delta^{13}C$	% abund	$\delta^{13}C$
MGDG	Control Dark	19.2	-0.4	-	-	27.5	-1.9	-	-	37.9	-2.6	3.7	-8.8	10.4	-3.4	1.4	-9.8
	Control Light	31.3	0.3	0.8	-6.7	28.2	0.7	0.5	-12.9	27.5	2.4	2.7	-5.9	7.4	-5.4	1.6	-4.8
	Bicarb. Dark	15.7	11.9	0.7	4.2	25.1	2.4	0.6	-7.4	37.9	3.3	3.2	1.1	14.4	-3.5	2.4	-2.8
	Bicarb. Light	26.3	414.5	-	-	24.8	170.8	1.0	269.3	23.0	49.6	6.0	316.9	17.6	20.0	1.4	13.1
	Glucose Dark	18.3	2.1	0.6	-1.1	23.9	16.3	1.5	20.9	27.6	74.8	5.1	6.0	20.5	38.4	2.4	-5.1
	Glucose Light	29.3	-0.3	1.2	5.5	23.4	5.6	0.9	-8.1	17.0	18.9	7.7	-0.1	19.1	13.0	1.4	-3.0
SQDG	Control Dark	7.4	0.9	-	-	31.4	-1.0	-	-	41.5	0.6	1.5	-13.2	16.1	-1.1	2.2	-7.6
	Control Light	6.3	6.4	0.7	4.8	26.3	0.8	1.3	-3.2	43.6	0.1	3.4	1.7	15.5	-1.8	2.9	-2.7
	Bicarb. Dark	4.0	-0.9	-	-	22.2	-1.1	1.7	-9.4	42.4	-1.0	5.6	-7.6	19.6	-2.5	4.5	-5.4
	Bicarb. Light	5.7	307.9	0.7	114.0	25.8	105.6	1.5	27.9	30.6	11.3	3.6	49.5	28.3	3.5	3.8	1.2
	Glucose Dark	5.1	4.3	0.7	2.2	26.0	2.1	0.9	-11.7	38.1	0.2	3.4	-7.5	22.4	-3.9	3.5	-2.6
	Glucose Light	6.3	3.6	1.3	-7.9	25.8	0.2	-	-	29.6	-2.4	3.5	-0.3	30.0	-3.8	3.4	-1.9
PG	Control Dark	1.3	-1.3	0.6	-10.8	23.8	-0.2	1.6	-2.9	53.4	-0.3	3.3	-4.6	12.7	-2.9	3.4	-2.3
	Control Light	1.9	11.4	0.6	-15.3	22.9	1.3	0.6	5.1	47.2	1.7	2.3	1.7	21.0	-0.5	3.5	-3.2
	Bicarb. Dark	1.3	-0.6	0.6	-15.8	22.8	-0.7	1.2	-6.5	51.9	-1.5	2.9	-8.7	15.2	-8.0	4.1	-5.8
	Bicarb. Light	1.4	67.2	-	-	23.9	9.3	0.9	-7.9	57.2	1.6	1.7	-5.2	12.3	-1.9	2.6	-2.7
	Glucose Dark	1.4	18.0	-	-	23.1	36.3	1.6	29.0	49.7	70.0	3.8	6.3	16.8	15.6	3.6	-1.3
	Glucose Light	2.2	9.4	0.6	-7.5	22.6	14.3	0.5	19.2	44.2	25.3	3.2	-6.4	23.1	0.6	3.7	-5.1
PE	Control Dark	2.8	0.9	-	-	35.4	1.6	5.1	7.6	40.6	2.5	2.9	-3.6	11.2	-5.0	2.0	-3.9
	Control Light	2.7	2.6	0.6	1.1	29.2	3.5	4.6	10.6	36.9	1.7	4.7	6.3	18.8	-5.2	2.4	-0.9
	Bicarb. Dark	2.5	3.4	-	-	28.4	2.4	4.7	4.1	38.8	-0.3	5.5	1.9	17.4	-0.5	2.7	-2.9
	Bicarb. Light	2.7	115.5	-	-	27.9	39.5	4.5	15.3	34.4	8.1	5.7	36.3	21.9	3.4	2.8	-4.2
	Glucose Dark	2.5	20.9	-	-	28.3	130.2	4.9	255.1	26.2	70.5	6.5	266.5	28.9	50.8	2.7	-7.4
	Glucose Light	2.9	12.0	0.6	-1.3	26.7	76.4	4.4	136.5	32.3	35.4	5.3	90.9	24.9	9.0	2.8	-4.3
PC	Control Dark	5.8	-0.7	1.3	-4.7	35.7	0.7	-	-	35.3	1.5	3.4	-4.2	16.0	-2.6	2.4	-7.0
	Control Light	5.1	3.5	-	-	36.3	2.7	-	-	43.7	-0.8	1.4	-2.8	11.8	-2.6	1.8	3.6
	Bicarb. Dark	4.6	0.2	1.0	-5.8	28.9	0.3	1.5	-1.8	38.0	-1.9	4.5	-3.6	18.1	-3.0	3.2	-4.5
	Bicarb. Light	4.6	158.8	1.0	45.5	29.6	64.8	0.9	4.6	32.2	12.1	2.5	71.0	26.8	5.1	2.4	-4.1
	Glucose Dark	4.1	7.0	1.0	5.7	29.1	43.1	1.6	5.4	28.1	71.5	5.2	73.7	27.4	29.3	3.5	3.7
	Glucose Light	4.7	4.2	0.9	10.3	26.7	30.1	1.8	16.5	34.8	27.2	4.6	23.1	23.5	1.2	3.0	-2.8
DGTS	Control Dark	4.1	-1.2	-	-	24.5	-0.4	-	-	49.4	-0.5	3.7	-3.4	15.9	-2.0	2.4	0.9
	Control Light	4.7	-2.2	1.3	0.7	23.0	-0.4	1.5	1.0	40.2	0.9	3.5	-3.1	22.5	0.5	3.3	-2.4
	Bicarb. Dark	3.1	3.3	-	-	22.2	-2.5	1.6	-9.8	47.8	-3.2	3.6	-4.5	18.1	-5.8	3.6	-7.1
	Bicarb. Light	4.3	231.0	1.2	26.0	23.1	22.4	0.9	-10.0	38.4	0.9	3.2	14.3	25.3	-2.7	3.6	-6.5
	Glucose Dark	3.4	19.3	-	-	22.1	0.3	1.6	0.0	32.4	0.7	3.7	-0.9	33.0	-1.1	3.8	-5.3
	Glucose Light	5.0	9.4	-	-	23.6	-1.7	-	-	33.0	1.9	1.1	2.3	33.5	-1.6	3.8	-1.9
DGTA	Control Dark	na	na	na	na	na	na	na	na	na	na	na	na	na	na	na	na
	Control Light	3.0	0.7	0.6	-18.6	26.9	2.6	1.9	1.9	36.3	1.0	4.4	0.5	23.9	-1.5	3.0	-6.6
	Bicarb. Dark	3.1	7.2	-	-	26.3	1.1	0.6	16.3	40.0	-0.8	5.6	-2.6	20.3	-3.7	4.1	-7.6
	Bicarb. Light	3.7	224.4	-	-	25.2	82.8	2.0	12.4	32.0	9.1	5.1	83.1	28.6	13.7	3.3	-5.6
	Glucose Dark	2.9	5.0	-	-	29.8	99.0	-	-	44.4	53.1	2.1	119.1	18.4	18.0	2.4	-6.5
	Glucose Light	3.0	6.8	-	-	27.2	32.5	1.2	11.7	39.2	24.7	3.7	16.5	22.6	4.8	3.2	-3.9
DGCC	Control Dark	4.3	2.7	0.9	-2.9	28.2	-0.1	-	-	45.8	0.8	2.2	2.4	15.9	-2.0	2.8	-7.0
	Control Light	2.5	0.5	-	-	23.0	-0.9	0.9	-10.3	50.6	-0.6	3.2	-4.2	16.3	0.7	3.6	-1.9
	Bicarb. Dark	3.5	2.9	0.7	0.2	23.7	1.1	1.6	1.6	44.9	-0.9	4.0	-2.0	17.9	-2.3	3.9	-6.6
	Bicarb. Light	3.4	209.6	0.7	71.0	24.5	71.1	1.5	13.7	41.5	11.0	3.7	58.3	21.4	31.3	3.3	-1.5
	Glucose Dark	3.6	4.4	0.7	6.0	24.7	4.2	1.5	-3.7	28.6	17.6	3.5	9.8	33.9	5.2	3.4	-3.8
	Glucose Light	4.0	-5.1	-	-	28.6	2.4	-	-	30.1	7.6	1.4	-11.1	33.0	9.5	2.9	-6.1

- fatty acid not detected
na IP-DAG headgroup class not analyzed

Fatty acid abundance and $\delta^{13}C$ of fatty acids per IP-DAG headgroup class, for the fatty acids of the most abundant chain lengths, C16 and C18. Saturated fatty acids and fatty acids with 1 unsaturation were positively identified by comparison of retention times with a standard (Sigma-Aldrich, Supelco 37-component FAME Mix 47885-U). Fatty acids with multiple unsaturations were binned together and presented as ":unsat". $\delta^{13}C$ values for binned fatty acids (unsat) are the weighted average enrichment of the composite fatty acids (the enrichment of each fatty acid multiplied by its abundance, summed, and divided by the total fatty acid abundance).

Table 2

		C16:0		C16:1		C16:unsat		C18:0		C18:1n9t		C18:unsat	
		% abund	$\delta^{13}C$	% abund	$\delta^{13}C$	% abund	$\delta^{13}C$	% abund	$\delta^{13}C$	% abund	$\delta^{13}C$	% abund	$\delta^{13}C$
MGDG	Control Dark	17.3	-1.7	8.3	-0.6	10.2	-2.4	5.9	-1.9	2.2	-1.2	32.0	-2.7
	Control Light	13.6	0.4	12.9	1.6	14.6	1.1	4.3	1.6	1.7	12.8	23.2	2.6
	Bicarb. Dark	16.4	-0.1	7.0	7.7	8.6	7.0	5.3	-1.9	1.6	-1.8	32.6	4.2
	Bicarb. Light	17.0	62.4	7.9	404.3	7.9	404.3	5.1	8.1	1.5	1.3	17.9	61.3
	Glucose Dark	16.1	20.3	6.7	9.9	7.8	7.9	5.2	24.4	1.8	1122.9	22.5	86.4
	Glucose Light	15.9	5.3	7.5	6.2	7.5	6.2	4.4	6.6	0.9	360.3	12.6	23.1
SQDG	Control Dark	28.7	-0.9	2.6	-2.1	2.6	-2.1	7.7	-1.3	2.9	1.3	33.8	1.0
	Control Light	24.0	0.5	2.4	4.7	2.4	4.7	5.8	-2.0	3.1	-1.3	37.8	0.4
	Bicarb. Dark	19.9	-0.8	1.0	4.9	2.3	-3.7	6.2	-2.0	2.5	1.2	36.3	-0.8
	Bicarb. Light	24.3	95.9	1.5	261.9	1.5	261.9	6.2	1.9	1.9	5.2	24.4	13.6
	Glucose Dark	24.0	0.3	2.0	23.4	2.0	23.4	6.4	-0.9	2.4	22.7	31.8	0.5
	Glucose Light	24.0	-0.4	1.8	8.8	1.8	8.8	5.9	-2.6	1.9	5.0	23.6	-2.4
PG	Control Dark	22.5	-0.5	1.3	4.2	1.3	4.2	6.6	-1.8	5.5	4.3	46.8	-0.1
	Control Light	22.2	0.2	0.7	35.5	0.7	35.5	7.0	1.2	4.3	26.8	40.2	1.8
	Bicarb. Dark	21.8	-1.2	1.0	8.5	1.0	8.5	6.7	-1.3	5.0	-1.6	45.2	-1.5
	Bicarb. Light	22.9	6.9	1.0	64.4	1.0	64.4	7.2	-0.2	5.6	11.9	49.9	1.9
	Glucose Dark	22.2	15.4	0.9	555.3	0.9	555.3	7.2	8.2	5.1	669.8	42.5	80.5
	Glucose Light	21.8	6.0	0.7	264.1	0.7	264.1	6.8	8.4	4.2	261.1	37.4	28.3
PE	Control Dark	29.5	0.7	5.8	6.0	5.8	6.0	6.1	2.2	7.2	6.4	34.5	2.5
	Control Light	24.2	1.6	5.0	12.8	5.0	12.8	5.8	2.3	5.7	11.0	31.2	1.6
	Bicarb. Dark	24.2	0.5	4.2	13.2	4.2	13.2	5.5	-0.4	5.0	4.2	33.3	-0.3
	Bicarb. Light	23.8	33.6	4.1	74.5	4.1	74.5	5.8	3.1	4.4	30.3	28.6	9.1
	Glucose Dark	25.3	73.4	2.9	618.7	2.9	618.7	5.8	13.1	3.4	464.0	20.4	86.9
	Glucose Light	22.8	41.2	3.8	285.8	3.8	285.8	6.2	15.4	4.3	227.3	26.0	40.2
PC	Control Dark	32.7	0.4	3.0	4.8	3.0	4.8	6.2	-0.2	3.8	5.5	29.1	1.8
	Control Light	33.2	0.9	3.1	21.9	3.1	21.9	6.7	-2.1	4.8	2.9	37.0	-0.5
	Bicarb. Dark	26.6	-0.2	2.3	5.9	2.3	5.9	5.9	-1.0	3.1	-1.1	32.1	-2.1
	Bicarb. Light	27.9	59.8	1.7	146.1	1.7	146.1	6.7	10.3	2.8	21.5	25.5	12.6
	Glucose Dark	27.0	21.4	2.1	327.3	2.1	327.3	6.1	6.0	2.6	757.5	22.0	89.7
	Glucose Light	24.4	12.5	2.4	211.2	2.4	211.2	5.8	4.4	2.8	319.3	29.0	31.8
DGTS	Control Dark	23.7	-0.5	0.9	0.8	0.9	0.8	7.5	-0.5	3.6	-2.5	41.9	-0.5
	Control Light	21.6	-0.6	0.9	5.8	1.4	2.7	6.7	-1.5	3.0	8.1	33.5	1.4
	Bicarb. Dark	21.5	-2.6	0.7	-0.4	0.7	-0.4	6.7	-3.4	3.0	-7.3	41.1	-3.2
	Bicarb. Light	21.7	15.5	0.8	185.1	1.4	131.8	6.8	1.6	2.6	-6.0	31.5	0.8
	Glucose Dark	22.1	0.3	-	-	-	-	7.1	0.3	2.0	21.7	25.3	0.8
	Glucose Light	23.6	-1.7	-	-	-	-	7.4	-1.7	2.2	18.7	25.6	3.0
DGTA	Control Dark	na	na	na	na	na	na	na	na	na	na	na	na
	Control Light	23.7	1.1	3.2	14.4	3.2	14.4	6.4	1.1	3.0	3.3	29.9	1.0
	Bicarb. Dark	22.2	-0.3	3.4	12.9	4.1	8.6	6.0	-1.0	3.0	-1.1	34.0	-0.8
	Bicarb. Light	22.8	66.8	2.4	231.3	2.4	231.3	6.3	4.5	2.5	22.8	25.8	10.2
	Glucose Dark	25.6	43.6	4.2	432.4	4.2	432.4	6.8	3.1	4.2	540.3	37.6	62.1
	Glucose Light	23.4	15.7	3.8	136.3	3.8	136.3	6.0	4.1	3.3	289.8	33.2	28.4
DGCC	Control Dark	27.3	-0.4	0.9	8.6	0.9	8.6	9.6	2.1	3.9	4.9	36.2	0.5
	Control Light	22.1	-1.1	0.9	4.3	0.9	4.3	6.6	-0.5	3.6	-3.6	44.0	-0.6
	Bicarb. Dark	22.8	0.8	0.9	7.8	0.9	7.8	6.1	-2.6	3.2	-1.7	38.8	-0.7
	Bicarb. Light	23.7	69.3	0.8	125.6	0.8	125.6	6.4	9.5	3.0	18.3	35.0	11.3
	Glucose Dark	24.7	4.2	-	-	-	-	6.8	-0.7	2.0	265.4	21.8	23.4
	Glucose Light	28.6	2.4	-	-	-	-	6.0	1.0	2.5	123.5	24.1	9.3

- fatty acid not detected
na IP-DAG headgroup class not analyzed

Appendix B

Phospholipid specific production rate in the light

Appendix B - Phospholipid specific production rate in light incubations

The relative rate of phospholipid specific production in the light versus the dark was studied at one location in the Mediterranean Sea, and in a regrowth experiment in the North Pacific subtropical gyre.

Figure 1
Depth profile of phospholipid specific production rate measured in the light and dark

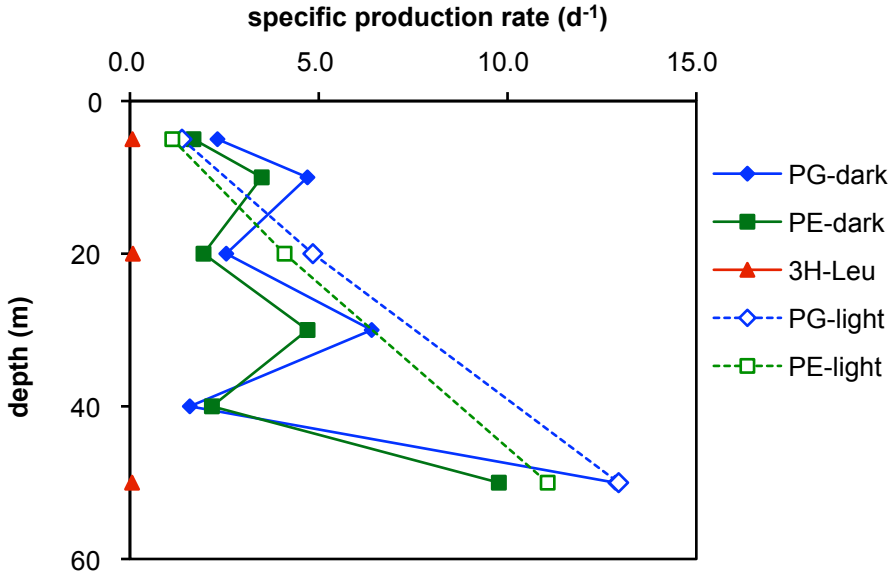

At one station on the BOUM cruise, station 17 in the Sicillian channel, parallel incubations were conducted for phospholipid specific production in the dark (blue and green solid lines, closed symbols), and in the light (blue and green dashed lines, open symbols); additionally specific production rate was calculated using the uptake rate of ^{3}H-Leucine in the dark. Specific production rate measured in the light versus the dark was not consistently different. For methods see Chapter 5.

Figure 2
North Pacific
Regrowth Experiment
in the light

Triplicate 20 L carboys (A, red circles, B, green triangles, and C, blue squares) were filled with 90% filtered seawater and 10% whole seawater from 5 m depth and incubated in the light (approximately 50% PAR) for 72 hours. Measurements were made at the beginning and end of the experiment for (A) heterotrophic bacterial cell concentration, (B) concentration of the phospholipid phosphatidylglycerol (PG, filled markers) and phosphatidylethanolamine (PE, open markers); measurements were made approximately every 12 hours for (C) production rate of the phospholipids PG (filled markers) and PE (open markers), and (D) uptake rate of 3H-leucine (Leu, filled markers) and 3H-thymidine (TdR, open markers). Incubations were conducted shipboard in the North Pacific subtropical gyre during the KM1013 cruise in July 2010. For full methods see Chapter 5.